Study on the roles of O-acetylserine (thiol) lyase and thiol dependent reductase 1 of *Leishmania*.

Lesley McCaig
BSc (Hons)

Thesis submitted in fulfilment of the requirements for the degree of Doctor of Philosophy in the Faculty of Biomedical and Life Sciences, University of Glasgow

Division of Infection and Immunity
Institute of Biomedical and Life Sciences
Glasgow Biomedical Research Centre
University of Glasgow
United Kingdom

May 2009

Abstract

Thiol dependent reductase 1 (TDR1) of *Leishmania* has been implicated in both the activation of pentavalent antimonial drugs and in the generation of drug-thiol conjugates facilitating drug-resistance. Reverse genetic studies were carried out on *TDR1* to elucidate the role of the enzyme and to assess its potential value as a drug target against *Leishmania*. In a similar study, O-acetylserine (thiol) lyase (OAS-TL), a key enzyme for the *de novo* synthesis of cysteine in *Leishmania*, was investigated as a potential target for new antileishmanial drugs.

TDR1 of *Leishmania* is a 49.9 kDa protein of which the physiological role remains unclear. The protein has shown both thiol transferase activity and dehydroascorbate reductase activity. Due to its ability to reduce pentavalent antimonials to the active trivalent form *in vitro*, TDR1 has been suggested as playing a vital role in antimonial resistance in *Leishmania*. This part of the study was undertaken to clarify the role TDR1 plays in the parasite by investigating the effects of deleting the gene.

Attempts were made to generate Δ*tdr1* null mutants in *Leishmania donovani*, but these were unsuccessful despite the fact that Δ*tdr1* null mutants exist for *L. major* and *L. infantum*. The mutants of these latter lines were studied to discover more on the roles of the proteins. *L. major* and *L. infantum* Δ*tdr1* null mutant promastigotes grow normally and do not display any change in total intracellular levels of cysteine, glutathione and trypanothione. The *L. major* Δ*tdr1* null mutants were able to survive and proliferate in parasitophorous vacuoles of peritoneal macrophages *in vitro*, with significantly higher numbers of parasites per infected macrophage compared to *L. major* wild-type. This suggests that the loss of *TDR1* is beneficial to *L. major* when establishing an infection in macrophages. However the loss of TDR1 also causes hypersensitivity to the antimonial drug sodium stibogluconate, under the conditions tested. The data generated in this study indicate that the physiological function of TDR1 does not lie in the activation of pentavalent antimonials as has been previously suggested.

The sulfur-containing amino acid cysteine plays a vital role in the synthesis of low molecular weight thiols, e.g. glutathione and trypanothione, as well as redox active thiol-containing proteins. In addition, cysteine is important for the stabilisation of tertiary and quaternary protein conformation due to its ability to form inter- and intra-chain disulfide bonds with other cysteine residues. In mammals, cysteine can either be taken up from the environment, or synthesised via the reverse trans-sulfuration pathway, involving the action of the enzymes cystathionine β-synthase and cystathionine γ-lyase, to generate cysteine from the essential amino acid methionine. In contrast, *Leishmania* parasites can synthesise cysteine in two ways but appear unable to salvage it effectively. They contain the reverse trans-sulfuration pathway, similar to mammals, and additionally, can generate cysteine through the sulfhydrylation pathway from serine, coenzyme A and sulfide, by utilising the enzymes serine acetyltransferase and O-acetylserine (thiol) lyase (OAS-TL).

The aim of this study was to assess the suitability of OAS-TL as a potential drug target against *Leishmania*. In this study, Δ*oas-tl* null mutants were generated in *L. donovani*, thus negating the sulfhydrylation pathway. The Δ*oas-tl* null mutant promastigotes displayed a slight growth defect as well as a severe morphological alterations directly affecting cell body and flagellum length. In addition, the Δ*oas-tl* null mutants were unable to survive in the parasitophorous vacuoles of peritoneal macrophages *in vitro*, suggesting that the exogenous supply of a source of cysteine (such as methionine) was not sufficiently high to support parasite proliferation. The finding that addition of high methionine concentrations to the medium facilitates parasite survival supports this idea. The data show that either differentiation of promastigotes into amastigotes or proliferation of amastigotes is detrimentally affected by the deletion of *OAS-TL*. Lines re-expressing OAS-TL were also generated in the Δ*oas-tl* null mutants and were found to complement the phenotypes of the Δ*oas-tl* null mutants identified in this study. The inability of *Leishmania* Δ*oas-tl* null mutants to survive within macrophages, together with the absence of OAS-TL in the mammalian host, make it a suitable candidate for the identification of new drug targets in the search for novel chemotherapeutic agents against leishmaniasis.

Acknowledgements

I'd like to thank my supervisors Graham Coombs and Sylke Müller for giving me the opportunity to study for a PhD in their labs. Thank you also to my assessor Mike Barrett for useful discussions and advice.

Thanks to all my colleagues in the lab, particularly to Rod Williams for teaching me so much and Jo McGregor for putting up with my endless questions! Thank you to Denise Candlish, Susan Baillie and Elaine Brown for technical advice and assistance over the past few years. I have to also thank the pub regulars for helping me forget the lab on a Friday night!

To my friends outside the lab, particularly Pauline, Jen, Dawn and Carol, thank you for years of friendship, for keeping my social life alive and for reminding me that life outside science does exist! To Keith, Liam and Max thanks for keeping me sane and spurring me on! And to my good friend Jeff, a big thank you has to go to you for the years of emotional support and professional advice. I hope I get to see you sometime soon!

For endless encouragement and support as well as scientific advice I'd like to thank my brother David. Thanks for all the help you've given me (since school!) and for inspiring me to do a PhD in the first place.

To Sylvain (thanks Subhash!), thank you for everything, not least reminding me what's important in life. I love you loads and can't wait till December...

I'd like to dedicate this thesis to my parents, John and Linda. I am so grateful to you for all the love, support and encouragement you've given me all my life, for believing I could do this and for 25 years of laughter! This is for you.

Author's Declaration

The research reported in this thesis is the result of my own original work, except where stated otherwise, and has not been submitted for any other degree.

Lesley McCaig

List of Abbreviations

ACR2	arsenate reductase 2
AMP	ampicillin
ANOVA	analysis of variance
AQP1	aquaglyceroporin 1
bp	base pair
BLEO	bleomycin
BSA	bovine serum albumin
CBS	cystathionine ß-synthase
CGL	cystathionine γ-lyase
CL	cutaneous leishmaniasis
Δ*tdr1*	null mutant for *TDR1* gene
Δ*oas-tl*	null mutant for *OAS-TL* gene
Δ*tdr1* [TDR1]	extra-chromosomal re-expression of TDR1 in Δ*tdr1*
Δ*oas-tl* [OAS-TL]	extra-chromosomal re-expression of OAS-TL in Δ*oas-tl*
DCL	diffuse cutaneous leishmaniasis
DTT	dithiothreitol
EDTA	ethylenediamine tetra acetic acid
ELF1α	elongation factor 1α
EPB	electroporation buffer
ER	endoplasmic reticulum
ETOH	ethanol
GCS	γ-glutamylcysteine synthetase
GPI	glycosylphosphatidylinositol
GS	glutathione synthetase
HDMS	hexamethyldisilazane
HEDS	2-hydroxyethyl disulfide
HIFCS	heat inactivated foetal calf serum
HRP	horseradish peroxidise
HSP	heat-shock protein
HYG	hygromycin B
IC_{50}	inhibitory concentration for 50 % inhibition
IPTG	isopropyl-ß-D-thiogalactopyranoside
KAN	kanamycin
kb	kilo base
kDa	kilo Dalton
kDNA	kinetoplast DNA
l	litre
LB	Luria-Bertani
LC	loading control
LPG	lipophosphoglycan
µ	micro
m	milli / metre
M	molar
MCL	mucocutaneous leishmaniasis
min	minute
MRPA	multi-drug resistance protein A
MST	mercaptopyruvate sulfurtransferase
MVT	multivesicular tubule

n	nano
OAS-TL	O-acetylserine (thiol) lyase
OD	optical density
ODC	ornithine decarboxylase
oGST	omega class glutathione S-transferase
PBS	phosphate buffered saline
PCR	polymerase chain reaction
PHLEO	phleomycin
PLP	pyridoxal-5'-phosphate
PMN	polymorphonuclear neutrophil granulocytes
PPG	proteophosphoglycan
PSG	promastigote secretory gel
SAT	serine acetyltransferase / nourseothricin acetyltransferase
SbIII	trivalent antimony
SbV	pentavalent antimony
SDS-PAGE	sodium dodecylsulfate polyacrilamide gel electrophoresis
SEM	standard error of the mean / scanning electron microscopy
TDR1	thiol dependent reductase 1
TR	trypanothione reductase
VL	visceral leishmaniasis
WT	wild type

Table of Contents

List of Figures

CHAPTER 1: INTRODUCTION

CHAPTER 2: MATERIALS AND METHODS

CHAPTER 3: *LEISHMANIA DONOVANI*, *L. MAJOR* AND *L. INFANTUM* TDR1: ANALYSIS OF GENE DELETION AND PRODUCTION OF RECOMBINANT PROTEIN

CHAPTER 4: O-ACETYLSERINE (THIOL) LYASE OF *LEISHMANIA DONOVANI*

List of Tables

CHAPTER 2: MATERIALS AND METHODS

CHAPTER 3: *LEISHMANIA DONOVANI*, *L. MAJOR* AND *L. INFANTUM* TDR1: ANALYSIS OF GENE DELETION AND PRODUCTION OF RECOMBINANT PROTEIN

CHAPTER 4: O-ACETYLSERINE (THIOL) LYASE OF *LEISHMANIA DONOVANI*

1. Introduction

1.1 *Leishmania*

Leishmania are obligate intracellular protozoa of the family Trypanosomatidae, and order Kinetoplastida. Over 20 species of *Leishmania* have been identified, each of which has specific mammalian reservoirs. The majority of mammalian reservoirs are rodents, but the human pathogens include *L. major*, *L. mexicana*, *L. donovani*, *L. braziliensis*, *L. aethiopica* and *L. tropica* (Lainson et al., 1979). Approximately 30 species of the phlebotomine sand-fly have been identified as vectors (Desjeux, 2004).

1.2 Leishmaniasis and geographic distribution of disease

Leishmaniasis is endemic in 88 countries worldwide (Figures 1.1 and 1.2), 66 of these are in the Old World and 22 in the New World (Desjeux, 2004). 72 of those countries affected are developing countries and a further 13 are among the least developed. At present, leishmaniasis affects 12 million people with a population of 350 million at risk. The clinical manifestation of leishmaniasis, which depends on the infective species as well as the immune response of the host, has been classified into four forms.

1.2.1 Cutaneous leishmaniasis

The most common clinical form is cutaneous leishmaniasis (CL), which is estimated to affect 1-1.5 million people annually (Desjeux, 2004). The disease involves the formation of up to 200 self-healing skin lesions on exposed parts of the body. When the lesions are multiple, CL can result in disability, and the disfiguring scars caused often create an aesthetic stigma. In the Old World, CL is mainly caused by *L. major*, *L. tropica* and *L. aethiopica*, and in the New World by *L. mexicana*, *L. guyanensis* and *L. panamensis* (Desjeux, 2004). 90 % of CL cases occur in Afghanistan, Algeria, Brazil, Iran, Peru, Saudi Arabia and Syria (Desjeux, 1996).

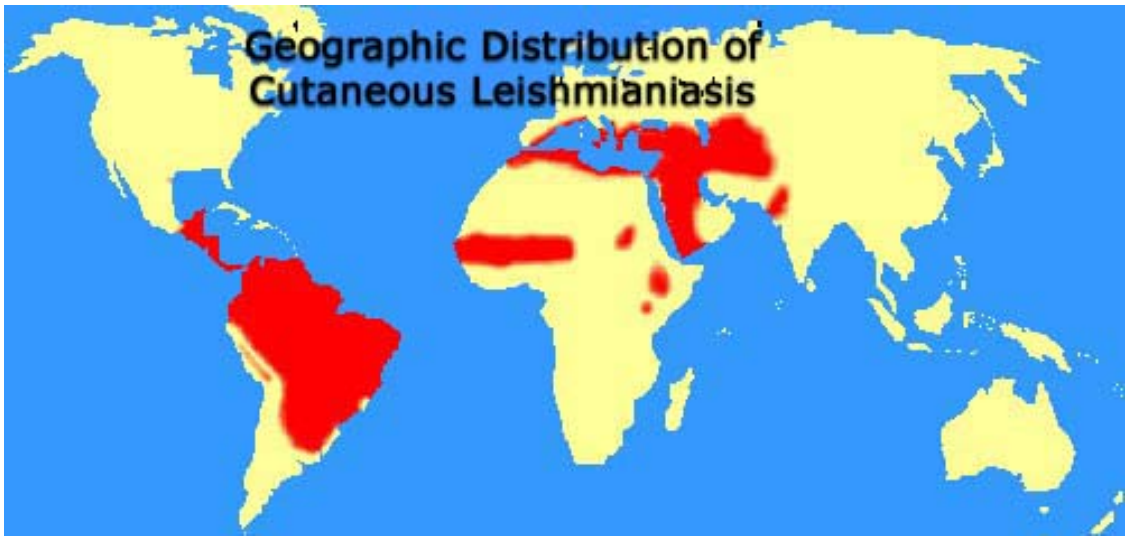

Figure 1.1 Geographic distribution of cutaneous leishmaniasis.
Map showing highly endemic regions of cutaneous leishmaniasis in red. Map taken from www.vet.uga.edu.

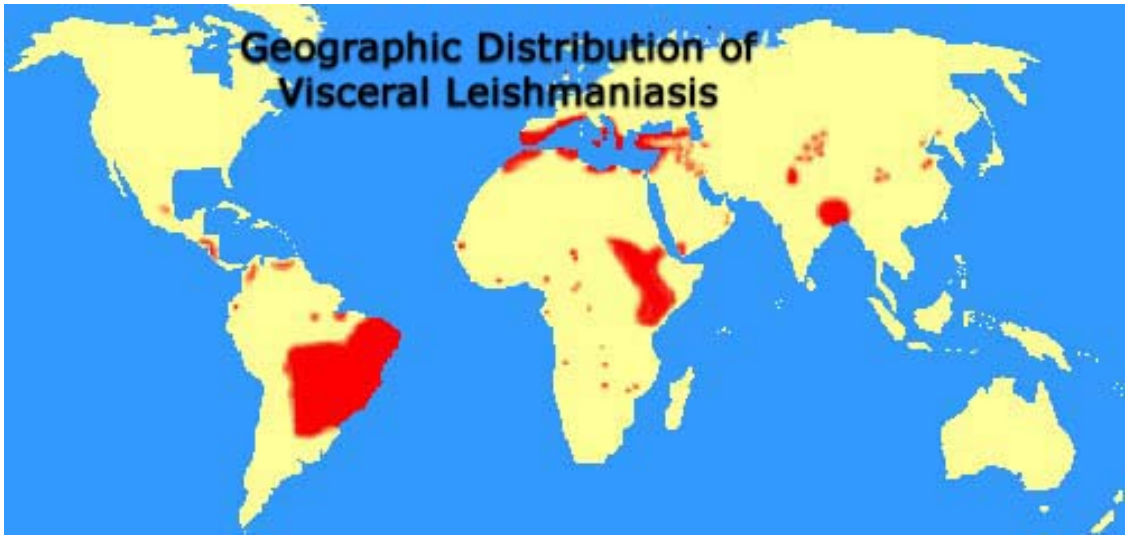

Figure 1.2 Geographic distribution of visceral leishmaniasis.
Map showing highly endemic regions of visceral leishmaniasis in red. Map taken from www.vet.uga.edu.

1.2.2 Diffuse cutaneous leishmaniasis

Diffuse cutaneous leishmaniasis (DCL) occurs in infected individuals that have a defective cell-mediated immune response. The disease is characterised by disseminated cutaneous lesions that resemble lepromatous leprosy. DCL does not self-heal and is prone to relapse after treatment with any of the drugs that are currently available (Desjeux, 2004). DCL is caused by *L. aethiopica* in the Old World and *L. mexicana* in the New World.

1.2.3 Mucocutaneous leishmaniasis

Mucocutaneous leishmaniasis (MCL), which is also known as espundia, is characterised by severely disfiguring lesions causing extensive destruction of the oral-nasal and pharyngeal cavities. This level of facial deformity causes affected individuals great suffering for life. Although most cases of MCL are caused by the New World species *L. braziliensis* and *L. guyanensis*, it has also been reported to be caused by *L. donovani*, *L. major* and, in the immune-suppressed, *L. infantum*, in the Old World (Desjeux, 2004).

1.2.4 Visceral leishmaniasis

Visceral leishmaniasis (VL), which is also known as kala azar, is a serious systemic infection characterised by irregular fever, severe weight loss, anaemia and swelling of the spleen and liver. The disease is fatal in the absence of treatment and is therefore considered of higher priority than CL. VL occurs in 65 countries worldwide, however 90 % of cases occur in poor rural and suburban areas of Bangladesh, India, Nepal, Sudan and Brazil (Desjeux, 1996). There are an estimated 500 000 cases of VL annually. Most cases that occur on the Indian subcontinent and Eastern Africa are caused by *L. donovani*, whereas most cases in the New World are caused by *L. infantum* (Olliaro et al., 2002).

1.3 *Leishmania* life-cycle

Leishmania are digenetic and exist in two hosts, the female phlebotomine sand-fly vector and the mammalian host. In the sand-fly, the parasite exists in its

flagellated promastigote form, and in the mammalian host, parasites reside intracellularly within phagolysosomes in amastigote form. A schematic representation of the *Leishmania* life-cycle is shown in Figure 1.3.

Leishmania amastigotes are taken up by the female phlebotomine sand-fly vector, when it takes a blood-meal from an infected mammal. In order to survive within the sand-fly, the parasites must transform into the promastigote form. They will subsequently differentiate through six promastigote stages, as they move anterially through the mid-gut (Rogers et al., 2002).

Members of the subgenus *Leishmania* undergo suprapylarian development taking place exclusively in the midgut and foregut of the vector whereas members of the subgenus *Viannia* also undergo a period of peripylarian development in the hindgut (Lainson et al., 1987). Amastigotes will transform into procyclic promastigotes which then differentiate into nectomonad promastigotes, then leptomonad promastigotes followed ultimately by the mammalian infective stage, metacyclic promastigotes (Rogers et al., 2002). Two further stages have been identified – haptomonad promastigotes and paramastigotes, but these have only been found in low numbers and the precursor form of each has never been established (Kamhawi, 2006). The time-dependent location of these distinct morphological forms of *Leishmania* promastigotes within the sand-fly are shown in Figure 1.4 (Kamhawi et al., 2006).

Infective metacyclics have been reported to take between 6-9 days to develop from amastigotes, depending on the species (Kamhawi, 2006). The metacyclic promastigotes accumulate at the stomodeal valve and the thoracic midgut fills with promastigote secretory gel. This gel is made up mostly of leptomonad and metacyclic promastigotes, and due to the blockage of the midgut, forces the stomodeal valve open (Rogers et al., 2002).

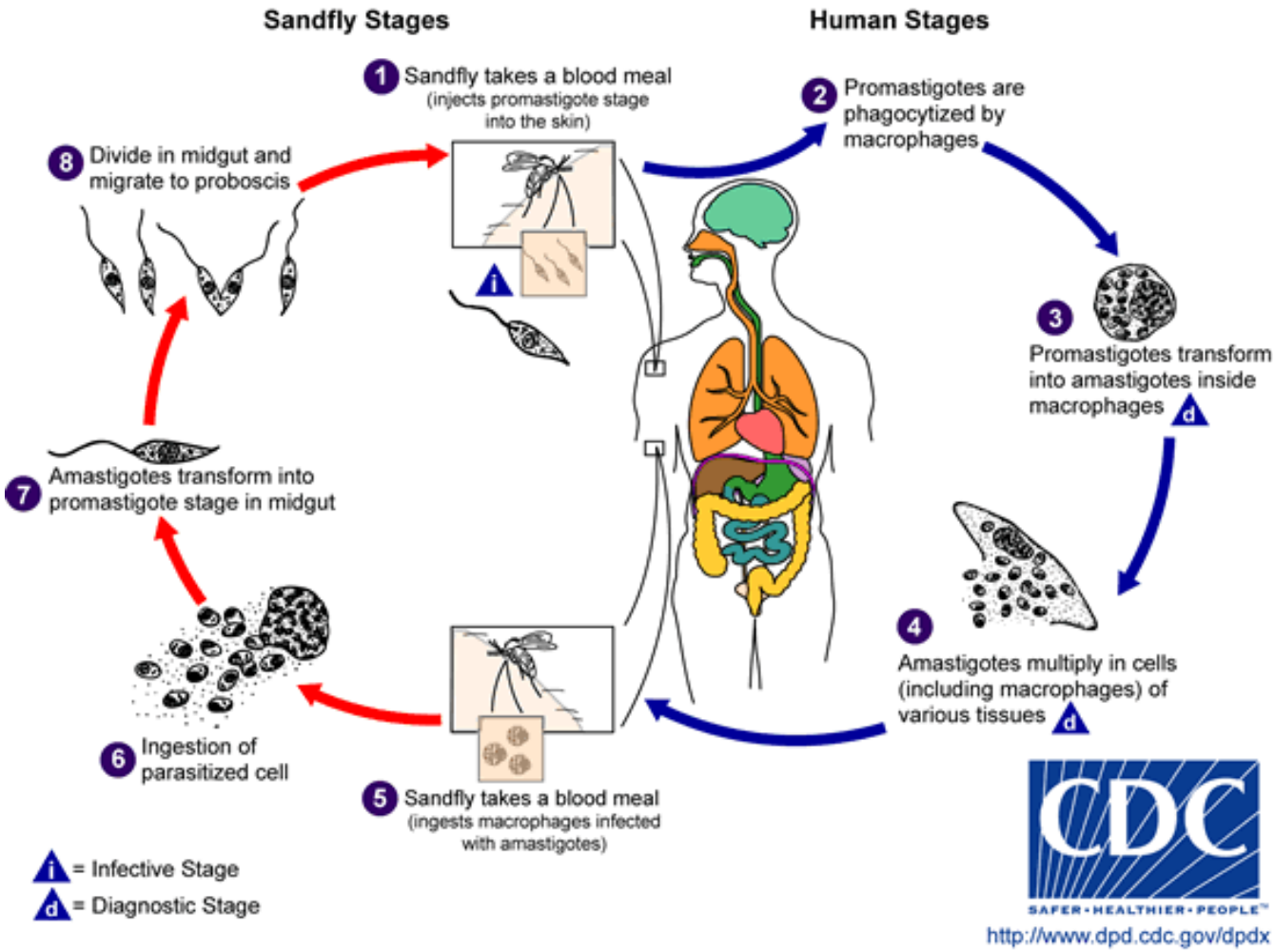

Figure 1.3 Life cycle of *Leishmania* spp.
Schematic diagram of the life cycle stages of *Leishmania*. The insect stages are shown on the left of the diagram, while the mammalian stages are shown on the right of the diagram. Taken from www.dpd.cdc.gov.

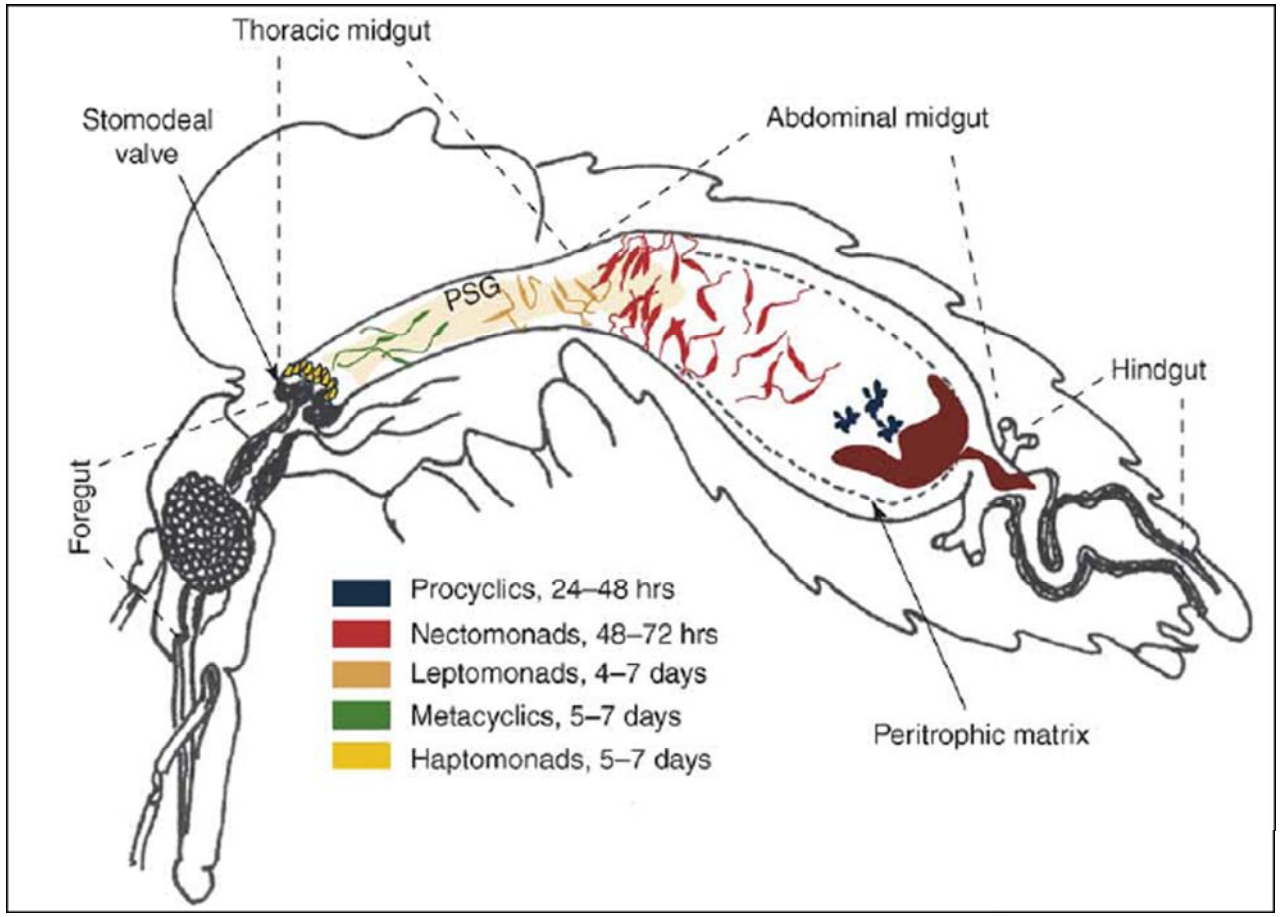

Figure 1.4 *Leishmania* promastigote stages within the sand-fly vector.
Schematic representation of a female phlebotomine sand-fly infected with *Leishmania*, showing the distinct morphological forms of promastigotes within the midgut. The thoracic midgut is shown filled with promastigote secretory gel (PSG) which holds the stomodeal valve open. Taken from Kamhawi, 2006.

When the sand-fly takes a blood-meal, approximately 1000 metacyclic promastigotes are regurgitated into the bite site as well as the promastigote secretory gel plug. The main component of this is filamentous proteophosphoglycan (PPG), and has been show to enhance disease progression (Rogers et al., 2004).

Within 10-24 h post-infection, polymorphonuclear neutrophil granulocytes (PMN) are recruited to the bite site, and the parasites are phagocytosed (Muller et al., 2001). The spontaneous apoptosis of the PMN is inhibited by *Leishmania* to prolong the lifespan of the cell until macrophages are recruited to the bite site (Aga et al., 2002). This normally occurs 1-2 days post-infection, and the macrophages will phagocytose the infected PMN (Aga et al., 2002). By taking up *Leishmania* in this way, the parasites are able to infect macrophages without activating the antimicrobial functions of the macrophage (Laskay et al., 2003). *Leishmania* are then able to differentiate into amastigotes (Figure 1.5), the mammalian replicative stage of the parasite.

Differentiation and replication both occur within a parasitophorous vacuole of a macrophage, and the lifecycle continues when a sand-fly takes a blood-meal from the infected mammal.

1.4 *Leishmania* ultrastructure

The structure of *Leishmania* promastigote and amastigotes stages are shown in Figure 1.6. *Leishmania* cells contain many of the organelles found in higher eukaryotes, but additionally contain a number of special organelles.

1.4.1 Surface Coat

Due to the digenetic life cycle of *Leishmania*, it goes through a number of distinct developmental stages. The specific shapes of these stages are maintained by an array of subpellicular microtubules that underly the plasma membrane (McConville et al., 2002).

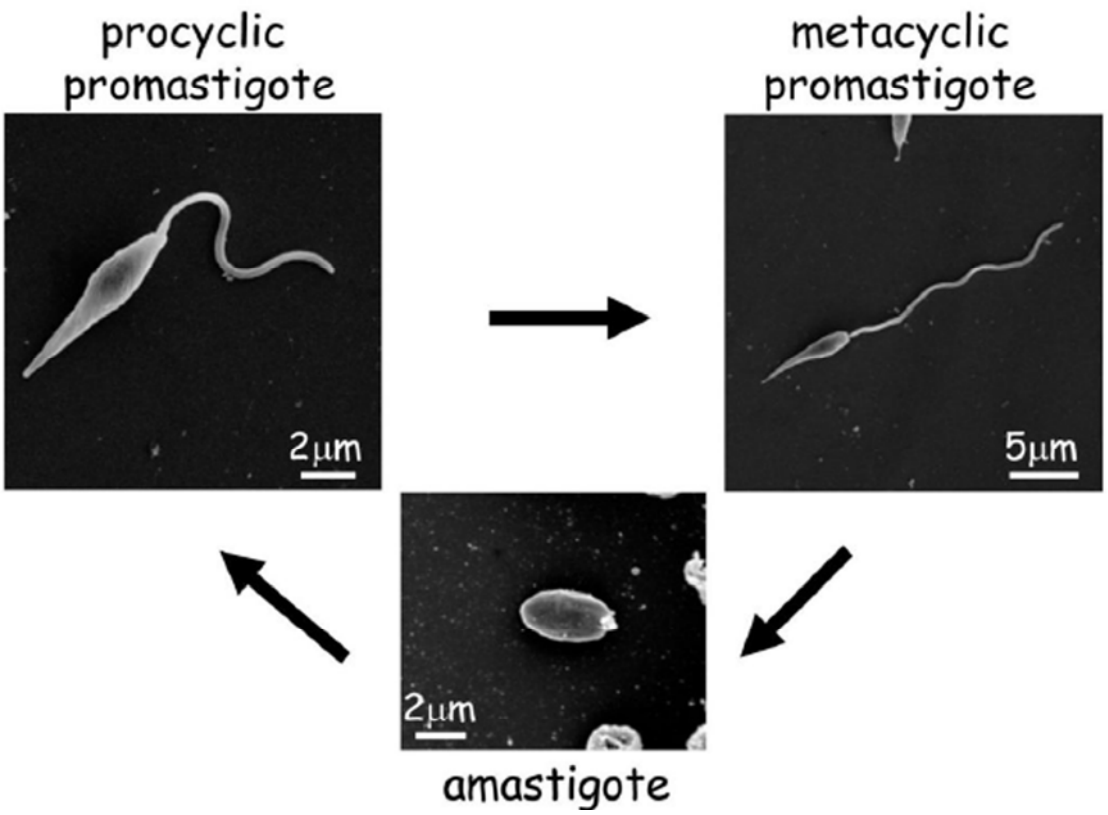

Figure 1.5 Changes in cell shape during the *Leishmania* life-cycle.
Scanning electron microscope images of the main life-cycle stages of *Leishmania major*. Taken from Besteiro et al., 2007.

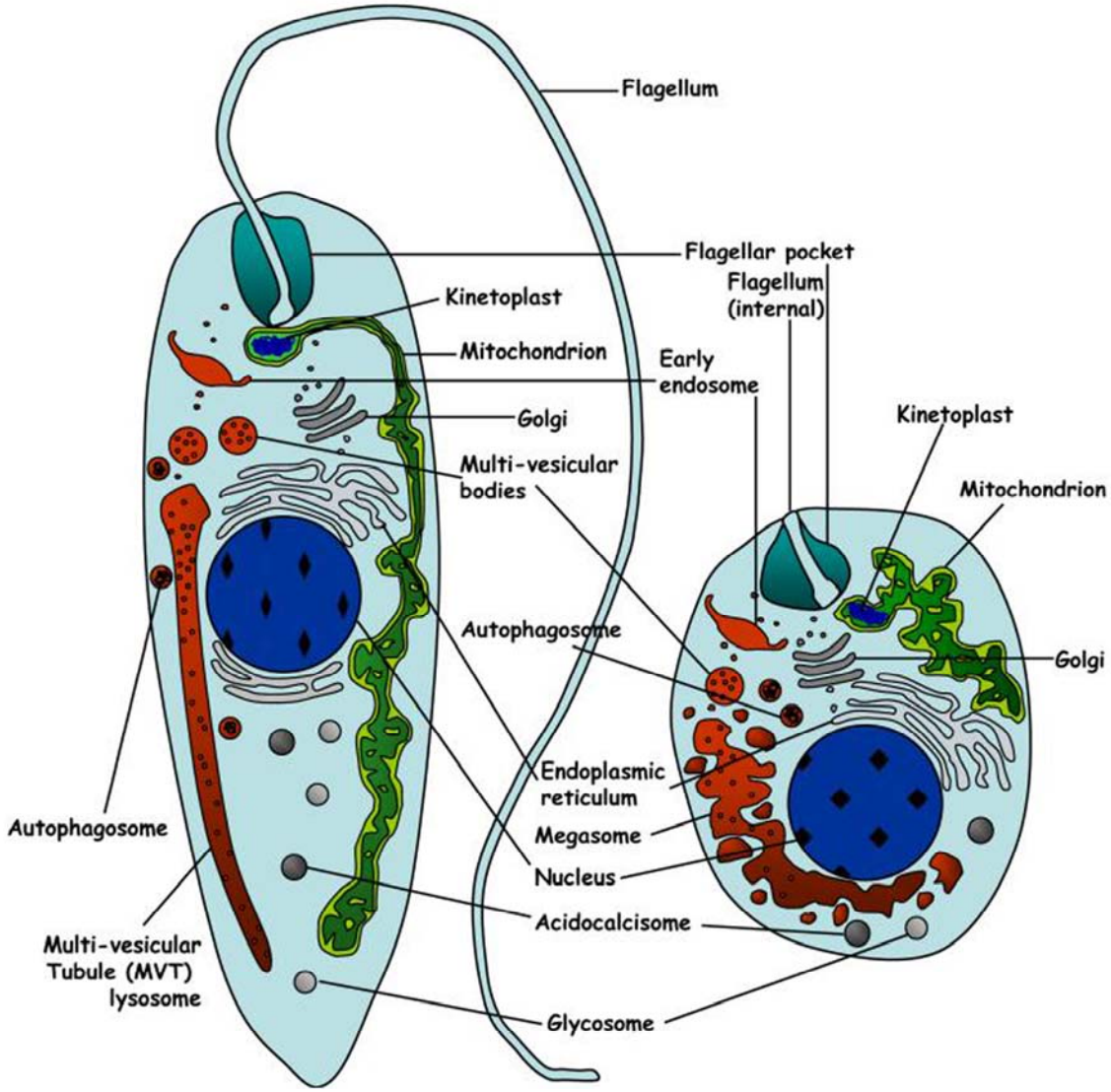

Figure 1.6 Cell structure of *Leishmania* promastigotes and amastigotes.
Schematic representation of the structural composition of *Leishmania* promastigotes (left) and amastigotes (right). The position of the flagellar pocket is indicative of the anterior end of the cell. Taken from Besteiro et al., 2007.

In promastigotes, the major macromolecule on the surface of the organism is lipophosphoglycan (LPG), the hyperglycosylated glycosylphosphatidylinositol (GPI) glycolipid (Mengeling et al., 1997). These surface molecules are made up of a conserved GPI anchor with a long phosphoglycan backbone that is elaborated with species- and stage-specific glycan side chains (Mengeling et al., 1997).

Polymorphisms in the LPG coat contribute to vector tropism in *Leishmania* (Sacks et al., 2000), and is also believed to play a role in protection of promastigotes from lysis by the alternative complement cascade and extracellular hydrolases (Puentes et al., 1990; Sacks, 2001). It has also been suggested that the LPG coat acts either directly or indirectly as a ligand for insect midgut and mammalian macrophage receptors (Mengeling et al., 1997; Sacks, 2000). The surface coat also contains various GPI proteins and proteophosphoglycans (PPGs), which are mostly masked on promastigotes by the LPG coat, and have been found to be important for resistance to complement lysis (Joshi et al., 1998).

The surface of *Leishmania* amastigotes is coated with a layer of free GPIs and host-derived glycosphingolipids, likely to be involved in the protection of essential plasma membrane transporters from proteolysis in the parasitophorous vacuole. Amastigotes lack a prominent surface glycocalyx of GPI proteins and other GPI-anchored macromolecules, which could contribute to immune evasion in the parasites (McConville et al., 2002).

As well as the pellicular plasma membrane, the surface membrane of *Leishmania* can be divided into a further two morphologically distinct subdomains; the flagellar membrane and the flagellar pocket. Despite their highly specialised biological functions, all three membranes are physically contiguous.

1.4.2 Flagellar pocket and flagellum

The flagellar pocket appears as a depression in the cell, formed by the invagination of the plasma membrane at the anterior region of the cell. Its membrane establishes a direct continuity with the membrane of the flagellum (De Souza, 2002), and it is the only region of the cell where the sub-pellicular microtubules associated with the membrane are not present (Landfear &

Ignatushchenko, 2001). The flagellar pocket has three main roles: the uptake of larger nutrients via receptor-mediated endocytosis, secretion of proteins into the extracellular medium and for integration of membrane proteins into the cell surface (Landfear & Ignatushchenko, 2001).

The flagellum is a motility organelle involved in movement of the parasite forward via wave-like beats of the microtubule-based flagellar axoneme. The flagellum also contains a fibrous body called the paraflagellar rod that consists of discrete filaments, and runs along the length of the flagellum attached to the flagellar axoneme (Landfear & Ignatushchenko, 2001). As well as being involved in the motility of promastigotes, it is also involved in the attachment of the parasites to the endothelium of the sand-fly gut (Killick-Kendrick et al., 1974a & 1974b). Amastigotes are immotile due to the fact that the flagellum is much shorter and does not emerge from the flagellar pocket in this stage.

1.4.3 Mitochondrion and kinetoplast

Each *Leishmania* cell contains a single mitochondrion, containing a single kinetoplast DNA (kDNA) network condensed into a disk-shaped structure. The kDNA disk is localised to a specific region of the mitochondrial matrix, near the flagellar basal body (Liu et al., 2005). The network of kDNA is comprised of two types of DNA rings: minicircles and maxicircles. The kinetoplast contains a few thousand minicircles and a few dozen maxicircles (Liu et al., 2005) comprising 10-20 % of the total DNA of the cell. Gene products of maxicircles are similar to those of mitochondrial DNAs of higher eukaryotes. The transcripts are cryptic and require editing to become functional mRNA, which involves the insertion or deletion of uridylate residues at precise internal sites (Liu et al., 2005). This editing is controlled by minicircle-encoded guide RNAs that serve as templates for uridylate-insertion and deletion. Therefore, the expression of kinetoplastid mitochondrial genes is a result of a cooperative effort between minicircle and maxicircle transcripts (Liu et al., 2005).

Leishmania promastigotes contain a single mitochondrion that extends throughout the cell. In stationary phase, the mitochondrion is asymmetric, with a single tubule extending from one edge of the kinetoplast portion of the cell. However, in dividing cells, the mitochondrion forms a symmetric circular

structure with mitochondrial tubules extending from both edges of the kinetoplast portion that join in the posterior region of the cell (Simpson & Kretzer, 1997). In *Leishmania* amastigotes, the mitochondrion forms a complex network that extends throughout the cell (Coombs et al., 1986).

1.4.4 The endocytic pathway

The morphology and function of organelles in the endocytic pathway of *Leishmania* changes as these parasites differentiate from the promastigote stage to the amastigote stage of the parasite. The main organelles in this pathway are the endoplasmic reticulum (ER) and the Golgi apparatus. The ER consists of a nuclear envelope and a system of cisternae, often closely associated with the plasma membrane (McConville et al., 2002). The Golgi apparatus is located between the nucleus and flagellar pocket, and consists of a stack of 3 to 10 cisternae and a polymorphic *trans*-Golgi network.

The endocytic pathway of *Leishmania* promastigotes is made up of three morphologically distinct compartments: i) a network of tubular endosomes that are localised close to the flagellar pocket, ii) a population of multivesicular bodies that are located to the anterior end of promastigotes and iii) a multivesicular tubule (MVT)-lysosome that runs along the anterior-posterior axis of the parasite (Waller & McConville, 2002). The MVT-lysosome is the terminal component in the promastigote endocytic pathway (Ghedin et al., 2001; Mullin et al., 2001) and increases in lytic capacity as the cells reach stationary growth phase (Mullin et al., 2001). As well as a marked difference in morphology, the differentiation of *Leishmania* from promastigotes to amastigotes is associated with significant alterations in the abundance and intracellular distribution of secretory and endocytic compartments. In amastigotes, the ER is minimal, comprising primarily of the nuclear envelope, and the Golgi apparatus is dispersed and often difficult to detect (Waller & McConville, 2002). However, amastigotes of some species of *Leishmania* contain an expanded lysosome system often containing one or a number of very large lysosomal vacuoles called megasomes (Coombs et al., 1986).

Endocytosis and lysosomal degradation provides a pathway by which *Leishmania* obtain essential nutrients, as well as being involved in the degradation and

turnover of endogenous proteins during differentiation (Waller & McConville, 2002).

1.4.5 Glycosomes

Glycosomes are apparently randomly distributed organelles that belong to the peroxisome family. They are bound by a single phospholipid bilayer and contain no DNA, while up to 90 % of the protein content of these organelles consists of glycolytic enzymes (Michels et al., 2006). The glycosome normally consists of a homogenous, slightly dense matrix, although in *L. mexicana* a crystalloid core has been described (Vickerman & Preston, 1974).

Glycosomes compartmentalise a number of metabolic functions and are believed to play an important role in metabolic adaptation of *Leishmania* to the different environments exposed to during the life-cycle. Ether-lipid synthesis and ß-oxidation of fatty acids takes place in the glycosomes (Zheng et al., 2004). The organelle also harbours the first seven enzymes of the glycolysis pathway and is therefore involved in energy production (Parsons et al., 2001).

1.4.6 Acidocalcisomes

Acidocalcisomes are spherical structures with an approximate diameter of 200 nm, and are preferentially located at the cell periphery. The structures are considered storage organelles for a range of elements including phosphorus, magnesium, calcium, sodium and zinc (Miranda et al., 2000).

1.5 Chemotherapy and drug resistance

1.5.1 Antimonial drugs

The pentavalent antimonials, e.g. sodium stibogluconate (Pentostam), were first introduced as a treatment against leishmaniasis in 1945. The drugs have been used to treat both VL and CL and since their introduction have been considered the cornerstone of anti-leishmanial therapy. Despite this, there are a number of factors decreasing the benefit of this drug. Antimonials require parenteral administration with long courses of treatment lasting up to 28 days, and a high

number of treatment failures in Nepal and India, particularly in Bihar State, are emerging that could be due to drug resistance. Bihar State is estimated to contain approximately 50% of annual cases of VL worldwide, with officially 430,000 cases in the past 11 years, although this figure is believed to be at least five times greater in reality (Lira et al., 1999). The precise mode of action of the pentavalent antimonials, how they are taken up by the *Leishmania* and how resistance occurs remain unknown.

1.5.1.1 Activation of antimonials

The pentavalent antimonials (SbV) are prodrugs and as such, must be reduced to the active trivalent form (SbIII) in order to be active against intracellular amastigotes (Ouellette et al., 2004) (Figure 1.7). The site of this activation together with the mechanism by which it occurs is unclear. Some studies provide evidence that the drug is reduced within the amastigote but not the promastigote form of the parasite (Shaked-Mishan et al., 2001). Other studies have suggested that the reduction of SbV to SbIII occurs in the macrophage, prior to uptake by the parasite (Sereno et al., 1998). Therefore, it is most likely that the drug may be reduced and thus activated both within the macrophage and in the amastigote. Activation is reported to take place both non-enymatically and enzymatically within the parasite. The macrophage specific thiols cysteine and cysteinyl-glycine are capable of reducing SbV to SbIII *in vivo* within the acidic parasitophorous vacuole (Ferreira et al., 2003). The same study also provides some evidence that suggests activation of the drug may be mediated by trypanothione (a parasite-specific thiol) within *Leishmania* parasites (Ferreira et al., 2003). Enzymatic activation has been reported recently. The thiol dependent reductase, thiol dependent reductase 1 (TDR1) – which is similar to the omega class glutathione S-transferases (oGSTs) – is known to reduce SbV to SbIII enzymatically using glutathione as a reductant (Denton et al., 2004). Additionally, a recent study involved the characterisation of ACR2 – an antimoniate reductase – capable of reducing SbV to SbIII in *Leishmania*. This study also showed that the presence of this enzyme increased the sensitivity of *Leishmania* to pentavalent antimony (Zhou et al., 2004).

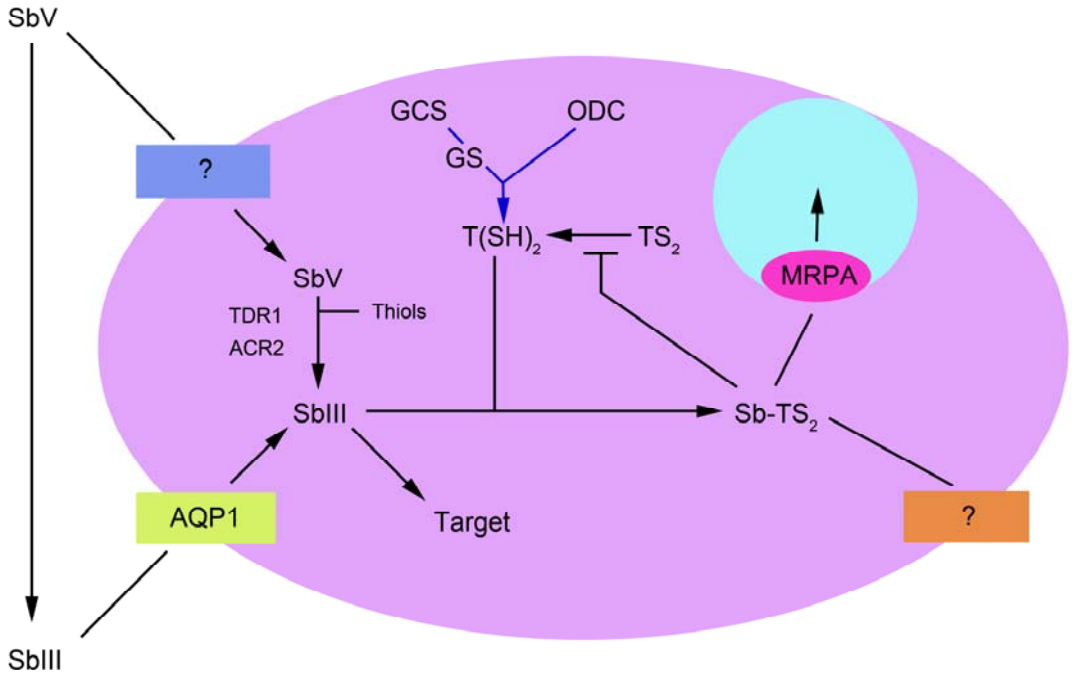

Figure 1.7 Entry, activation, action and efflux of antimonial drugs.
Schematic representation of the pathways involved in entry, activation, action and efflux of antimonial drugs in *Leishmania* amastigotes. TR, trypanothione reductase; MRPA, multidrug resistance protein A; AQP1, aquaglyceroporin 1; TDR1, thiol dependent reductase 1; ACR2, arsenate reductase 2; ODC, ornithine decarboxylase; GCS, γ-glutamylcysteine synthetase; GS, glutathione synthetase. Activation of SbV may occur outside the amastigotes, and can therefore enter the parasite as SbV, via an unknown transporter (blue box) or as SbIII, via AQP1. SbV can be reduced within the amastigotes enzymatically by TDR1 or ACR2 or non-enzymatically by thiols. The active form of the drug can then affect the intracellular target, which is at present unknown. Possible mechanisms of resistance include the conjugation of the drug with thiols, which can then be extruded from the cell via an unknown transporter (orange box) or sequestered by MRPA into intracellular organelles (pale blue). Alterations in the expression of proteins involved in the synthesis of thiols (GCS, GS and ODC) have also been suggested as contributing factors in the resistance of *Leishmania* to antimonials.

1.5.1.2 Thiol dependent reductase 1

Thiol dependent reductase 1 of *Leishmania major* is a 49.9 kDa protein, which forms a trimer of approximately 155 kDa (Denton et al., 2004). The enzyme displays a two-domain nature consisting of an N-terminal domain containing the characteristic motif of glutaredoxin and thioredoxin, and a C-terminal domain where the active site is more similar to the omega class of glutathione S-transferases (Denton et al., 2004). TDR1 bears some similarity to the arsenate reductases, but uses glutathione as the reducing agent, as opposed to glutaredoxin and thioredoxin, which are utilised by the arsenate reductases (Denton et al., 2004).

The precise role of the enzyme is as yet unknown, but it has been shown *in vitro* to have the ability to reduce pentavalent antimonials to trivalent antimonials (Denton et al., 2004). The amount of TDR1 in amastigotes has been found to be ten times the amount present in promastigotes (Denton et al., 2004). As *Leishmania* amastigotes are 50 – 600 times more sensitive to SbV than promastigotes (Roberts et al., 1995; Sereno et al., 1998; Callahan et al., 1997; Ephros et al., 1999), this increase in TDR1 has been implicated as the potential reason for the specificity of antimonial drugs to the amastigote stage, suggesting that the activation of SbV to SbIII is the physiological role of the enzyme.

On the other hand, it has also been suggested that TDR1 plays a role in the detoxification of arsenic, due to its similarity with to the arsenate reductases (Styblo et al., 2000). Antimony is a metal related to arsenic, and organisms resistant to arsenic are often cross-resistant to antimony. If this hypothesis is true, the upregulation of TDR1 could play an important role in resistance of *Leishmania* to antimonial drugs.

Tc52 of *Trypanosoma cruzi* is similar to glutathione S-transferase and has an overall identity of 45.7 % to TDR1 of *L. major* (Denton et al., 2004). Tc52 is a 52 kDa protein which plays an important role in the regulation of intracellular thiol-disulphide redox balance by reducing glutathione disulphide (Moutiez et al., 1997). The active site residues of TDR1 and Tc52 are identical in the N-terminal domains, but differ in the C-terminal domains (Denton et al., 2004). Tc52 has

been shown to be essential for parasite survival and helps to modulate the host's immune response to infection (Allaoui et al., 1999; Garzon et al., 2003).

1.5.1.3 Uptake of antimonials

Before SbIII/SbV can have an effect, it must be taken up by the amastigote. Entry of the drug into the amastigote is believed to occur both in its pentavalent form and its reduced, active trivalent form. SbV is known to enter and accumulate in *Leishmania* cells, supporting the hypothesis that activation occurs within the parasite (Shaked-Mishan, 2001). Evidence has also been provided which suggests the active SbIII enters amastigotes via the *Leishmania* aquaglyceroporin 1 (AQP1) (Gourbal et al., 2004). A recent study has shown that the routes of entry of SbV and SbIII to *Leishmania* are likely to differ and therefore the uptake of SbV into the cell must be via an, as yet, uncharacterised transporter (Brochu et al., 2003).

1.5.1.4 Antileishmanial effects of antimonials

Fatty acid β-oxidation has been reported as a potential cellular target of SbIII as well as the inhibition of glycolytic enzymes (Berman et al., 1989). However, the trivalent antimonial Triostam and the trivalent arsenical melarsen oxide were shown not to affect the activity of leishmanial hexokinase, phosphofructokinase, pyruvate kinase, malate dehydrogenase and phosphoenolpyruvate carboxykinase (Mottram & Coombs, 1985). It has also been shown that the active SbIII has two different mechanisms of action against *Leishmania* parasites. Firstly, SbIII induces the quick efflux of intracellular glutathione and trypanothione, thus decreasing thiol buffering capacity within the cell (Wyllie et al., 2004). In addition, the active drug is known to inhibit the action of trypanothione reductase, causing an increase in intracellular levels of the disulfide forms of glutathione and trypanothione (Wyllie et al., 2004). These effects combine to significantly compromise the redox potential of the cell, ultimately affecting the ability of the cells to withstand oxidative stress. Recent evidence has shown that antimony kills the parasite by a process of apoptosis involving DNA fragmentation and externalisation of phosphatidylserine on the outer surface of the membrane (Sudhandiran & Shaha, 2003).

1.5.1.5 Resistance to antimonials

As is often the case with bacterial drug resistance, reduced drug uptake and increased drug efflux are two possible mechanisms by which resistance occurs in *Leishmania* parasites. Since resistance of *Leishmania* to antimonials has been associated with its reduced accumulation, it has been suggested that alteration in AQP1 gene transcript levels could be partly responsible for antimonial resistance in these organisms. Although changes have not been observed in AQP1 gene copy numbers or in copy numbers of AQP homologues, it has been shown that AQP1 RNA levels are down-regulated in several promastigote species of *Leishmania* that are resistant to antimonials (Marquis et al., 2005). The intracellular organelle membrane protein multi-drug resistant protein A (MRPA), which is an ABC transporter, has been shown to transport metal/thiol conjugates (Legare et al., 1997). It is believed that MRPA may cause antimonial resistance by sequestration of these drug/thiol conjugates into cellular organelles ready for efflux from the cell. Furthermore, transfection of the *MRPA* gene has recently been shown to confer sodium stibogluconate resistance in *L. infantum* amastigotes (El Fadili et al., 2005).

In addition, these metal/thiol conjugates could be exported out of the cell via an, as yet, uncharacterised efflux mechanism as well as or subsequent to sequestration into cellular organelles (Dey et al., 1994).

Alternatively, both the over-expression and down-regulation of proteins involved in thiol biosynthesis have been reported to affect the sensitivity of *Leishmania* to antimonial drugs. Levels of trypanothione have been shown to be elevated in heavy metal arsenate-resistant *Leishmania* parasites (Haimeur et al., 1999). This increase in trypanothione is mediated by the over-expression of the rate limiting enzyme involved in polyamine biosynthesis - ornithine decarboxylase (ODC). Both the overexpression of γ-glutamylcysteine synthetase (GCS) and ODC would cause an increase in intracellular thiol levels. Consequently, this would increase the levels of thiols available to form conjugates with the drug and undergo extrusion from the cell or become sequestered into cellular organelles, thus aiding resistance. It has also been suggested that a decrease in thiol metabolism may induce antimonial resistance in these parasites (Ouellette et al., 2004).

More recent evidence states that the expression of ODC is significantly reduced within *Leishmania* parasites that are resistant to antimonials, compared to drug sensitive wild type parasites (Decuypere et al., 2005). In addition, this particular study shows that the expression of GCS is down-regulated in antimonal-resistant *Leishmania* compared to the drug sensitive wild-type parasite although this difference was not found to be statistically significant (Decuypere et al., 2005). This down-regulation of thiol-biosynthetic enzymes would result in an overall decrease in thiols within the cell, which could consequently inhibit both enzymatic and non-enzymatic drug activation. Since an increase in total thiols is observed in antimonial resistant *Leishmania*, it is generally considered that lower trypanothione levels may reduce the incidence of resistance.

This has been supported by the reversal of resistance using buthionine sulfoxamine and difluoromethylornithine (two glutathione and spermidine biosynthesis inhibitors) in combination with metals (Arana et al., 1998, Haimeur et al., 1999, Legare et al., 2001).

The over-expression of heat-shock proteins (HSP) by transfection of an Hsp70 gene increases the tolerance of the cells to metals (Ashutosh, 2007). However, it is not known how Hsp70 confers resistance and whether this mechanism operates in antimonial resistant field isolates.

1.5.2 Pentamidine

The aromatic diamidine pentamidine is now considered one of the first-line drugs used in the treatment of both cutaneous and visceral leishmaniasis. The efficacy of pentamidine is currently decreasing in India, which suggests the emergence of resistant parasites (Sundar et al., 2001). Significant toxicity is associated with the administration of the drug (including hypotension, hypoglycemia, diabetes and nephrotoxicity) and consequently use of the drug is decreasing (Ouellette et al., 2004).

The mode of action of pentamidine, as well as mechanisms of resistance, are not well understood at present, but pentamidine is known to compete with polyamines for nucleic acid binding and may also preferentially bind to kinetoplast DNA, interfering with replication and transportation at the

mitochondrial level (Sands et al., 1985). Studies have also shown that pentamidine is a competitive inhibitor of arginine transport in *L. donovani* (Kandpal et al., 1996) and a non-competitive inhibitor of putrescine and spermidine transport in *L. infantum* (Reguera et al., 1994). More recent studies suggest that pentamidine greatly enhances the efficacy of mitochondrial respiratory chain complex II inhibitors, creating a 4-fold increase in intracellular Ca^{2+} ultimately leading to apoptosis (Mehta & Shaha, 2004).

In kinetoplastids, it was recently found that the mitochondrion is an important target of pentamidine and in some resistant lines is associated with a decrease in drug accumulation in this organelle (Basselin et al., 2002). A decreased mitochondrial membrane potential could be responsible for this pentamidine resistance. Furthermore, the cytosolic fraction of the drug is extruded outside the cell in resistant lines which is possibly mediated by the ABC transporter PRP1 (Coelho et al., 2003).

1.5.3 Amphotericin B

The polyene antibiotic, amphotericin B, is a valuable antifungal agent used in the treatment of systemic fungal infections. The drug is highly effective against visceral leishmaniasis caused by antimonial-resistant *L. donovani* and against some cases of cutaneous leishmaniasis that have not responded well to the first line treatment of the antimonials (Thakur et al., 1999). In areas where resistance to the pentavalent antimonials is endemic, amphotericin B is the drug of choice. The drug must be administered parenterally by slow infusion over a period of four hours. This coupled with its high toxicity and association with severe side effects including fever and chills, nephrotoxicity and first-dose anaphylaxis, make treatment rather unpleasant for the patient. Despite this, amphotericin B has replaced antimonials as the first-line treatment of VL in Bihar, India (Chappuis, et al., 2007). Lipid formulations of the drug, e.g. AmBisome®, although much more expensive, have greatly reduced toxicity and have proved effective against VL and mucocutaneous leishmaniasis (Meyerhoff et al., 1999). The high cost of these have prevented their use in endemic areas until recently, when the WHO announced a reduction in cost from around $ 2 800 to $ 200 per treatment in VL endemic countries (Chappuis et al., 2007).

The antifungal effect of the Amphotericin B results from an interaction with sterols in the fungal membrane. The drug forms complexes with 24-substituted sterols, e.g. ergosterol in the cell membrane of the parasite, creating pores and ultimately causing an ion imbalance and cell death (Roberts et al., 2003). The similarity between the major sterols of fungi and *Leishmania* (ergostane-based sterols) explains the high efficacy of this drug against leishmaniasis.

Although resistance to amphotericin B does not develop quickly, it has been induced *in vitro* and found to be associated with a detrimentally altered membrane fluidity which affects the binding affinity of amphotericin B to the modified cell membrane. Additionally, the major sterol of the cell membrane was found to be an ergosterol precursor in the resistant strains, rather than ergosterol itself as was the case with the amphotericin B-sensitive parent (Mbongo et al., 1998).

1.5.4 Miltefosine

Originally developed as an antitumour agent, miltefosine is an alkylphosphocholine and a membrane-active synthetic ether-lipid analogue. It is an oral drug and in 2002 was registered in India as a therapy against visceral leishmaniasis (Davies et al., 2003). Miltefosine is well absorbed and widely distributed after administration. The mechanism of action of the drug involves the interference with cellular membranes without interacting with DNA. More specifically, miltefosine modulates membrane permeability and fluidity, membrane lipid composition, metabolism of phospholipids and proliferation signal transduction (Palumbo, 2008). Miltefosine has been shown to be safe for treatment of both children and adults, and is approximately 90 % effective against visceral leishmaniasis (Palumbo, 2008).

Clinically-resistant *Leishmania* parasites have not yet been reported, however, this is not surprising as the drug was only registered for use fairly recently. However, the drug has a narrow therapeutic index and long half-life (Sundar, 2001) which are both factors thought to favour the emergence of resistance. Resistance to miltefosine can be easily induced in vitro and the subsequent characterisation of these mutant strains has shown that reduced drug uptake, increased drug efflux, changes in plasma membrane permeability and increased

drug metabolism are all possible mechanisms by which resistance to the drug occurs in *Leishmania*. Recently, miltefosine resistant *Leishmania* cells were shown to over-express the P-glycoprotein gene, *MDR1*, which is an ABC transporter involved in the multidrug resistance of cancer cells (Perez-Victoria, 2001). It has been hypothesised that since MDR1 is associated with a number of endocytic and secretory compartments, it transports substrate into these secretory compartments ready for export from the cell (Dodge et al., 2004).

1.5.5 Paromomycin

Paromomycin is currently in phase IV clinical trials against leishmaniasis (Jhingran et al., 2009). It is an aminoglycoside antibiotic which acts primarily by impairing the macromolecular synthesis and altering the membrane properties of *Leishmania* (Mishra et al., 2007). The effectiveness of paromomycin was determined to be the same as amphotericin B when subjected to trial (Sundar et al., 2007). A dose of 16 mg/kg intramuscularly for a period of 21 days has been shown to cure 93 % of patients (Jha et al., 1998).

A major advantage of paromomycin is its low cost, however some minor drawbacks exist, including the requirement for administration by intramuscular injection, the drug can cause reversible damage to the inner ear in 2 % of patients and may produce mild pain at the site of injection (Chappuis et al., 2007).

1.6 Cysteine Acquisition

1.6.1 Functions of cysteine

Cysteine is one of the main sulfur-containing amino acids and acts as the central precursor of all organic molecules containing reduced sulfur. It plays a vital role in the stabilization of tertiary and quaternary protein conformation due to its ability to form inter- and intra-chain disulfide bonds with other cysteine residues (Brosnan & Brosnan, 2006). Due to the reactive sulfhydryl (CH_2**SH**) functional group, cysteine is the principal amino acid precursor for low molecular weight thiols, e.g. glutathione and trypanothione, as well as redox active thiol-

containing proteins. The catalytic activities of free thiols as well as thiol containing proteins, which are involved in the detoxification of metals, nucleophilic drugs and reactive oxygen, depends upon the sulfur atoms of thiol groups (Gilbert, 1990). The conversion of free thiol groups to disulfide bridges and *vice versa* produces a reactive system that forms the basis for redox switches in protein. These switches play an essential role in the modulation of essential metabolic function and regulation of metabolism (Paget & Buttner, 2003). Cysteine is also involved in the synthesis of essential bio-molecules like antioxidants, vitamins and cofactors, e.g. thiamine, lipoic acid, biotin and coenzyme A (Wirtz & Droux, 2005). The catalytic mechanism of these molecules is based upon the reactivity of the thiol group.

1.6.2 Cysteine biosynthesis pathways

Organisms can aquire cysteine either by taking it up from the environment or through biosynthesis, which has been reported to occur via two pathways. The sulfhydrylation pathway, which involves the enzymes serine acetyltransferase (SAT) and O-acetylserine (thiol) lyase (OAS-TL) (Morzycka et al., 1979) and the reverse trans-sulfuration pathway which involves the enzymes cystathionine ß-synthase (CBS) and cystathionine γ-lyase (CGL) (Morzycka et al., 1979) (Figure 1.8). However, both of these biosynthesis pathways do not operate in all organisms and therefore cysteine synthesis often depends upon one of these pathways only.

1.6.2.1 Mammals

Animals and humans lack the ability to reduce inorganic sulfur and as a result humans and most animals rely partly on diet for the acquisition of cysteine (Zhao et al., 2000). In mammals, cysteine is synthesised via the reverse trans-sulfuration pathway from methionine. Methionine is converted to homocysteine by the action of methionine adenosyltransferase, various S-adenosylmethionine methyltransferases and adenosylhomocysteinase (Griffith, 1987). Cystathionine ß-synthase (CBS) catalyses the condensation of homocysteine and serine to form cystathionine, which is ultimately converted to cysteine by cystathionine γ-lyase (Mino & Ishikawa, 2003). The absence of the sulfhydrylation pathway in mammals makes it a potential candidate for investigation as a drug target in

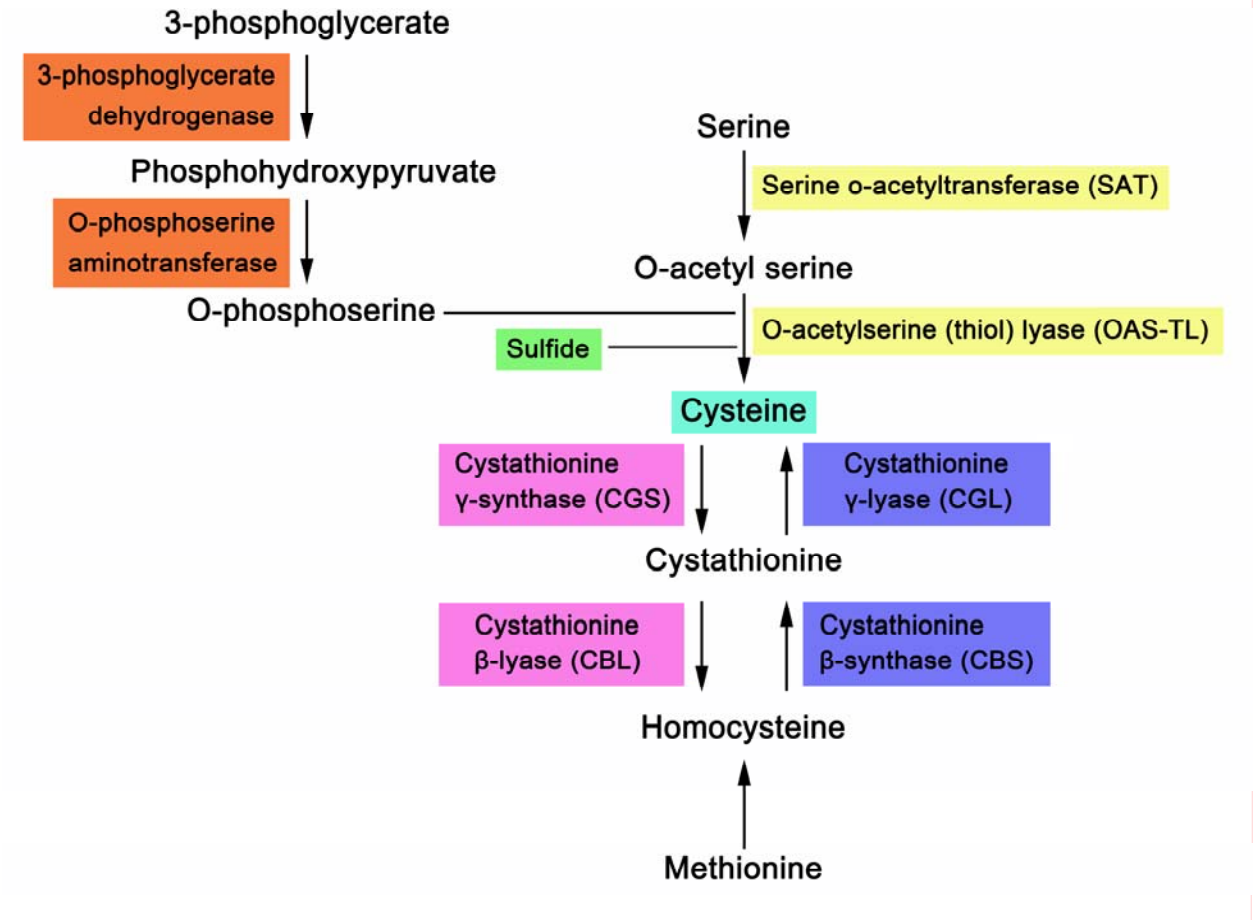

Figure 1.8 Cysteine synthesis pathways of parasitic protozoa.
Schematic representation of the enzymes involved in the biosynthesis of cysteine. The sulfhydrylation pathway is shown in yellow, the trans-sulfuration pathway is shown in pink, the reverse trans-sulfuration pathway is shown in blue and the O-phosphoserine pathway of *T. vaginalis* is shown in orange.

organisms that possess and utilise this pathway and cause human or animal diseases.

1.6.2.2 Plants

Cysteine synthesis in plants occurs via the sulfhydrylation pathway (Figure 1.8), by two sequential reactions catalysed by SAT and OAS-TL. The conversion of serine to O-acetylserine by SAT occurs in plastids, mitochondria and cytosol of plants. In *Arabidopsis thaliana*, five SATs exist. SAT1 and SAT3 are plastid and mitochondria located, respectively (Kawashima et al., 2005). SAT2, SAT4 and SAT5 are cytosolic, but the amino acid sequences of these substantially differ from the other SATs (Kawashima et al., 2005). The second step of cysteine biosynthesis in this pathway involves the conversion of O-acetylserine to cysteine and is catalysed by OAS-TL. In *Arabidopsis*, three genes exist that encode cytosolic OAS-TL, plastid OAS-TL and mitochondrial OAS-TL (Jost et al., 2005). A further four *OAS-TL* genes exist in *Arabidopsis*, but these are weakly expressed and show either little or no cysteine synthase activity (Wirtz and Hell, 2006; Heeg et al., 2008). 40-45 % of *Spinacia oleracea, Brassica oleracea* and *Datura innoxia* OAS-TL activity is localised to the plastids and cytosol, whereas approximately 5 % is attributed to mitochondria (Lunn et al., 1990; Rolland et al., 1992; Kuske et al., 1996).

1.6.2.3 Bacteria

The biosynthesis of cysteine in bacteria occurs, in most cases, via the sulfhydrylation pathway (Figure 1.8). In this pathway SAT catalyses the acetylation of the ß-hydroxyl of serine giving O-acetylserine. This is followed by the ß elimination of acetate from O-acetylserine and the addition of sulfide to produce cysteine. This process has been described in *Escherichia coli* and *Salmonella typhimurium* (Kredich & Tomkins, 1966). In most bacteria the step catalysing the formation of cysteine from O-acetylserine is catalysed by two isoforms of OAS-TL, OAS-TL A and OAS-TL B

(Kredich et al., 1979), which are produced under aerobic and anaerobic conditions respectively (Mino & Ishikawa, 2003).

The filamentous bacteria *Streptomyces phaeochromogenes* has been shown to possess a reverse trans-sulfuration pathway similar to yeast and moulds (Nagasawa et al., 1984). Therefore the actinomycetaceae may utilise this pathway for cysteine biosynthesis.

1.6.2.4 Fungi

The biosynthesis of cysteine in fungi takes place through the sulfhydrylation pathway and the reverse trans-sulfuration pathways. Some species, e.g. *Saccharomyces lipolytica*, use both cysteine synthesis pathways (Morzycka et al., 1979). *Neurospora crassa* and *Aspergillus nidulans* possess both cysteine biosynthesis pathways, but only the sulfhydrylation pathway is active (Paszewski et al., 1974). The reverse trans-sulfuration pathway has been shown to be activated when the sulfhydrylation pathway was impaired (Paszewski et al., 1984).

However in the yeasts *Saccharomyces pombe, Pichia membranofaciens and Candida valida*, the enzymes involved in the reverse trans-sulfuration pathway, cystathionine ß-synthase (CBS) and cystathionine γ-lyase (CGL) are absent. This suggests that these organisms only synthesise cysteine via the sulfhydrylation pathway (Brzywczy et al., 1993, 2002; Piotrowska et al., 1990; Piotrowska, 1993).

1.6.2.5 Parasitic organisms

The methods by which parasitic organisms synthesise cysteine have not been extensively studied, however, some information does exist. The sulfhydrylation pathway exists in *Trichomonas vaginalis* (Goodall, 2001; Westrop et al., 2006), as well as the amoebae *Entamoeba histolytica* and *Entamoeba dispar* (Nozaki et al., 1998), in which the trans-sulfuration pathway does not exist. *Panagrellus redvivus*, a parasitic nematode, and the

fluke *Fasciola hepatica* have been shown to have a functional reverse trans-sulfuration pathway (Papadopoulos et al., 1996; Bankov et al., 1996). Like fungi, the trypanosomatids *Trypanosoma cruzi* and *Leishmania spp*. possess both the sulfhydrylation and reverse trans-sulfuration pathways (Nozaki et al., 2001; Williams et al., 2009). Some differences exist between *T. cruzi* and *T. brucei*, in the metabolism of the sulfur-containing amino acids. The enzymes involved in the trans-sulfuration pathway have been detected in bloodstream trypomastigotes of *T. brucei*, compared to a down regulation of CBS activity observed in *T. cruzi* mammalian forms (Yarlett & Bacchi, 1988; Goldberg et al., 2000).

It is possible that trypanosomatid parasites are able to take up cysteine from the environment, although this has not been extensively studied. A total of 30 possible amino acid transporters have been identified in *Leishmania major*, of which only 3 have been characterised (Genedb LmjF31.1790, LmjF31.1820 and LmjF31.1800) (Mazareb et al., 2001).

1.6.3 Enzymes involved in cysteine biosynthesis

1.6.3.1 Serine acetyltransferase

Serine acetyltransferase (SAT) catalyses the acetyl CoA-dependent acetylation of the side chain hydroxyl group of serine, resulting in the formation of O-acetylserine. This is the first step in cysteine synthesis via the sulfhydrylation pathway. The molecular mass of the monomeric unit of SAT ranges from 30-35 kDa. The X-ray crystallographic structure of SAT from the gram negative bacterium *Haemophilus influenza* has been determined showing a hexameric structure arranged as a dimer of trimers (Olsen et al., 2004).

SAT is the rate-limiting enzyme involved in cysteine biosynthesis via the sulfhydrylation pathway (Harms et al., 2000), and the enzyme exists with an excess of OAS-TL. The association of OAS-TL and SAT in complex plays a regulatory role in both sulfur assimilation and cysteine biosynthesis. SAT

requires binding to OAS-TL for full activity (Wirtz & Hell, 2006). SATs from bacteria, plants and protozoa are feedback inhibited by cysteine (Kredich et al., 1966; Nozaki et al., 2001), and the binding site is located at the C-terminal end of the protein. SATs bound to cysteine are still able to form complexes with OAS-TL, suggesting that the two events are independent (Mino et al., 1999).

Kinetic analyses of purified SATs have yielded K_m values ranging from 0.1 mM to 5.1 mM for serine, and 0.1 mM to 0.56 mM for acetyl CoA. The pH optimum for the enzyme has also been shown to range from 7.5 – 8.5 (Kredich et al., 1966; Smith et al., 1971; Burnell et al., 1977).

1.6.3.2 O-acetyl serine (thiol) lyase

O-acetylserine (thiol) lyase (OAS-TL) is a pyridoxal-5'-phosphate dependent enzyme, which catalyses the second step of cysteine biosynthesis via the sulfhydrylation pathway. The formation of cysteine via sulfhydrylation is a two-step reaction mechanism involving: i) the reversible interaction of O-acetylserine and pyridoxal phosphate, which results in the ß-elimination of acetate to form α-aminoacrylate (Cook & Wedding, 1976) and ii) the reaction of α-aminoacrylate with sulfide to form cysteine (Cook & Wedding, 1976). The first of these steps is the overall rate limiting step in the formation of cysteine from O-acetylserine and sulfide (Woehl et al., 1996). Multiple isoforms of OAS-TL exist in most organisms that use the sulfhydrylation pathway, however *T. cruzi* and *T. vaginalis* appear to only possess one isoform of the enzyme. OAS-TL usually exists as a homodimer, with monomeric units ranging from 30 – 35 kDa, but higher oligomeric forms have been identified in *T. cruzi*, where the enzyme exists as a dimer, trimer and oligotetramer (Nozaki et al., 2001). Kinetic analyses of purified OAS-TLs have yielded K_m values ranging from 0.02 mM to 2.7 mM for sulphide and 1.25 mM to 50 mM for O-acetylserine.

In enteric bacteria, two isoforms of OAS-TL have been identified, type A and type B OAS-TLs. Type A OAS-TL is a homodimeric protein with a molecular

weight of approximately 68.9 kDa (Mino & Ishikawa, 2003). The dimer is arranged such that entry to the two active sites occurs on the same side (Mino & Ishikawa, 2003). Type A OAS-TL occurs as a bifunctional protein complex together with SAT, and is governed by the *cysK* gene (Nakamura et al., 1983). Type B OAS-TL is also a homodimeric protein, with a molecular weight of approximately 64.0 kDa (Mino & Ishikawa, 2003). Type B OAS-TL is encoded by the *cysM* gene and has been reported to exist as a monomeric protein (Hulanicka et al., 1974). Type B OAS-TL of *Salmonella typhimurium* is preferentially used for the biosynthesis of cysteine under anaerobic growth conditions within host epithelial cells, and is capable of utilizing thiosulfate instead of sulfide, to produce S-sulfocysteine (Nakamura et al., 1984).

Cysteine synthesis in plants is performed by a protein system of compartment-specific isoforms. In most plants, cysteine synthesis occurs in most cells in the plastids, cytosol and mitochondria (Wirtz & Hell, 2007). It has been suggested that these subvolumes of cellular space facilitate the thermodynamic or kinetic character of the metabolic process to differ from that of the bulk cellular space. Enhanced specificity and reaction velocity can therefore be achieved as a result of reduced interference with other cellular reactions (Srere, 1987; Ovadi, 1991; Winkel, 2004). Plant OAS-TL monomer size ranges between 68 and 75 kDa (Wirtz & Hell, 2006).

Leishmania OAS-TL monomeric units range in size between 34.3 and 35.4 kDa. OAS-TL of *L. major* is similar to type A OAS-TL of bacteria and has been shown to have K_m values of 17.5 and 0.13 mM for the substrates O-acetylserine and sulfide respectively (Williams et al., 2009). The enzyme has the ability to utilise sulfide produced by the action of mercaptopyruvate sulfurtransferase. When grown in medium with limited availability of sulfur-containing amino acids, OAS-TL is upregulated (Williams et al., 2009). The parasite *Trichomonas vaginalis* has multiple type B *OAS-TL* genes but lacks the *SAT* gene. Instead the organism has a functional 3-phosphoglycerate dehydrogenase and an O-phosphoserine aminotransferase, which together

produce O-phosphoserine, used by *T. vaginalis* instead of serine as the precursor for cysteine synthesis (Westrop et al., 2006).

1.6.3.3 The SAT/OAS-TL multi-enzyme complex

The biosynthesis of cysteine by the sufhydrylation pathway involves, in plants, the bienzyme SAT/OAS-TL complex, which is comprised of two OAS-TL dimers and one SAT hexamer (Feldman-Salit et al., 2009). In plants, the nature of the SAT enzyme varies depending on the cellular compartmentalisation and sensitivity to cysteine inhibition. Cytosolic SAT from *Citrullus vulgaris* and *Arabidopsis thaliana* are highly sensitive to feedback inhibition by cysteine at the physiological concentration (3 μM) (Saito et al., 1995; Noji et al., 1998; Howarth et al., 1997). On the other hand, the plastid SAT and mitochondrial SAT isoforms of *A. thaliana* have been shown to be insensitive to cysteine inhibition (Noji et al., 1998).

Similarly, *Leishmania major* OAS-TL forms a bi-enzyme complex not only with *L. major* SAT, but also with *Arabidopsis* SAT (Williams et al., 2009). Residues K222, H226 and K227 of *L. major* OAS-TL are involved in the formation of the complex (Williams et al., 2009). These residues exist in bacterial type A OAS-TL, which forms complexes with SATs, whereas bacterial type B OAS-TL lacks them and does not form SAT/OAS-TL complexes (Liszewska et al., 2007). OAS-TL of *Mycobacterium tuberculosis* also forms a bi-enzyme complex with SAT (Schnell et al., 2007).

The main form of kinetic regulation of cysteine synthesis via sulfhydrylation occurs by feedback inhibition of SAT by the end product, cysteine. Cysteine competes with serine to bind to the active site of SAT resulting in a conformational change of the C-terminal segment of the enzyme stopping the binding of the cofactor, CoA (Olsen et al., 2004; Pye et al., 2004). This activity has been confirmed by kinetic studies on SAT from *E. coli* using serine analogs, as well as studies showing reduced enzyme activity in cysteine-desensitised mutants (Nakamori et al., 1998). The regulation of cysteine biosynthesis in mycobacteria via sulfhydrylation is similar to plants.

A domain rotation occurs at the same time as the formation of the bienzyme complex which results in the closure of the active site of OAS-TL (Schnell et al., 2007).

The formation of the bi-enzyme complex is not affected by the binding of cysteine to the SAT active site, indicating that these processes are independent of one another (Mino et al., 1999). The dissociation of the bi-enzyme complex with 1 mM O-acetylserine restores OAS-TL activity (Mino et al., 1999).

1.6.3.4 Cystathionine β-synthase

Cystathionine ß-synthase (CBS) is the first and rate-limiting step in the reverse trans-sulfuration pathway, catalysing the formation of cystathionine from serine and homocysteine. The enzyme exists as heterotetramers with subunit sizes of 55 – 63 kDa.

Mammalian CBSs are heme-dependent enzymes and therefore consist of a heme domain, a catalytic core with a pyridoxal-5'-phosphate motif and a regulatory domain composed of two CBS domains (Bateman, 1997). Heme is incorporated into mammalian CBSs during folding and is essential for enzyme activity as it is a prerequisite for pyridoxal-5'-phosphate binding (Kery et al., 1994), as well as activating or binding homocysteine and regulation of the redox potential within the cell (Taoka et al., 1998; Taoka et al., 1999). The C-terminal CBS domain is the site of S-adenosylmethionine binding (Taoka et al., 1999), which is an allosteric activator of mammalian CBSs. Binding of S-adenosylmethionine decreases the K_m for homocysteine eight-fold (Roper et al., 1992).

CBSs from yeasts and trypanosomatids are heme-independent and lack the heme motif (Jhee et al., 2000; MacLean et al., 2000; Nozaki et al., 2001). The method by which the CBSs of these organisms bind homocysteine is therefore different to the mammalian CBSs, but the precise mechanism is as yet unknown. Increased levels of CBS have been shown to result in an

increase in cysteine and glutathione levels in humans, which have subsequently caused an increase in resistance against oxidative stress (Taoka et al., 1998).

1.6.3.5 Cystathionine γ-lyase

Cystathionine γ-lyase (CGL), a 140 kDa homo-tetrameric protein, also functions in the trans-sulfuration pathway that converts homocysteine to cysteine (Smacchi & Gobbetti, 1998). CGL is a pyridoxal-5'-phosphate dependent enzyme that catalyses the α, γ-elimination reaction of cystathionine to produce cysteine, α-ketobutyrate and ammonia (Bruinenberg et al., 1996). The activity of CGL is regulated by feedback inhibition of the product cysteine (Cherest et al., 1993; Kanzaki et al., 1987).

CGL is widely distributed in filamentous bacteria of the genera *Streptomyces, Micromonospora, Micropolyspora, Mycobacterium, Nicardia, Streptosporangium* and *Streptoverticillium* (Nagasawa et al., 1984). In these organisms the reverse trans-sulfuration pathway is similar to yeasts and moulds (Nagasawa et al., 1984). CGL is also present in *Lactobacillus reuteri* where its principal role is in cysteine-mediated oxidative defence by producing reducing equivalents (Lo et al., 2009). CGL exists in yeasts, such as *Saccharomyces cerevisiae* where its expression is induced by sulfur starvation and repressed by the addition of cysteine to the growth medium (Hiraishi et al., 2008).

In mammals, several mutations in CGL have been described in cases of cystathioninuria, a poorly understood rare genetic disease (Zhu et al., 2008). In addition, a single nucleotide polymorphism converting serine at position 403 to isoleucine is linked to an increase in plasma homocysteine levels (Zhu et al., 2008).

1.6.3.6 Cysteine biosynthesis enzymes as potential drug targets

The enzymes involved in cysteine biosynthesis have been suggested as potential drug targets for the development of novel chemotherapeutics against leishmaniasis. The development of inhibitors of OAS-TL has not been extensively studied, however some studies have been carried out in plants. The pyridoxal-5'-phosphate-dependent enzyme inhibitors amino-oxyacetate and hydroxylamine have been found to successfully inhibit *Echinochloa crus-galii* OAS-TL by 96 and 98 % respectively (Hirase & Molin, 2001).

Cysteine is vital to all organisms because it is the main sulfur containing amino acid, and a range of cellular pathways depend upon its availability. Since mammals synthesize cysteine via the reverse trans-sulfuration pathway, OAS-TL is not present in these organisms and it has therefore been suggested as a possible drug target against a number of human pathogens, including *Trichomonas vaginalis* (Westrop et al., 2006) and other parasitic protozoa (Nozaki et al., 2005). The removal of cytosolic and plastid OAS-TL in *Arabidopsis thaliana,* causing it to rely on mitochondrial OAS-TL for cysteine biosynthesis, showed a 25 % growth retardation (Heeg et al., 2008), highlighting the validity of OAS-TL as a target for herbicides. Other enzymes involved in cysteine biosynthesis have also been suggested as worthwhile investigating as potential drug targets. SAT, which is also involved in the sulfhydrylation pathway, has been identified as a potential drug target in *Entamoeba hystolytica* (Agarwal et al., 2008). In addition, *Leishmania* CBS has been shown to be significantly different to CBS of mammals and as a result has been suggested as a possible drug target against the organism (Williams et al., 2009).

1.7 Aims of this study

The overall aims of this study were divided into two main sections:

1.7.1 Thiol dependent reductase 1

i) To evaluate the potential of TDR1 as an anti-leishmanial drug target, by:

   a. Generating *TDR1* null mutants in the Nepalese field isolate *L. donovani* BPK 206 clone 10.

   b. Using available *L. major* and *L. infantum TDR1* null mutants to elucidate the role of the enzyme in *Leishmania* and highlight any potential alteration in sensitivity to antimonial drugs caused by the genetic manipulation.

ii) To investigate the role of TDR1, by:

   a. Producing recombinant TDR1 and trypanothione reductase from *L. donovani*.

1.7.2 O-acetylserine (thiol) lyase

i) To evaluate the potential of OAS-TL as an anti-leishmanial drug target, by:

   a. Generating *OAS-TL* null mutants in the Nepalese field isolate *L. donovani* BPK 206 clone 10.

   b. Evaluating the potential use of OAS-TL as an anti-leishmanial drug target by characterisation of the null mutant parasites.

2. Materials and Methods

2.1 Buffers, solutions, media and antibiotics

2.1.1 General buffers

1x PBS	140 mM NaCl, 3 mM KCl, 10 mM Na_2HPO_4, 1.8 mM KH_2PO_4, pH 7.4
1x TAE	40 mM Tris-Acetate, 1 mM EDTA, pH 8.0
TE	10 mM Tris/HCl pH 8.0, 1 mM EDTA, pH 8.0

2.1.2 DNA analysis

DNA loading dye	0.25 % (w/v) bromophenol blue, 0.25 % (w/v) orange-G, 40 % (w/v) sucrose
Buffer A	100 mM Tris/HCl, 300 mM NaCl, pH 9.5
1x SSC	15 mM Tri-sodium citrate, 150 mM NaCl, pH 7-8
Primary wash buffer	2 M urea, 0.1 % (w/v) SDS, 50 mM sodium Phosphate pH 7.0, 150 mM NaCl, 1 mM $MgCl_2$, 0.2 % (w/v) Blocking Reagent (GE Healthcare))
Secondary wash buffer	50 mM Tris base, 100 mM NaCl, 2 mM $MgCl_2$, pH 7.0

2.1.3 Protein analysis

6x loading buffer	62.5 mM Tris/HCl pH 6.8, 2 % (w/v) SDS, 10 % (v/v) glycerol, 0.001 % (w/v) bromophenol blue, 5 % (v/v) 2-mercaptoethanol
1x running buffer	25 mM Tris, 192 mM glycine, 0.1 % (w/v) SDS

1x MOPS buffer	50 mM 3-[N-morpholino]propane sulphonic acid, 50 mM Tris, 3.5 mM SDS, 1 mM EDTA, pH 7.2
Coomassie stain	40 % (v/v) methanol, 10 % (v/v) acetic acid, 0.1 % (w/v) Coomassie brilliant blue R-250
Destain	20 % (v/v) methanol, 10 % (v/v) acetic acid
Towbin buffer	25 mM Tris, 192 mM glycine, 20 % (v/v) methanol, pH 8.3

2.1.4 Bacterial culture

Luria-Bertani medium	10 g/L tryptone, 5 g/L yeast extract, 5 g/L NaCl (15 g/L agar was added to make LB plates)
Ampicillin	100 mg/ml in distilled, deionised H_2O (ddH_2O) (1000x stock), stored at -20 °C. Used at a concentration of 100 µg/ml.
Kanamycin	50 mg/ml in ddH_2O (1000x stock), stored at -20 °C. Used at a concentration of 50 µg/ml.

2.1.5 *Leishmania* culture

Electroporation buffer	120 mM KCl, 0.15 mM $CaCl_2$, 10 mM K_2HPO_4, 25 mM HEPES, 2 mM EDTA, 2 mM $MgCl_2$, pH 7.6
Freezing solution	70 % (v/v) heat inactivated foetal calf serum (HIFCS), 30 % (v/v) glycerol
Nourseothricin	50 mg/ml in ddH_2O (1000x stock), stored at 4 °C. Used at a concentration of 75 µg/ml.

PSGEMKA buffer	108 ml of 0.02 M $Na_2HPO_4.2H_2O$, 34.5 ml of 0.02M $NaH_2PO_4.2H_2O$, 15.75 g of NaCl, 15 g of glucose, 0.285 g of EDTA, 3.04 g of $MgCl_2.6H_2O$, 1.11 g of KCl and 0.30 g of albumin (bovine) in 1.3575 l of ddH_2O), pH 7.3

2.1.6 HPLC buffers

Lysis buffer	40 mM N-[2-hydroxyethyl]-piperazine-N'[3-propanesulphonic acid] (HEPPS), 4 mM diethylenetriamine pentaacetic acid (DTPA), pH 8.0 (adjusted with lithium hydroxide)
Solvent A	0.25 % (v/v) acetic acid, 99.75 % (v/v) ddH_2O
Solvent B	100 % acetonitrile

2.1.7 Bacteria strains

DH5α (Invitrogen)

F- *φ*80*dlac*ZM15 (*lac*ZYA-*arg*F)U169 *deo*R *rec*A1 *end*A1 *hsd*R17(r k-, m k+) *pho*A *sup*E44 *thi-1 gyrA*96 *rel*A1 *λ*-

BL21(DE3) (Promega)

F^-, *omp*T, *hsd*S_B(r_B-, m_B-), *dcm*, *gal*, λ(DE3)

2.2 Antibodies and antibiotics

	Western Blot	Source
Anti-CS (rabbit)	1 : 5 000	SAPU
Anti-CBS (rabbit)	1 : 10 000	SAPU
Anti-MST (rabbit)	1 : 5 000	SAPU
Anti-TDR1 (sheep)	1 : 5 000	SAPU
Anti-Elf1α (mouse)	1 : 20 000	Upstate Cell Signaling Solutions

Table 2.1 Primary and secondary antibodies and their dilutions.

	Bacterial culture – using concentration	*Leishmania* culture – using concentration
Ampicillin	100 µg/ml	
Kanamycin	50 µg/ml	
Hygromycin		50 µg/ml
Phleomycin		20 µg/ml
Nourseothricin		75 µg/ml
G418		50 µg/ml

Table 2.2 Antibiotics used and their concentrations.

2.3 Methods

2.3.1 Bioinformatics

All DNA and protein analyses, including the construction of cloning and expression plasmids and searching for reading frames and restriction sites, were carried out using Vector NTI (v 10.0) software (Informax Inc). Sequence alignments were performed using the program T-Coffee (Notredame et al., 2000, Poirot et al., 2003).

The following web-based resources were also used: The Sanger Institute (http://www.sanger.ac.uk), NCBI (http://www.ncbi.nlm.gov) and GeneDB (http://www.genedb.org).

2.3.2 *Leishmania* species culture methods

2.3.2.1 Cell lines

Throughout this research, wild type *L. major* (MHOM/IL/80/Friedlin) and the field isolate *L. donovani* (MHOM/NP/2003/BPK 206/0) were used. All cell lines were derived from these parent lines.

The *L. donovani* BPK 206/0 was isolated from a Nepalese visceral leishmaniasis patient living in the Sunsari district. The patient was recruited at the B.P. Koirala Institute of Health Sciences on the 6th April 2003, which was also the date of isolation, for the study LeishNatDrug-R. Ethical clearance was obtained from the institutional review boards of the Nepal Health Research Council, Kathmandu, Nepal and the Institute of Tropical Medicine, Antwerp, Belgium.

The patient was a twelve year old male suffering from visceral leishmaniasis for the first time. He had been suffering from bouts of fever for approximately eight weeks before hospitalization. The bone marrow aspirate showed high parasite load (5+, on a scale of 0-6). The patient was treated with 30 doses of sodium stibogluconate at 20 mg/kg/day, and responded very well to treatment. He remained healthy during the twelve months follow-up period and was considered to be cured.

The strain BPK 206/0 was isolated from the bone marrow taken at the time of clinical recruitment and was tested several times with both generic (Albert David SAG) and branded (Pentostam) sodium stibogluconate, and the results indicated that the strain is susceptible to antimonials. (Personal communication – Dr. Saskia Decuypere.)

The clones derived from the isolate were also sensitive to antimonials. *Leishmania donovani* BPK 206 clone 10 was used in this study, and will be referred to as wild type (WT).

2.3.2.2 Cultivation and electroporation of *L. major* and *L. donovani* promastigotes

L. major, *L. infantum* and *L. donovani* promastigotes were grown at 25 ˚C in HOMEM medium (Invitrogen, Paisley, UK, ref. 041-946-99M), a modified Eagle's minimal essential medium with Spinner's salts (Berens et al., 1976), supplemented with 10 % (v/v) heat-inactivated fetal bovine serum (HIFCS) (Labtech International, Ringmer, UK), in the case of *L. major*, and 20 % (v/v) HIFCS in the case of *L. donovani*. Cultures were grown at 25 ºC (*L. major* and *L. donovani*) or 27 ºC (*L. infantum*) with air as the gas phase, in phenolic-style lidded flasks. Parasites were kept in liquid culture for a maximum of 20 sub-passages, which were performed once per week. For tranfections, cells were used at as low a passage number as possible (typically 1-4).

Transfections were carried out according to the procedure of Robinson and Beverley (2003). 10 ml of *Leishmania* were grown to late log phase (approximately 1 x 10^7 cells/ml) and harvested by centrifugation at 1000 *g* for 10 min before being washed in half the original volume of ice cold electroporation buffer (EPB) (120 mM KCl, 0.15 mM $CaCl_2$, 10 mM K_2HPO_4, 25 mM HEPES, 2 mM EDTA, 2 mM $MgCl_2$, pH 7.6). Before electroporation the cells were adjusted to a concentration of 2 x 10^8/ml in EPB (usually 1 ml). 500 µl of this suspension (1 x 10^8 cells) were transferred to a pre-chilled 4 mm electroporation cuvette (Biorad), containing 10-30 µg of the appropriate linearised/circular DNA. Cells were electroporated twice using a Genepulser II apparatus at 25 µF capacitance, 1500 V (3.75 kV/cm), with 10 s between pulses. After electroporation, cells were allowed to recover, on ice, for 10 min before being transferred to flasks

containing 10 ml of fresh HOMEM medium + 20 % (v/v) HIFCS, to aid recovery. Flasks of transfected parasites were then incubated overnight at 25 ˚C in HOMEM medium with 20 % (v/v) HIFBS without drug selection. Cells were seeded, at a concentration of 1 parasite per ml in HOMEM with 20% (v/v) HIFBS and the appropriate antibiotic and transferred into 96 well culture plates, 100 µl per well. Cells were grown to a high density (approximately 3 x 10^8 cells/ml), then later transferred to a 1 ml culture, and subsequently to a 10 ml culture, all grown at 25 ˚C. To maintain all cell lines, early stationary phase cells (approximately 2 x 10^7 cells/ml) were inoculated into HOMEM medium containing the correct percentage HIFBS and appropriate antibiotics (Table 1.2), at approximately 1 x 10^6 cells/ml. Cell numbers were determined by counting using an improved Neubauer haemocytometer.

2.3.2.3 Clone selection

After 24 h at 25 ˚C, antibiotics were added directly to flasks of transfected cells, generating a population of tranfectants. This was sufficient for transfections with extra-chromosomal vectors and controls. Transfectants of integrative vectors required selection of single cells to produce clonal cell lines. Transfected parasites were diluted to 1 parasite per ml and added to 96 well microplates (100 µl per well). Plates were incubated at 25 ˚C for 1-2 weeks. Theoretically, 9 wells out of the 96 should yield parasites which were assumed to arise from a single transfection event and analysed further.

Alternatively, serial dilutions of transfected parasite populations were performed in 96 well microplates and incubated at 25 ˚C for 1 – 2 weeks. Parasites in the most dilute wells were assumed to arise from a single transfection event and analysed further.

2.3.2.4 Growth curves

Parasites were seeded at a start concentration of 2.5 x 10^5 cells/ml in HOMEM with 10-20 % (v/v) HIFCS, supplemented with the appropriate antibiotic (Table 1.2). Cultures were incubated at 25 ˚C and counted every 24 h for a period of seven days. Growth curves were constructed using Grafit 5.0 (Erathicus).

2.3.2.5 Preparation of stabilates for long-term storage of cell lines

0.5 ml of log phase cultures were diluted with an equal volume of HIFCS containing 30% (v/v) glycerol in Cryotube™ vials (Nunc), mixed and left on ice for 5 min. The vials were stored at -70 °C overnight and then transferred to liquid nitrogen storage until required.

When required, stabilates were removed from liquid nitrogen, thawed at room temperature and immediately transferred into 10 ml of HOMEM supplemented with 10 % (v/v) HIFCS (for *L. major*) or 20 % (v/v) HIFCS (for *L. donovani*) and the appropriate drug selection if necessary.

2.3.2.6 Passage of *L. donovani* from Golden Hamster spleen

Golden hamsters were culled after approximately five months post-infection with *L. donovani* or when they began to show clinical signs of disease. The skin of the hamster and all equipment were sterilised with 70% (v/v) ethanol (ETOH). The spleen was removed and weighed, cut into small pieces and ground in sterile phosphate buffered saline (PBS) using a masticating tube. The volume of the cell suspension was made up to 5 ml with sterile PBS and then centrifuged at 2766 *g* for 10 min. The pellet was washed once more and resuspended to a final concentration of 1 x 10^9 amastigotes/ml. 100 µl of cell suspension was then injected, intra-peritoneally, into a new animal.

2.3.2.7 Rapid passage of *Leishmania* parasites *in vivo*.

Leishmania parasites were grown to late stationary phase, harvested by centrifugation (1000 *g* for 10 min, at room temperature) and washed twice in sterile PBS. Parasites were then resuspended in sterile PBS at a final concentration of 2 x 10^8 cells/ml. Passage into BALB/c mice was performed via sub-cutaneous injection into the footpad, using a 1 ml plastic syringe with a 26 G needle. 40 µl of cell suspension was injected into each mouse (8 x 10^6 parasites). Popliteal lymph-nodes were harvested from the mice after either 4 weeks or 8 weeks post-infection and placed in flasks containing 10 ml of HOMEM medium with 20 % (v/v) HIFCS, 1 % (v/v) penicillin/streptomycin. Flasks were incubated at 25 °C and monitored for outgrowth of promastigote parasites.

To quantify the approximate number of viable parasites in the lymph node, each lymph node was pushed through a 70 µm cell strainer (Scientific Laboratory Supplies), into a known volume of HOMEM medium with 20 % (v/v) HIFCS, 1 % (v/v) penicillin/streptomycin. Each cell suspension was then plated out into 96 well tissue culture plates, and incubated at 25 ˚C. The most dilute well containing parasites was assumed to have originally contained one viable parasite and the number of parasites within each popliteal lymph node was calculated from this.

2.3.2.8 Purification of *L. major* from mouse skin lesion

Cutaneous lesions of *L. major* were removed from infected Balb/c mice. The lesions were cut into small pieces and ground in a tissue grinder in PSGEMKA buffer (108 ml of 0.02 M $Na_2HPO_4.2H_2O$, 34.5 ml of 0.02M $NaH_2PO_4.2H_2O$, 15.75 g of NaCl, 15 g of glucose, 0.285g of EDTA, 3.04 g of $MgCl_2.6H_2O$, 1.11 g of KCl and 0.30 g of albumin (bovine) in 1.3575 l of ddH_2O). The cell suspension was then made up to 400 ml with PSGEMKA buffer. 100 µl of the suspension was removed to estimate the number of amastigotes using a haemocytometer. 50 mg of saponin dissolved in 1 ml PSGEMKA buffer was added to the cell suspension, mixed and incubated at room temperature for 3-4 min to lyse any red blood cells present. The suspension was subsequently centrifuged for 10 min at 2766 *g*, and the pellets were resuspended in a total volume of 200 ml PSGEMKA. The amastigote preparation was washed a further three times and resuspended in a final volume of 100 ml.

To prepare the column, 2.5 g of sephadex was weighed out and swelled in 100 ml of PSGEMKA buffer at room temperature overnight, and added to a glass column connected to a short tube with a screw clamp stopcock, containing plastic mesh (to retain the chromatography medium) and a small quantity of glass wool. The column was mounted vertically on a clamp stand and washed with 50 ml of PSGEMKA buffer at a flow rate of approximately 1 drip/sec. The cell suspension was then passed through this Sephadex CM-25 cation exchange column, allowing the elution of amastigotes. 100 µl of amastigote suspension was removed to estimate the number of amastigotes. The final amastigote suspension was centrifuged as before and washed three times in PSGEMKA

buffer. The pellets were given a final wash in 0.25 M sucrose, centrifuged once more and pellets were stored at -70 ˚C.

2.3.2.9 Preparation of parasite protein extract

Stationary phase parasites (2-3 x 10^7 cells/ml) were harvested by centrifugation at 1500 *g* for 10 min at 4 ˚C followed by two washes in sterile PBS. Parasite lysates were produced by resuspension of parasite pellets in 100 µl of lysis buffer (0.25 M sucrose, 0.25% Triton X-100, 10 mM EDTA and the following protease inhibitors: 10 µM E-64, 2 mM 1,10-phenanthroline, 4 µM pepstatin A and 1 mM phenylmethylsulfonyl fluoride). The resulting suspension was incubated on ice for 10 min and insoluble and soluble protein fractions were separated by centrifugation at 13000 *g* for 30 min at 4 ˚C. The resulting supernatant (soluble fraction) was retained for western blot analysis.

2.3.3 Molecular Biology Methods

2.3.3.1 Oligonucleotide primer design

DNA oligonucleotides were synthesised by Eurogentec. Primers were designed complementary to the N- and C- termini of the DNA fragment or gene to be amplified. The oligonucleotides used in this study are listed below. The restriction sites used for cloning are given in bold type.

Recombinant protein expression

L. donovani trypanothione reductase

1 5’ GT**G CGG CCG C**TC AGA GGT TGC TGC TGA G 3’ (*Not*I)

2 5’ GC**C ATA TG**T CCC GCG CGT ACG ACC TCG TGG 3’ (*Nde*I)

L. donovani thiol dependent reductase 1 (TDR1)

1 5’ AT**G CGG CCG C**TT ACC CGC TCT GGG CCC TCC GTT GAC 3’ (*Not*I)

2 5’ GA**C ATA TG**G CCG CCC GCG CGC TAA AGC TAT ACG TG 3’ (*Nde*I)

Gene manipulation studies in *L. donovani*

***O-acetylserine thiol lyase* (*OAS-TL*) null mutant**

3’ flank

1 5’ **CCC GGG** TAG TCG ATG CCT CGG AGC TGC AGG 3’ (*Sma*I)

2 5’ **AGA TCT** ACA AGA CGT AGT GCG CTG CAT CAG CTG TAT GCA TAC 3’ (*Bgl*II)

5’ flank

1 5’ **AAG CTT** GAG GTG CAG GTC GGC GAG CGG CTA GGT GTA 3’ (*Hind*III)

2 5’ **GTC GAC** GCG TGA TGG GAT CAC TTA AAG GGG GGG 3’ (*Sal*I)

OAS-TL re-expresser

1 5’ **CCC GGG** ATG GCG GCA CCG TTC GAC AAG TCA 3’ (*Sma*I)

2 5’ **GGA TCC** CTA CGG GCA GGG ACG ACA CCT CAT CCC 3’ (*BamH*I)

***TDR1* null mutant**

3' flank

1 5’ **CCC GGG** AGG CTC GTC GAG GGG ATC GAC GTG 3’ (*sma*I)

2 5’ **AGA TCT** GGG GAG GGA GGG AAT GTA GTA GTC CTC TGT GCC TGT 3’ (*Bgl*II)

5' flank

1 5’ **AAG CTT** TGT GCA GCG TTT CTT AGT ACC GCT GTG CAG TTT TG 3’ (*Hind*III)

2 5’ **GTC GAC** CCT CGA CGC CAG GCA CGC AGT GGC TTA GTT 3’ (*Sal*I)

TDR1 re-expresser

1 5’ **CCC GGG** ATG GCC GCC CGC GCG CTA AAG CTA 3’ (*Sma*I)

2 5’ **GGA TCC** TTA CCC GCT CTG GGC CCT CCG TTG ACG 3’ (*BamH*I)

2.3.3.2 Polymerase chain reaction (PCR)

Two commercially available PCR mixes were used to amplifiy fragments of *Leishmania* DNA. PCR SuperMix, which has no proof reading ability, was used in diagnostic PCRs, e.g. to verify the integration of fragments of DNA in the correct position, and AccuPrime *Pfx* SuperMix, which has proof reading abilities, was used to amplify genes for recombinant protein production and generation constructs for genetic manipulation of *Leishmania*.

PCR SuperMix

PCR Supermix (Invitrogen) is a ready to use mix containing 1.65 mM $MgCl_2$, 220 µM dNTP and 22 U/ml *Taq* DNA polymerase. The SuperMix was added to 100 ng of gDNA in a final reaction volume of 25 µl, with a final concentration of 400 nM of each oligonucleotide. The PCR was carried out under the following conditions:

Initial Denaturation	94 °C, 5 min
30 cycles of:	
Denaturation	94 °C, 1 min
Annealing	Oligonucleotide specific temperature, 1 min
Elongation	72 °C, 1 min per kb to be amplified
Final Elongation	72 °C, 10 min

All PCR products were analysed on 1 % agarose gels and fragments of the expected size were cloned into the pGEM-T easy Vector (Promega) (Figure 2.1).

AccuPrime *Pfx* SuperMix

AccuPrime *Pfx* SuperMix (Invitrogen) is a ready to use mix containing 1.1 mM $MgSO_4$, 330 µM dNTPs and 22U/ml *Pfx* DNA polymerase. The *Pfx* SuperMix was added to 100 ng gDNA in a final reaction volume of 25 µl, with a final concentration of 400 nM of each oligonucleotide. The PCR was carried out under the following conditions:

Initial Denaturation	94 °C, 5 min
30 cycles of:	
Denaturation	94 °C, 1 min
Annealing	Oligonucloetide specific temperature, 1 min
Elongation	68 °C, 2 min per kb to be amplified
Final Elongation	68 °C, 10 min

All PCR products were analysed on 1% agarose gels and fragments of the expected size were cloned into the StrataClone Blunt PCR Cloning Vector (pSC-B) (Stratagene) (see Figure 2.2).

2.3.3.3 Sub-cloning of PCR products

Ligation of DNA fragments with commercially available vectors was carried out according to the manufacturer's instructions. Fragments of DNA amplified using *Taq* polymerase produced adenine overhangs at the 3' ends and therefore the pGEM-T easy vector (Promega) was used. PCR products amplified using *Pfx* polymerase had blunt ends and therefore the StrataClone Blunt PCR Cloning Vector (Stratagene) was used according to the manufacturer's recommendations.

2.3.3.4 Selection of colonies

Both the pGEMT-easy and StrataClone blunt PCR cloning vectors contain the *LacZ* gene which encodes beta-galactosidase. The multiple cloning sites present of the vectors are contained within the *LacZ* gene sequence, which means that when foreign DNA is introduced to the multiple cloning site (MCS), the transcription of *LacZ*, and consequently the activity of beta-galactosidase, are disrupted. 5-bromo-4-chloro-3-indolyl-[beta]-D-galactopyranoside (X-Gal) is a colourless modified galactose sugar which produces a coloured (blue) product when hydrolysed by beta-galactosidase. The hydrolysis of colourless X-Gal by the beta-galactosidase causes characteristically blue bacterial colonies and shows that the colonies contain recircularised vector, whereas white colonies indicate the insertion of DNA into the MCS and the loss of the cells' ability to hydrolyse the marker.

White colonies were selected and used to inoculate Luria-Bertani (LB) medium supplemented with 100 µg/ml ampicillin. Clones were verified by DNA miniprep and digestion with appropriate restriction enzymes. Clones with the correct vector and insert band size were verified by DNA sequencing.

2.3.3.5 Sub-cloning into destination vectors

Fragments of DNA verified by DNA sequencing were digested from the plasmid, gel purified and ligated together with the destination plasmid. The ligation reactions were transformed into the commercially available *E. coli* strain DH5α (Invitrogen).

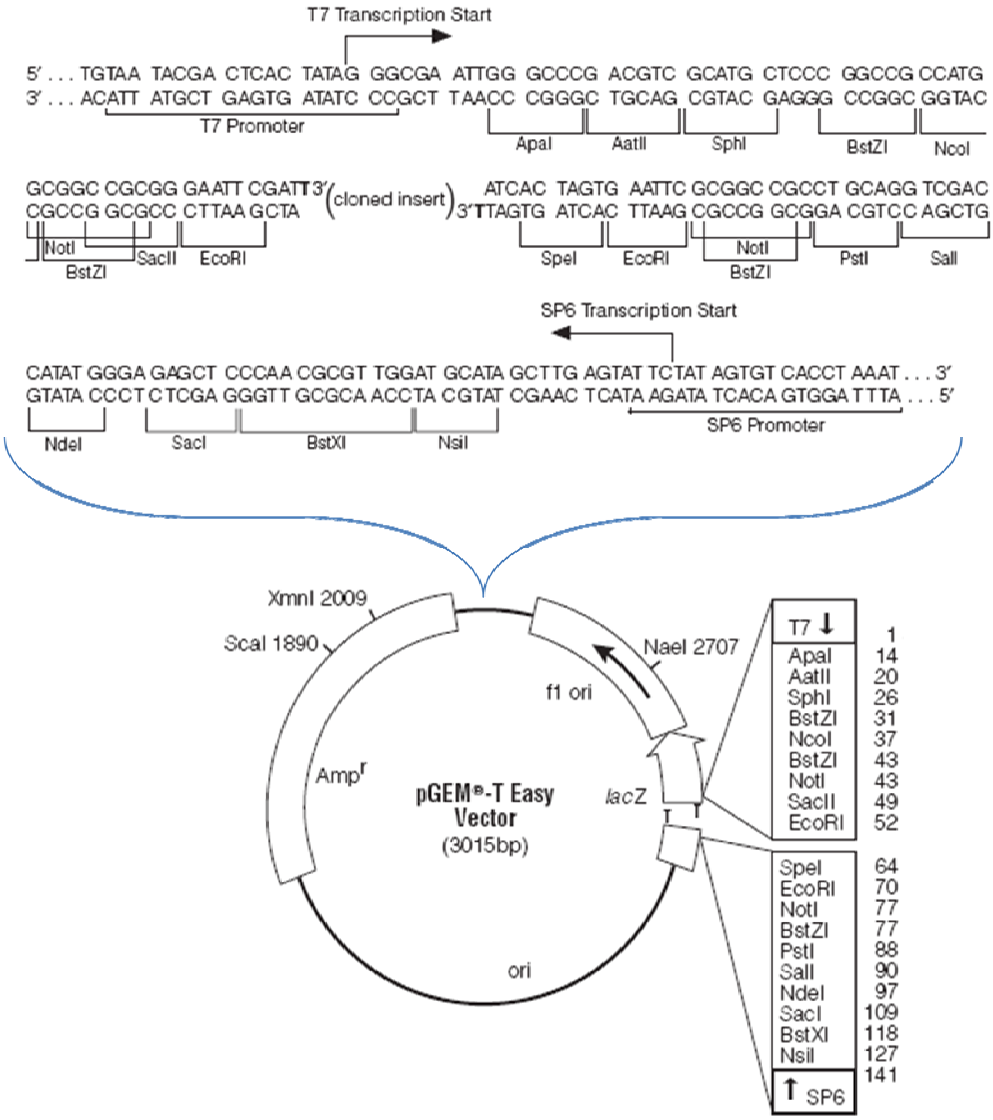

pGEM®-T Easy Vector sequence reference points:

T7 RNA polymerase transcription initiation site	1
multiple cloning region	10–128
SP6 RNA polymerase promoter (–17 to +3)	139–158
SP6 RNA polymerase transcription initiation site	141
pUC/M13 Reverse Sequencing Primer binding site	176–197
*lac*Z start codon	180
lac operator	200–216
β-lactamase coding region	1337–2197
phage f1 region	2380–2835
lac operon sequences	2836–2996, 166–395
pUC/M13 Forward Sequencing Primer binding site	2949–2972
T7 RNA polymerase promoter (–17 to +3)	2999–3

Figure 2.1 pGEM-T Easy Vector.
This figure displays the important features of the pGEM-T Easy plasmid (Promega) that was used to clone PCR products amplified with the PCR supermix containing Taq polymerase. These include the multiple cloning site and the T7 and SP6 primers that were used for DNA sequencing. This figure was taken from www.promega.com.

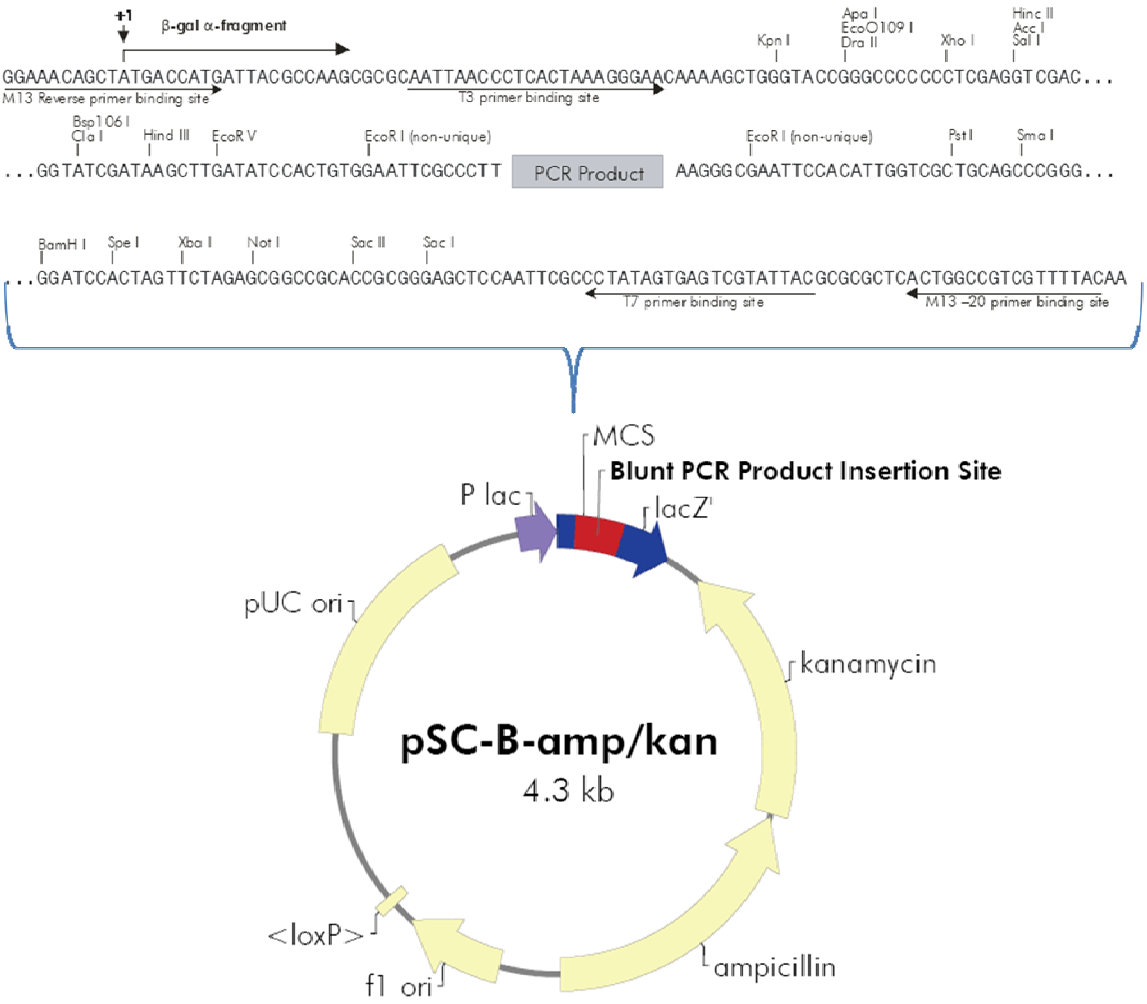

Feature	Nucleotide Position
β-galactosidase α-fragment coding sequence (lacZ´)	1–354
Multiple cloning site (MCS)	57–197
PCR product insertion site	123
kanamycin resistance ORF	465-1256
ampicillin resistance (*bla*) ORF	1268–2125
f1 origin of ss-DNA replication	2317–2623
<loxP> (mutant *loxP*-derived sequence *lox66/71*; nonfunctional in Cre-mediated recombination)	2690-2723
pUC origin of replication	3264–3931
lac promoter	4153-4272

Figure 2.2 pSC-B Blunt PCR Cloning Vector.
This figure displays the important features of pSC-B, the StrataClone blunt PCR cloning vector that was used to clone PCR products amplified with *Pfx* Supermix, such as the ampicillin and kanamycin resistance cassettes, the multiple cloning site and the positions of the M13 and M13 reverse primers that were used for DNA sequencing. This figure was taken from www.stratagene.com.

Restriction enzymes were used according to the manufacturer's instructions. Typically, 1 µg of plasmid DNA was digested in a 20 µl reaction containing the appropriate enzyme and buffer. Reactions were incubated overnight at the optimum temperature, specified by the manufacturer. Digested plasmids were separated by agarose gel electrophoresis and DNA fragments (either plasmids or inserts) were isolated by gel purification.

Following electrophoresis, DNA fragments were visualised under low intensity UV light, and any fragments of interest were excised from the gel using a sterile scalpel blade. Purification of DNA from the agarose gel was performed using the Qiaquick Gel Extraction Kit (Qiagen), according to the manufacturer's instructions.

For ligation of purified DNA fragments into destination vectors, plasmid and DNA insert were mixed at a molar ratio of 1:3 in a 20 µl reaction containing 1 unit of T4 DNA ligase (New England Biolabs) and 1 x T4 ligase buffer. Reactions were incubated overnight at 16 ˚C.

2.3.3.6 Transformation of competent *E. coli*

Plasmid DNA was transformed into the chemically competent *E. coli* strain DH5α (Invitrogen) for general cloning and BL21 (DE3) (Stratagene) for recombinant protein expression. Transformations were performed by heat-shock according to the manufacturer's instructions, and resulting bacteria were plated onto LB agar (LB medium, 1.5 % Bacto-agar (Oxoid), pH 7.0) plates with the appropriate antibiotic selection and incubated overnight at 37 ˚C. Possible positive clones were verified by plasmid DNA miniprep and digestion with appropriate restriction enzymes, as described above. Plasmids containing the correct sized inserts were sent for nucleotide sequencing.

2.3.3.7 Long-term storage of bacteria

E. coli cells were plated onto LB agar containing the appropriate antibiotic and incubated overnight at 37 ˚C. A single colony was used to inoculate 5 ml of LB media containing the appropriate antibiotic, which was then incubated overnight at 37 ˚C, with shaking at 200 rpm. 0.5 ml of the overnight culture was mixed

with an equal volume of sterile 98 % (v/v) glycerol, 2 % (v/v) PBS, and stored at -70 ˚C.

2.3.3.8 Isolation of plasmid DNA from *E. coli*

Single bacterial colonies from transformation plates were inoculated into 5 ml LB medium containing either 50 µg/ml kanamycin (for recombinant expression clones) or 100 µg/ml ampicillin (for all other vector clones and destination clones produced). These cultures were incubated overnight at 37 ˚C with shaking at 200 rpm. Plasmid DNA isolation was then performed using the Qiaprep spin miniprep kit (Qiagen) according to the manufacturer's instructions. Correct ligation of DNA fragments into plasmids was verified by either diagnostic double digests using appropriate restriction enzymes or by DNA sequencing using relevant oligonucleotide primers.

2.3.3.9 DNA sequencing

DNA sequencing was carried out by The Sequencing Service, School of Life Sciences, University of Dundee (www.dnaseq.co.uk) using Applied Biosystems Big-Dye Ver 3.1 chemistry on an Applied Biosystems model 3730 automated capillary DNA sequencer. For each sequencing reaction, 200-300 ng of plasmid DNA and 3.2 pmoles of sequencing primer was required.

2.3.3.10 DNA gel electrophoresis

Analysis of DNA fragments was typically carried out on gels containing 1 % agarose in TAE buffer (40 mM TrisAcetate and 1 mM Na_2EDTA, pH 7.6). Prior to loading the gel, samples were mixed with 6x DNA loading buffer (0.25 % (w/v) bromophenol blue, 0.25 % (w/v) orange-G, 40% (w/v) glycerol) to a final concentration of 1x loading buffer. Gels were electrophoresed at 100 V until the dye in the loading buffer could be seen to have migrated approximately two thirds of the length of the gel.

2.3.3.11 Southern blot analysis

Leishmania genomic DNA was analysed by Southern blot. 2-5 µg of DNA was digested with appropriate restriction enzymes (typically 20-100 units) overnight. The digested DNA was run on a 0.8 % agarose gel overnight at 15-20 V, and then transferred to positively charged nylon membrane Hybond-N+ (GE Healthcare), using a VacuGene XL apparatus (GE Healthcare). The gel was placed on top of the membrane and covered with depurination solution (0.25 N HCl) and a vacuum was applied at 50-60 mbar pressure.

After approximately 25 min, the colour of the loading dye changed from blue to yellow and the remaining depurination solution was removed. The gel was then covered with denaturation solution (1.5 M NaCl, 0.5 M NaOH) for approximately 25 min until the loading dye had changed colour from yellow back to blue. The remaining denaturation solution was removed and replaced with 20x SSC for 1 h, to transfer the DNA onto the membrane. The DNA was crosslinked to the membrane by using a UV crosslinker (UVP Laboratory Products). The membrane was blocked with pre-warmed pre-hybridization buffer (5x SSC, 0.1 % (w/v) dextran sulphate and 1:20 dilution of liquid block (GE Healthcare)), at 55 °C for at least 1 h. After pre-hybridization, a DNA probe labelled with a thermostable alkaline phosphatase enzyme was added, which had been synthesized using the AlkPhos Direct Labelling Reagents (GE Healthcare) according to the manufacturer's guidelines. The blot was incubated at 55 °C overnight. The blot was then washed twice in pre-warmed primary wash buffer (2 M urea, 0.1 % (w/v) SDS, 50 mM sodium phosphate pH 7.0, 150 mM NaCl, 1 mM $MgCl_2$, 0.2 % (w/v) Blocking Reagent (GE Healthcare) at 55 °C), for 10 min each wash. After the primary washes, the blot was transferred to a clean container and washed in secondary wash buffer (50 mM Tris base, 100 mM NaCl, 2 mM $MgCl_2$) twice at room temperature, for 5 min.

Excess secondary wash buffer was removed from the blot and CDP-Star detection reagent (GE Healthcare) was applied to the membrane (30-40 µl/cm^2) and incubated at room temperature for 2-5 min. Chemiluminescence was detected on autoradiography film (Kodak), for 2-24 h.

2.3.4 Biochemical methods

2.3.4.1 Estimation of protein concentration

Concentration of protein was determined using Protein assay reagent (BioRad). Varying dilutions of protein of an unknown concentration were added to wells of a 96 well microplate in total volumes of 10 µl. Protein assay reagent was diluted 1:5 in sterile water, filtered and 200 µl added to each well containing protein. Bovine serum albumin (BSA) was used to determine a standard curve of the concentrations 0, 0.5, 1.0, 1.5 and 2.0 mg protein/ml.

The absorbance of unknown protein solutions and standards with added Protein assay reagent was measured at 595 nm and the concentration of protein was determined by reference to the standard curve of known BSA concentrations. Measurements were taken using a Versamax microplate reader (Molecular Devices). A standard curve of BSA concentrations was made for each estimation of protein concentration, using the software Grafit 5.0 (Erathicus).

2.3.4.2 SDS-PAGE analysis

Protein samples were separated by sodium dodecyl sulphate polyacrylamide gel electrophoresis (SDS-PAGE) using the NuPAGE Bis/Tris electrophoresis system (Invitrogen). Proteins for analysis were quantified by the method described in Section 2.3.4.1 and heated to 100 ˚C for 5 min in 1 x SDS loading buffer (10.4 mM Tris-HCl pH 6.8, 0.3 % (w/v) SDS, 1.7 % (v/v) glycerol, 0.0002 % (w/v) bromophenol blue, 0.8 % (v/v) 2-mercaptoethanol), before being loaded into Novex Bis/Tris pre-cast gels (4-12 % polyacrylamide). Gels were run in Xcell Surelock™ Mini-cell apparatus with 1 x MOPS buffer (50 mM 3-[N-morpholino] propane sulphonic acid, 50 mM Tris base, 3.5 mM SDS, 1 mM EDTA) (all Invitrogen). Electrophoresis was performed according to the manufacturer's instructions. SDS-PAGE gels were stained by incubation in Coomasie stain (40 % (v/v) methanol, 10 % (v/v) acetic acid, 0.1 % (w/v) coomasie brilliant blue R-250) for 10 min and washing in destain solution (20 % (v/v) methanol, 10 % (v/v) acetic acid).

2.3.4.3 Western blot analysis

1-20 µg of protein separated by SDS-PAGE was transferred to Protran nitrocellulose (Schleicher & Schuell) using a Transblot semi-dry blotting system (Biorad) according to the manufacturer's guidelines. Transfer occurred in a downward direction in a sandwich consisting of, from top to bottom, six sheets of blotting paper soaked in cold Towbin buffer (25 mM Tris, 192 mM glycine, 20 % (v/v) methanol), SDS-PAGE gel, nitrocellulose and a further six sheets of blotting paper soaked in cold Towbin buffer. The transfer was performed at 20 V for 40 min per gel. After transfer, nitrocellulose membranes were stained with Ponceau S stain (Sigma) to visualise transferred proteins and to ensure the transfer was successful and to allow marking of the gel lanes. The membranes were blocked by incubating in PBS with 5 % (w/v) Marvel milk powder overnight at 4 °C, with shaking.

Rabbit polyclonal antibodies raised against *Leishmania* recombinant proteins by the Scottish Antibody Production Unit (SAPU, Carluke, UK), using standard protocols. Primary antibodies were diluted to the appropriate concentration (Table 1.1) in PBS with 1 % (w/v) Marvel milk powder, and incubated on membranes at room temperature for 60 min, with shaking. The membranes were then washed three times in PBS with 0.1 % (v/v) Tween 20, for 10 min each wash, with shaking. Horse radish peroxidise (HRP) conjugated secondary antibodies were applied at the appropriate dilution in 1 % (w/v) Marvel milk powder in PBS, for 60 min at room temperature, with shaking. The wash steps were then repeated as before. The ECL-plus detection kit (GE Healthcare) was used to detect HRP conjugated secondary antibodies. The blots were exposed to ECL film (GE Healthcare) from 15 s to 5 min in a hyperfilm cassette (GE Healthcare).

2.3.4.4 Recombinant protein constructs

L. donovani TDR1 and *trypanothione reductase* genes were amplified from genomic DNA using the oligonucleotide primers described in Section 2.3.3.1. The restriction sites *Not*I and *Nde*I were added to the 3' and 5' ends respectively, to facilitate cloning. The genes were first cloned into pGEMT-easy (Figure 2.1), then competent *E. coli* was transformed and plasmid DNA extracted from 6 ml

overnight cultures of the bacteria. The *TDR1* and *trypanothione reductase* genes were then digested out of the pGEMT-easy vector using the restriction enzymes *Not*I and *Nde*I (typically 20-50 units) and the products were run on a 1 % agarose gel, to isolate the gene insert. Digested *TDR1* and *trypanothione reductase* were then cloned into the expression vector pET28a+ (Novagen) (Figure 2.3). Recombinant expression of gene products in this vector is under control of the T7 promoter and is therefore inducible by addition of isopropyl-beta-D-thiogalactopyranoside (IPTG). pET28a+ contains a multiple cloning site and a kanamycin resistance cassette. The *L. donovani* TDR1 and *L. donovani* trypanothione reductase expression constructs were cloned into *Not*I/*Nde*I sites, resulting in the addition of an N-terminal $(His)_6$ tag.

2.3.4.5 Production of recombinant *L. donovani* trypanothione reductase and TDR1

A single colony of BL21 DE3 cells harbouring the appropriate expression construct was inoculated into 5 ml of LB medium with kanamycin (25 µg/ml) and allowed to grow at 37 °C overnight. The overnight culture was then diluted 1:50 with LB containing 25 µg/ml of kanamycin and grown at 37 °C until OD_{600} reached 0.7 – 0.8. Expression was induced with 2 mM IPTG and growth was continued for 16 h at 15°C for TDR1 (previously optimised by other lab members) and 20 °C for trypanothione reductase (Mittal et al., 2005). The induced culture was harvested by centrifugation at 1500 *g* for 20 min then resuspended in 6 ml of buffer A (20 mM Tris/500 mM NaCl, pH 7.9) containing 5 mM imidazole. The cells were lysed by sonication with a power of 50 W (six times 10 s pulse with 10 s cooling interval) and the resulting suspension was centrifuged at 15000 *g* for 20 min at 4 °C to remove cell debris. The clear supernatant was applied on to a 2.5 ml Ni^{2+}-nitrilotriacetate column, pre-equilibrated in buffer A containing 5 mM imidazole. The column was washed first with 50 ml of buffer A with 60 mM imidazole and the His-tagged recombinant protein was eluted with 250 mM imidazole in buffer A. Samples from each stage of the purification process were prepared as described in Section 2.3.4.2 and analysed on 12% SDS-PAGE gel.

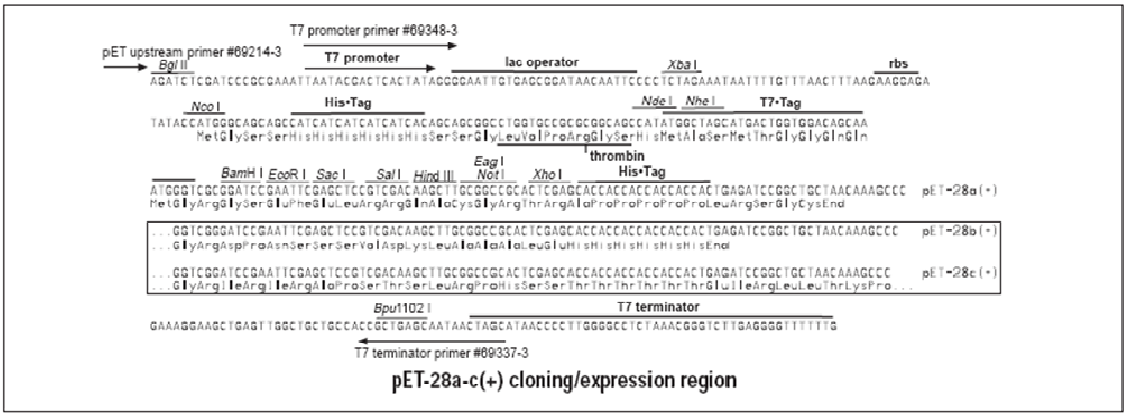

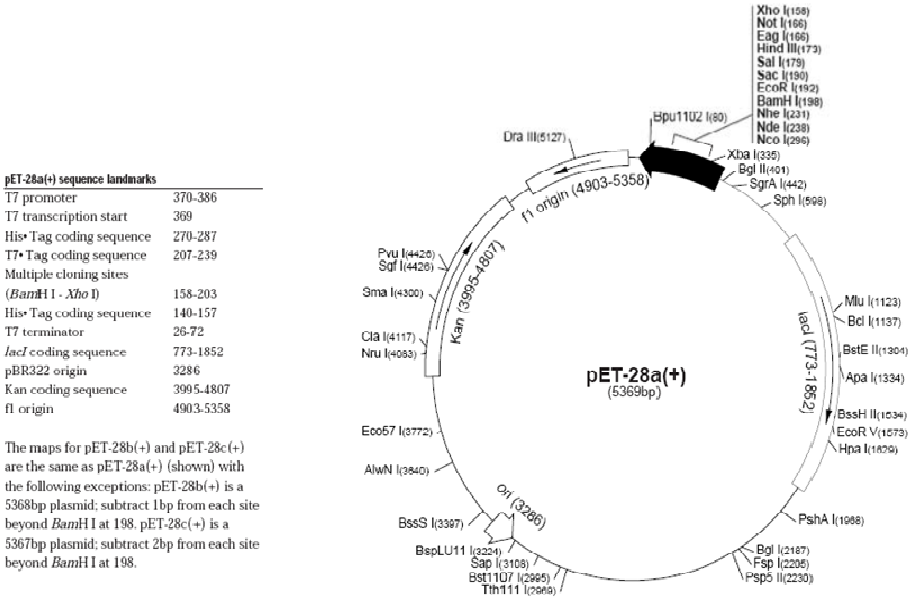

Figure 2.3 pET28a+ Recombinant Expression Plasmid.
Schematic representation of the pET28a+ recombinant expression plasmid and its important features, including the kanamycin resistance cassette, for selection in *E. coli*, and the multiple cloning site. The *L. donovani* trypanothione reductase expression construct was subcloned using *Not*I/*Nde*I. The *L. donovani* TDR1 expression construct was subcloned using *Not*I/*Nde*I. Recombinant expression using this plasmid is under the control of the T7 promoter and attaches a $His_{(6)}$ tag at the N-terminus of the expressed protein. This figure was taken from www.novagen.com.

2.3.4.6 Activity of trypanothione reductase

This assay was performed according to Hamilton et al., 2003, to ensure the recombinant trypanothione reductase was active. The standard assay mixture contained, in a final volume of 1 ml, 40 mM Hepes (pH 7.5), 1 mM EDTA, 0.15 mM NADPH, 1 µM $T[S]_2$, 25 µM DTNB and various concentrations of trypanothione reductase. The basis of the assay involves the reaction of each trypanothione molecule with one DTNB molecule, producing one TNB molecule which is yellow in colour and detectable spectrophotometrically at 412 nm. This is a cycling reaction in which the initial rate is proportional to the concentration of trypanothione. The assay components were preincubated with NADPH for 5 min at 27 °C, before initiating the reaction by the addition of $T[S]_2$. Enzyme activity was monitored as the increase in absorbance at 412 nm due to the formation of TNB.

2.3.4.7 Thiol transferase activity of TDR1

The ability of TDR1 of using glutathione and trypanothione as electron donors to reduce the synthetic disulphide – 2-hydroxyethyl disulfide (HEDS) was investigated as described in Denton et al., 2004. The standard assay mixture contained, in a final volume of 200 µl, 50 mM Tris/HCl (pH 7.0), 5 mM EDTA, 300 µM NADPH, 1 mM GSH, 0.75 mM HEDS and 1 unit/ml GSH reductase. When using trypanothione as an electron donor, all assay components were the same except 1 mM GSH was replaced by 400 µM trypanothione, 1 unit/ml of GSH reductase was replaced by 1 unit/ml of trypanothione reductase and the concentration of NADPH was reduced from 300 µM to 200 µM. The assay mixture was preincubated at 30 °C for 10 min, before initiation of the reaction by the addition of TDR1. Activity was monitored as the decrease in absorbance at 340 nm. Specific activities were calculated from the linear rate during the first 1 min of the reaction.

2.3.5 DNA manipulation techniques for *L. major* and *L. donovani*

2.3.5.1 Production of a knock-out cassette

The plasmids pGL345, pGL158 and pGL1033 were obtained from Prof. J. C. Mottram, Glasgow (Mottram et al., 1996). pGL345 contains the *hygromycin phosphotransferase* (*HYG*) gene, conferring resistance to Hygromycin, pGL158 contains the *nourseothricin acetyltransferase* (*SAT*) gene, conferring resistance to Nourseothricin and pGL1033 contains the *dihydroxybiphenyl dioxygenase* (*BLEO*) gene, conferring resistance to Bleomycin/Phleomycin.

Approximately 1 kb of the 3' flanking region of the *L. donovani OAS-TL* gene was amplified using the oligonucleotide primers described in Section 2.3.3.1, and the amplification conditions described in Section 2.3.3.2. *Hind*III and *Bam*HI sites were introduced at the 5' and 3' ends of the amplified 5' flanking region and *Sma*I and *Bgl*II sites were introduced to the 5' and 3' ends of the amplified 3' flanking region.

The 1 kb 3' flanking region of the antibiotic resistance genes of the plasmid pGL345 was removed by digestion with the restriction enzymes *Hind*III and *Bam*HI (20-50 units). The amplified 3' flanking region of the *OAS-TL* gene was then subcloned into the pSD-B plasmid (Figure 2.2), released using the restriction enzymes *Hind*III and *Bam*HI (20-50 units) and sub-cloned into the plasmid pGL345 pre-digested with the same restriction enzymes. Competent *E. coli* was transformed with pGL345 + *OAS-TL* 3' flank and the plasmid DNA was purified from a 6 ml overnight bacterial culture. This procedure was repeated to replace the 5' flanking region of the antibiotic resistance gene with the 5' flanking region of the *OAS-TL* gene creating the construct pGL345 with *OAS-TL* 3' and 5' flanks.

Since the sequence of pGL345, pGL158 and pGL1033 are identical apart from the antibiotic resistance genes, the *nourseothricin acetyltransferase* and *dihydroxybiphenyl dioxygenase* genes were isolated from pGL158 and pGL1033 respectively, by digest with *Spe*I and *Bam*HI. These fragments of DNA were then used to replace the *hygromycin phosphotransferase* gene in the construct pGL345 + *OAS-TL* 3' and 5' flanks. This method was used to generate *TDR1* knock

out constructs in the same way. Figure 2.4 shows the constructs designed to knock-out *TDR1* in *L. donovani* and *L. infantum*, and Figure 2.5 shows the constructs designed to knock-out *OAS-TL* in *L. donovani*.

2.3.5.2 Production of over-expression plasmids

The pGL102 plasmid was obtained from Prof. J. C. Mottram, Glasgow, and used to create *Leishmania* lines in which a particular gene was re-expressed or over-expressed. pGL102 contains the neomycin phosphotransferase gene, which confers resistance to G418 and neomycin (Figure 2.6).

The *OAS-TL* gene (975 bp in length) and the *TDR1* gene (1353 bp in length) were amplified using the oligonucleotide primers described in Section 2.3.3.1. A *Bam*HI site and an ATG initiation codon were added to the 5' end of the oligonucleotide N-terminal primers and a *Sma*I restriction site and a stop codon were added to the C-terminal end. In the case of *OAS-TL*, the *Sma*I restriction site was replaced with *Eco*RV, because the gene itself contains a *Sma*I restriction site. The PCR products were cloned into the pGEMT-easy vector (Qiagen) and then used to transform *E. coli* DH5α cells. Plasmid DNA was purified from a 6 ml overnight bacterial culture. The *TDR1* and *OAS-TL* inserts were digested out with *Bam*HI and *Sma*I (20-50 units) in the case of *TDR1,* and *Bam*HI and *Eco*RV (20-50 units) in the case of *OAS-TL*, and ligated into the pre-digested *Sma*I/*Bam*HI pGL102 plasmid. Plasmids were used to transform *E. coli* DHα cells. Plasmid DNA was purified from a 6 ml overnight bacterial culture.

2.3.5.3 Preparation of plasmid for transfection

Extra-chromasomal plasmids for over-expression of OAS-TL and TDR1 were prepared by using the Qiaprep spin miniprep kit (Qiagen) with 6 ml of overnight *E. coli* cultures, to purify plasmid DNA. The plasmid DNA was then sterilised by ethanol precipitation. DNA was washed twice in 70 % (v/v) ethanol and resuspended in 20 µl of sterile water.

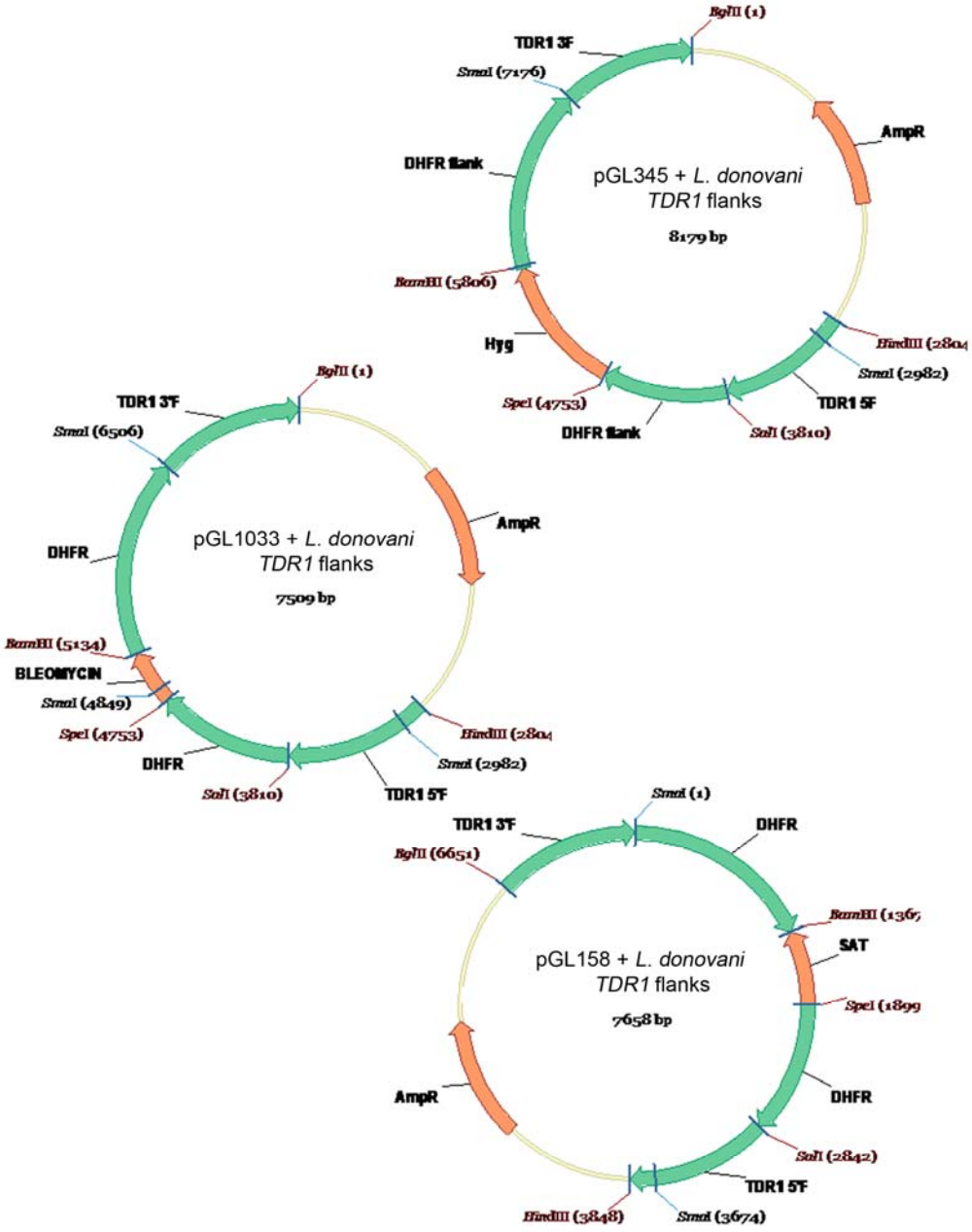

Figure 2.4 Constructs for the gene knock-outs of *TDR1*.
Schematic representation of the pGL345 with *TDR1* flanks (Panel A), pGL1033 with *TDR1* flanks (Panel B) and the pGL158 with *TDR1* flanks (panel C). *Hyg,* hygromycin phosphotransferase; *Bleomycin,* dihydroxybiphenyl dioxygenase*; SAT,* nourseothricin acetyltransferase; *AmpR,* ampicillin resistance gene; *DHFR*, flanking regions of the *Leishmania* dihydrofolate reductase. All contain the ampicillin resistance gene (AmpR; 858 bp) for selection in *E. coli*. The restriction sites used to clone the *TDR1* flanks into the plasmids are shown in red. *Hind*III and *Bgl*II were used to cut out the flank-containing linear knock-out construct for transfection into *L. donovani*.

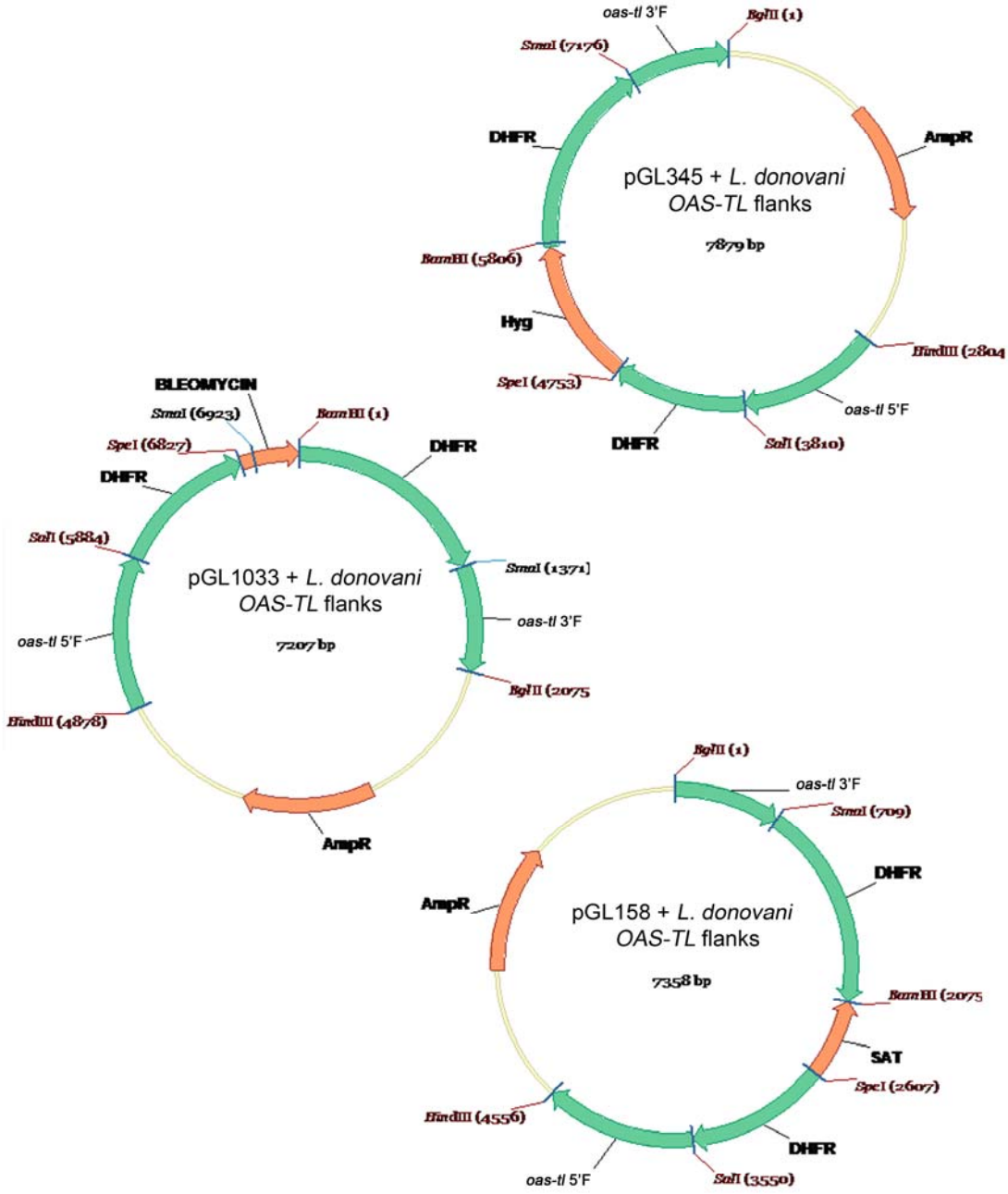

Figure 2.5 Constructs for the gene knock-outs of *OAS-TL*.
Schematic representation of pGL345 with *OAS-TL* flanks (Panel A), pGL1033 with *OAS-TL* flanks (Panel B) and pGL158 with *OAS-TL* flanks (Panel C). *Hyg,* hygromycin phosphotransferase; *Bleomycin,* dihydroxybiphenyl dioxygenase*; SAT,* nourseothricin acetyltransferase; *AmpR*, ampicillin resistance gene; *DHFR*, flanking regions of the *Leishmania* dihydrofolate reductase. All contain the ampicillin resistance gene (AmpR; 858 bp) for selection in *E. coli*. The restriction sites used to clone the *OAS-TL* flanks into the plasmids are shown in red. *Hind*III and *Bgl*II were used to cut out the flank-containing linear knock-out construct for transfection into *L. donovani*.

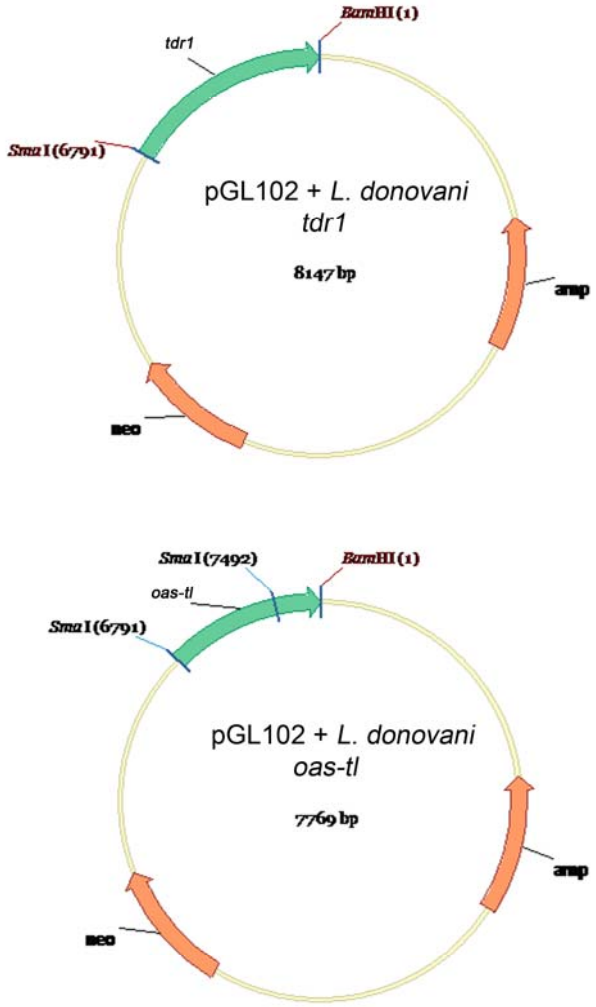

Figure 2.6 Plasmids for the re-expression/over-expression of OAS-TL and TDR1.
Schematic representation of the pGL102 plasmid for re-expression or over-expression of genes in *Leishmania*. pGL102 with *OAS-TL* (Panel A) for re-expression/over-expression of OAS-TL and pGL102 with *TDR1* (Panel B) for re-expression/over-expression of TDR1. *Neo*, neomycin resistance gene; *AmpR*, ampicillin resistance gene for selection in *E. coli*. The restriction sites used to clone *OAS-TL* and *TDR1* into the plasmids are shown.

Plasmid DNA containing the knock-out constructs for *OAS-TL* and *TDR1* were also prepared using the Qiaprep spin miniprep kit (Qiagen) with 6 ml of overnight *E. coli* cultures, to purify plasmid DNA. 20 µg of knock-out plasmid DNA was linearised by overnight digest with *Hind*III and *Bgl*II, in a 60 µl reaction volume, according to the manufacturer's instructions. Digested knock-out DNA was electrophoresed on 1 % agarose TAE gels, purified using the Qiaquick Gel Extraction Kit (Qiagen) and sterilised by ethanol precipitation. DNA was washed twice in 70 % (v/v) ethanol and resuspended in 20 µl of sterile water.

2.3.5.4 Isolation of genomic DNA

Genomic DNA was isolated from *Leishmania* promastigotes according to a method based on the mini-prep procedure described by Medina-Acosta and Cross (1993). Up to 2 x 10^8 cells were harvested at 1000 *g* for 10 min, resuspended in 150 µl of TELT lysis buffer and incubated at room temperature for 5 min. The cell lysate was extracted after the addition of phenol/chloroform (1:1) followed by centrifugation at 13000 *g*, 5 min. DNA was ethanol precipitated by washing twice in 70 % (v/v) ethanol. The precipitated DNA was allowed to air dry for 5 min before being resuspended in sterile TE buffer. The quantity and quality of DNA were analysed by agarose gel electrophoresis.

2.3.6 HPLC

2.3.6.1 Preparation of thiol standards for analysis by HPLC

Mixes containing stock concentrations of 0, 50, 100, 150, 200, 250, 300 and 350 pmoles of each of cysteine, γ-glutamyl cysteine, cysteinyl glycine, glutathionyl spermidine, glutathione, homocysteine and trypanothione were diluted in 50 µl of 40 mM N-[2-hydroxyethyl]-piperazine-N'[3-propanesulphonic acid] (HEPPS), 4 mM diethylenetriamine pentaacetic acid (DTPA) buffer, 1 mM dithiothreitol (DTT), pH 8.0 (adjusted with lithium hydroxide). Thiols were derivatised by the addition of 50 µl 2 mM monobromobimane in absolute ethanol and heated for 3 min at 70 ˚C. After a brief cooling period, standards were deproteinised by the addition of 100 µl of 4 M methanesulphonic acid, pH adjusted to 1.6 with lithium hydroxide, and incubated on ice for 30 min. Standards were centrifuged at 15000 *g* for 5 min. Supernatant was carefully removed and stored at -80 ˚C until

analysis, typically no longer than 4 weeks. The correlation between peak area and thiol concentration was shown to be linear in the range 0 – 350 pmoles.

2.3.6.2 Preparation of parasite extracts for analysis by HPLC

5 x 10^7 *L. donovani* cells, in amber coloured microcentrifuge tubes (Eppendorf), were pelleted at 1 500 *g* for 10 min at 4˚C and stored at -20 ˚C overnight. The cells were resuspended in 50 µl of 40 mM N-[2-hydroxyethyl]-piperazine-N'[3-propanesulphonic acid] (HEPPS), 4 mM diethylenetriamine pentaacetic acid (DTPA) buffer, 1 mM DTT, pH 8.0 (adjusted with lithium hydroxide), and incubated on ice for 1 h. Intracellular thiols were derivatised by the addition of 50 µl 2 mM monobromobimane in absolute ethanol and heated for 3 min at 70 ˚C. After a brief cooling period, cells were deproteinised by the addition of 100 µl of 4 M methanesulphonic acid, pH 1.6 (adjusted with lithium hydroxide) and incubated on ice for 30 min. The denatured cell protein was removed by centrifugation at 15 000 *g* for 5 min. Supernatant was carefully removed and stored at -20 ˚C until analysis.

2.3.6.3 Separation of thiols by HPLC analysis

Solvent A (0.25 % acetic acid) and solvent B (100 % acetonitrile) were made fresh for each HPLC run, and were de-gassed by vaccum filtration using 0.2 µm filters (Phenomenex). HPLC was performed by an UltiMate HPLC system, consisting of the UltiMate 3000 pump, autosampler and variable wavelength detector, the RF 2000 fluorescence detector and a UCI-50 universal chromatography interface.

Prepared samples were defrosted at room temperature and transferred, by pipette, into 0.3 ml HPLC crimp vials with snap caps (Kinesis), and placed in the autosampler. Separation of labelled thiols was performed using a Gemini C18 chromatography column fitted with a SecurityGuard guard column (Phenomenex), at a flow rate of 0.55 ml min^{-1} by application of the following gradient (% of solvent B): 0 min, 0%; 10 min, 0%; 40 min, 8%; 100 min, 15%; 110 min, 50%; 111 min 0%; 121 min, 0%. Thiols were detected by a fluorescence spectrophotometer (excitation, 365 nm; emission, 480 nm). The mobile phases consisted of 0.25% acetic acid (solvent A) and 100% acetonitrile (solvent B).

Peak area was used to calculate the amount of γ-glutamyl-cysteine, cysteine, cysteinyl-glycine, glutathione, homocysteine and trypanothione in a given sample. Values were calculated using the straight line equation y = mx + c and the appropriate standard curves. To allow for slight differences in retention time between columns, the standard curves were re-plotted when the column was changed, and during every run, a standard thiol mix of known concentrations was run to ensure the validity of the results.

2.3.7 Macrophage infections

2.3.7.1 Purification of macrophages from mice

Culled ICR mice and all equipment to be used were sterilised by spraying with 70 % (v/v) ethanol. A small incision was created in the middle of the abdomen of the mouse and the skin was pulled off to reveal the peritoneum, which was sterilised by spraying with 70 % (v/v) ethanol. 10 ml of RPMI 1640 with 1 % (v/v) gentamycin (both Invitrogen) was injected into the peritoneal cavity of the mouse and, holding the tail and shoulders, was gently agitated for approximately 20 s. The fluid (macrophage suspension) within the peritoneal cavity of the mouse was removed using a syringe, and centrifuged at 691 g for 10 min. The cell pellet was resuspended in fresh RPMI 1640 with 10 % (v/v) HIFCS and the cell number determined. The number of cells was adjusted to 5 x 10^5 cells/ml.

2.3.7.2 *In vitro* macrophage infections

Peritoneal macrophages were harvested as described in Section 2.3.7.1. 100 µl of cell suspension (5 x 10^4 cells/ml) was pipetted into each well of 16-well Lab-tek™ tissue culture slides (Nunc) and incubated at 37 °C, in 5 % CO_2 95 % air for 24 h. Stationary phase promastigotes were counted using a haemocytometer and diluted to the relevant concentration for the desired ratio (typically 5 promastigotes: 1 macrophage) in HOMEM with 20% (v/v) HIFCS. 100 µl of this parasite suspension was added to each of the wells containing macrophages. The slides were then incubated for a further 2 h at 37 °C with 5 % CO_2, 95 % air.

The medium was then carefully removed from each well and replaced with fresh HOMEM medium with 20 % HIFCS. Slides were fixed and stained after various

time points including 2 h, 12 h, 24 h, 55 h and 144 h post-infection with promastigote parasites. Slides were always incubated at 37 ˚C, in 5 % CO_2, 95 % air, fixed in 100% methanol and stained with 10% Geimsa for 10 min. The percentage of macrophages infected was determined using light microscopy by counting 100 macrophages. The number of parasites per macrophage, or per infected macrophage, was determined by counting the number of parasites in 50 macrophages per well, and calculating the average. Counts were always performed at least in triplicate and standard errors were calculated using the computer program Grafit 5.0 (Eraticus).

The effect of supplementing the medium with glutathione (1 mM) and L-methionine (5 mM), was investigated by setting up macrophage infections and infecting them with stationary phase parasites as described above. At all experimental stages, the medium was supplemented with the appropriate amino acid. 2 h post infection, the medium was replaced with HOMEM + 20 % HIFCS supplemented with the appropriate amino acid. Slides were fixed in 100 % methanol after 2 h, 12 h, 24 h and 55 h post infection, and stained using 10 % Geimsa stain for 10 min. Percentage infection and mean number of parasites per infected macrophage were calculated as described previously.

2.3.7.3 Sodium Stibogluconate Sensitivity Assay

Peritoneal macrophages were harvested as described in Section 2.3.7.1. 100 µl of cell suspension was pipetted into each well of 16-well Lab-tek™ tissue culture slides (Nunc) and incubated at 37 ˚C, in 5% CO_2, 95% air for 24 h. Stationary phase promastigotes were counted using a haemocytometer and diluted to the relevant concentration for the desired ratio (7 promastigotes:1 macrophage) in RPMI1640 with 10% (v/v) HIFCS. 100 µl of this parasite suspension was added to each of the wells containing macrophages. The slides were then incubated for a further 24 h at 37 ˚C with 5% CO_2, 95% air. The medium was then carefully removed from each well and sodium stibogluconate added in the following concentrations: 500 µM, 250 µM, 125 µM, 62.5 µM, 31.3 µM, 15.6 µM, 7.8 µM and 0 µM. The sodium stibogluconate was dissolved in PBS, filter sterilised and diluted in HOMEM with 10 % HIFCS. Drug dilutions were prepared in duplicate for each parasite line being tested (*L. major* FNM, *L. major Δtdr1* (*tdr1* null mutant)

and *L. major* Δ*tdr1* [TDR1] (TDR1 re-expresser)). The slides were incubated for a further 72 h at 37 °C with 5% CO_2, 95% air. The removal of medium and application of fresh sodium stibogluconate was then repeated using the concentrations described previously. The slides were then incubated for a further 48 h at 37 °C with 5% CO_2, 95% air. All slides were fixed with 100% methanol and stained with 10% Geimsa for 10 min. The percentage of macrophages infected was determined using light microscopy by counting 100 macrophages per well, and calculating the percentage of those infected. IC_{50} values and standard errors were determined by Grafit 5.0 (Erathicus).

2.3.8 Statistical tests

Unpaired t-tests were used routinely throughout this project to determine whether there is a difference between two means. Macrophage infection data were analysed in this way. All unpaired t-tests were carried out using the statistical program Minitab 15.

In order to compare the data collected on flagellum and body length of *L. donovani* WT, Δ*oas-tl* A, Δ*oas-tl* B, Δ*oas-tl* A [OAS-TL] and Δ*oas-tl* A [OAS-TL], the one way analysis of variance (ANOVA) was used. The ANOVA compares the means of several populations and depends on the following assumptions: each data set must be a random sample from each population, all populations must have the same variance and each population must have a normal distribution. Minitab 15 was used to carry out four separate analyses of variance to compare the means of the following groups: *L. donovani* WT, Δ*oas-tl* A and Δ*oas-tl* A [OAS-TL] flagellum length; *L. donovani* WT, Δ*oas-tl* B and Δ*oas-tl* B [OAS-TL] flagellum length; *L. donovani* WT, Δ*oas-tl* A and Δ*oas-tl* A [OAS-TL] body length; *L. donovani* WT, Δ*oas-tl* B and Δ*oas-tl* B [OAS-TL].

2.3.9 The effects of stressors on promastigote growth of *Leishmania*

2.3.9.1 The effect of peroxides on growth of *Leishmania* promastigotes

To investigate the effect of hydro-peroxides on growth of *Leishmania* promastigotes, wild type and transgenic parasite lines were seeded at 2.5 x 10^5

cells/ml in white bottom 96-well tissue culture plates and cultured for 72 h at 25 ˚C, with hydrogen peroxide (10, 5, 2.5, 1.3, 0.6, 0.3, 0.2, 0.08, 0.04, 0.02 or 0.01 mM), cumene hydroperoxide or tert-butyl hydroperoxide (both at 1, 0.5, 0.3, 0.1, 0.06, 0.03, 0.02, 0.008, 0.004, 0.002 or 0.001 mM) in total volumes of 200 µl. 20 µl of 500 µM resazurin sodium salt was then added to each well and the plates were incubated for a further 48 h at 25 ˚C before absorbance values were determined by dual wavelength using a FLUOStar OPTIMA fluorescent plate reader at 490 and 595 nm.

Resazurin sodium salt is used for the measurement of the metabolic activity of living cells. The bioreduction of the dye reduces the amount of the oxidised form (blue) and subsequently increases the fluorescent intermediate (red).

2.3.9.2 The effect of heavy metals on growth of *L. donovani* promastigotes

To investigate the effect of heavy metals on growth of *L. donovani* promastigotes, wild type and transgenic lines were seeded at 2.5 x 10^5 cells/ml in white bottom 96-well tissue culture plates and cultured for 72 h at 25 ˚C, with copper sulphate, potassium arsenate or cadmium chloride (all at 5, 2.5, 1.3, 0.6, 0.3, 0.2, 0.08, 0.04, 0.02 0.01 or 0.005 mM), in total volumes of 200 µl. 20 µl of 500 µM resazurin sodium salt was then added to each well and the plates were incubated for a further 48 h at 25 ˚C before absorbance values were determined with an excitation of 490 nm and emission of 595 nm, using a FLUOStar OPTIMA fluorescent plate reader.

2.3.10 Scanning Electron Microscopy

2.3.10.1 Preparation of samples for Scanning Electron Microscopy

10 mm glass coverslips were coated with poly-L-lysine and allowed to dry at room temperature for approximately 1 h. Mid-log phase cells (approximately 3 x 10^6 cells/ml) were centrifuged at 1000 *g* for 5 min, washed in PBS once, centrifuged again at 1000 *g* for 5 min and resuspended in 2.5 % glutaraldehyde, 0.1 M sodium phosphate. Samples were fixed by incubation at room temperature for 40 min. Cells were pelleted by centrifugation at 1000 *g* for 5 min and washed in 0.1 M sodium phosphate buffer. This was repeated twice to ensure the

complete removal of glutaraldehyde. Droplets of fixed cells were placed, by pipette, onto 10 mm glass coverslips pre-coated with poly-L-lysine. Cells were allowed to settle and adhere to the coverslips for 30 min at room temperature. The coverslips were washed twice in 0.1 M sodium phosphate buffer, for 5 min each wash, by placing them specimen-side down onto droplets of buffer on nescofilm wax paper. The coverslips were then transferred, specimen-side down onto droplets of osmium tetroxide where they were incubated for 1 h at room temperature. Following incubation with osmium tetroxide, the samples were washed three times in distilled water by placing the coverslips specimen-side down onto droplets on wax paper. Each wash was performed at room temperature and lasted 5 min. The coverslips were transferred, specimen-side up, into a 24 well tissue culture plate containing distilled water, for 5 min at room temperature, then into filtered uranyl acetate and incubated in darkness for 30 min-1 h. Following staining in uranyl acetate the coverslips were washed once in distilled water and then dehydrated by incubation for 10 min in each of the following; 30 % (v/v) ethanol, 50 % (v/v) ethanol, 70 % (v/v) ethanol, 90 % (v/v) ethanol, absolute ethanol and dried absolute ethanol. The absolute ethanol incubation was performed twice. The coverslips were placed specimen-side up in hexamethyldisilazane (HMDS) for 5 min at room temperature. This step was repeated once before removing coverslips from the 24 well tissue culture plate and placing them, specimen-side up, onto blotting paper to dry out. To allow specimens to dry out completely, they were placed in a dessicator overnight. Samples were then mounted onto aluminium pin stubs (Agar Scientific), secured by double-sided copper tape (Agar Scientific). Conductivity was increased by painting a layer of silver paint (Agar Scientific) around the edge of the glass coverslip, connecting it to the aluminium stub. Samples were then coated in a layer of gold palladium, 20 nm in thickness, using a Polaron SC515 SEM coating system.

2.3.10.2 Visualisation of samples by Scanning Electron Microscopy

Imaging was performed using a JSM 6400 scanning electron microscope at 6kV. Digital images were acquired via an ADDA 3 capture system at 2048 x 1536 pixel resolution.

2.4 Companies from which equipment, chemicals and kits were purchased

Agar Scientific	Aluminium pin stubs, double-sided copper tape, silver paint
BDH	Giemsa stain, saponin
Beckman	GS-15R centrifuge
Beckman Coulter	Avanti J-26xP centrifuge, Allegra™ X-12R centrifuge
Beckton Dickinson	10 ml, 5 ml, 2 ml and 1 ml sterile plastic syringes, Microlance™ 3 needles (26 G x 5/8”) and (21 G x 1 1/2”)
BioRad	Transblot SD semi-dry transfer cell, precision plus all blue protein standards, gene pulser electroporation cuvette (0.4 cm), GenePulser® II electoporator, Capacitance extender II, Protein assay reagent
Calbiochem	G418 sulfate
ClonNAT	Nourseothricin
Dionex	UltiMate HPLC system (UltiMate 3000 pump, autosampler and variable wavelength detector, RF 2000 fluorescence detector and UCI-50 universal chromatography interface)
Eppendorf	Microcentrifuge 5415D, Amber microcentrifuge tubes (1.5 ml)
Eurogentec	All oligonucleotide primers
Floustar	OPTIMA fluorescence plate reader

GE Healthcare	Hyperfilm ECL, ECL-plus detection kit, Hypercassettes (18 x 24 cm), AlkPhos direct labelling reagents, CDP-Star detection reagent, Hybond-N+ nylon membrane
Invitrogen	Accuprime *Pfx* Supermix, PCR Supermix, chemically competent *E. coli* TOP10 cells, chemically competent *E. coli* DH5α cells, RPMI 1640 (with 25 mM HEPES, L-Glutamine), gentamycin, penicillin/streptomycin, NuPAGE 10 % Bis/Tris gels, 20 x MOPS buffer, Xcell Surelock™ Mini-cell apparatus, phleomycin 20 mg/ml, HOMEM medium (ref 041-946-99M)
Kinesis	HPLC crimp vials (0.3 ml), HPLC vial snap caps
Kodak	Autoradiography film
Melford	Ampicillin, Isopropyl-beta-D-thiogalactopyranoside (IPTG), NADPH
Molecular Devices	Versamax tunable microplate reader
New England Biolabs	All restriction endonucleases, T4 DNA ligase
Novagen	pET28a+ expression vector
Nunc	1.0 ml cryotubes, 16-well Lab-tek™ tissue culture slides
Phenomenex	Gemini C18 chromatography column, SecurityGuard guard column kit, 0.2 µm nylon filters
Polaron	SC515 SEM coating system
Promega	pGEMT-easy cloning kit, 1 kb DNA ladder
Qiagen	Qiaprep spin DNA miniprep kit, Qiaquick gel extraction kit, Ni-NTA agarose

Roche	Hygromycin B
Sartorius	0.2 µm syringe filters
Schleicher & Schuell	Protran nitrocellulose
Shimadzu	UV-2501 PC spectrophotometer
Sigma	6k15 centrifuge, all chemicals unless otherwise stated
Stratagene	StrataClone blunt PCR cloning kit
UVP Laboratory Products	UV crosslinker
Zeiss	Axioplan 2 microscope

3. *Leishmania donovani, L. major* and *L. infantum* TDR1: Analysis of gene deletion and production of recombinant protein.

3.1 Introduction

Thiol dependent reductase 1 (TDR1) of *Leishmania* is a 49.9 kDa protein of which the physiological role remains unclear (Denton et al., 2004). The amino acid sequence alignment of TDR1 of various *Leishmania* species with a thiol dependent reductase, TcAc2, of the related organism *Trypanosoma cruzi* (Schöneck et al., 1994), is shown in Figure 3.1.

The protein is made up of two domains with differing active site residues. The N-terminal domain contains the characteristic glutaredoxin/thioredoxin active site, CXXC, while the C-terminal domain active site is more similar to the active sites of the omega class glutathione S-transferases. Although the precise function of TDR1 remains unclear, it has been suggested that the two domains may function together as an electron donor and a reductase, respectively. TcAc2 has a conserved N-terminal active site, but the active site residues of the C-terminal domain differ.

TDR1 has been shown to reduce inactive pentavalent antimonials, SbV, to the active trivalent form, SbIII, *in vitro* (Denton et al., 2004), suggesting that the protein may be involved in the activation of SbV *in vivo*. This possible physiological role of the protein is supported by the evidence that TDR1 is expressed approximately 10-fold higher in amastigotes than promastigotes, possibly explaining the specificity of the drug to the amastigote stage of the parasite (Denton et al., 2004). TDR1 also shows some similarity and a conserved active site (Figure 3.1) to the three classes of arsenate reductases that have been described previously (Mukhopadhyay et al., 2002). The arsenate reductases have a role in the detoxification of arsenic by reduction followed by excretion of drug-thiol conjugates from the cell. Therefore it has been suggested that TDR1 could be involved in the detoxification of arsenic and other heavy metals from *Leishmania*.

The sequence homology between TDR1 of different *Leishmania* species suggests the conservation of an important function, particularly given that the presumed active sites are highly conserved. Table 3.1 shows the percentage identity of the different proteins included in the alignment.

The aim of this study was to investigate the role of TDR1 in *L. donovani* through over-expression and gene replacement studies and subsequent analysis of phenotype.

3.2 Gene deletion of *TDR1* in *L. major*

The removal of the *TDR1* gene from *L. major*, by two rounds of homologous recombination, was anticipated to result in a phenotypic effect that may clarify the role of TDR1 in the parasites. The design of the knock-out plasmids as well as both rounds of transfection were carried out by a previous PhD student in the laboratory.

3.3 Analysis of *L. major* Δ*tdr1* A and Δ*tdr1* B

The replacement of both *TDR1* alleles of the two clones generated, *L. major* Δ*tdr1* A and Δ*tdr1* B, with DNA from the plasmids pGL345 and pGL1033, was confirmed by Southern blot analysis. *L. major* wild-type (WT) as well as Δ*tdr1* A and Δ*tdr1* B were harvested from stationary growth phase and the genomic DNA was extracted. 1-2 µg of DNA was digested overnight using the restriction endonuclease *Xho*I, and separated by DNA gel electrophoresis before Southern blotting. The sizes of the expected DNA fragments can be seen in Figure 3.2. The blot was probed with the labelled 3' flanking region of *TDR1*, and the resulting Southern blot in shown in Figure 3.3. The 4.9 kb band that was seen in the WT lane represents the fragment of DNA detected by the labelled 3' flanking region of the gene. In each of the lanes corresponding to Δ*tdr1* A and Δ*tdr1* B, two bands were seen at 7.0 kb and 7.7 kb, indicating that the knock-out DNA had integrated in the correct place. However, a faint band was visible in the lane containing Δ*tdr1* A at 4.9 kb, suggesting that the clone selection procedure was not optimal and resulted in a mixed population of knock-out and WT parasites.

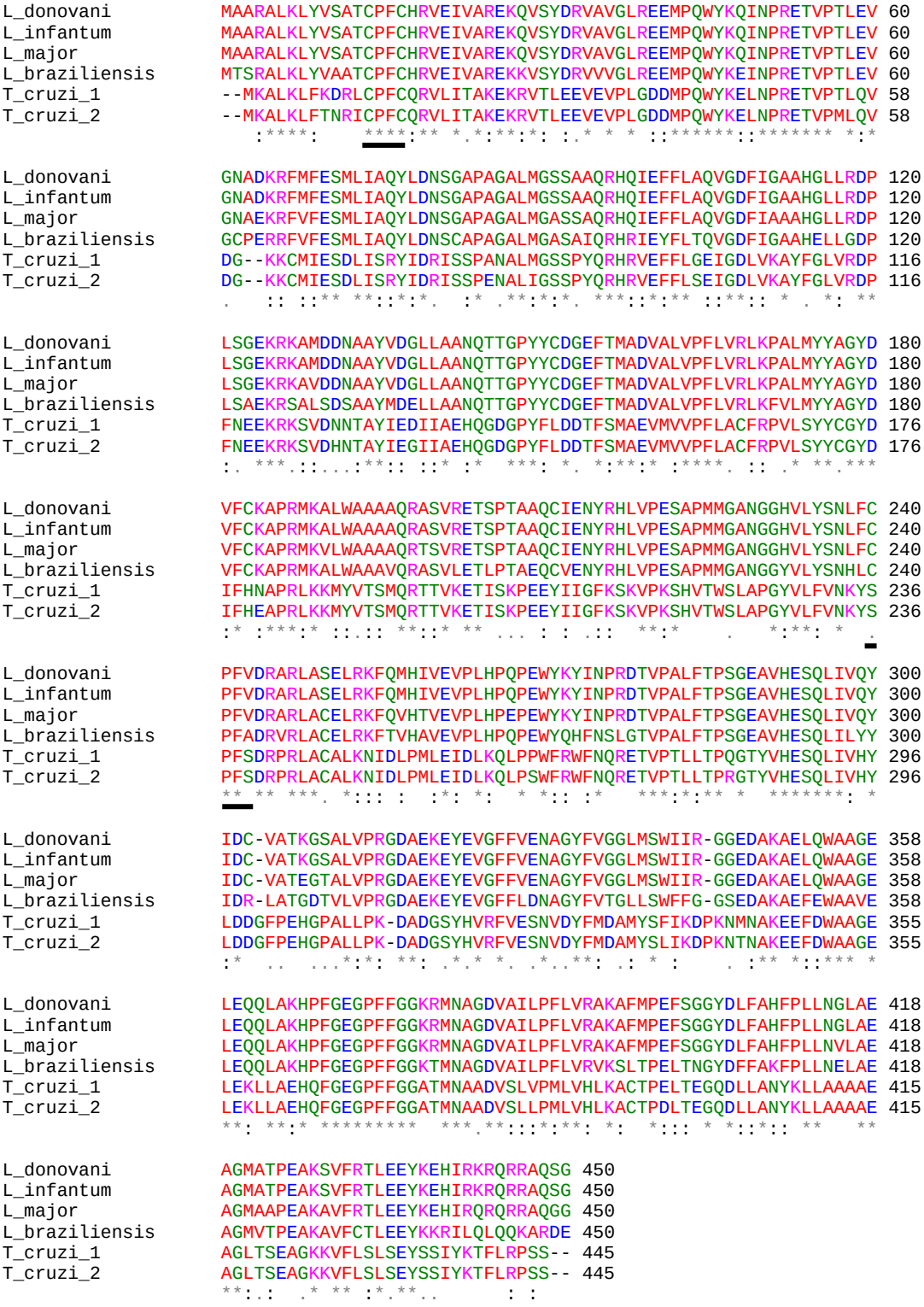

Figure 3.1 Amino acid alignment of *L. donovani* TDR1 with TDR1 of other *Leishmania* and TcAc2 of *T. cruzi*.
ClustalW alignments of *L. donovani* TDR1 (sequenced), *L. infantum* TDR1 (Genedb LinJ33_V3.0260), *L. major* TDR1 (Genedb LmjF33.0240), *L. braziliensis* TDR1 (Genedb LbrM31_V2.0550), *T.cruzi* TcAc2 (Genedb Tc00.1047053503419.30) and *T. cruzi* TcAc2 (Genedb Tc00.1047053509105.70), were combined using the program T-Coffee (Notredame et al., 2000, Poirot et al., 2003) showing (*) identical residues, (:) conserved residues and (.) homologous residues. Residues are coloured as follows: A, V, F, P, M, I, L and W are shown in red; D and E are blue; R, H and K are magenta; S, T, Y, H, C, N, G and Q are green and all other residues are grey. Presumed active sites are underlined. T_cruzi_1 and T_cruzi_2 are variant haplotypes of TcAc2.

	Tc_2	Tc_1	Lb	Lm	Li	Ld
Tc_2		96	44	46	45	45
Tc_1			44	46	46	46
Lb				80	80	80
Lm					96	96
Li						100
Ld						

Table 3.1 Amino acid sequence identities of TDR1 and TcAc2 of trypanosomatids.
Percentage identities of the amino acid sequences of TDR1 of *L. donovani*, *L. infantum*, *L. major* and *L. braziliensis* and TcAc2 of *T. cruzi*. Ld, *L. donovani* TDR1 (sequenced); Li, *L. infantum* TDR1 (Genedb LinJ33_V3.0260); Lm, *L. major* TDR1 (Genedb LmjF33.0240); Lb, *L. braziliensis* TDR1 (Genedb LbrM31_V2.0550); Tc_1, *T.cruzi* TcAc2 (Genedb Tc00.1047053503419.30); Tc_2, *T. cruzi* TcAc2 (Genedb Tc00.1047053509105.70).

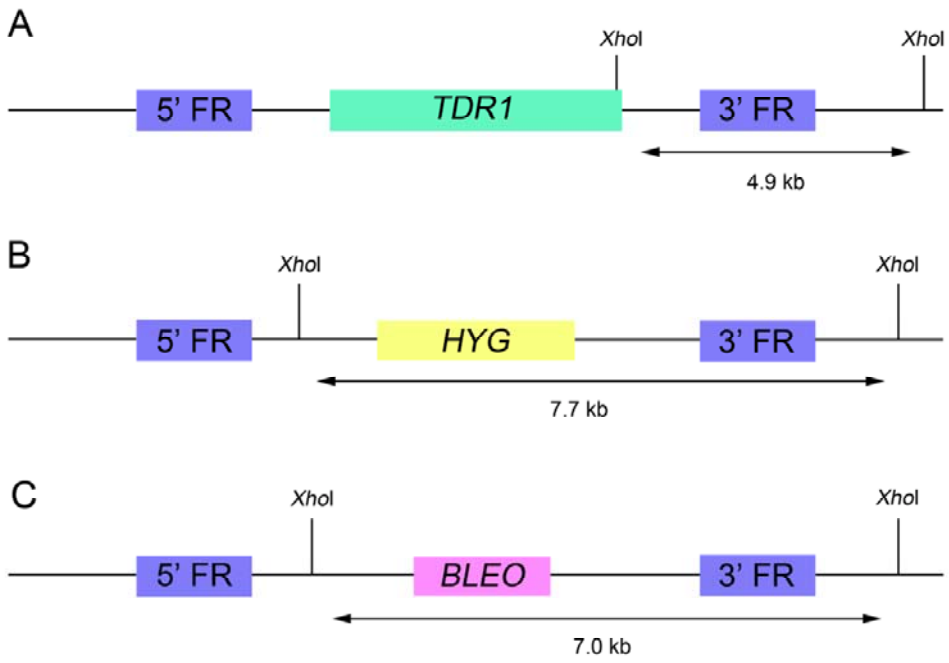

Figure 3.2 Schematic representation of the *TDR1* locus and plasmid constructs used for gene replacement in *L. major*.
A = *TDR1* locus, B = pGL345 and C = pGL1033. Positions of *Xho*I restriction sites are shown, with the sizes of DNA fragments expected when digested with *Xho*I and probed with the 3' flanking region.

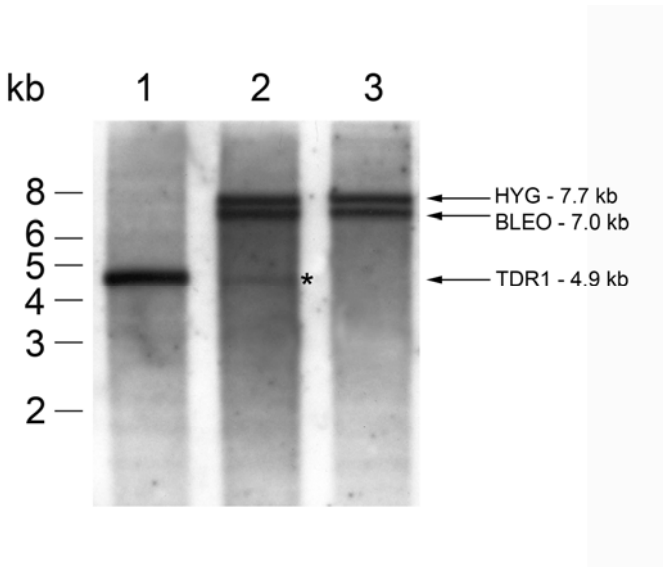

Figure 3.3 Southern blot analysis of *L. major* Δ*tdr1* lines
Genomic DNA (1 µg) from *L. major* WT (lane 1), *L. major* Δ*tdr1* A (lane 2) and *L. major* Δ*tdr1* B (lane 3) was digested overnight at 37 ºC with *Xho*I and resolved on a 0.8 % agarose gel. The blot was probed with the 3' flanking region of *L. major tdr1* labelled with an alkaline phosphatase, detected by CDP-Star detection reagent (G.E. Healthcare) and chemiluminescence was detected by autoradiography film. The band at 4.9 kb represents the endogenous gene and the bands at 7.7 kb and 7.0 kb show the correct integration of the *HYG* and *BLEO* knock-out cassettes, respectively. The 4.9 kb band visible in lane 2 means that the endogenous gene still exists in a proportion of the cells.

Alternatively, the gene, chromosome or the entire genome of the organism may have been duplicated in some of these parasites to try and counteract any detrimental effect that the loss of TDR1 may have (Cruz et al., 1993).

Due to the existence of only one verified *TDR1* null mutant, Δ*tdr1* B will be referred to as *L. major* Δ*tdr1* from here on.

3.4 Generation of *L. donovani Δtdr1* null mutant lines

Specific oligonucleotide primers were designed using the *L. infantum* genome due to the lack of an available *L. donovani* sequence at the time, which were then used to amplify the 3' and 5' flanking regions of *tdr1*. PCR products were subcloned into pGEMT-Easy and ultimately into the vectors pGL345, pGL1033 and pGL158, which contain the *hygromycin phosphotransferase*, *dihydroxybiphenyl dioxygenase* and *nourseothricin acetyltransferase* genes respectively, conferring resistance to hygromycin, bleomycin/phleomycin and nourseothricin (Figure 2.4). The constructs containing the 3' and 5' flanking regions and the antibiotic resistance markers were digested out of the vectors and the linear DNA was purified, sterilised by ethanol precipitation and used to transfect mid-log phase *L. donovani* promastigotes. Two independent rounds of transfection were carried out. After each one, parasites were allowed to recover for 24 h during which time the knock-out DNA was expected to integrate into the genomic DNA of a proportion of cells, by homologous recombination. The corresponding selective drugs were added after this time and the cultures were diluted to obtain clonal lines.

3.5 Analysis of attempts to generate *L. donovani* Δ*tdr1*

Clones that were selected by serial dilution with the appropriate drug pressure were subjected to further analysis by either PCR, to amplify a region of DNA from a point within the knock-out cassette to a point outside the 1 kb flanking region of *TDR1*, or by Southern blot, probing with a labelled flanking region. Table 3.2 details the attempts that were made to create a *TDR1* null mutant in *L. donovani*. Three attempts were made in total to create single allele knock-outs of *TDR1*. Integration of the knock-out DNA in the correct place and

subsequent removal of one copy of *TDR1* was shown to have occurred in all of the clones that grew from selection plates. However, all attempts to replace the second allele of *TDR1* appeared to be unsuccessful. Over the course of three attempts, a total of 76 'clones' were selected using two different selection methods and each one grown under the pressure of the two relevant antibiotics corresponding to the two knock-out cassettes used to transfect. Each of the 76 'clones' were then analysed by PCR or Southern blot and the results clearly showed that the knock-out DNA had correctly integrated into the parasite genome, which would explain the ability of the parasites to grow under the selective drug pressure. However, the endogenous gene was still shown to exist in all the clones. Figure 3.4 shows an example Southern blot of two *L. donovani* double allele *TDR1* gene replacement clones, given the names Δ*tdr1* A and Δ*tdr1* B, clearly showing bands of the at 7.0 and 7.7 kb indicating integration of the knock-out DNA in the correct places, but also show bands at 4.9 kb, which indicate at least one copy of the *TDR1* gene is still present.

In some cases, when attempts are made to replace essential genes in *Leishmania*, the genome duplicates itself to try to overcome the detrimental effect that would inevitably occur if the gene replacement was successful. This has been previously reported by Cruz et al., 1993. The genomic content of the clonal lines was investigated further by FACS analysis and an example of both *L. donovani* WT and one of the clonal lines created using knock-out DNA derived from the plasmids pGL345 and pGL1033 are shown in Figure 3.5.

The large peaks at 200 FL2-area on both of the tracings represent the vast majority of parasites with the genomic content corresponding to one nucleus and one kinetoplast. The small peak at approximately 400 FL2-area represents a small proportion of the cells that are preparing to divide and consequently have double the genomic content of *L. donovani* that are not dividing. The results are as expected as the cells used in this experiment were taken at stationary phase, so fewer cells would be expected to be preparing for division. Since the genomic content of the cells from the clonal lines was not found, in any case, to be different to the genomic content of WT parasites, the endogenous gene could not have still been present due to a duplication of the parasite's entire genomic content.

	Single allele gene replacement		Double allele gene replacement	
Attempt	No. of clones selected	No. of clones verified	No. of clones selected	No. of clones verified
1	4	4	2	0
2	4	4	4	0
3	3	3	70*	0

Table 3.2 Attempts to create *L. donovani* Δ*tdr1*.
The number of clones selected after one and two rounds of transfection with knock-out DNA, and the number of clones verified, either by Southern blot or by PCR. * The increased number of clones selected in this case was due to a different method used. Both methods are detailed in Section 2.3.2.3. Plasmids derived from pGL345, pGL1033 and pGL158 were used during the first round of transfection, indicating that they are not deficient in any way, and are capable of replacing genes in the correct location.

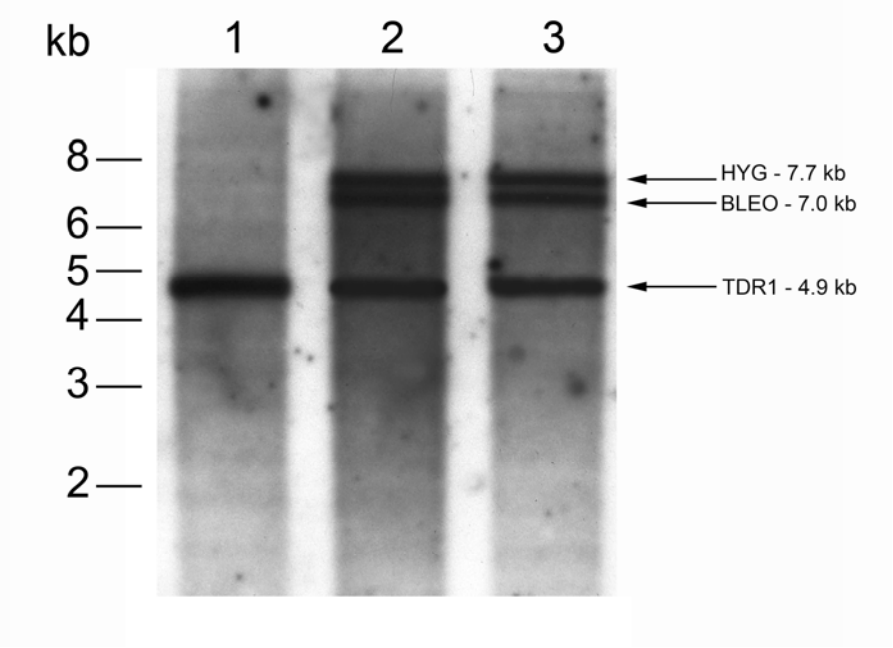

Figure 3.4 Southern blot analysis of two *L. donovani* double allele *TDR1* gene replacement clones.
Genomic DNA (1 µg) from *L. donovani* WT (lane 1), *L. donovani* Δ*tdr1* A (lane 2) and *L. donovani* Δ*tdr1* B (lane 3) was digested overnight at 37 ºC with *Xho*I and resolved on a 0.8 % agarose gel. The blot was probed with the 3' flanking region of *TDR1* labelled with an alkaline phosphatase, detected by CDP-Star detection reagent (G.E. Healthcare) and chemiluminescence was detected by autoradiography film. The band at 4.9 kb represents the endogenous gene and the bands at 7.7 kb and 7.0 kb show the correct integration of the *HYG* and *BLEO* knock-out cassettes respectively. The 4.9 kb band visible in all lanes is indicative of the presence of the endogenous gene.

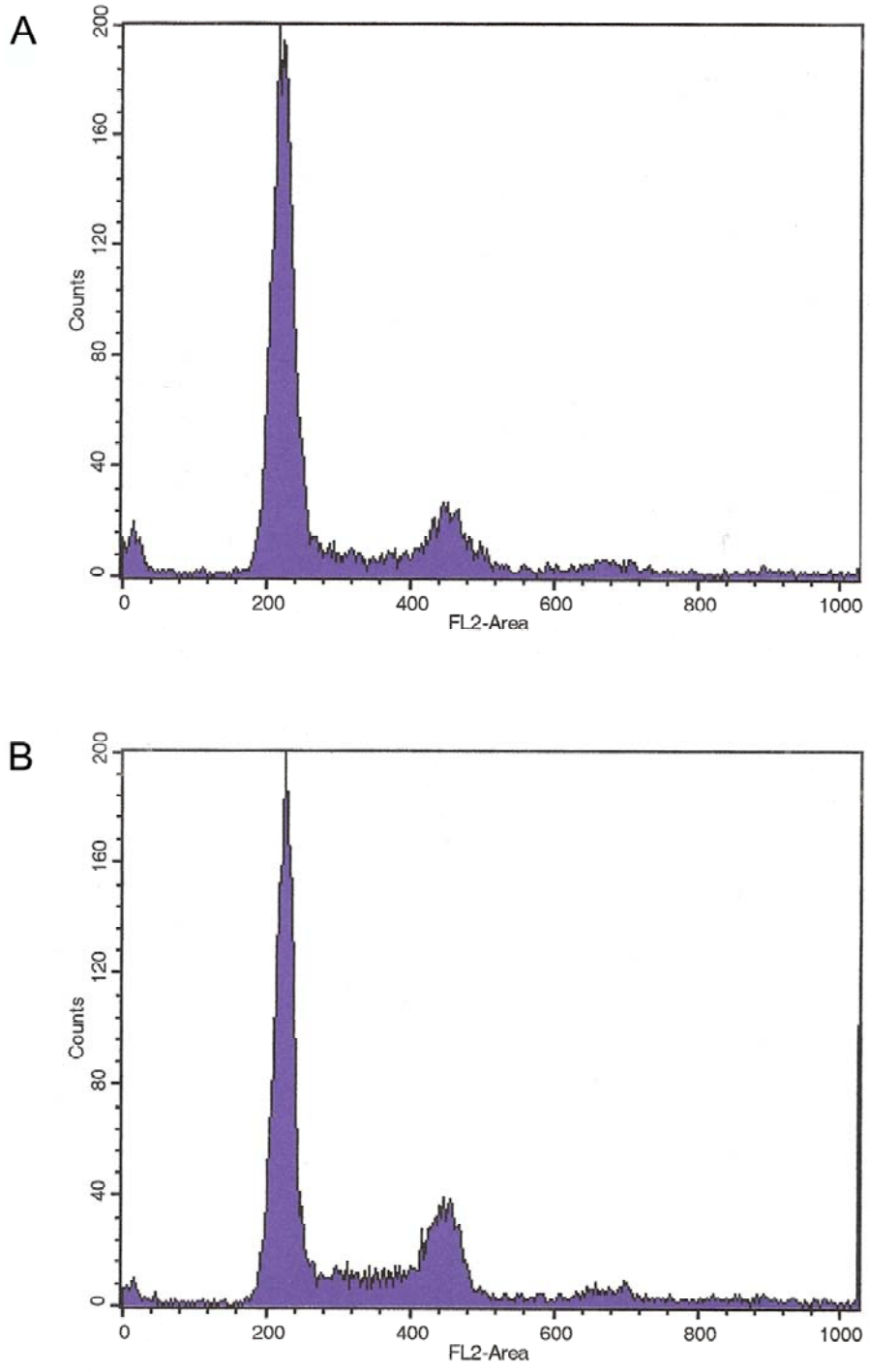

Figure 3.5 Effect of duplication of chromosome 33 on ploidy of *L. donovani* promastigotes. FACS analysis was performed on *L. donovani* WT promastigotes and *L. donovani* promastigotes that had been subjected to two rounds of gene replacement, but retained at least one copy of the endogenous gene. A = *L. donovani* WT, B = *L. donovani* pGL345/pGL1033. Peaks at 200 FL2-area represent cells containing 1 nucleus and 1 kinetoplast and peaks at 400 FL2-area represent cells containing double the genomic content.

The results suggest that given the integration of the knock-out DNA in the correct place, the ability of the parasite lines to grow in the presence of drugs and the results of the FACS analysis, the parasites have undergone a chromosome duplication that was not detectable by FACS.

The PCR primers used to amplify the 3' and 5' flanking regions of *TDR1* and make the knock-out constructs for *L. donovani*, were also used by another PhD student, Ana Marta Silva, to attempt to create a *L. infantum TDR1* null mutant line. One clonal line was verified as *L. infantum* Δ*tdr1* and was analysed along with *L. major* Δ*tdr1* to clarify any phenotypic effect of the loss of TDR1 in the two *Leishmania* species that cause two different clinical manifestations of disease. Due to time constraints, a parasite line re-expressing TDR1 in the *L. infantum* Δ*tdr1* was not generated.

3.6 Generation of *L. major* TDR1 re-expressing line

To ensure any phenotypic difference observed between the *L. major* WT and the *TDR1* null mutant lines was due entirely to the loss of the gene and not a result of the genetic manipulation techniques, a re-expressing line was created in which TDR1 was expressed, extra-chromasomally, in *L. major* Δ*tdr1*.

Specific oligonucleotide primers were designed, using the *L. major* genome, and used to amplify *TDR1*. PCR products were subcloned into pGEMT-Easy and ultimately into the vector pGL102 which contains the *neomycin phosphotransferase* gene which confers resistance to neomycin (Figure 2.6). pGL102 containing *TDR1* was used to transfect mid-log phase *L. major* Δ*tdr1* promastigotes. Cultures were allowed to recover overnight before being subjected to the selective drug pressure of neomycin phosphotransferase.

3.7 Phenotypic analysis of *L. major* Δ*tdr1* and *L. infantum* Δ*tdr1* null mutant parasite lines

3.7.1 Western blot analysis of *L. major* Δ*tdr1* and Δ*tdr1* [TDR1]

Western blot analysis confirmed that *L. major* Δ*tdr1* [TDR1] was indeed expressing TDR1 (Figure 3.6). When compared to the expression of TDR1 in *L. major* WT cells, the blot suggests that the protein is, in fact, over-expressed in Δ*tdr1* [TDR1]. No visible band at 49.9 kDa in the lane containing protein extract from Δ*tdr1*, confirms that TDR1 is not expressed by this line.

3.7.2 Growth and morphology

Growth of *L. major* WT, Δ*tdr1* and Δ*tdr1* [TDR1] was monitored to identify any differences between the parasites due to the gene deletion. Promastigote cultures were counted and diluted to the same concentration, then counted at 24 h intervals for 7 days.

Figure 3.7 shows the growth of *L. major* WT, Δ*tdr1* and Δ*tdr1* [TDR1] over 7 days. The results suggest that there is no growth defect between any of the parasite lines. Each of the parasite lines go through the same lag, exponential growth and stationary phases at the same time and also reach a similar cell density.

The growth of *L. infantum* WT and Δ*tdr1* was also monitored over 7 days and the results are shown in Figure 3.8. Similarly, there is no growth defect between either of the *L. infantum* lines, with the same final cell density achieved by both WT and Δ*tdr1* after going through the typical growth stages.

L. major Δ*tdr1* and Δ*tdr1* [TDR1] were compared with *L. major* WT by phase contrast microscopy, and no morphological differences could be identified. In addition, *L. infantum* Δ*tdr1* was compared with *L. infantum* WT in the same way and, again, there were no visible differences in morphology.

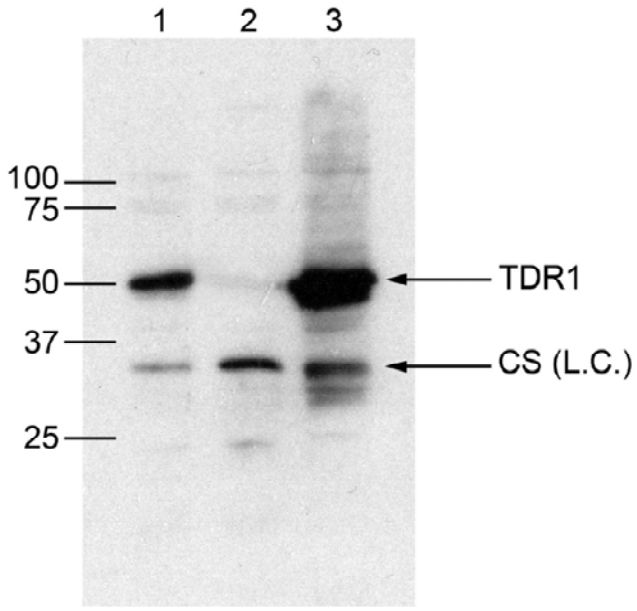

Figure 3.6 Western blot analysis of *TDR1* expression in *L. major* promastigotes.
Lane 1, *L. major* WT; lane 2, *L. major* Δ*tdr1*; lane 3, *L. major* Δ*tdr1* [TDR1]. 2.5 µg of soluble parasite lysate was loaded per lane. CS was used as a loading control (L.C.). The positions of the proteins are indicated to the right of the image.

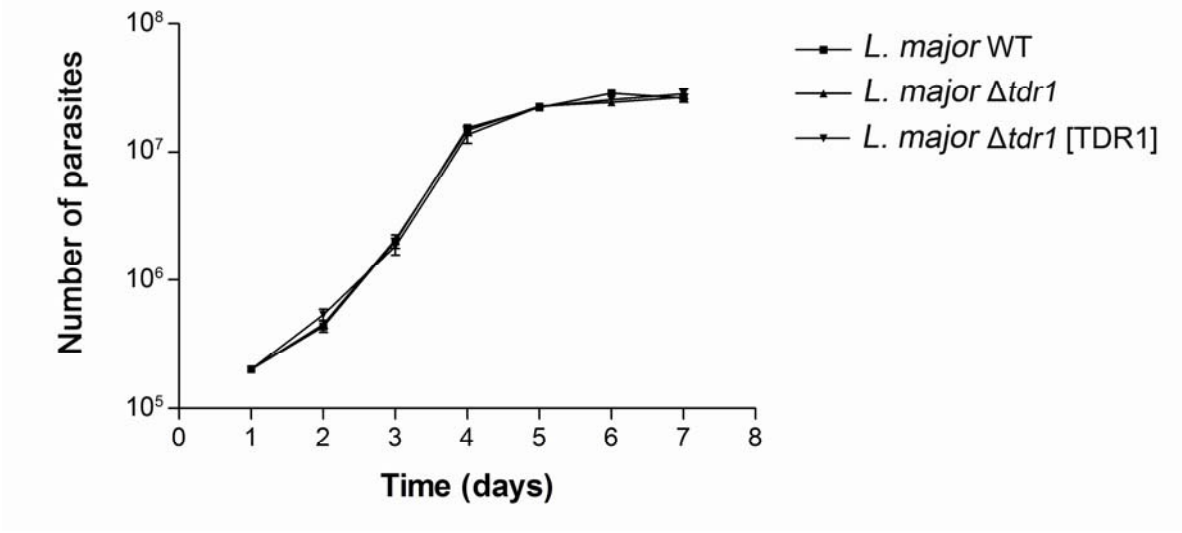

Figure 3.7 Growth curve of *L. major* WT, Δ*tdr1* and Δ*tdr1* [TDR1] promastigotes.
Cultures were seeded at a concentration of 2 x 10^5 parasites/ml and were counted daily. Δ*tdr1* : TDR1 was grown in 50 µg/ml G418.

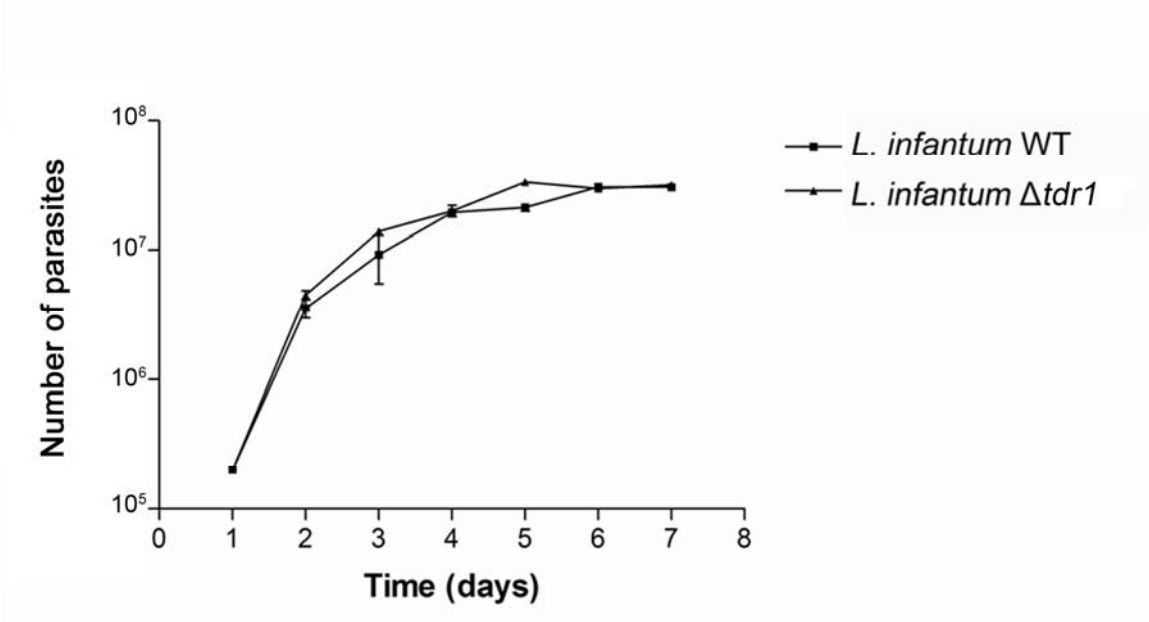

Figure 3.8 Growth curve of WT and Δ*tdr1 L. infantum* promastigotes.
Cultures were seeded at a concentration of 2 x 10^5 parasites/ml and were counted daily.

3.8 *In vitro* infectivity of *L. major* Δ*tdr1* and Δ*tdr1* [TDR1] in macrophages

The ability of *L. major* WT, Δ*tdr1* and Δ*tdr1* [TDR1] to infect murine peritoneal macrophages was assessed *in vitro*. Macrophages were extracted and incubated for 24 h in tissue culture slides at 37 ºC with 5 % CO_2, 95 % air, before infecting with stationary phase promastigotes at a ratio of 5:1. Infections were incubated for a further 6 days at 37 ºC with 5 % CO_2, 95 % air, carefully replacing used medium with fresh after 3 days post-infection.

To investigate the ability of these parasites to infect macrophages, the percentage infection was determined over the course of three independent experiments and the results are shown in Figure 3.9. After 6 days, *L. major* WT parasites had established an infection in 78 % of macrophages, and there was no difference between the level of infection of *L. major* Δ*tdr1*, which shows a percentage infection of 84 %. However, the results show that Δ*tdr1* [TDR1] only infects 45 % of macrophages, almost half that of the WT and Δ*tdr1*. According to these findings, there appears to be no effect on the infection of macrophages due to the deletion of *TDR1* in *L. major*. The re-expressing line shows a statistically significant difference ($p = <0.001$) in percentage infection when compared to the WT. Since these parasites are actually over-expressing TDR1, these findings suggest that the over-expression of TDR1 reduces the ability of the parasites to establish an infection of macrophages *in vitro*.

In order to examine the ability of *L. major* WT, Δ*tdr1* and Δ*tdr1* [TDR1] to proliferate within peritoneal macrophages, the mean number of parasites per infected macrophage was also determined and the results are shown in Figure 3.10. Despite the similar infection levels of *L. major* WT and Δ*tdr1*, after a period of 6 days post-infection, there is an average of 4.7 parasites per macrophage infected with *L. major* WT, while *L. major* Δ*tdr1* shows an average

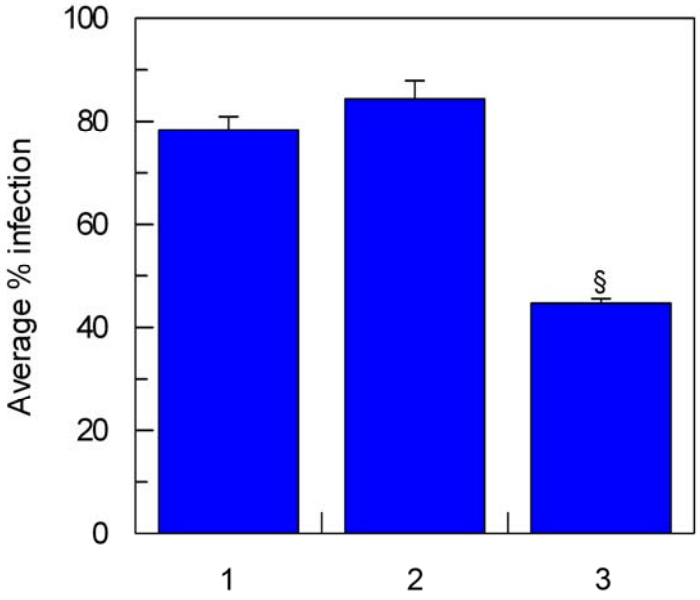

Figure 3.9 Infectivity of *L. major* WT, *tdr1* and Δ*tdr1* [TDR1] promastigotes in macrophages.
Stationary phase promastigotes were used to infect peritoneal macrophages at a ratio of 5:1 and were incubated for 6 days. Each value is the mean of 3 replicates ± S.E.M. §, $p < 0.001$, compared to *L. major* WT, by unpaired t-test.

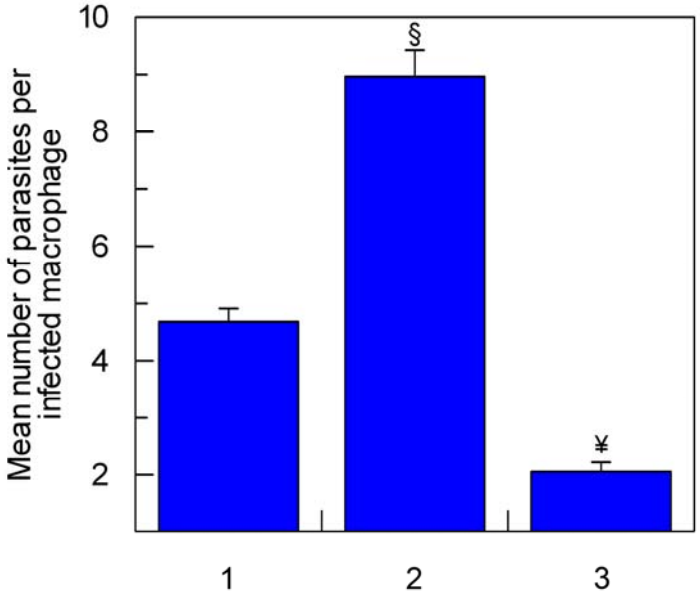

Figure 3.10 Proliferation of *L. major* WT, *tdr1* and Δ*tdr1* [TDR1] promastigotes in macrophages.
Stationary phase promastigotes were used to infect peritoneal macrophages at a ratio of 5:1 and were incubated for 6 days. Each value is the mean of 3 replicates ± S.E.M. §, $p = 0.001$ and ¥, $p = 0.001$, compared to *L. major* WT, by unpaired t-test.

of 9.0 parasites per macrophage. This difference is statistically significant, yielding a p-value of 0.001 when compared by unpaired t-test. This suggests that the deletion of *TDR1* is, in fact, of benefit to the parasites when establishing an infection in macrophages. The mean number of parasites per macrophage infected with *L. major* Δ*tdr1* [TDR1] is significantly less than WT, with a mean number of 2.1 parasites per infected macrophage. This is less than half the number seen in macrophages infected by WT parasites and approximately 4-fold less than the number of parasites seen in macrophages infected by Δ*tdr1*. This is again a statistically significant difference (P-value = 0.001) when compared to WT by unpaired t-test, and suggests that the benefit of the absence of TDR1 is reversed when the protein is re-expressed and actually results in both a percentage infection and mean number of parasites per infected macrophage even lower than WT, due to the over-expression of TDR1 in this line.

In summary, Δ*tdr1* [TDR1] infects approximately half the percentage of macrophages as WT and Δ*tdr1*. The mean number of Δ*tdr1* parasites per infected macrophage is double that of the WT and approximately 4-times higher than that of Δ*tdr1* [TDR1].

3.9 Thiol analysis of *L. major* and *L. infantum tdr1* mutant parasite lines

As part of the phenotype analysis of the *L. major* and *L. infantum TDR1* null mutant lines, total intracellular thiol levels in these parasites were analysed by HPLC. The level of expression of TDR1 undoubtedly affects the ability of the *L. major* parasites to infect and proliferate within macrophages. By quantifying the levels of intracellular thiols, any differences observed between *L. major* WT, Δ*tdr1* and Δ*tdr1* [TDR1] may shed light on reasons that ultimately may have an effect on the ability of these parasites to infect and proliferate within macrophages.

A number of tests were performed prior to the thiol quantification of any parasite lines, to ensure the complete derivatisation of thiols, after being reduced by DTT. Initially known amounts of thiol standards were reduced by two different concentrations of DTT, 1 mM and 10 mM, before derivatisation with

monobromobimane, and subsequent analysis by HPLC. No differences in thiol amounts were detected between the samples that had been reduced by 1 mM DTT and those that had been reduced by 10 mM DTT. Therefore, 1 mM DTT was used throughout this study with the confidence that it was sufficient to fully reduce the thiols in the samples.

Standard curves were generated for the six thiols to be detected; cysteine, glutathione, trypanothione, γ—glutamyl cysteine, cysteinyl glycine and homocysteine, by reduction with 1 mM DTT, derivatisation with monobromobimane and analysis by HPLC. 0 – 350 pmoles of each thiol was used, as linear relationships between peak area (mV) and thiol amounts were identified within this range. Analysis of individual thiols was performed from six independent replicates, each replicate consisting of two injections. Thiol mixes of the concentration range already tested were also analysed by HPLC, to confirm the standard curves. Again, these mixes were analysed from six independent replicates, replicate consisting of two injections. The C18 reversed-phase chromatography column was replaced once during this study and the generation of standard curves was repeated for the new column, as described above. Figure 3.11 shows an example chromatogram of a mix of 250 pmoles of each of the six thiol standards as well as an example chromatogram of *L. major* WT parasites.

To ensure the complete reduction and subsequent derivatisation of thiols in a parasite extract, samples were spiked with known amounts of cysteine, trypanothione and glutathione, and the results are shown in Table 3.3. The amounts that were quantified were compared with the amounts of thiols that were quantified for the same parasite line without any addition. The results show that the difference between the appropriate thiol is approximately equal to the amount that was added to the parasite extract. Since this amount is rather small, the detection of the added amount can be looked on as evidence not only of the sensitivity of the technique, but that the thiol content of the entire samples were both fully reduced and derivatised.

Stationary phase promastigotes to be analysed were counted and harvested, before lysing the cells, reducing thiols with DTT and derivatising intracellular

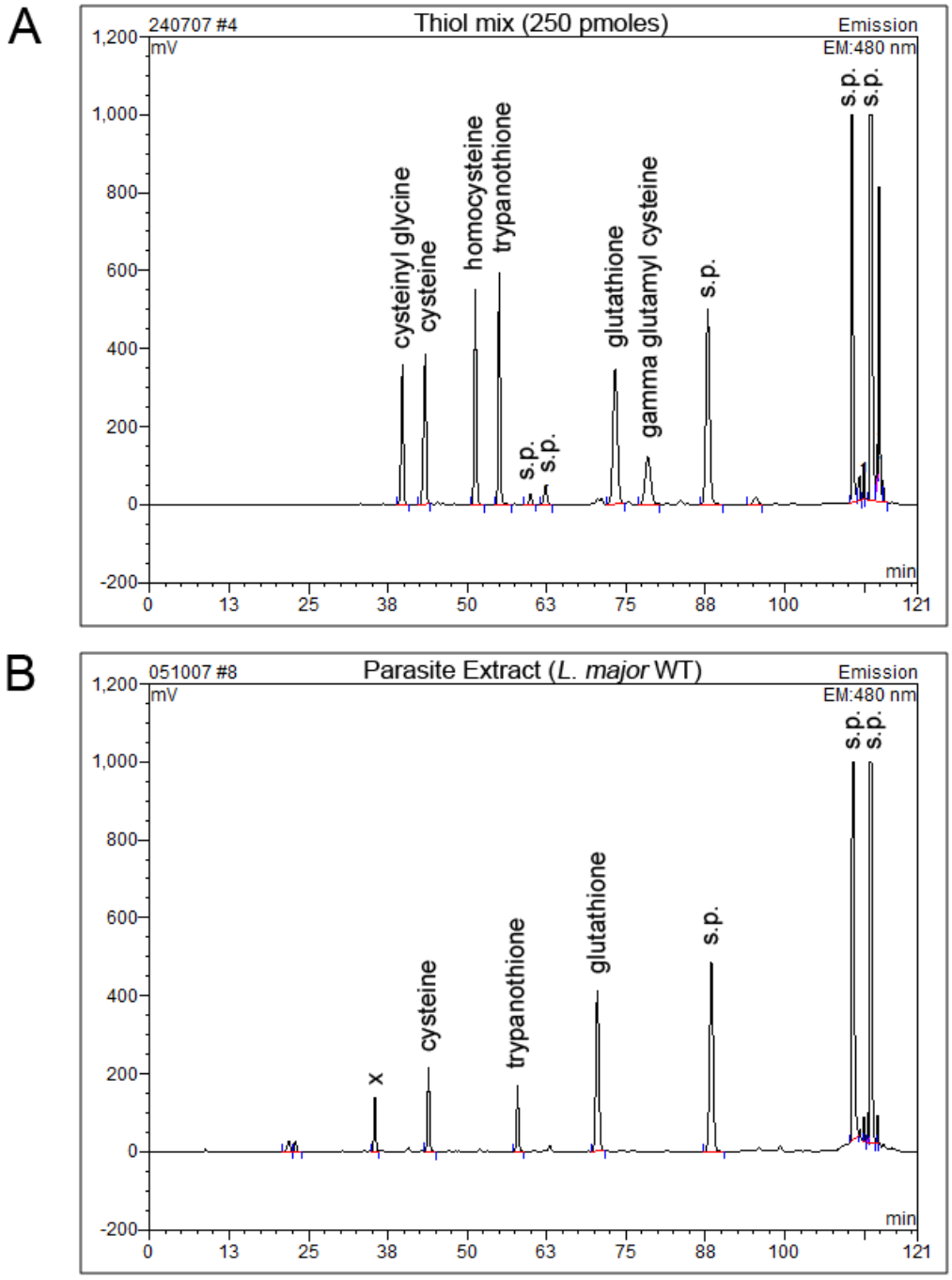

Figure 3.11 HPLC analysis of low-molecular-weight thiols of *Leishmania*.
A = Reversed-phase HPLC separation of a mixture of monobromobimane-derivatized thiol standards. A mixture of cysteine, cysteinyl-glycine, homocysteine, trypanothione, glutathione and gamma glutamyl cysteine (all 250 pmoles) were injected after reduction with DTT. B = An example chromatogram of the thiol pattern of *L. donovani* WT. X, unidentified peak, s.p., solvent peak. Derivatization and chromatographic conditions are described in Sections 2.3.6.2 and 2.3.6.3.

	Amount of thiol detected (pmoles)		
	Cysteine	Trypanothione	Glutathione
L. major WT	37.9	22.5	101.6
+ 40 pmoles cysteine	73.8	21.7	77.1
+ 40 pmoles trypanothione	32	67.9	107.3
+ 40 pmoles glutathione	31.5	25.4	141.5
L. donovani WT	30.1	56.2	202.3
+ 40 pmoles cysteine	78.1	71.1	209.9
+ 40 pmoles trypanothione	18.6	99.7	203.9
+ 40 pmoles glutathione	18.4	66.5	230.0

Table 3.3 Thiol content of parasite extracts supplemented with known amounts of cysteine, trypanothione and glutathione.
Stationary phase *L. major* and *L.donovani* promastigotes were harvested and lysed. Known amounts of cysteine, trypanothione and glutathione were added, individually, to the samples and they were then reduced by the addition of DTT and subsequently monobromobimane-derivatised. Thiols were derivatised by reversed-phase HPLC. Derivatization and chromatographic conditions are described in Sections 2.3.6.2 and 2.3.6.3.

thiols with fluorescent monobromobimane. Thiols were separated by HPLC using a C18 reversed-phase chromatography column, using the mobile phases 0.25 % acetic acid and 100 % acetonitrile. Up to 350 pmoles of each thiol was detected, as this was the concentration range shown to have a linear relationship between peak area and thiol concentration. Results were then multiplied to express the results in nmoles/10^8 parasites. Details of the derivatisation method as well as the separation program are given in materials and methods Sections 2.3.6.2 and 2.3.6.3.

The proportion of cysteine, glutathione and trypanothione, that make up the total thiol content of the parasites, changes quite significantly over the 6 day period in liquid culture. Figure 3.12 shows the thiol profile of *L. donovani* WT cells that have been harvested between days 2-7 of culture, and then reduced by DTT, derivatised and quantified by HPLC. In this study, all parasites used to infect macrophages were used at day 7 of liquid culture; therefore all parasites used in HPLC analysis were also taken at this time-point.

Thiol levels of *L. major* WT, Δ*tdr1* and Δ*tdr1* [TDR1] as well as *L. infantum* WT and Δ*tdr1* were quantified by HPLC and the results are shown in Table 3.4. There is clearly no significant difference in total intracellular levels of cysteine, trypanothione or glutathione between the *L. major* and *L. infantum* WT lines and their corresponding *TDR1* null mutant lines. There is also no difference between the total cysteine and total glutathione levels between the two groups of parasites. However, the total intracellular amount of trypanothione appears to be higher in the *L. infantum* lines compared to the *L. major* lines. It is possible, however, that due to the differences in thiol levels seen for *L. donovani* WT over the different growth stages of the parasites, that there is an effect on thiol levels caused by the deletion of *TDR1* that remains undetected. Future studies may involve quantification of total cysteine, trypanothione and glutathione levels at an earlier stage of culture, perhaps when the parasites are dividing and growing.

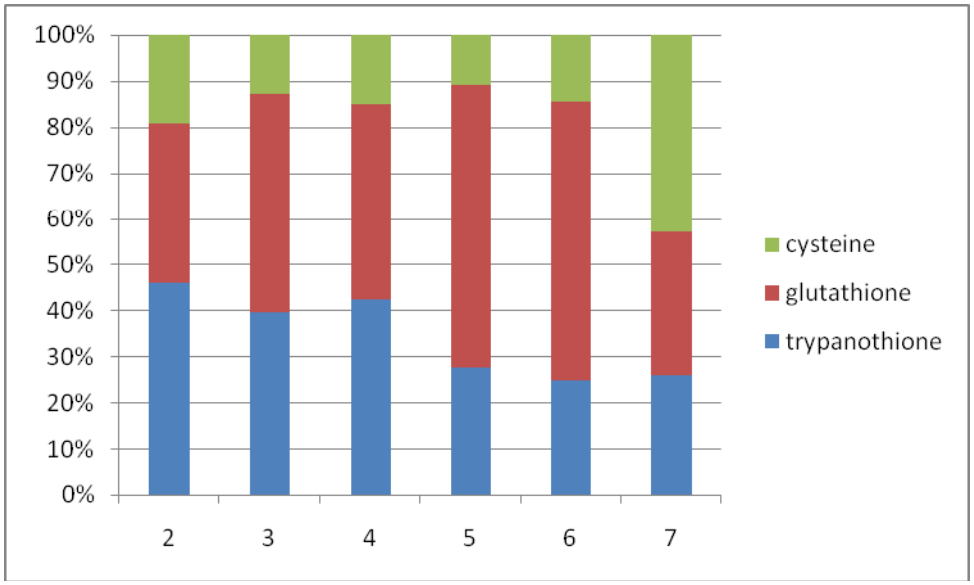

Figure 3.12 Thiol levels of *L. donovani* WT promastigotes over 6 days.
L. donovani WT promastigotes were harvested between day 2 and day 7 of liquid culture. Parasite extracts were monobromobimane-derivatized after reduction of thiols with DTT, and were separated by reversed-phase HPLC. Derivatization and chromatographic conditions are described in Sections 2.3.6.2 and 2.3.6.3.

	Thiol levels (nmoles per 10^8 parasites) ± S.E.		
	Cysteine	Trypanothione	Glutathione
L. major WT	2.1 ± 0.1	0.5 ± 0.1	3.4 ± 0.2
L. major Δ*tdr1*	1.9 ± 0.2	0.3 ± 0.02	3.8 ± 0.6
L. major Δ*tdr1* [TDR1]	2.1 ± 0.3	0.5 ± 0.1	3.7 ± 0.4
L. infantum WT	1.6 ± 0.2	1.0 ± 0.2	3.3 ± 1.0
L. infantum Δ*tdr1*	2.7 ± 0.8	0.7 ± 0.1	4.3 ± 0.9

Table 3.4 Thiol levels of *L. major* and *L. infantum* promastigotes.
Total cysteine, trypanothione and glutathione levels in *L. major* and *L. infantum* promastigotes per 10^8 parasites ± S.E.M. Parasite extracts were monobromobimane-derivatized after reduction of thiols with DTT, and were separated by reversed-phase HPLC. Derivatization and chromatographic conditions are described in Sections 2.3.6.2 and 2.3.6.3. Parasites were harvested at day 7 in liquid culture (Figures 3.7 and 3.8).

3.10 Effect of sodium stibogluconate on *L. major Δtdr1* and *Δtdr1* [TDR1] *in vitro* macrophage infection

Two possible physiological roles of TDR1 have been suggested. TDR1 has been shown *in vitro* to enzymatically reduce inactive pentavalent antimonials to the leishmanicidal trivalent form. Alternatively, the protein may be involved in the detoxification of heavy metals from the cell, due to its homology to other arsenate reductases. To help elucidate the true function of TDR1, the susceptibility of *L. major* WT, Δ*tdr1* and Δ*tdr1* [TDR1] to sodium stibogluconate was investigated.

Stationary phase promastigotes were used to infect peritoneal macrophages at a ratio of 10:1 and incubated for 24 h at 37 ºC with 5 % CO_2, 95 % air. Medium containing extracellular parasites was carefully removed from the macrophages and replaced with fresh medium containing varying concentrations of sodium stibogluconate; 0, 7.8, 15.6, 31.3, 62.5, 125, 250 and 500 µg/ml, and incubated for a further 6 days, refreshing the drug containing medium after 3 days. The percentage of infected macrophages was determined by counting 100 macrophages and calculating the percentage infected. The results are shown in Table 3.5. Due to time constraints, only two biological replicates exist, which is not enough to analyse the data statistically. The data is variable and would require further investigation, but there is a clear general trend.

Compared to *L. major* WT, Δ*tdr1* is more sensitive to sodium stibogluconate. When exposed to 500 µg/ml SbV, the highest concentration tested, Δ*tdr1* is completely cleared from macrophages, whereas 1.7 and 2.5 % of macrophages are still infected with WT. *L. major* Δ*tdr1* [TDR1] is much less sensitive to the drug at this concentration, with 22.8 % and 46.5 % of macrophages remaining infected. The higher values may be explained by the over-expression of TDR1 in these parasites. It is worth noting that when these experiments were carried out, a similar trend in percentage infection was seen as with the *in vitro* macrophage infections shown in Figures 3.9 and 3.10. A higher percentage of macrophages were infected with *L. major* Δ*tdr1* than WT and Δ*tdr1* [TDR1], with Δ*tdr1* [TDR1] infecting almost half the percentage of macrophages than the WT.

		Percentage infection							
		Concentration of Sb(V) (μg/ml)							
		0	7.8	15.6	31.3	62.5	125	250	500
L. major WT	Expt 1	100	100	86.8	81.0	82.8	46.6	28.2	1.7
	Expt 2	100	94.4	91.9	78.2	88.3	54.1	20.3	2.5
L. major Δ*tdr1*	Expt 1	100	65	58	59	37	9	0	0
	Expt 2	100	78	82.8	93.9	84.8	40.4	7.1	0
L. major Δ*tdr1* [TDR1]	Expt 1	100	96.2	105.4	94.1	85.4	87.6	56.8	46.5
	Expt 2	100	105.4	98.2	86.2	64.1	46.1	27.0	22.8

Table 3.5 Susceptibility of *L. major* WT, Δ*tdr1* and Δ*tdr1* [TDR1] to sodium stibogluconate.
Stationary phase promastigotes were used to infect peritoneal macrophages at a ratio of 10:1 and incubated for 24 h at 37 ºC with 5 % CO_2, 95 % air. Medium was replaced with fresh medium containing varying concentrations of sodium stibogluconate; 0, 7.8, 15.6, 31.3, 62.5, 125, 250 and 500 μM, and incubated for a further 6 days, replacing the medium once after 3 days with fresh medium containing the same concentration of sodium stibogluconate. The percentage of infected macrophages was determined by counting 100 macrophages and calculating the percentage infected. The control values (no drug) were taken as 100 % and all other values were adjusted accordingly. Two biological replicates are shown.

3.11 Recombinant expression of *L. donovani* TDR1 and trypanothione reductase

Recombinant *L. donovani* TDR1 was generated to try to elucidate potential roles of the enzyme and clarify its function in the parasite. *L. major* TDR1 has already been produced recombinantly, and some investigation into functionality has been carried out (Denton et al., 2004). It was decided that TDR1 from a species of *Leishmania* that is the causative organism of a different clinical form of the disease should be produced and investigated. TDR1 was hypothesised to possibly be involved in antimonial resistance, therefore *L. donovani* BPK 206 clone 10 was used. This line is a field isolate line from a region in Nepal where antimonial drug resistance is endemic. To test the ability of TDR1 to use trypanothione as a reducing agent, trypanothione reductase was also required to carry out several spectrophotometric functional assays. Therefore, *L. donovani* trypanothione reductase was produced recombinantly.

The ORFs of *L. donovani TDR1* and *trypanothione reductase* were amplified by PCR using oligonucleotide primers and PCR conditions described in Materials and Methods Sections 2.3.3.1 and 2.3.3.2. PCR products were first sub-cloned into pGEMT-easy and subsequently into pET28a+ (Figure 3.13). *L. donovani tdr1* and *trypanothione reductase* genes were expressed and purified as soluble proteins from *E. coli*. The recombinant TDR1 was 49.9 kDa in size and approximately 17.8 mg of protein per litre of *E. coli* culture was produced. Recombinant trypanothione reductase was 54.7 kDa in size and approximately 27.3 mg of protein per litre of *E. coli* culture was produced. The purification procedures used to purify recombinant TDR1 and trypanothione reductase are described in Section 2.3.4.5. Figures 3.14 and 3.15 show the stages of purification of trypanothione reductase and TDR1 respectively.

At the end of the processes used to purify the proteins (Section 2.3.4.5) imidazole was removed from the buffer containing TDR1 and trypanothione reductase. The imidazole was dialysed out of the buffer containing TDR1, and the protein was aliquoted into small volumes and stored at -80 ºC for a maximum of 8 months, as described by Denton et al., 2004.

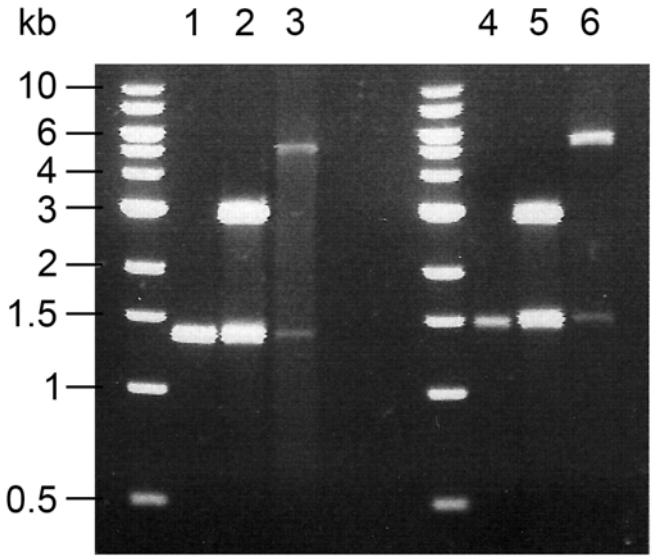

Figure 3.13 Cloning of *L. donovani TDR1* and *trypanothione reductase* into pGEM T-easy and pET28a+.
Sybr safe stained 1 % agarose gel showing the PCR products and digested products of recombinant protein expression constructs. **1**, 1.4 kb *TDR1* PCR product; **2**, 1.4 kb *TDR1* digested out of pGEMT-easy by *Not*I and *Nde*I; **3**, 1.4 kb *TDR1* digested out of pET28a+ by *Not*I and *Nde*I; **4**, 1.5 kb *trypanothione reductase* PCR product; **5**, 1.5 kb *trypanothione redutcase* digested out of pGEMT-easy by *Not*I and *Nde*I; **6**, 1.5 kb *trypanothione reductase* digested out of pET28a+ by *Not*I and *Nde*I.

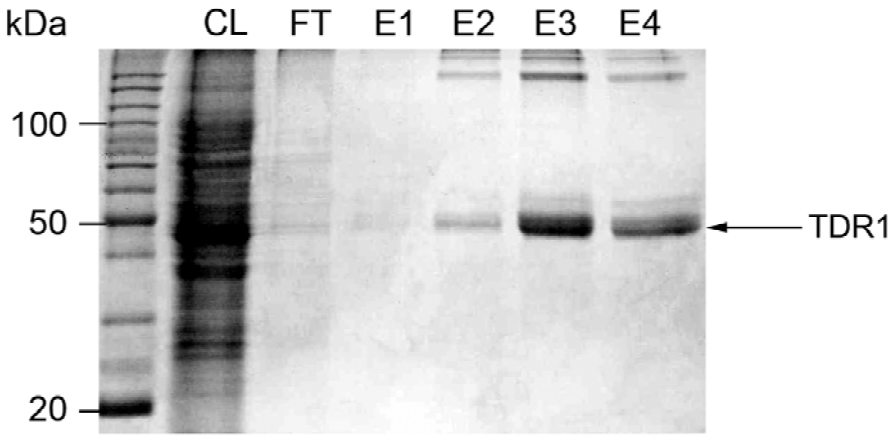

Figure 3.14 SDS-PAGE analysis of expression and purification of recombinant *L. donovani* TDR1 at 15 ºC.
CL, clear lysate; FT, flow through; E1-E4, elutes. Arrow indicates TDR1. 20 µl of extract containing up to 20 µg of protein was loaded in each lane. The recombinant TDR1 is 49.9 kDa in size and 17.8 mg of protein was produced per litre of *E. coli* culture.

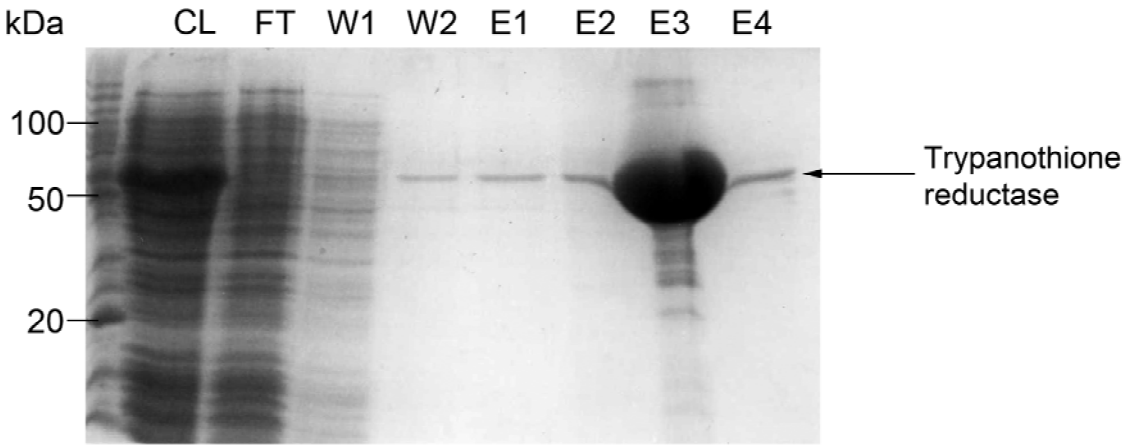

Figure 3.15 SDS-PAGE analysis of expression and purification of recombinant L. donovani trypanothione reductase at 20 ºC.
CL, clear lysate; FT, flow through; W1-W2, washes 2; E1-E4, elutes. Arrow indicates trypanothione reductase. 20 µl of extract containing up to 20 µg of protein was loaded in each lane. The recombinant trypanothione reductase is 54.7 kDa in size and 27.3 mg of protein was produced per litre of *E. coli* culture.

Activity [µmol/min/mg protein]	
Glutathione	Trypanothione
11.6 ± 1.9	4.4 ± 0.1

Table 3.6 Thiol transferase activity of recombinant *L. donovani* TDR1.
Activities are expressed in terms of µmol/min/mg of protein and are means ± S.D. for 3 determinations.

Activity [µmol/min/mg protein]	
TNB produced	4.6 ± 0.5

Table 3.7 Activity of recombinant *L. donovani* trypanothione reductase.
Activities are expressed in terms of µmol/min/mg of protein and are means ± S.D. for 3 determinations.

The imidazole from the purification buffer was dialysed out of the buffer containing trypanothione reductase. The protein was then aliqouted into small volumes and stored at 4 ºC for a maximum of 4 weeks, as described by Mittal et al., 2005.

3.11.1 Activity of recombinant *L. donovani* TDR1

To confirm whether or not recombinant *L. donovani* TDR1 was active, the thiol transferase activity of the enzyme was tested. The ability of TDR1 of using glutathione and trypanothione as electron donors to reduce the synthetic disulphide – 2-hydroxyethyl disulphide (HEDS) was investigated as described in Denton, et al., 2004. The standard assay mixture contained, in a final volume of 200 µl, 50 mM Tris/HCl (pH 7.0), 5 mM EDTA, 300 µM NADPH, 1 mM GSH, 0.75 mM HEDS and 1 unit/ml GSSG reductase. When using trypanothione as an electron donor, all assay components were the same except 1 mM GSH was replaced by 400 µM trypanothione, 1 unit/ml of GSSG reductase was replaced by 1 unit/ml of trypanothione reductase and the concentration of NADPH was reduced from 300 µM to 200 µM. The assay mixture was preincubated at 30 ˚C for 10 min, before initiation of the reaction by the addition of TDR1. Activity was monitored as the decrease in absorbance at 340 nm. Specific activities were calculated from the linear rate during the first 1 min of the reaction, using the molar extinction coefficient of NADPH of 6220 M^{-1} cm^{-1}.

The results are given in Table 3.6 and show that recombinant *L. donovani* TDR1 is active, with a similar activity to *L. major* TDR1, as shown by Denton et al., 2004. The protein is capable of using both glutathione and trypanothione as substrates, however, it is unclear whether TDR1 prefers to use glutathione or trypanothione as an electron donor. Further investigation would have to be carried out before this can be established.

3.11.2 Activity of recombinant *L. donovani* trypanothione reductase

A spectrophotometric assay was performed to confirm the activity of recombinant trypanothione reductase. The assay was performed according to

Hamilton et al., 2003, and the standard assay mixture contained, in a final volume of 1 ml, 40 mM Hepes (pH 7.5), 1 mM EDTA, 0.15 mM NADPH, 1 μM $T[S]_2$, 25 μM DTNB and various concentrations of trypanothione reductase. The basis of the assay involves the reaction of each trypanothione molecule with one DTNB molecule, producing one TNB molecule which is yellow in colour and detectable spectrophotometrically at 412 nm. This is a cycling reaction in which the initial rate is proportional to the concentration of trypanothione. The assay components were pre-incubated with NADPH for 5 min at 27 °C, before initiating the reaction by the addition of $T[S]_2$. Enzyme activity was monitored as the increase in absorbance at 412 nm due to the formation of TNB. The results of the assay confirm that trypanothione reductase is active (Table 3.7), with a specific activity of 4.57 μmol/min/mg protein.

3.12 Discussion

The attempts made to generate a *L. major TDR1* null mutant were successful (Dr Joanne McGregor), as were the attempts to generate a *L. infantum TDR1* null mutant (Miss Marta Silva). However, all the attempts made to generate a *L. donovani* TDR1 null mutant were unsuccessful. In all parasites that had undergone two rounds of transfection with knock-out DNA, the knock-out DNA was shown to have integrated in the correct place, thus making the parasites resistant to the two drugs used in culturing at this stage. However, Southern blot analysis of these lines suggested that, despite integration of knock-out DNA in the correct place, at least one WT allele still existed. FACS analysis showed that the parasites had a normal genomic content, indicating that it was likely that the parasites had duplicated chromosome 33, the location of *TDR1*. This phenomenon was first observed in *L. major* by Cruz et al., 1992, where it was suggested that this may be an indicator for assessing essentiality of genes. However, the fact that *TDR1* null mutants have been generated in *L. major* and *L. infantum* suggest that *TDR1* is unlikely to be essential for *L. donovani*, particularly since *L. infantum* is so closely related to *L. donovani*. More recently aneuploidy has been shown in *L. infantum* to be a result of antimonial drug selection (Leprohon et al., 2009), indicating that this process can facilitate the development of drug resistance in *Leishmania*. The effects of the *TDR1* gene deletion have been shown to be complemented by the line re-expressing TDR1,

indicating that this is a true null mutant. The analysis of the *L. infantum TDR1* null mutant did not show any phenotype that could be complemented by re-expressing TDR1, therefore it may be that this is not a true null mutant. The gene duplication observed in the attempts to generate *L. donovani* Δ*tdr1* were also observed in the attempts to generate *L. infantum* Δ*tdr1*. Only one clonal line from multiple attempts carried out over the course of a year was verified as *L. infantum* Δ*tdr1*. In contrast, the first attempt to generate *L. major* Δ*tdr1* was fruitful, suggesting that it is much easier to create a *TDR1* null mutant in *L. major* than *L. infantum* and *L. donovani*. *L. infantum* and *L. donovani* are closely related species that are very different to *L. major*, which could account for the differences in ease of removing *TDR1*.

Both TDR1 and the similar *T. cruzi* enzyme Tc52 show similarity in both amino acid sequence and function *in vitro*. Both enzymes have thiol transferase activity and dehydroascorbate reductase activity (Denton et al., 2004). It has been reported that Tc52 is an excretory-secretory product that plays a role in parasite modulation of the host's immune response to infection (Garzon et al., 2003). Indeed, under experimental infection, Tc52 appears to be immunologically silent, failing to cause an antibody response and lymphocyte proliferation during the initial acute phase infection (Fernandez-Gomez et al., 1998). *T. cruzi* tolerates the deletion of one *Tc52* allele, but deletion of both alleles causes the death of the parasite (Allaoui et al., 1999). This indicates that *Tc52* is essential for parasite survival and the gene cannot be deleted. Due to the similarity between TDR1 and Tc52 it is possible that this could explain the lack of success found when trying to generate *TDR1* null mutants in *L. donovani*.

The growth and morphology of promastigotes of the *L. major* and *L. infantum TDR1* null mutants were analysed, and found not to be different to the corresponding WT of each parasite line. Therefore the lack of TDR1 has no effect on the growth and morphology of *L. major* and *L. infantum*.

The sensitivity of the HPLC method developed for the analysis of intracellular thiol levels was checked, as well as the ability of DTT to reduce the entire samples. The results clearly show the entire reduction of samples, and the extent of the sensitivity of detection. These results give confidence of the validity of the procedure used. The retention times for the low molecular weight

thiols were found to be different to those previously determined (Spies et al., 1994, Ariyanayagam & Fairlamb, 1999, Mandal et al., 2007). However, the HPLC program used in this study was developed to separate a greater number of thiols and would account for the differences observed in retention time between this and previous studies.

No significant differences were found in intracellular amounts of cysteine, glutathione and trypanothione between the *L. major* WT and *TDR1* null mutant lines and the *L. infantum* WT and *TDR1* null mutant lines. Thiol levels of *L. major* have recently been quantified by HPLC, showing similar levels of cysteine and glutathione and a much higher amount of trypanothione than the levels shown in this study (Williams et al., 2009). Alternative studies have shown glutathione levels in *L. major* to be 0.8 nmol/10^8 parasites (Romao et al., 2006), which is much lower than the levels detected in this study. However, the detection method used was not HPLC, and may be the cause of the differences observed. HPLC analysis of the low molecular weight thiols of *L. tarentolae* indicated levels of 0.13 nmol/10^8 parasites, 0.09 nmol/10^8 parasites and 0.1 nmol/10^8 parasites for cysteine, glutathione and trypanothione respectively (Mukhopadhyay et al., 1996). These findings are again much less than those detected in this study, but this could be explained by the lack of a reducing agent in the sample preparation. Only thiols that were reduced would be derivatised and ultimately detected by HPLC, resulting in the quantification of only cysteine, glutathione and trypanothione that were reduced at the time of cell harvest. It is also to be expected that some variation in thiol levels exists between different species of *Leishmania* (Romao et al., 2006).

The most significant effect of the lack of *TDR1* in *Leishmania* was observed when the infectivity of *L. major* Δ*tdr1* was assessed using *in vitro* macrophage infections. The lack of TDR1 did not have any effect on average percentage infection of macrophages compared to WT, but it did cause a significant increase in the number of parasites per macrophage. Almost double the number of parasites was observed per macrophage compared to WT. When TDR1 was re-expressed extra-chromasomally, the protein was in fact over-expressed and the infectivity of these parasites was assessed. Interestingly, the average percentage of macrophages infected with *L. major* Δ*tdr1* [TDR1] was almost half that of the WT and the mean number of parasites observed per infected macrophage was

less than half that of the WT, and less that 25 % of *L. major* Δ*tdr1*. Clearly the lack of TDR1 gives the parasites an advantage when infecting and proliferating within macrophages *in vitro*. It is, however, unclear whether the parasites that over-express TDR1 are less efficient in establishing an infection or in proliferation after infecting. This could be further analysed by carrying out macrophage infections for time periods indicative of specific stages of infection, differentiation to amastigotes and proliferation as amastigotes within macrophages. The precise stage affected by the lack of TDR1 could then be elucidated.

Analysis of the susceptibility of *L.major* WT, Δ*tdr1* and Δ*tdr1* [TDR1] to sodium stibogluconate showed that the lack of TDR1 resulted in an increase in sensitivity to the drug. Additionally, the over-expression of TDR1 caused an increase in resistance to sodium stibogluconate. Although this particular experiment was only carried out twice, the general trend remains clear. It is also worth noting that although the numbers have been adjusted, the raw data reflect the same trend even when the differences in macrophage infectivity, seen in Section 3.8, were taken into account.

Ten times the amount of TDR1 is present in *L. major* amastigotes compared to promastigotes (Denton et al., 2004), which adds weight to the theory that the particular function of this protein lies in amastigotes. The protein has been shown to be capable of reducing inactive pentavalent antimonials, SbV, to the active trivalent form, SbIII, *in vitro* (Denton et al., 2004). Although the non-enzymatic chemical conversion of SbV to SbIII can occur spontaneously *in vitro* involving thiols, the reaction is significantly faster in the presence of TDR1 (Denton et al., 2004), suggesting that the role of TDR1 lies in the activation of SbV to SbIII, within the parasite. However, TDR1 bears some similarity to arsenate reductases, which play a role in the detoxification of arsenate (Mukhopadhyay & Rosen, 2002), with reduction followed by excretion from the cell. Since arsenic and antimony are related metalloids, arsenical resistant *Leishmania* strains are frequently cross-resistant to antimonials. This is supported by evidence that the *Leishmania* arsenate reductase LmACR2 increases susceptibility to Pentostam when over-expressed (Zhou et al., 2004). The results of this study add weight to this latter proposed function of TDR1, that the protein aids in the detoxification of drugs and heavy metals in

Leishmania parasites. The removal of a drug activator would be expected to cause resistance to the drug, but the opposite is, in fact, true when TDR1 was removed. The removal of a protein involved in de-toxification of drugs and other xenobiotics from the cell would be expected to result in sensitivity to antimonials, as was seen for Δ*tdr1* in this study.

Recombinant *L. donovani* TDR1 and trypanothione reductase were successfully produced. The extent to which these proteins were analysed is minimal, however they were shown to be active. The thiol transferase activity of recombinant L. major TDR1 was previously shown to be 11.2 ± 2.2 µmol/min/mg protein (Denton et al., 2004), which is very similar to the thiol transferase activity of recombinant *L. donovani* TDR1, which was determined as 11.6 ± 1.9 µmol/min/mg protein. It was also shown that recombinant *L. donovani* TDR1 is able to utilise trypanothione as an electron donor. However, it remains unclear whether glutathione or trypanothione is preferentially used by TDR1, and further investigation is required before this could be determined. Recombinant *L.donovani* trypanothione reductase was required to facilitate the execution of the thiol transferase assay using trypanothione as a substrate, however, it was also subject to activity analysis to ensure any difference between the two thiol transferase assays using glutathione and trypanothione was not due to poor activity of the enzyme. The activity of the recombinant *L. donovani* trypanothione reductase was similar to that reported of *L. donovani* trypanothione reductase (Mittal et al., 2005) as well as trypanothione reductase of other trypanosomatids (Castro-Pinto et al., 2008).

3.12.1 Conclusions and future directions

TDR1 null mutants can be generated in *L. major* and *L. infantum*, and have been attempted unsuccessfully in *L. donovani*. It is therefore not an essential gene in *L. major* and *L. infantum* promastigotes, and therefore unlikely to be an essential gene in *L. donovani*, despite the lack of success generating the null mutant.

The intracellular thiol levels of *L. major* Δ*tdr1* and *L. infantum* Δ*tdr1* remained no different to WT, and the parasites showed no defect in growth or morphology. Since the parasites were harvested for HPLC analysis in stationary

phase, it may also be worthwhile quantifying the thiol levels in these promastigotes in mid-log phase, to elucidate whether levels of cysteine, glutathione and trypanothione are affected by the gene deletion during growth.

L. major Δ*tdr1* [TDR1] showed a decreased ability to survive in macrophages. This finding was supported by the increased number of parasites per macrophage shown by *L. major* Δ*tdr1*. This suggests that TDR1 plays a role in either establishing an infection or proliferating within macrophages, however it remains unclear exactly what stage of the infection process is inhibited by higher levels of TDR1. Further investigation could easily clarify this by carrying out macrophage infections for periods of time indicative of the particular developmental stages of the parasites. The proportion of metacyclic promastigotes in stationary phase cultures could also be quantified, which may shed light on the reasons behind the differences observed in their ability to maintain an infection. It would also be interesting to investigate the effect of the lack of TDR1 in *L. major* on *in vivo* infectivity, by conducting mouse footpad infections. In addition, these macrophage infections should be repeated using the *L. infantum TDR1* null mutant to confirm the *L. major* findings, with re-expression of TDR1 in the null mutant being necessary to confirm any deficiencies observed.

L. major Δ*tdr1* showed a slight increase in sensitivity to sodium stibogluconate compared to WT, and *L. major* Δ*tdr1* [TDR1] showed a marked increase in resistance to the drug. Although the general trend from these results is clear, the actual values were quite variable and, since the experiment was only carried out twice, should undoubtedly be repeated to ensure the reliability of the findings.

Finally, in depth analysis of the *L. donovani* recombinant protein is required, including the analysis of different substrates under varied conditions, before a greater understanding of the physiological function of TDR1 is achieved.

4. O-acetylserine (thiol) lyase of *Leishmania donovani*

4.1 Introduction

The *de novo* synthesis of cysteine occurs via the sulfhydrylation pathway, in which cysteine is formed from serine by a two-step reaction. In most cases the reaction is initiated by SAT to form O-acetylserine, which then condenses with sulfide to form cysteine, which is catalysed by OAS-TL. *Trichomonas vaginalis* lacks SAT and instead has a functional 3-phosphoglycerate dehydrogenase and an O-phosphoserine aminotransferase, which together result in the production of O-phosphoserine which is used as a substrate for OAS-TL (Westrop et al., 2006). OAS-TL of other organisms, including *Mycobacterium tuberculosis*, also use O-phosphoserine as a substrate (Agren et al., 2008). Plants (Blaszczyk et al., 1999), fungi (Marzluf, 1997), bacteria (Kredich et al., 1969) and some protozoa (Nozaki et al., 2001; Williams et al., 2009) are capable of fixing sulfur and synthesising cysteine via the sulfhydrylation pathway. However, since mammals do not contain the sulfhydrylation pathway, they synthesise cysteine solely through the reverse trans-sulfuration pathway.

SAT forms a complex with OAS-TL, while OAS-TL exists either bound to SAT or free (Ruffet et al., 1994). OAS-TL is inactive when bound to SAT, but SAT in complex with OAS-TL, is highly active and displays a high affinity for its substrates. The activity of SAT results in the production of O-acetylserine. The OAS-TL unbound dimer is highly active and is capable of catalysing the formation of cysteine. The SAT/OAS-TL complex is not only regulated by the product cysteine, but also by its substrates. A high concentration of O-acetylserine causes the dissociation of the complex (Saito et al., 1994), while a high concentration of sulfide regulates the stabilisation of the complex (Kredich, 1971; Droux et al., 1998). Cysteine is also capable of regulating cysteine biosynthesis via sulfhydrylation, by feedback inhibition (Saito et al., 1995).

The tight regulation of the activity of SAT and OAS-TL through interaction within the SAT/OAS-TL complex suggests that the genetic manipulation of either of these enzymes would result in a significant disruption in cysteine biosynthesis via the sulfhydrylation pathway.

Transgenic studies on OAS-TL of parasitic protozoa are not documented, but the effect of genetic manipulation of OAS-TL in plants has been studied extensively. Null mutants created for the cytosolic OAS-TL isoform in *Arabidopsis thaliana* were shown to result in a decrease in the total amount of intracellular cysteine and glutathione (Lopez-Martin et al., 2008). This subsequently caused an increase in sensitivity to the heavy metal cadmium and the lack of OAS-TL was also found to promote a perturbation in hydrogen peroxide homeostasis (Lopez-Martin et al., 2008). Similarly, the over-expression of cytosolic OAS-TL in a *Populus sieboldi* x *P. grandidentata* hybrid displayed several-fold increases in cysteine and glutathione levels, resulting in an increased resistance to hydrogen sulfide, sulfur dioxide, sulfite and hydrogen peroxide (Nakamura et al., 2009). Transgenic tobacco plants over-expressing OAS-TL in the cytosol, chloroplasts and both organelles together showed higher resistance to cadmium, selenium and nickel (Kawashima et al., 2004). These findings highlight the importance of OAS-TL in detoxification of heavy metals and the maintenance of the redox potential of the cell, and ultimately the defence against oxidative stress.

The parasite line used in the reverse genetic studies, *Leishmania donovani* BPK 206 clone 10, is a field isolate from an area of Nepal where visceral leishmaniasis is endemic (Section 2.3.2.1). The efficacy and cost-effectiveness of the pentavalent antimonials has made them the cornerstone of anti-leishmanial therapy since their introduction in 1945. The high toxicity of the drugs coupled with difficulty in administering and ensuring patients receive full courses of treatment make the use of pentavalent antimonials less than ideal. However, the emerging problem of drug resistance, which is endemic in the region where *L. donovani* BPK 206 clone 10 was isolated, is perhaps posing the biggest problem of all. Therefore, the development of novel chemotherapeutic agents is an urgent research priority, but before these can be developed valid drug targets must be identified.

Given the wide range of vital roles of the sulfur containing amino acid cysteine in *Leishmania*, and the absence of the enzymes involved in the sulfhydrylation pathway in the mammalian host, OAS-TL was investigated as a potential drug target in *L. donovani*.

4.2 Alignment of O-acetylserine (thiol) lyase amino acid sequences

The amino acid sequence of *L. donovani* O-acetylserine (thiol) lyase (OAS-TL) was used to perform alignments firstly with the amino acid sequences of OAS-TL of other trypanosomatids (Figure 4.1) and then with other organisms (Figure 4.2), using the program T-Coffee (Notredame et al., 2000, Poirot et al., 2003).

The amino acid sequence of *L. donovani* OAS-TL has significant identities with other trypanosomatids (Table 4.1). *L. major* OAS-TL bears the closest resemblance to *L. donovani* OAS-TL with a percentage identity of 94 %, closely followed by *L. infantum* (92 %) and *L. braziliensis* (88 %). The two forms of OAS-TL of *Trypanosoma cruzi* that were included in the alignment had sequence identities of 71 and 72 % when compared to *L. donovani*. Of all the organisms included in the alignment, the PLP binding sites and the SAT binding sites are 100 % identical.

The amino acid sequence of *L. donovani* OAS-TL was also compared to the OAS-TL sequence of a selection of other organisms. Of those compared, two *Chlamydomonas reinhardtii* OAS-TLs showed the highest sequence identity to *L. donovani* OAS-TL (53 %), and the OAS-TL of *Arabidopsis thaliana* and *Dictyostelium discoideum* show the lowest, both with identities of 30 %. It is worth noting that the SAT binding site was identical between most of the organisms except *A. thaliana, D. discoideum* and *S. cerevisiae*. The lysine residues essential for sulfhydrylase activity and also for binding PLP were not found to be conserved between OAS-TLs of the organisms included in the alignment.

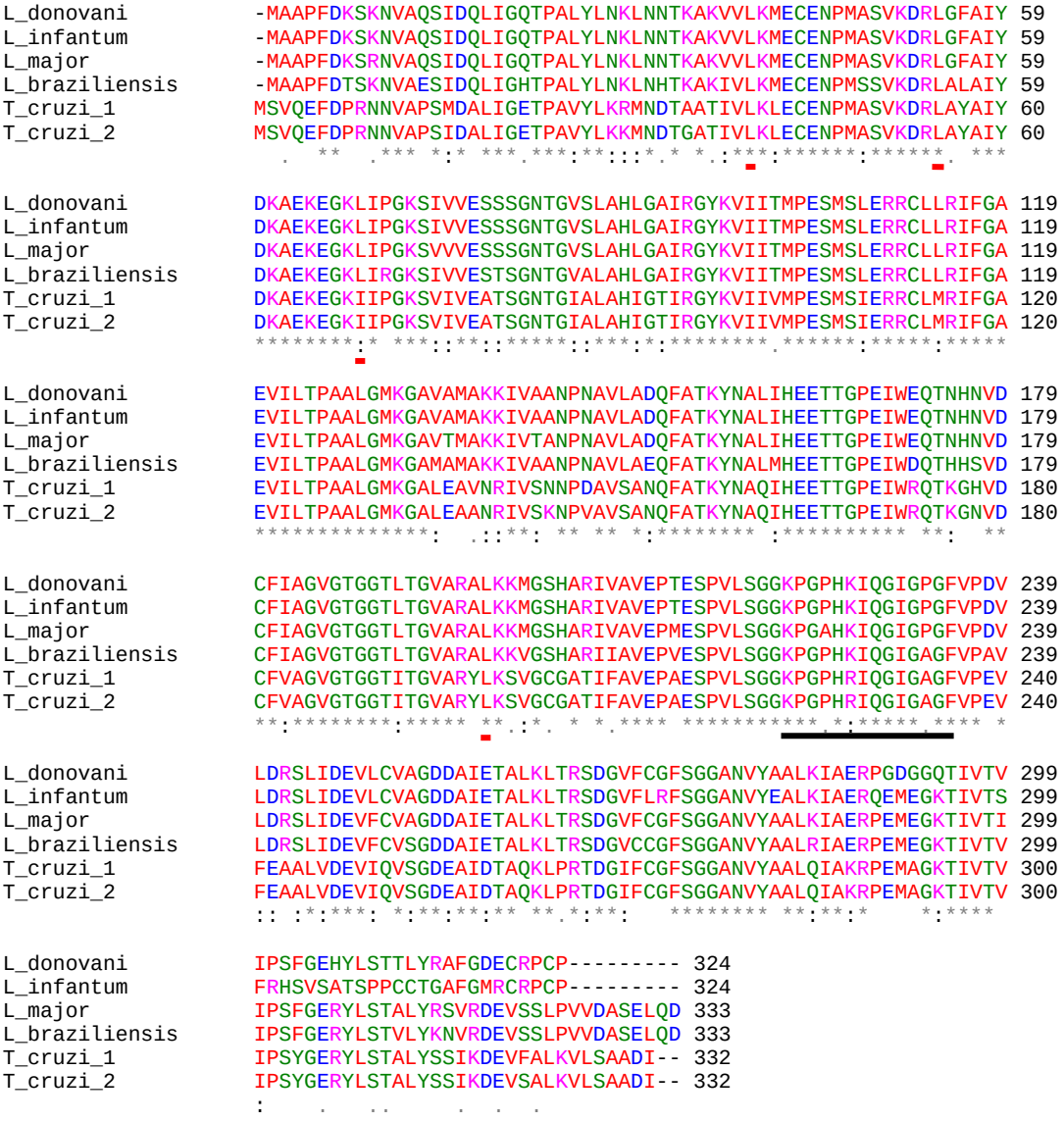

Figure 4.1 Amino acid alignment of *L. donovani* OAS-TL with OAS-TL of other trypanosomatids.
ClustalW alignments of *L. donovani* OAS-TL (sequenced), *L. infantum* OAS-TL (Genedb LinJ36_V3.3750), *L. major* OAS-TL (Genedb LmjF36.3590), *L. braziliensis* OAS-TL (Genedb LbrM35_V2.3820), *T.cruzi* OAS-TL 1 (Genedb Tc00.1047053507165.50) and *T. cruzi* OAS-TL 2 (Genedb Tc00.1047053507793.20), were combined using the program T-Coffee (Notredame et al., 2000, Poirot et al., 2003) showing (*) identical residues, (:) conserved residues and (.) homologous residues. Residues are coloured as follows: A, V, F, P, M, I, L and W are shown in red; D and E are blue; R, H and K are magenta; S, T, Y, H, C, N, G and Q are green and all other residues are grey. The four lysine residues that are essential for sulfhydrylase activity and binding pyridoxal phosphate (PLP) are underlined in red. The SAT binding site is underlined in black.

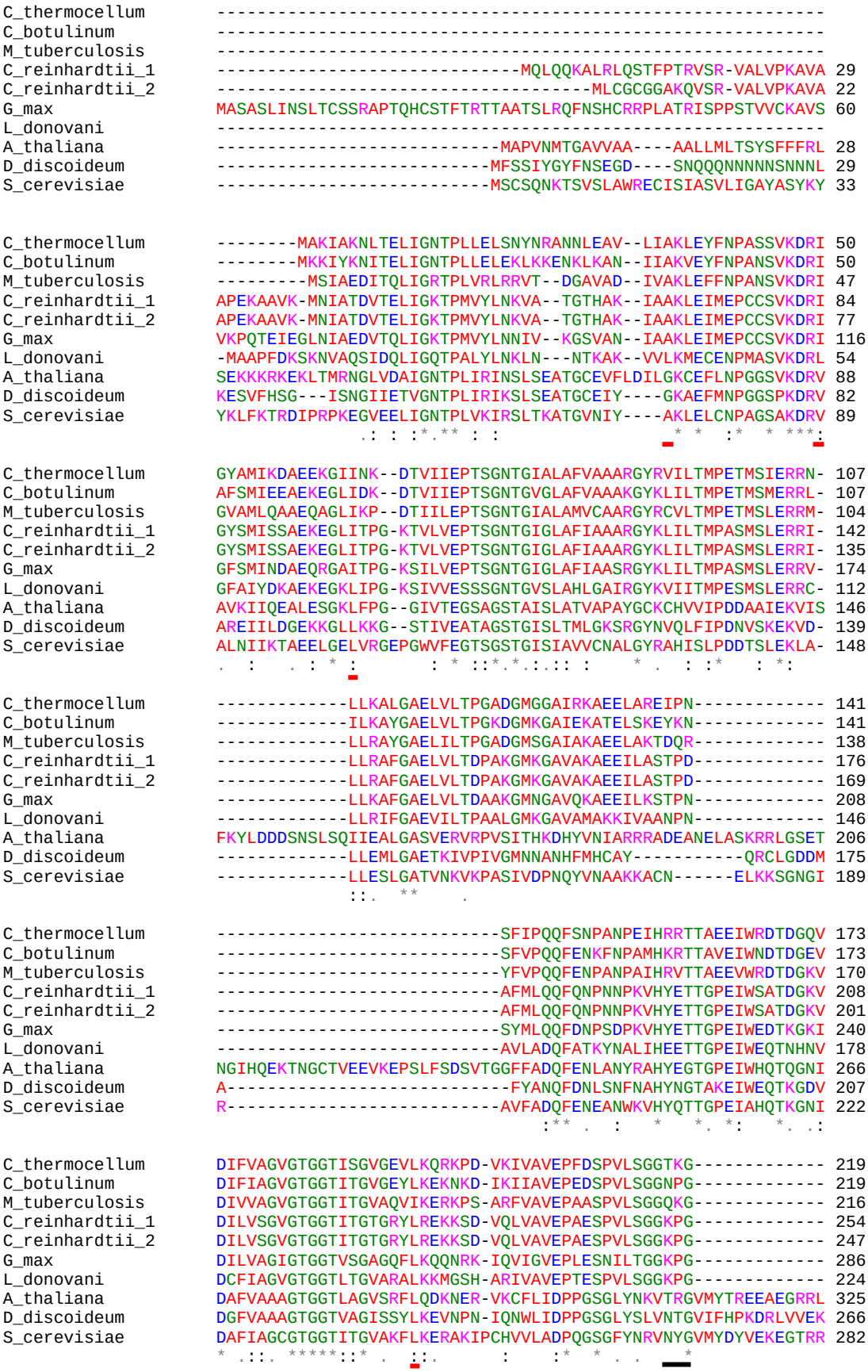
C_thermocellum
C_botulinum
M_tuberculosis
C_reinhardtii_1
C_reinhardtii_2
G_max
L_donovani
A_thaliana
D_discoideum
S_cerevisiae

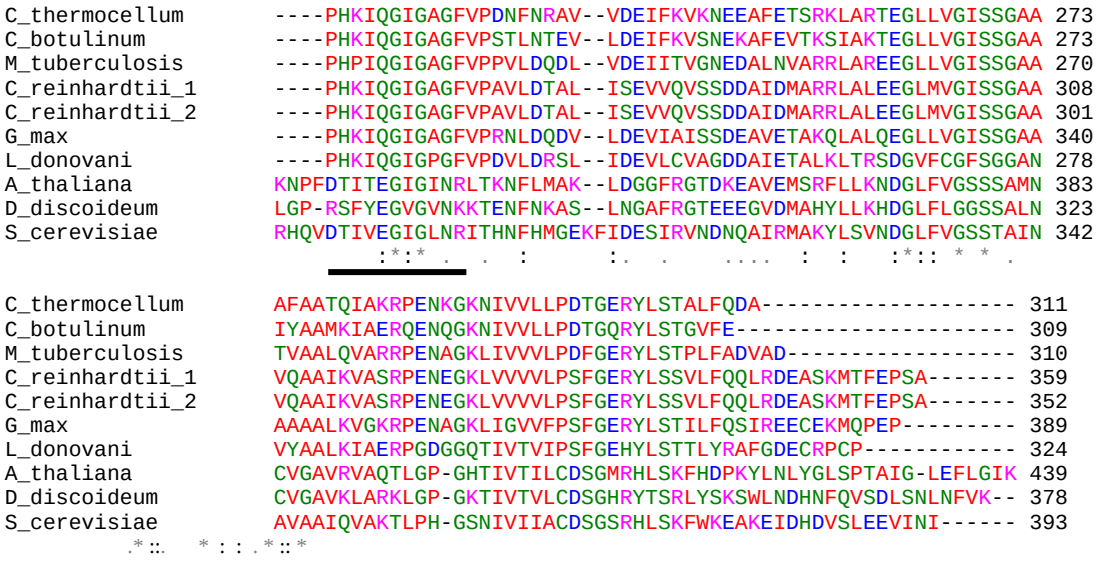

Figure 4.2 Amino acid alignment of *L. donovani* OAS-TL with OAS-TL of other organisms. ClustalW alignments of *L. donovani* OAS-TL (sequenced), *Clostridium thermocellum* OAS-TL (GenBank accession no. NC_009012.1), *Clostridium botulinum* OAS-TL (GenBank accession no. NC_009495.1), *Mycobacterium tuberculosis* OAS-TL (GenBank accession no. NC_002755.2), *Chlamydomonas reinhardtii* OAS-TL 1 (GenBank accession no. XM_001691883.1), *Chlamydomonas reinhardtii* OAS-TL 2 (GenBank accession no. XM_001691884.1), *Glycine max* OAS-TL (GenBank accession no. EF584900.1), *Arabidopsis thaliana* OAS-TL (GenBank accession no. AC002304.3), *Dictyostelium discoideum* OAS-TL (GenBank accession no. XM_629377.1) and *Saccharomyces cerevisiae* OAS-TL (GenBank accession no. EDN61611.1), were combined using the program T-Coffee (Notredame et al., 2000, Poirot et al., 2003) showing (*) identical residues, (:) conserved residues and (.) homologous residues. Residues are coloured as follows: A, V, F, P, M, I, L and W are shown in red; D and E are blue; R, H and K are magenta; S, T, Y, H, C, N, G and Q are green and all other residues are grey. The four lysine residues that are essential for sulfhydrylase activity and binding pyridoxal-5'-phosphate (PLP) are underlined in red. The SAT binding site is underlined in black.

	Cb	Ct	Mt	Dd	At	Sc	Tc_2	Tc_1	Lb	Lm	Li	Ld	Cr_2	Cr_1	Gm
Cb		72	61	34	31	34	48	47	51	49	46	48	58	58	55
Ct			68	34	33	36	52	52	49	52	45	48	58	58	57
Mt				32	30	36	52	52	51	50	46	50	62	62	57
Dd					43	37	33	33	30	29	29	30	29	28	29
At						44	29	29	29	30	29	30	28	27	27
Sc							34	33	34	34	33	34	32	32	31
Tc_2								98	74	73	67	72	54	54	49
Tc_1									72	72	66	71	53	53	49
Lb										90	83	88	54	54	49
Lm											89	94	53	53	49
Li												92	49	49	45
Ld													53	53	49
Cr_2														97	66
Cr_1															66
Gm															

Table 4.1 Sequence identities of OAS-TL of various organisms.
Percentage identity of the amino acid sequences of various organisms when compared to OAS-TL of *L. donovani* BPK 206 clone 10. Cb, *Clostridium botulinum* (GenBank accession no. NC_009495.1); Ct, *Clostridium thermocellum* (GenBank accession no. NC_009012.1); Mt, *Mycobacterium tuberculosis* (GenBank accession no. NC_002755.2); Cr_1 *Chlamydomonas reinhardtii* (GenBank accession no. XM_001691883.1), Cr_2 *Chlamydomonas reinhardtii* (GenBank accession no. XM_001691884.1); Gm, *Glycine max* (GenBank accession no. EF584900.1); At, *Arabidopsis thaliana* (GenBank accession no. AC002304.3); Dd, *Dictyostelium discoideum* (GenBank accession no. XM_629377.1); Sc, *Saccharomyces cerevisiae* (GenBank accession no. EDN61611.1); Li, *L. infantum* (Genedb LinJ36_V3.3750); Lm, *L. major* (Genedb LmjF36.3590); Lb, *L. braziliensis* (Genedb LbrM35_V2.3820); Tc_1, *T.cruzi* (Genedb Tc00.1047053507165.50) and Tc_2, *T. cruzi* (Genedb Tc00.1047053507793.20) were combined using the program T-Coffee (Notredame et al., 2000, Poirot et al., 2003) and sequences identities were calculated.

4.3 Knocking out of *OAS-TL* in *L. donovani*

The removal of the *OAS-TL* gene from *L. donovani*, by two rounds of homologous recombination, was anticipated to result in a phenotypic effect that would clarify the role of OAS-TL in the parasites. Analysis of various aspects of the biology of the knock-out parasites would also clarify whether the reverse trans-sulfuration pathway was able to compensate for the loss of OAS-TL, and further elucidate the role of OAS-TL.

4.4 Generation of *L. donovani OAS-TL* null mutant parasite lines

Specific oligonucleotide primers were designed, using the *L. infantum* genome, and used to amplify the 3' and 5' flanking regions of *OAS-TL*. The *L. infantum* genome was used because no *L. donovani* genome was available at the time the primers were designed and *L. infantum* is believed to be the most similar to *L. donovani*. PCR products were subcloned into pGEMT-Easy and ultimately into the vectors pGL345, pGL1033 and pGL158 (Mottram et al., 1996), which contain the *hygromycin phosphotransferase*, *dihydroxybiphenyl dioxygenase* and *nourseothricin acetyltransferase* genes respectively, conferring resistance to hygromycin, bleomycin/phleomycin and nourseothricin (Figure 2.5). The constructs containing the 3' and 5' flanking regions and the antibiotic resistance markers were excised from the vectors and the linear DNA fragments were purified and used to transfect mid-log phase *L. donovani* promastigotes. Figure 4.3 shows the sizes of the 500 bp 3' and the 1 kb 5' flanking regions of *OAS-TL* when they were digested out of pGL1033 with *OAS-TL* flanks, pGL158 with *OAS-TL* flanks and pGL345 with *OAS-TL* flanks. Following two independent rounds of transfection, where gene replacement occurs by homologous recombination, the corresponding selective drugs were added and the cultures were diluted to obtain clonal lines. Two independent rounds of transfection were carried out. After each one, parasites were allowed to recover for 24 h during which time the knock-out DNA integrates into the genomic DNA of a proportion of cells, by homologous recombination. The corresponding selective drugs were added after this time and the cultures were diluted to obtain clonal lines. Two lines, Δ*oas-tl* A and Δ*oas-tl* B, were generated in this way resulting from transfection with the

plasmids pGL158 (*nourseothricin acetyltransferase*) followed by pGL345 (*hygromycin phosphotransferase*). These parasite lines were produced independently.

4.5 Analysis of Δ*oas-tl* A and Δ*oas-tl* B

The replacement of the *OAS-TL* gene from Δ*oas-tl* A and Δ*oas-tl* B with DNA from the plasmids pGL158 and pGL345, was assessed by Southern blot analysis. *L. donovani* WT as well as Δ*oas-tl* A and Δ*oas-tl* B were harvested from stationary growth phase and the genomic DNA was extracted. 1-2 µg of DNA was digested overnight using the restriction endonuclease *Xho*I, and separated by DNA gel electrophoresis before Southern blotting. The sizes of the resulting DNA fragments can be seen in Figure 4.4. The blot was then probed with labelled *hygromycin phosphotransferase* and *nourseothricin acetyltransferase* (Figure 4.5). No band was seen in the WT lane because *hygromycin phosphotransferase* and *nourseothricin acetyltransferase* do not exist in this parasite line. In each of the lanes corresponding to Δ*oas-tl* A and Δ*oas-tl* B, two bands were seen at 7.0 kb and 7.4 kb, indicating that the DNA fragments carrying the selection markers had replaced both *OAS-TL* alleles.

To ensure that the *OAS-TL* had been completely removed from the genome, and that no chromosome duplications had occurred (Cruz et al., 1992), the blot was stripped and re-probed with labelled *OAS-TL* (Figure 4.6). In the WT lane a clear band of 4.7 kb was visible, however the expected band at 0.6 kb was too small to be seen clearly on the blot. This indicated that the *OAS-TL* gene is present in the WT line. In the lanes containing Δ*oas-tl* A and Δ*oas-tl* B DNA, no bands corresponding to *OAS-TL* were seen, demonstrating that both of the *OAS-TL* alleles were replaced with the selectable markers (Figure 4.5). Therefore Δ*oas-tl* A and Δ*oas-tl* B are two independently generated parasite lines in which the *OAS-TL* gene has been replaced.

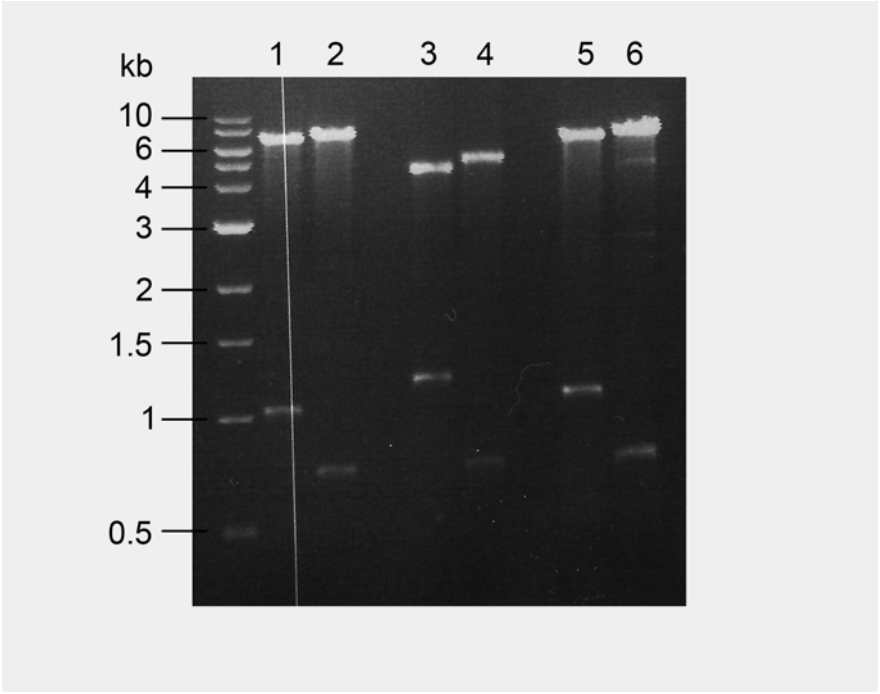

Figure 4.3 Cloning of *L. donovani OAS-TL* 5' and 3' flanks into pGL1033, pGL158 and pGL345.
Sybr safe stained 1 % agarose gel showing the DNA products of digested pGL1033 with *OAS-TL* flanks, pGL158 with *OAS-TL* flanks and pGL345 with *OAS-TL* flanks. **1**, 1 kb 5' flank of pGL158 with *OAS-TL* flanks digested with *Hind*III and *Sal*I; **2**, 500 bp 3' flank of pGL158 with *OAS-TL* flanks digested with *Sma*I and *Bgl*II; **3**, 1 kb 5' flank of pGL1033 with *OAS-TL* flanks digested with *Hind*III and *Sal*I; **4**, 500 bp 3' flank of pGL1033 with *OAS-TL* flanks digested with *Sma*I and *Bgl*II; **5**, 1 kb 5' flank of pGL345 with *OAS-TL* flanks digested with *Hind*III and *Sal*I; **6**, 500 bp 3' flank of pGL345 with *OAS-TL* flanks digested with *Sma*I and *Bgl*II.

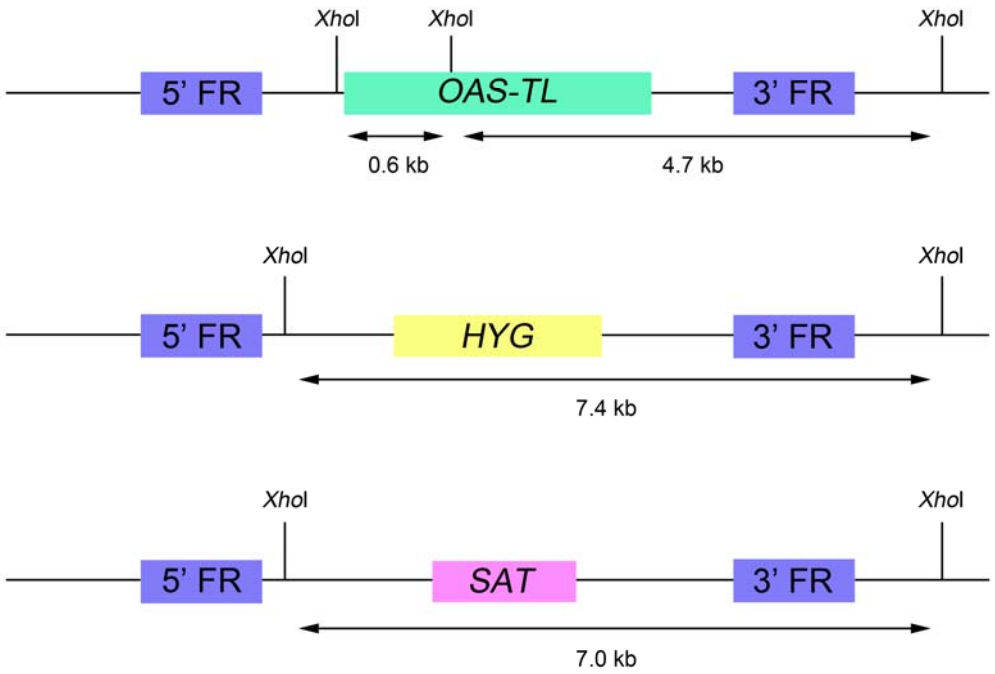

Figure 4.4 Knock out strategy of *OAS-TL* in *L. donovani*.
Schematic representation of one gene copy of *OAS-TL* and the two knock-out cassettes that will replace the endogenous genes by homologous recombination following two independent rounds of transfection. The positions of *Xho*I restriction sites and the sizes of DNA fragements expected from *Xho*I digest are given.

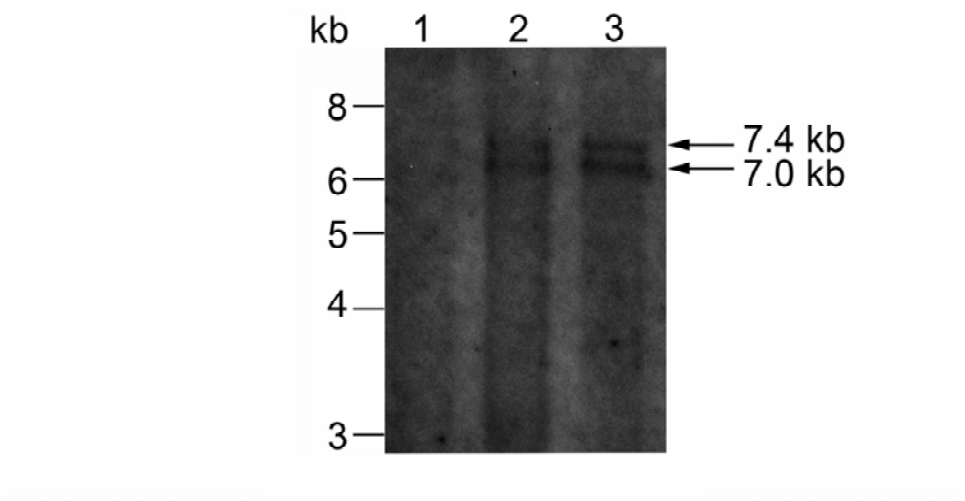

Figure 4.5 Southern blot analysis of *L. donovani OAS-TL* null mutant lines.
Genomic DNA (1 µg) from *L. donovani* WT (lane 1), *L. donovani* Δ*oas-tl* A (lane 2) and *L. donovani* Δ*oas-tl* B (lane 3) was digested overnight at 37 ºC with *Xho*I and resolved on a 0.8 % agarose gel. The blot was probed with the *hygromycin phosphotransferase* and *nourseothricin acetyltransferase* labelled with an alkaline phosphatase, detected by CDP-Star detection reagent (G.E. Healthcare) and chemiluminescence was detected by autoradiography film. The bands at 7.0 and 7.4 kb indicate the correct integration of the *HYG* and *SAT* knock-out cassettes respectively. As expected, there are no visible bands in the WT lane, as the *hygromycin phosphotransferase* and *nourseothricin acetyltransferase* genes do not exist in this line.

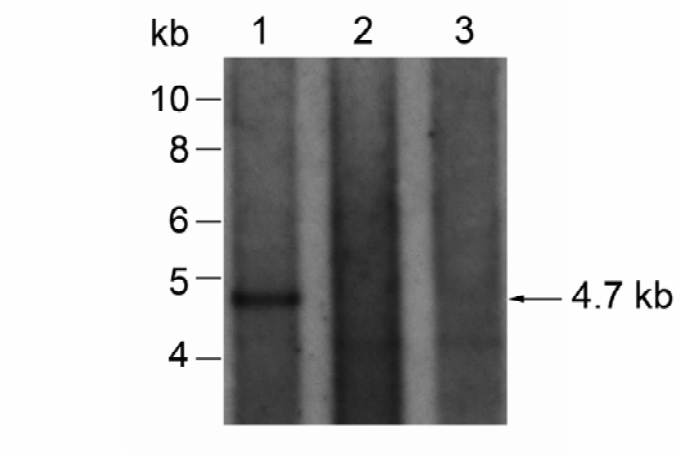

Figure 4.6 Southern blot analysis of *L. donovani OAS-TL* null mutant lines.
Genomic DNA (1 µg) from *L. donovani* WT (lane 1), *L. donovani* Δ*oas-tl* A (lane 2) and *L. donovani* Δ*oas-tl* B (lane 3) was digested overnight at 37 ºC with *Xho*I and resolved on a 0.8 % agarose gel. The blot was probed with *OAS-TL* labelled with an alkaline phosphatase, detected by CDP-Star detection reagent (G.E. Healthcare) and chemiluminescence was detected by autoradiography film. The band at 4.7 kb in lane 1 represents the endogenous gene, which is no longer present in Δ*oas-tl* A and Δ*oas-tl* B.

4.6 Generation of OAS-TL re-expressing lines

To ensure any phenotypic differences observed between the WT and the *OAS-TL* null mutant lines was due entirely to the loss of the gene and not a result of the genetic manipulation techniques, re-expressing lines were generated in which OAS-TL was expressed, extra-chromasomally, in Δ*oas-tl* A and Δ*oas-tl* B.

Specific oligonucleotide primers were designed, using the *L. infantum* genome, and used to amplify *OAS-TL*. PCR products were subcloned into pGEMT-Easy and ultimately into the vector pGL102 which contains the *neomycin phosphotransferase* gene which confers resistance to neomycin (Figure 2.6). pGL102 containing *OAS-TL* was used to transfect mid-log phase *L. donovani* Δ*oas-tl* A and Δ*oas-tl* B promastigotes. Cultures were allowed to recover overnight before being subjected to the selective drug pressure of neomycin.

4.7 Phenotypic analysis of *OAS-TL* null mutant lines

4.7.1 Western blot analysis of OAS-TL mutant lines

Western blot analysis confirmed that *L. donovani* Δ*oas-tl* A [OAS-TL] and Δ*oas-tl* B [OAS-TL] expressed the protein (Figure 4.7). The level of expression compared to *L. donovani* WT, Δ*oas-tl* A and Δ*oas-tl* B was confirmed by quantification of the band intensity of the blot (Table 4.2). The relative band intensity of OAS-TL suggests that the protein level of OAS-TL present in *L. donovani* Δ*oas-tl* A [OAS-TL] and Δ*oas-tl* B [OAS-TL] is approximately half the level found in WT. The protein level of mercaptopyruvate sulfurtransferase (MST) and cystathionine ß-synthase (CBS) in *L. donovani* WT, Δ*oas-tl* A, Δ*oas-tl* B, Δ*oas-tl* A [OAS-TL] and Δ*oas-tl* B [OAS-TL] was investigated in the same way. Interestingly, CBS is present at a similar level as WT in Δ*oas-tl* A and Δ*oas-tl* B, but in Δ*oas-tl* A [OAS-TL] and Δ*oas-tl* B [OAS-TL] the level of protein is roughly half that found in *L. donovani* WT. Although the values representing the expression of MST are slightly more variable than those representing the expression of OAS-TL and CBS, the results suggest that there is no difference in the amount of MST between the various parasite lines.

4.7.2 Growth

Growth of *L. donovani* WT, Δ*oas-tl* A, Δ*oas-tl* B, Δ*oas-tl* A [OAS-TL] and Δ*oas-tl* B [OAS-TL] was monitored to assess whether the loss of *OAS-TL* affected promastigote growth. Growth was monitored by determining cell density at 24 h intervals for 7 days.

The knock-out parasites go through the same lag, exponential and stationary phases as WT, but appear to show a slight growth defect. The lack of OAS-TL causes the parasites to grow to a lower density at all stages of growth, compared to WT (Figure 4.8). A stationary phase culture of Δ*oas-tl* A and Δ*oas-tl* B is approximately 1 x 10^7 cells/ml, compared to WT which reaches a maximum of approximately 4 x 10^7 cells/ml. When OAS-TL is expressed extra-chromasomally in Δ*oas-tl* A and Δ*oas-tl* B, the deficiency in density is restored to WT levels.

4.7.3 Morphology

It appears that *L. donovani* Δ*oas-tl* A and Δ*oas-tl* B follow the same growth pattern as the WT parasites, but it was found that their density in stationary phase was reduced compared to *L. donovani* WT. While assessing parasite growth it was found that *L. donovani* Δ*oas-tl* A and Δ*oas-tl* B had a very different morphology compared to WT parasites, which appeared to be restored to WT in the parasite lines re-expressing OAS-TL. The knock-out lines were significantly shorter in body length than the WT. The flagella were also shorter in these parasites compared to WT, and in some cases seemed to lack the flagellum entirely. In addition to the difference in size, the knock-out parasites also look severely deformed. Morphological features that can be clearly seen in WT cells, like the overall spindle-like shape of the body and the 'spiral' effect of the membrane, are grossly altered in Δ*oas-tl* A and Δ*oas-tl* B (Figure 4.9). *L. donovani* Δ*oas-tl* A [OAS-TL] and Δ*oas-tl* B [OAS-TL] appear more similar to WT parasites, with both the spindle-like shape and 'spiral' effect recovered. Overall body length, however, was not recovered.

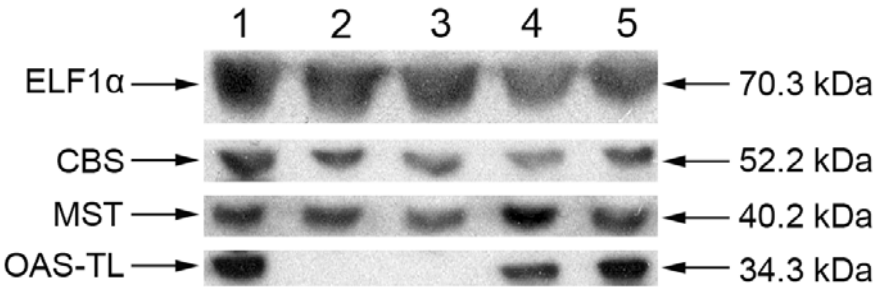

Figure 4.7 Western blot analysis of the expression of ELF1α, CBS, MST and OAS-TL in WT, Δ*oas-tl* A, Δ*oas-tl* B, Δ*oas-tl* A [OAS-TL] and Δ*oas-tl* B [OAS-TL] *L. donovani* promastigotes.
1 µg of soluble cell extract was subjected to western blot analysis using the rabbit anti-OAS-TL (1:7,500), rabbit anti-MST (1:7,500), rabbit anti-CBS (1:10,000) and mouse anti-ELF1α (1:30,000) antisera. WT, lane 1; Δ*oas-tl* A, lane 2; Δ*oas-tl* B, lane 3; Δ*oas-tl* A [OAS-TL], lane 4 and Δ*oas-tl* B [OAS-TL], lane 5.

	WT	Δ*oas-tl* A	Δ*oas-tl* B	Δ*oas-tl* A [OAS-TL]	Δ*oas-tl* B [OAS-TL]
OAS-TL	1	0.00	0.00	0.54	0.55
CBS	1	0.85	0.96	0.58	0.56
MST	1	1.19	0.93	0.78	0.82

Table 4.2 Relative density of bands detected by western blot representing OAS-TL, CBS and MST in *L. donovani* promastigotes.
1 µg of soluble cell extract was subjected to western blot analysis using the rabbit anti-OAS-TL (1:7,500), rabbit anti-MST (1:7,500), rabbit anti-CBS (1:10,000) and mouse anti-ELF1α (1:30,000) antisera. Chemiluminescence was detected and density determined using a Molecular Imager ChemiDoc XRS System with Quantity One 4.6.3 software. Values were adjusted using the values obtained for the loading control, ELF1α, and then WT values were taken as 1 and the data for the other cell lines were adjusted accordingly.

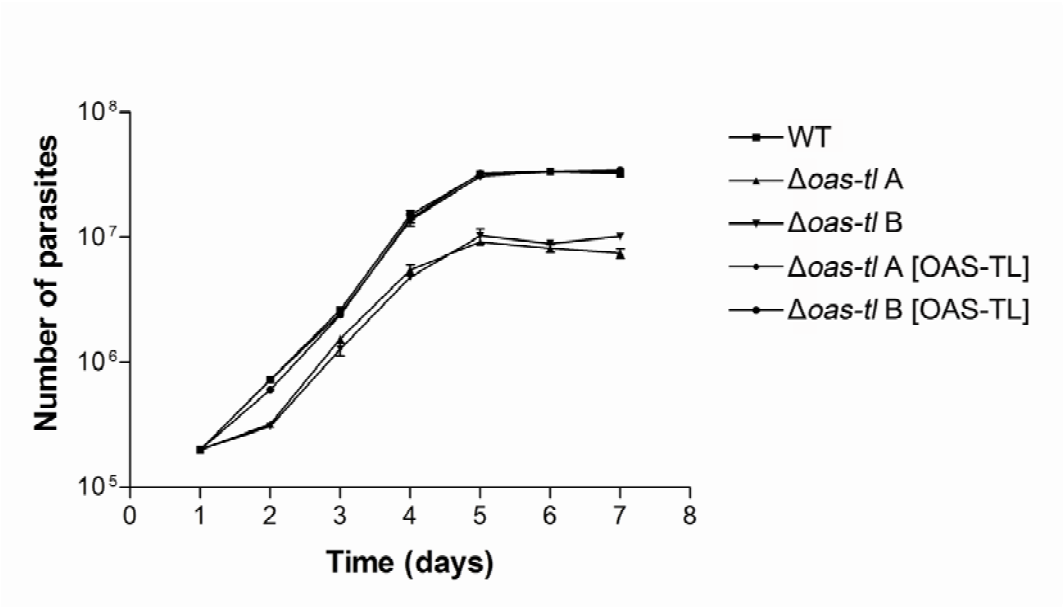

Figure 4.8 Growth curve of WT, Δoas-tl A, Δoas-tl B, Δoas-tl A [OAS-TL] and Δoas-tl B [OAS-TL] *L. donovani* promastigotes.
Cultures were seeded at a concentration of 2 x 10^5 parasites/ml and were counted daily. Δ*oas-tl* A [OAS-TL] and Δ*oas-tl* B [OAS-TL] were grown in 50 µg/ml G418.

These observations suggest that the lack of OAS-TL results in dramatic morphological changes in promastigotes. Scanning Electron Microscopy (SEM) was used to capture images of a sample of each of the parasite lines, to facilitate the visualisation of the morphological differences in more detail, while also enabling the quantification of these differences by using measurement software. Measurements of flagellum length and body length of *L. donovani* WT, Δ*oas-tl* A, Δ*oas-tl* B, Δ*oas-tl* A [OAS-TL] and Δ*oas-tl* B [OAS-TL] were taken, and the means and standard errors were calculated from a random sample of 100 parasites from each line. The data were statistically analysed by analyses of variance (ANOVA), to compare the means of three populations, with Tukey's post-tests to provide confidence intervals for all pairwise differences between group means.

Figure 4.9 A shows a representative image of a *L. donovani* WT promastigote. The mean length of the flagella in the parasite population at late log phase was determined to be 14.2 ± 0.4 μm. The two *OAS-TL* null mutant lines (Δ*oas-tl* A and Δ*oas-tl* B), shown in Figure 4.9 B and C, show an obvious reduction of flagellum lengths. The mean lengths of the flagella of Δ*oas-tl* A and Δ*oas-tl* B were determined to be 6.7 ± 0.4 μm and 4.8 ± 0.5 μm respectively. Figure 4.9 D and E show examples of the parasite lines re-expressing OAS-TL (Δ*oas-tl* A [OAS-TL] and Δ*oas-tl* B [OAS-TL]). The mean flagella lengths of these parasite populations was found to be 10.2 ± 0.3 μm and 8.3 ± 0.2 μm, suggesting that the re-expression of OAS-TL causes the partial recovery of this phenotypic defect. ANOVA tests were used to analyse the difference between WT, Δ*oas-tl* A and Δ*oas-tl* A [OAS-TL] flagella lengths and the difference between WT, Δ*oas-tl* B and Δ*oas-tl* B [OAS-TL] flagella lengths. The null hypothesis of no statistically significant difference between the mean flagellum lengths of the *L. donovani* WT, Δ*oas-tl* A and Δ*oas-tl* A [OAS-TL] was rejected [$F_{2,297} = 123.3$, $p < 0.001$]. Tukey's post test shows significant differences between all three mean values. The null hypothesis of no statistically significant difference between the mean flagellum lengths of *L. donovani* WT, Δ*oas-tl* B and Δ*oas-tl* B [OAS-TL] was also rejected [$F_{2,297} = 166.4$, $p < 0.001$]. Tukey's post test shows significant differences between all three mean values. The results of the statistical test on flagellum lengths are shown in Figure 4.10. The data are graphically summarised in Figure 4.12 A.

The body length of the *OAS-TL* null mutants also appeared to have a detrimental effect on the parasites due to the loss of the gene. The mean body length of *L. donovani* WT promastigotes at late log phase (Figure 1.9 A) was found to be 11.4 ± 0.3 μm, which is much higher than the mean body lengths of Δ*oas-tl* A and Δ*oas-tl* B (Figure 1.9 B and C), which were determined to be 6.4 ± 0.2 μm and 6.7 ± 0.2 μm respectively. Despite the recovery of body shape in the re-expressing lines (Δ*oas-tl* A [OAS-TL] and Δ*oas-tl* B [OAS-TL], Figure 1.9 D and E), the mean body lengths of these parasite populations were determined to be 6.8 ± 0.2 μm and 5.6 ± 0.2 μm. ANOVA tests were performed to determine whether or not statistically significant differences existed between the WT, Δ*oas-tl* A and Δ*oas-tl* A [OAS-TL] body lengths and WT, Δ*oas-tl* B and Δ*oas-tl* B [OAS-TL] body lengths. The tests confirmed that the differences between the mean body length of WT and Δ*oas-tl* A and the difference between WT and Δ*oas-tl* B were statistically significant, and the results are shown in Figure 4.11. The null hypothesis of no statistically significant difference between the mean body lengths of the *L. donovani* WT, Δ*oas-tl* A and Δ*oas-tl* A [OAS-TL] was rejected [$F_{2,297}$ = 155.5, $p < 0.001$]. Tukey's post test shows a significant difference between mean body lengths of WT and Δ*oas-tl* A, and WT and Δ*oas-tl* A [OAS-TL], but no significant difference between Δ*oas-tl* A and Δ*oas-tl* A [OAS-TL]. The null hypothesis of no statistically significant difference between the mean body lengths of *L. donovani* WT, Δ*oas-tl* B and Δ*oas-tl* B [OAS-TL] is rejected [$F_{2,297}$ = 155.2, $p < 0.001$]. Tukey's post test shows a significant difference between mean body lengths of WT and Δ*oas-tl* B, and WT and Δ*oas-tl* B [OAS-TL], but no significant difference between Δ*oas-tl* B and Δ*oas-tl* B [OAS-TL]. The data are graphically summarised in Figure 1.12 B.

Therefore, the lack of OAS-TL in promastigotes has a severe, negative effect on the flagellum length of *L. donovani*, which is partially recovered by the extra-chromasomal re-expression of OAS-TL. The mean body lengths of the *OAS-TL* null mutant parasites were also significantly shorter due to the gene deletion. When OAS-TL was re-expressed, morphological features such as the spindle-like shape and the twisted effect of the membrane were restored, but the mean body length remained similar to the null mutant lines. It is likely that the partial nature of the recovery of the morphological defects in the re-expressing lines is

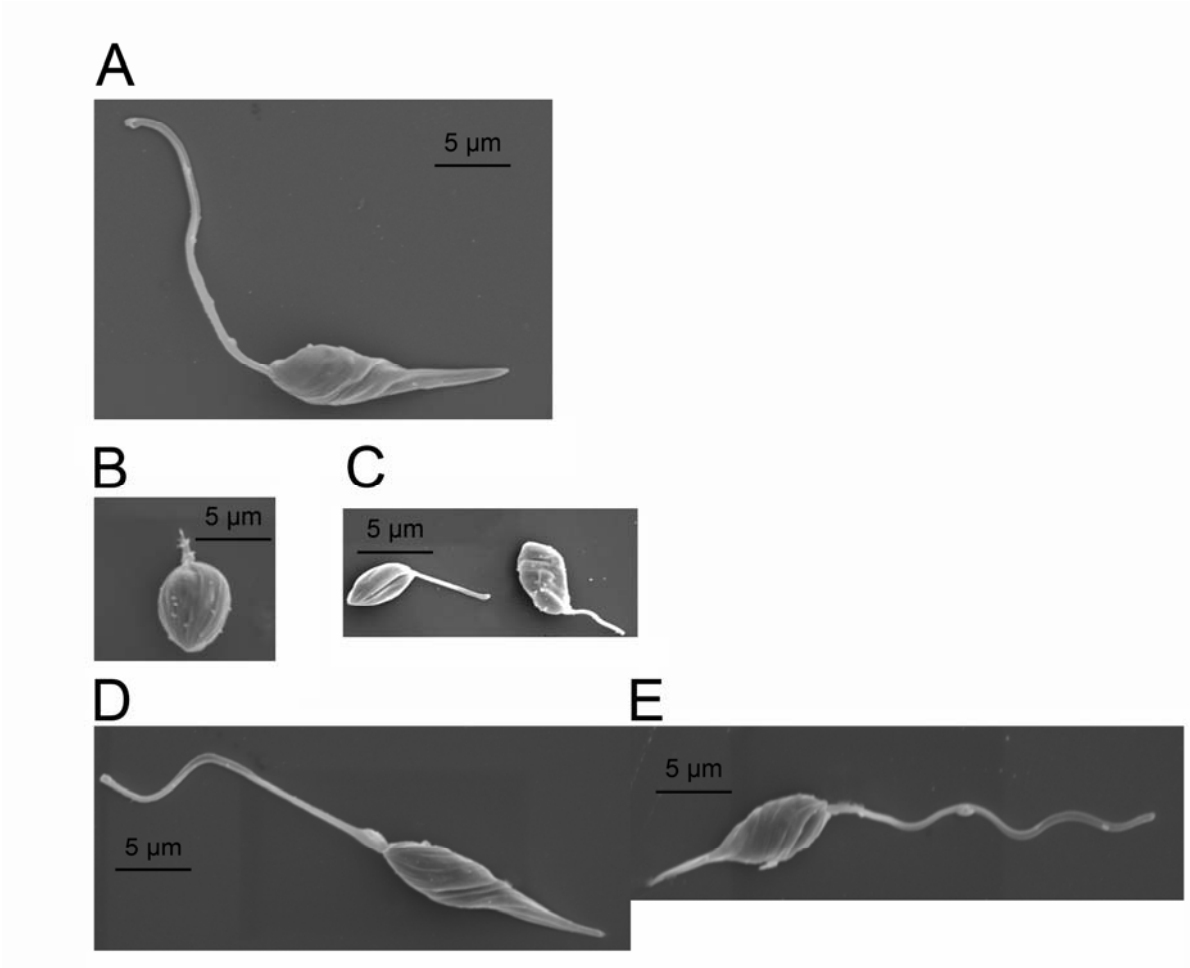

Figure 4.9 SEM images of WT, Δ*oas-tl* A, Δ*oas-tl* B, Δ*oas-tl* A [OAS-TL] and Δ*oas-tl* B [OAS-TL] *L. donovani* promastigotes.
Log phase promastigotes (approximately 5 x 10^6 cells/ml) were fixed, mounted and viewed using scanning electron microscopy. **A**, WT; **B**, Δ*oas-tl* A; **C**, Δ*oas-tl* B; **D**, Δ*oas-tl* A [OAS-TL]; **E**, Δ*oas-tl* B [OAS-TL]. The range of values observed for flagellum length are; WT, 5.5 – 21.7 µm; Δ*oas-tl* A, 0 – 15.8 µm; Δ*oas-tl* B, 0 – 18.9 µm; Δ*oas-tl* A [OAS-TL], 4.7 – 17.5 µm; Δ*oas-tl* B [OAS-TL], 4.3 – 17.9 µm. The range of values observed for body length are; WT, 6.1 – 23.7 µm; Δ*oas-tl* A, 3.3 – 11.9 µm; Δ*oas-tl* B, 0.4 – 14.7 µm; Δ*oas-tl* A [OAS-TL], 3.7 – 12.2 µm; Δ*oas-tl* B [OAS-TL], 2.0 – 16.9 µm.

A

L. donovani WT, Δ_oas-tl_ A, Δ_oas-tl_ A [OAS-TL] flagellum length.
One-way ANOVA: C1 versus C2

```
Source   DF          SS          MS       F      P
C2        2  2846285177  1423142589  123.33  0.000
Error   297  3427276178    11539650
Total   299  6273561355

S = 3397   R-Sq = 45.37%   R-Sq(adj) = 45.00%


                          Individual 95% CIs For Mean Based on
                          Pooled StDev
Level    N   Mean  StDev  ------+---------+---------+---------+---
1      100  14250   3556                                (--*--)
2      100   6713   3568  (--*--)
3      100  10170   3040               (--*-)
                          ------+---------+---------+---------+---
                             7500     10000     12500     15000

Pooled StDev = 3397


Tukey 95% Simultaneous Confidence Intervals
All Pairwise Comparisons among Levels of C2

Individual confidence level = 98.01%


C2 = 1 subtracted from:

C2  Lower  Center  Upper  -----+---------+---------+---------+----
2   -8661   -7536  -6412  (--*---)
3   -5204   -4080  -2955            (--*---)
                          -----+---------+---------+---------+----
                           -7000     -3500         0      3500


C2 = 2 subtracted from:

C2  Lower  Center  Upper  -----+---------+---------+---------+----
3    2332    3457   4581                                 (--*--)
                          -----+---------+---------+---------+----
                           -7000     -3500         0      3500
```

B

L. donovani WT, Δ_oas-tl_ B, Δ_oas-tl_ B [OAS-TL] flagellum length.
One-way ANOVA: C2 versus C1

```
Source   DF          SS          MS       F      P
C1        2  4566393504  2283196752  166.42  0.000
Error   297  4074639994    13719327
Total   299  8641033498

S = 3704   R-Sq = 52.85%   R-Sq(adj) = 52.53%
```

```
                          Individual 95% CIs For Mean Based on
                          Pooled StDev
Level    N   Mean  StDev  ------+---------+---------+---------+---
1      100  14250   3556                                  (-*--)
2      100   4795   4615  (-*-)
3      100   8320   2686            (--*-)
                          ------+---------+---------+---------+---
                             6000      9000     12000     15000

Pooled StDev = 3704


Tukey 95% Simultaneous Confidence Intervals
All Pairwise Comparisons among Levels of C1

Individual confidence level = 98.01%


C1 = 1 subtracted from:

C1   Lower  Center  Upper  -------+---------+---------+---------+--
2   -10681   -9455  -8229  (--*--)
3    -7156   -5930  -4704           (--*--)
                            -------+---------+---------+---------+--
                               -8000     -4000         0      4000


C1 = 2 subtracted from:

C1  Lower  Center  Upper  -------+---------+---------+---------+--
3    2300    3526   4752                                  (--*--)
                          -------+---------+---------+---------+--
                             -8000     -4000         0      4000
```

Figure 4.10 Statistical analysis of the flagellum lengths of *L. donovani* parasite lines.
ANOVA analysis was used to determine whether or not a difference exists between the flagellum lengths of the parasite lines, and Tukey's post-test was used to particularly identify where the differences lie. ANOVA analysis of the mean flagellum lengths of **A**, *L. donovani* WT, Δ*oas-tl* A and Δ*oas-tl* A [OAS-TL] and **B**, *L. donovani* WT, Δ*oas-tl* B and Δ*oas-tl* B [OAS-TL]. In the case of A, the null hypothesis of no statistically significant difference between the mean flagellum lengths of the *L. donovani* WT, Δ*oas-tl* A and Δ*oas-tl* A [OAS-TL] is rejected [$F_{2,297} = 123.3$, $p < 0.001$]. Tukey's post test shows significant differences between all three mean values. In the case of B, the null hypothesis of no statistically significant difference between the mean flagellum lengths of *L. donovani* WT, Δ*oas-tl* B and Δ*oas-tl* B [OAS-TL] is rejected [$F_{2,297} = 166.4$, $p < 0.001$]. Tukey's post test shows significant differences between all three mean values.

A

L. donovani WT, Δ_oas-tl_ A and Δ_oas-tl_ A [OAS-TL] body length.
One-way ANOVA: C1 versus C2

```
Source   DF          SS         MS       F      P
C2        2  1570008932  785004466  155.46  0.000
Error   297  1499724128    5049576
Total   299  3069733059

S = 2247   R-Sq = 51.14%   R-Sq(adj) = 50.82%


                          Individual 95% CIs For Mean Based on Pooled StDev
Level    N   Mean  StDev     +---------+---------+---------+---------
1      100  11444   2899                                      (--*--)
2      100   6369   1681     (-*--)
3      100   6850   1979        (--*--)
                             +---------+---------+---------+---------
                           6000      7500      9000     10500

Pooled StDev = 2247


Tukey 95% Simultaneous Confidence Intervals
All Pairwise Comparisons among Levels of C2

Individual confidence level = 98.01%


C2 = 1 subtracted from:

C2  Lower  Center  Upper  ---------+---------+---------+---------+
2   -5819   -5075  -4332  (---*--)
3   -5338   -4595  -3851    (---*---)
                           ---------+---------+---------+---------+
                                -4000     -2000         0      2000


C2 = 2 subtracted from:

C2  Lower  Center  Upper  ---------+---------+---------+---------+
3    -263     481   1225                              (--*---)
                           ---------+---------+---------+---------+
                                -4000     -2000         0      2000
```

B

L. donovani WT, Δ_oas-tl_ B and Δ_oas-tl_ B [OAS-TL] body length.
One-way ANOVA: C1 versus C2

```
Source   DF          SS         MS       F      P
C2        2  1934505719  967252860  155.20  0.000
Error   297  1850962128    6232196
Total   299  3785467847

S = 2496   R-Sq = 51.10%   R-Sq(adj) = 50.77%
```

```
                          Individual 95% CIs For Mean Based on
                          Pooled StDev
Level    N   Mean  StDev  ----+---------+---------+---------+-----
1      100  11444   2899                              (-*--)
2      100   6682   2445       (-*--)
3      100   5598   2077  (-*-)
                          ----+---------+---------+---------+-----
                           6000      8000     10000     12000

Pooled StDev = 2496


Tukey 95% Simultaneous Confidence Intervals
All Pairwise Comparisons among Levels of C2

Individual confidence level = 98.01%


C2 = 1 subtracted from:

C2  Lower  Center  Upper  -------+---------+---------+---------+--
2   -5589   -4763  -3936       (--*--)
3   -6673   -5846  -5020  (---*--)
                          -------+---------+---------+---------+--
                             -5000     -2500         0      2500


C2 = 2 subtracted from:

C2  Lower  Center  Upper  -------+---------+---------+---------+--
3   -1910   -1083   -257                    (---*--)
                          -------+---------+---------+---------+--
                             -5000     -2500         0      2500
```

Figure 4.11 Statistical analysis of the body lengths of *L. donovani* parasite lines.
ANOVA analysis was used to determine whether a difference exists between the body lengths of the parasite lines, and Tukey's post-test was used to particularly identify where the differences lie. ANOVA analysis of the mean body lengths of **A**, *L. donovani* WT, Δ*oas-tl* A and Δ*oas-tl* A [OAS-TL] and **B**, *L. donovani* WT, Δ*oas-tl* B and Δ*oas-tl* B [OAS-TL]. In the case of A, the null hypothesis of no statistically significant difference between the mean body lengths of the *L. donovani* WT, Δ*oas-tl* A and Δ*oas-tl* A [OAS-TL] is rejected [$F_{2,297}$ = 155.5, $p < 0.001$]. Tukey's post test shows a significant difference between mean body lengths of WT and Δ*oas-tl* A, and WT and Δ*oas-tl* A [OAS-TL], but no significant difference between Δ*oas-tl* A and Δ*oas-tl* A [OAS-TL]. In the case of B, the null hypothesis of no statistically significant difference between the mean body lengths of *L. donovani* WT, Δ*oas-tl* B and Δ*oas-tl* B [OAS-TL] is rejected [$F_{2,297}$ = 155.2, $p < 0.001$]. Tukey's post test shows a significant difference between mean body lengths of WT and Δ*oas-tl* B, and WT and Δ*oas-tl* B [OAS-TL], but no significant difference between Δ*oas-tl* B and Δ*oas-tl* B [OAS-TL].

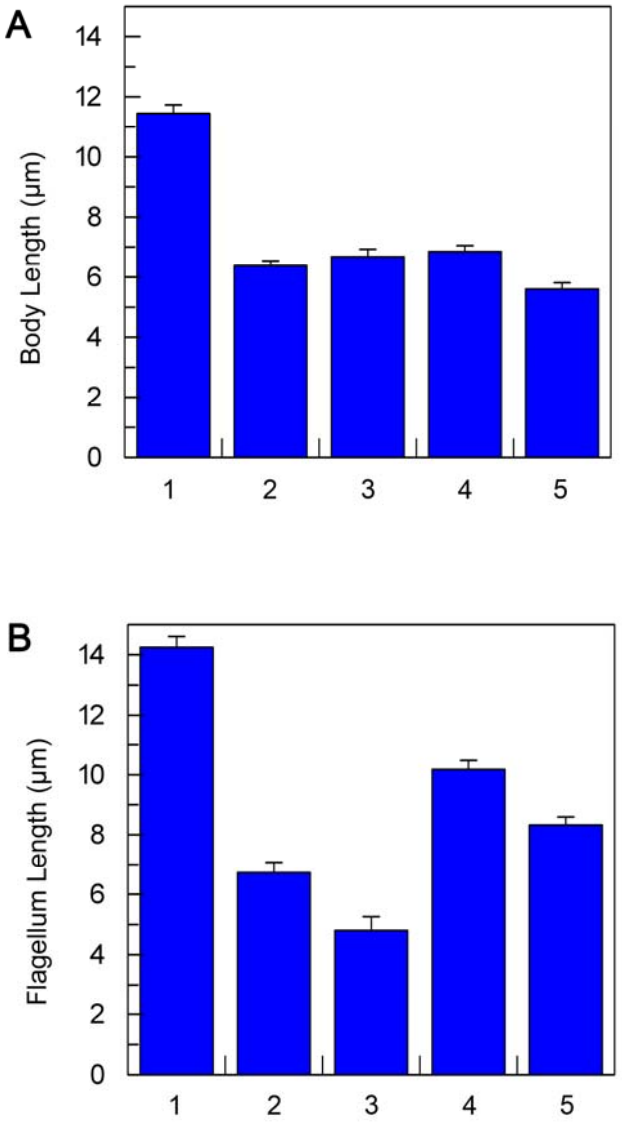

Figure 4.12 Body length and flagellum length of *L. donovani* promastiogtes.
L. donovani WT (**1**), Δ*oas-tl* A (**2**), Δ*oas-tl* B (**3**), Δ*oas-tl* A [OAS-TL] (**4**) and Δ*oas-tl* B [OAS-TL] (**5**) mid-log phase promastigotes were harvested and fixed and coated with a layer of gold palladium before being visualised by scanning electron microscopy (SEM). 1, *L. donovani* WT; 2, Δ*oas-tl* A; 3, Δ*oas-tl* B; 4, Δ*oas-tl* A [OAS-TL]; 5, Δ*oas-tl* B [OAS-TL]. **A**, Mean body lengths of *L. donovani* promastigotes. Graph shows the means and standard errors of 50 parasites measured from each parasite line; **B**, Mean flagellum lengths of *L. donovani* promastigotes. Graph shows the means and standard errors of 50 parasites measured from each parasite line.

due to the levels of OAS-TL in these lines being approximately 50 % less than the WT (Figure 4.7 and Table 4.2).

4.7.4 Thiol analysis of *L. donovani* WT, Δ*oas-tl* A and Δ*oas-tl* B

In order to elucidate the potential reasons for the differences in growth and morphology of Δ*oas-tl* A and Δ*oas-tl* B when compared to WT, the levels of cysteine, glutathione and trypanothione were quantified in the WT and knock-out lines by HPLC. Stationary phase cultures to be analysed were counted and harvested, before lysing the cells and derivatising intracellular thiols with fluorescent monobromobimane. Thiols were separated by HPLC using a C18 reversed-phase chromatography column, using the mobile phases 0.25 % acetic acid and 100 % acetonitrile. Values were calculated using the appropriate standard curves.

Table 4.3 shows the amount of cysteine, glutathione and trypanothione detected in derivatised parasite extract of WT, Δ*oas-tl* A and Δ*oas-tl* B. Each value is a mean of six biological replicates, each of which is a mean of two injections. The data show no difference between any of the three parasite lines, therefore the absence of OAS-TL appears not to affect the amount of thiols available in the cell, which means that the differences observed in growth and morphology of the *OAS-TL* knock-out lines cannot be attributed to a reduction of intracellular thiol levels.

4.7.5 Susceptibility of *L. donovani* Δ*oas-tl* A and B to heavy metals

Parasites lacking OAS-TL clearly have no difference in intracellular thiol levels, however the experiments to determine this were carried out under normal culture conditions. Thiols have been shown to be involved in the detoxification of heavy metals from a number of organisms including *Leishmania* (Ashutosh et al., 2007). It may be the case that parasites lacking OAS-TL are capable of maintaining thiol levels under normal conditions, but when the parasites are exposed to stress, may have very little capability of synthesising enough thiols to create sufficient defence.

	Thiol levels (nmoles per 10^8 parasites) ± S.E.		
	Cysteine	Trypanothione	Glutathione
L. donovani WT	1.7 ± 0.3	0.6 ± 0.1	4.9 ± 0.6
L. donovani Δ*oas-tl* A	1.7 ± 0.2	0.6 ± 0.1	5.3 ± 0.5
L. donovani Δ*oas-tl* B	1.6 ± 0.1	0.6 ± 0.1	4.3 ± 0.5

Table 4.3 Thiol levels of WT, Δ*oas-tl* A and Δ*oas-tl* B *L. donovani* promastigotes.
Total cysteine, trypanothione and glutathione levels in *L. donovani* WT, Δ*oas-tl* A and Δ*oas-tl* B promastigotes, per 10^8 parasites ± S.E. Parasite extracts were monobromobimane-derivatized after reduction of thiols with DTT, and were separated by reversed-phase HPLC. Derivatization and chromatographic conditions are described in Sections 2.3.6.2 and 2.3.6.3.

Since the most commonly used drugs against leishmaniasis are the antimonials, which may have a similar mode of action to heavy metals, the susceptibility of *L. donovani* WT, Δ*oas-tl* A, Δ*oas-tl* B, Δ*oas-tl* A [OAS-TL] and Δ*oas-tl* B [OAS-TL] to a range of heavy metals was investigated. Cultures were counted and seeded at 2.5 x 10^5 cells/ml in 96-well plates and incubated at 25 ºC for 72 h with copper sulphate, potassium arsenate or cadmium chloride (all at 5, 2.5, 1.3, 0.6, 0.3, 0.2, 0.08, 0.04, 0.02, 0.01 or 0.005 mM). Resazurin sodium salt was then added and the plates incubated for a further 48 h at 25 ºC. The bioreduction of this dye reduces the amount of the blue oxidised form and increases the fluorescent intermediate, thus allowing the metabolic activity of the cells to be quantified and indicate cell viability. Values were used to construct IC_{50} graphs (Figures 4.13, 4.14 and 4.15), and IC_{50} values are shown in Table 4.4.

Δ*oas-tl* A and Δ*oas-tl* B are more susceptible to copper sulphate than the WT, with IC_{50} values of 87.7 and 90.7 μM compared to 178.3 μM. When OAS-TL is re-expressed extra-chromasomally, the IC_{50} is restored close to that of the WT, with values of 137.3 and 159.4 μM for Δ*oas-tl* A [OAS-TL] and Δ*oas-tl* B [OAS-TL] respectively. This evidence supports the hypothesis that although able to achieve normal intracellular thiol levels under normal conditions, parasites lacking OAS-TL are less able to cope with heavy metal stress. A similar pattern is seen when the parasite lines were exposed to cadmium chloride. The IC_{50} values for Δ*oas-tl* A and Δ*oas-tl* B are 10.8 and 12.4 μM compared to the WT value of 68.8 μM. Δ*oas-tl* A [OAS-TL] and Δ*oas-tl* B [OAS-TL] have IC_{50} values of 26.2 and 28.1 respectively, which are higher than those of the two null mutant lines, but still lower than the WT value. In the case of potassium arsenate the WT and knock-out lines follow a similar pattern to those observed for the other heavy metals tested, with a WT IC_{50} value of 227.5 μM compared to Δ*oas-tl* A and Δ*oas-tl* B which have IC_{50} values of 169.7 and 177.1 μM respectively. Surprisingly, the re-expression lines do not show any recovery of this phenotype. Δ*oas-tl* A [OAS-TL] and Δ*oas-tl* B [OAS-TL] have IC_{50} values of 161.0 and 92.3 μM, which are even less than the corresponding knock-out lines.

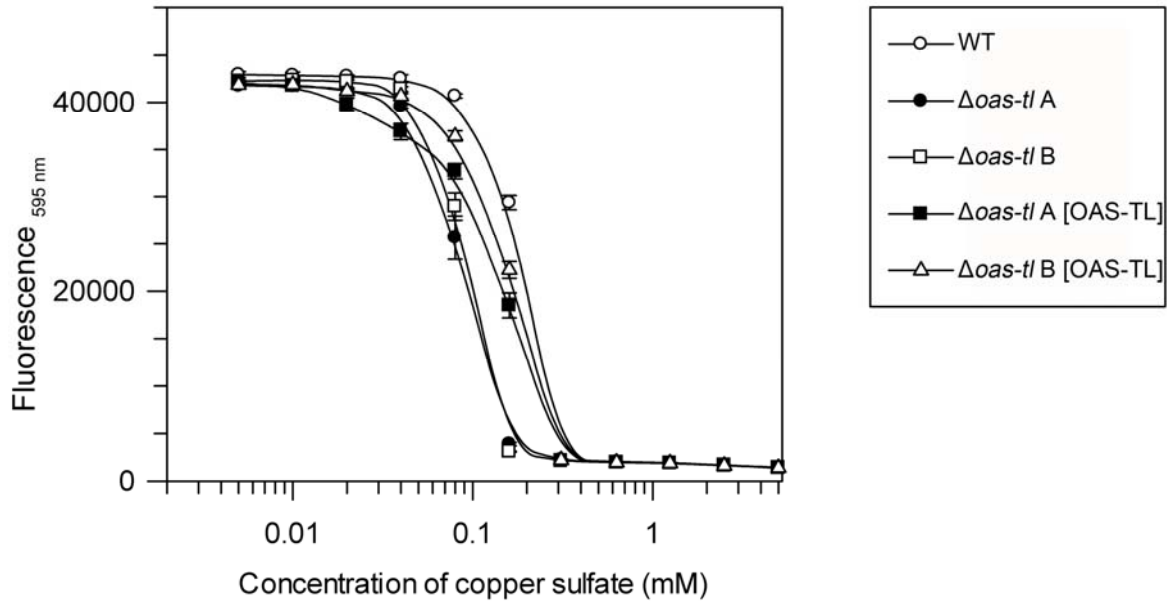

Figure 4.13 IC_{50} determination of *L. donovani* promastigotes exposed to copper sulfate for 5 days.
L. donovani WT, Δ*oas-tl* A, Δ*oas-tl* B, Δ*oas-tl* A [OAS-TL] and Δ*oas-tl* B [OAS-TL] promastigotes were exposed to varying concentrations of copper sulphate, ranging from 0.005 mM to 5 mM. Initial cell density was 2.5 x 10^5 cells/ml. Metabolic activity of cells was determined by the addition of resazurin sodium salt, 48 h before the end of incubation. Absorbance values were determined with an excitation of 490 nm and emission of 595 nm, using a fluorescent plate reader.

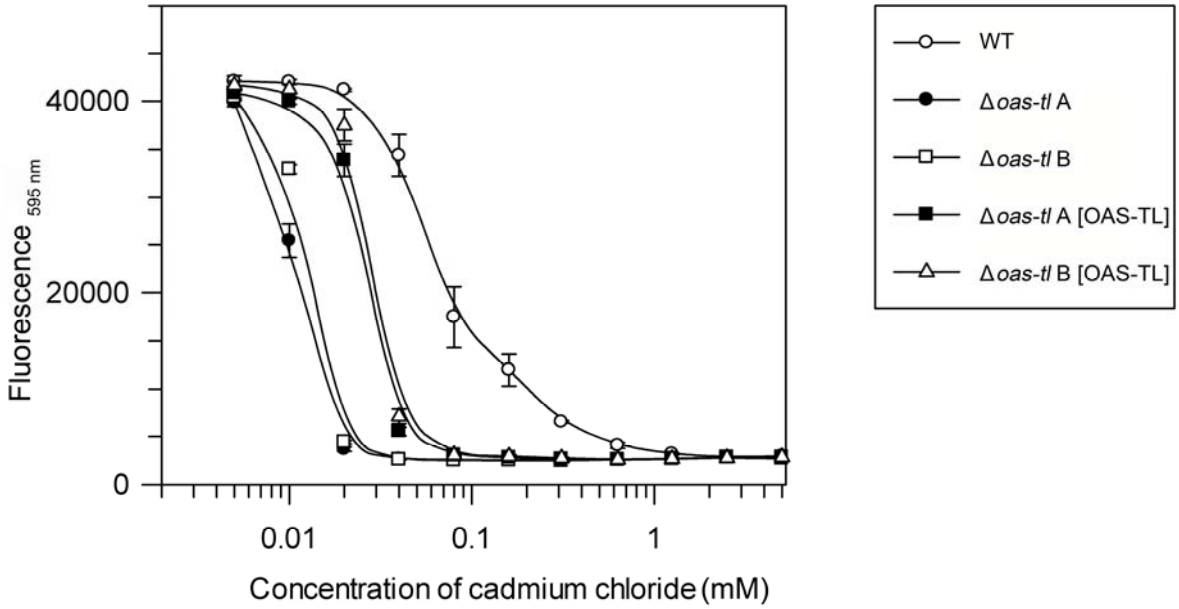

Figure 4.14 IC_{50} determination of *L. donovani* promastigotes exposed to cadmium chloride for 5 days.
L. donovani WT, Δ*oas-tl* A, Δ*oas-tl* B, Δ*oas-tl* A [OAS-TL] and Δ*oas-tl* B [OAS-TL] promastigotes were exposed to varying concentrations of cadmium chloride, ranging from 0.005 mM to 5 mM. Initial cell density was 2.5 x 10^5 cells/ml. Metabolic activity of cells was determined by the addition of resazurin sodium salt, 48 h before the end of incubation. Absorbance values were determined with an excitation of 490 nm and emission of 595 nm, using a fluorescent plate reader.

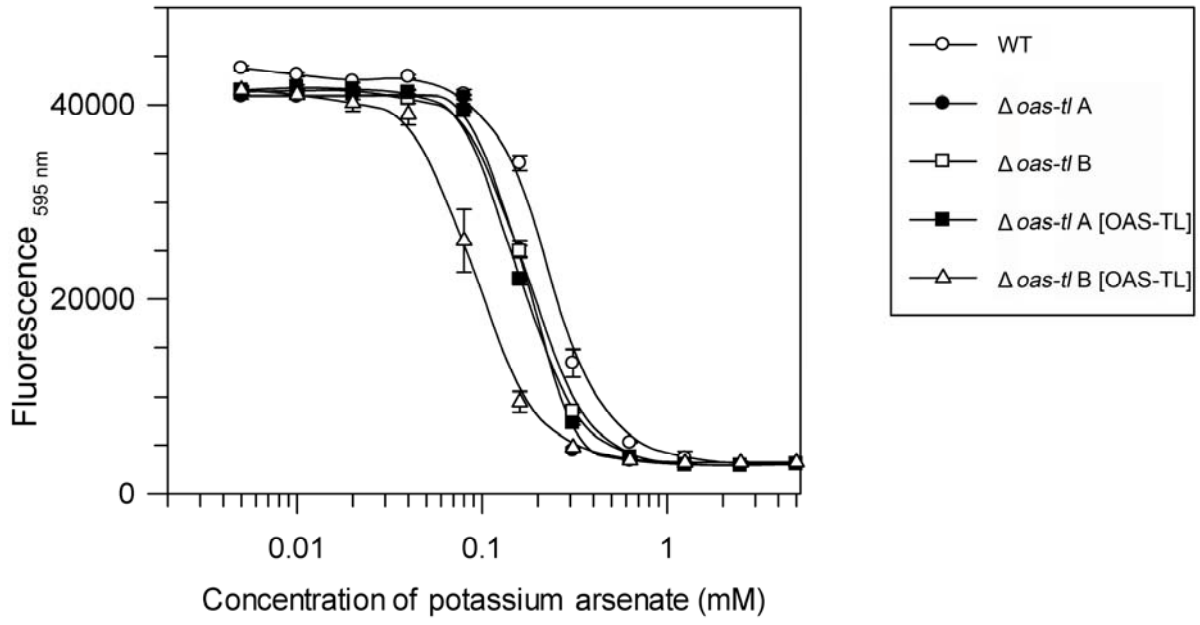

Figure 4.15 IC_{50} determination of *L. donovani* promastigotes exposed to potassium arsenate for 5 days.
L. donovani WT, Δ*oas-tl* A, Δ*oas-tl* B, Δ*oas-tl* A [OAS-TL] and Δ*oas-tl* B [OAS-TL] promastigotes were exposed to varying concentrations of potassium arsenate, ranging from 0.005 mM to 5 mM. Initial cell density was 2.5 x 10^5 cells/ml. Metabolic activity of cells was determined by the addition of resazurin sodium salt, 48 h before the end of incubation. Absorbance values were determined with an excitation of 490 nm and emission of 595 nm, using a fluorescent plate reader.

Parasite Line	IC_{50} $CuSO_4$ [µM]	IC_{50} $CdCl_2$ [µM]	IC_{50} KH_2AsO_4 [µM]
L. donovani WT	178.3 ± 0.1	68.8 ± 0.1	227.5 ± 0.1
L. donovani Δ*oas-tl* A	87.7 ± 0.1	10.8 ± 0.1	169.7 ± 0.1
L. donovani Δ*oas-tl* B	90.7 ± 0.1	12.4 ± 0.1	177.1 ± 0.1
L. donovani Δ*oas-tl* A [OAS-TL]	137.3 ± 0.1	26.2 ± 0.1	161.0 ± 0.1
L. donovani Δ*oas-tl* B [OAS-TL]	159.4 ± 0.1	28.1 ± 0.1	92.3 ± 0.1

Table 4.4 Effect of heavy metals on *L. donovani* promastigote viability.
IC_{50} values were determined as described in Materials and Methods Section 2.3.9.2 using resazurin sodium salt as an indicator of metabolic activity in promastigote stages of *L. donovani* WT and *oas-tl* mutant lines.

4.7.6 Susceptibility of *L. donovani* Δ*oas-tl* A and B to hydroperoxides

As well as being an essential defence against heavy metal toxicity, thiols also play a vital role in protecting *Leishmania* against oxidative stress (Castro et al., 2002). The results of the heavy metal stress experiments led to the hypothesis that parasites lacking OAS-TL may also be significantly more sensitive to hydroperoxides. To investigate this, IC_{50} values were obtained for hydrogen peroxide (H_2O_2), cumene hydroperoxide ($C_6H_5C(CH_3)_2OOH$) and tert-butyl hydroperoxide ($(CH_3)_3COOH$) against of *L. donovani* WT, Δ*oas-tl* A, Δ*oas-tl* B, Δ*oas-tl* A [OAS-TL] and Δ*oas-tl* B [OAS-TL], and are presented in Figures 4.16, 4.17 and 4.18 and Table 4.5.

Experiments were set up similar to the heavy metal experiments described in Section 2.3.9.2, with the following concentrations used, hydrogen peroxide (10, 5, 2.5, 1.3, 0.6, 0.3, 0.2, 0.08, 0.04, 0.02 or 0.01 mM), cumene hydroperoxide and tert-butyl hydroperoxide (both at 1, 0.5, 0.3, 0.1, 0.06, 0.03, 0.02, 0.008, 0.004, 0.002 or 0.001 mM).

No significant differences were found between the parasite lines when exposed to H_2O_2. *L. donovani* Δ*oas-tl* A and Δ*oas-tl* B are approximately twice as susceptible to cumene hydroperoxide than the WT, with IC_{50} values of 9.3 and 13.8 μM respectively compared to 22.1 μM. The sensitivity of the re-expressing lines was reduced back to WT levels, with IC_{50} values of 20.2 and 20.5 μM for Δ*oas-tl* A [OAS-TL] and Δ*oas-tl* B [OAS-TL] respectively.

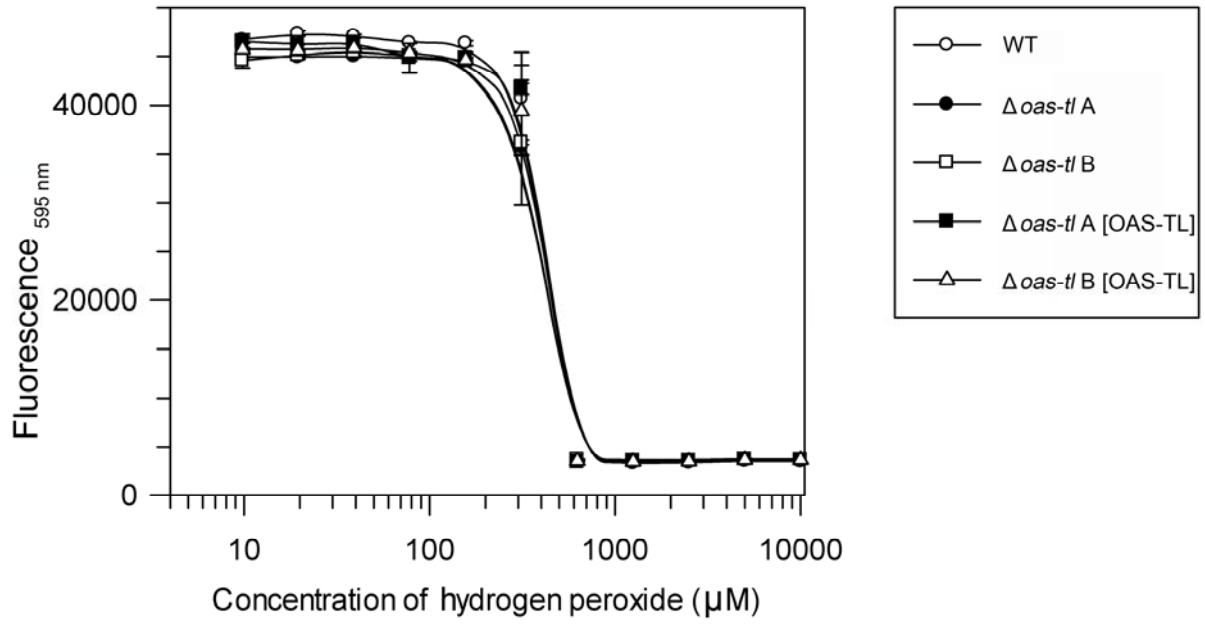

Figure 4.16 IC_{50} determination of *L. donovani* promastigotes exposed to hydrogen peroxide for 5 days.
L. donovani WT, Δ*oas-tl* A, Δ*oas-tl* B, Δ*oas-tl* A [OAS-TL] and Δ*oas-tl* B [OAS-TL] promastigotes were exposed to varying concentrations of hydrogen peroxide, ranging from 0.01 mM to 10 mM. Initial cell density was 2.5 x 10^5 cells/ml. Metabolic activity of cells was determined by the addition of resazurin sodium salt, 48 h before the end of incubation. Absorbance values were determined with excitation of 490 nm and emission of 595 nm, using a fluorescent plate reader.

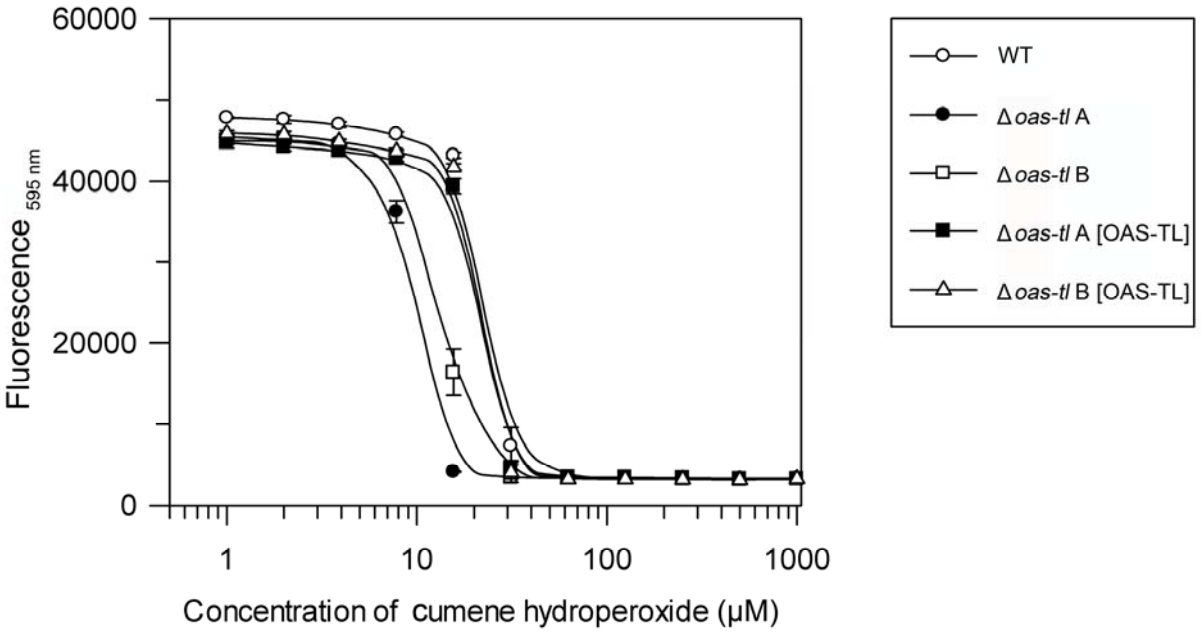

Figure 4.17 IC_{50} determination of *L. donovani* promastigotes exposed to cumene hydroperoxide for 5 days.
L. donovani WT, Δ*oas-tl* A, Δ*oas-tl* B, Δ*oas-tl* A [OAS-TL] and Δ*oas-tl* B [OAS-TL] promastigotes were exposed to varying concentrations of cumene hydroperoxide, ranging from 0.001 mM to 1 mM. Initial cell density was 2.5 x 10^5 cells/ml. Metabolic activity of cells was determined by the addition of resazurin sodium salt, 48 h before the end of incubation. Absorbance values were determined with excitation of 490 nm and emission of 595 nm, using a fluorescent plate reader.

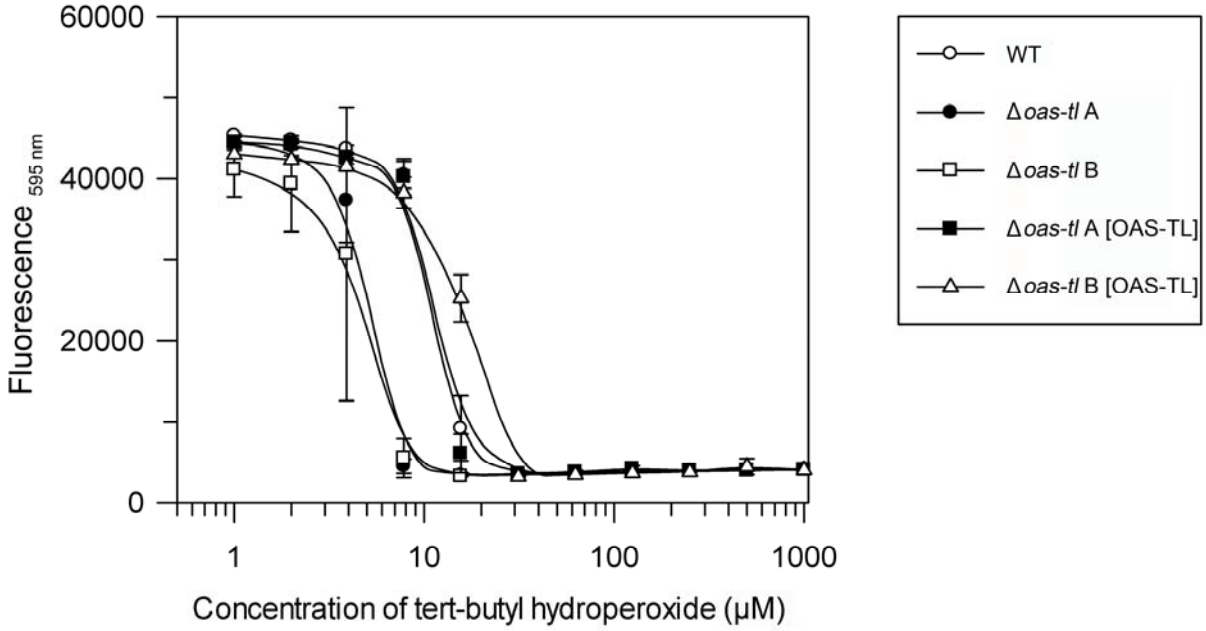

Figure 4.18 IC_{50} determination of *L. donovani* promastigotes exposed to tert-butyl hydroperoxide for 5 days.
L. donovani WT, Δ*oas-tl* A, Δ*oas-tl* B, Δ*oas-tl* A [OAS-TL] and Δ*oas-tl* B [OAS-TL] promastigotes were exposed to varying concentrations of tert-butyl hydroperoxide, ranging from 0.001 mM to 1 mM. Initial cell density was 2.5 x 10^5 cells/ml. Metabolic activity of cells was determined by the addition of resazurin sodium salt, 48 h before the end of incubation. Absorbance values were determined with an excitation of 490 nm and an emission of 595 nm, using a fluorescent plate reader.

Parasite Line	IC_{50} for hydrogen peroxide (H_2O_2) [µM]	IC_{50} for cumene hydroperoxide $C_6H_5C(CH_3)_2OOH$ [µM]	IC_{50} for tert-butyl hydroperoxide $(CH_3)_3COOH$ [µM]
L. donovani WT	364.0 ± 35.9	22.1 ± 0.4	11.2 ± 0.2
L. donovani Δ*oas-tl* A	350.9 ± 24.8	9.3 ± 0.1	4.8 ± 0.2
L. donovani Δ*oas-tl* B	353.6 ± 31.4	13.8 ± 0.1	4.6 ± 0.1
L. donovani Δ*oas-tl* A [OAS-TL]	367.2 ± 31.5	20.2 ± 0.5	10.6 ± 0.3
L. donovani Δ*oas-tl* B [OAS-TL]	354.4 ± 55.5	20.5 ± 0.7	16.2 ± 0.6

Table 4.5 Effect of hydroperoxides on *L. donovani* promastigote viability.
IC_{50} values were determined as described in Section 2.3.9.1 using resazurin sodium salt as an indicator of metabolic activity in promastigote stages of *L. donovani* WT and *OAS-TL* mutant lines.

IC_{50} concentrations of tert-butyl hydroperoxide showed a similar pattern between the WT, knock-out and re-expressing lines, with IC_{50} values of 4.8 and 4.6 µM for Δ*oas-tl* A and Δ*oas-tl* B respectively, compared to a WT value of 11.2 µM. Δ*oas-tl* A [OAS-TL] and Δ*oas-tl* B [OAS-TL] have IC_{50} values of 10.6 and 16.2 µM respectively, higher than the values corresponding to the *OAS-TL* knock-out lines.

4.7.7 Infectivity of peritoneal macrophages *in vitro*

The ability of *L. donovani* WT, Δ*oas-tl* A, Δ*oas-tl* B, Δ*oas-tl* A [OAS-TL] and Δ*oas-tl* B [OAS-TL] to infect murine peritoneal macrophages was assessed *in vitro*. Macrophages were extracted and incubated for 24 h in tissue culture slides at 37 ºC with 5 % CO_2, 95 % air, before infecting them with stationary phase promastigotes. These were allowed to infect for 2 h before being washed off and replaced with fresh medium. Infections were incubated for a further 6 days at 37 ºC with 5 % CO_2, 95 % air, changing spent medium after 3 days. Percentage infection and number of parasites per macrophage were determined and the results are shown in Figure 4.19.

After 6 days, *L. donovani* WT parasites had established an infection level of 20.0 % ± 6.2. Δ*oas-tl* A and Δ*oas-tl* B did not appear to infect macrophages at all (0 % and 0%), while Δ*oas-tl* A [OAS-TL] and Δ*oas-tl* B [OAS-TL] infected their host cells to about the same level as WT parasites (18.7 % ± 6.3 and 20.0 ± 5.0). When OAS-TL is re-expressed in the knock-out lines, the level of infection was restored to a similar percentage to the WT. This indicates that Δ*oas-tl* A and Δ*oas-tl* B must be unable to develop an infection of macrophages. This could be due to an inability to infect, an inability to transform to amastigotes or an inability to survive as amastigotes.

4.7.8 Time course in vitro infectivity to macrophages

To dissect exactly which stage of the 'infection' process was hindered by the lack of OAS-TL in the null mutants, macrophages were exposed to promastigotes as before. This time the experiments were stopped after 2 h, 12 h, 24 h and 55 h, and only WT and one of the null mutant lines, Δ*oas-tl* B, were used to infect. The 2 h time-point was chosen as an indicator of the ability of the parasites to

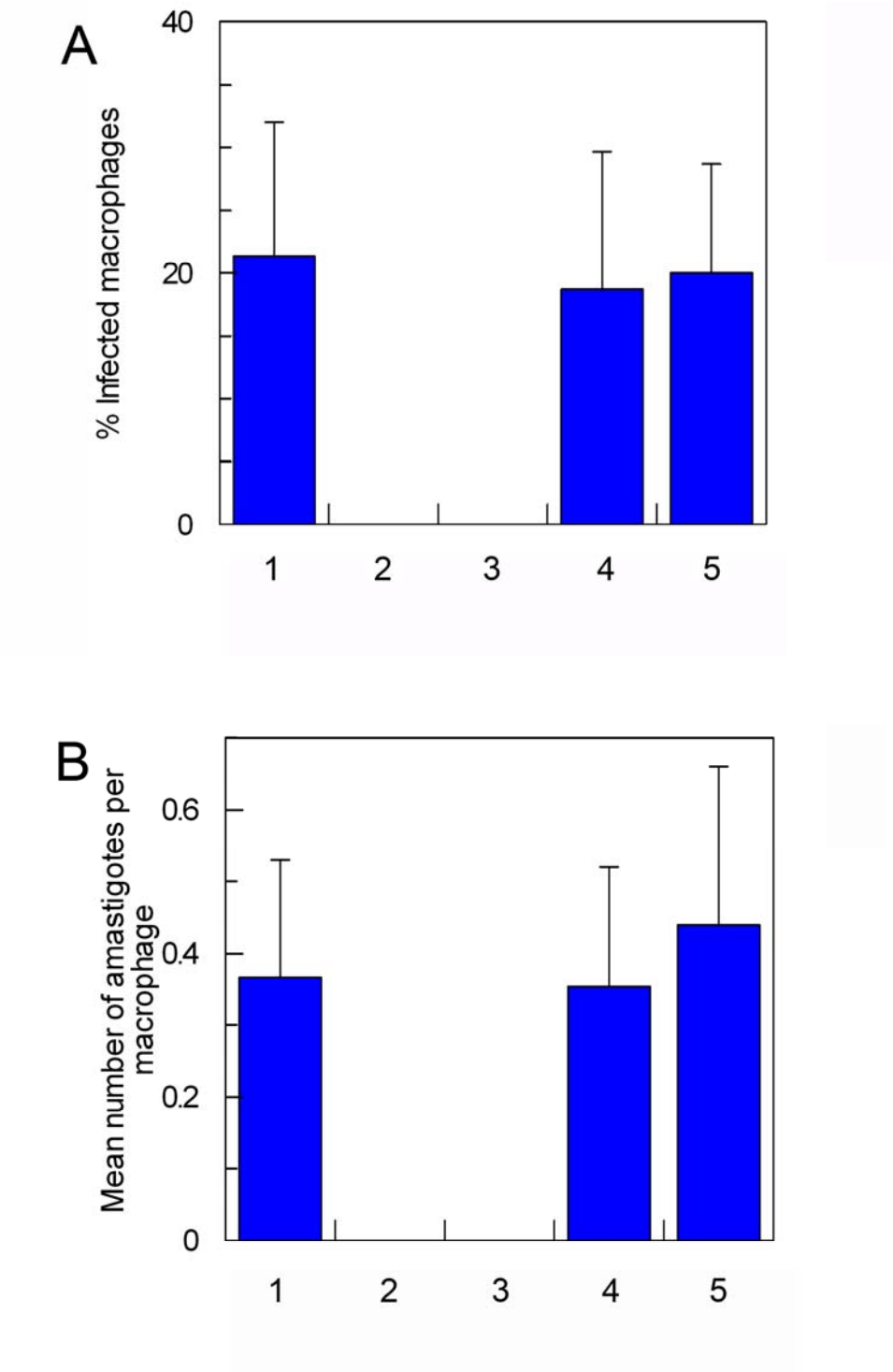

Figure 4.19 Infectivity of *L. donovani* WT, Δ*oas-tl* A, Δ*oas-tl* B, Δ*oas-tl* A [OAS-TL] and Δ*oas-tl* B [OAS-TL] promastigotes to macrophages.
Stationary phase promastigotes were used to infect peritoneal macrophages at a ratio of 5:1, and slides were incubated for 6 days post-infection. 1, WT; 2, Δ*oas-tl* A; 3, Δ*oas-tl* B; 4, Δ*oas-tl* A [OAS-TL]; 5, Δ*oas-tl* B [OAS-TL]. **A**: Percentage of infected macrophages per 100 counted. Results show the mean ± S.E.M. of three replicates. **B**: Mean number of amastigotes per 50 macrophages. Results show the mean ± S.E.M. of three replicates.

infect macrophages, the 12 h time-point was indicative of survival within macrophages, the 24 h time-point was the estimated time taken for promastigotes to transform into amastigotes and the 55 h time-point was chosen as an indicator of proliferation within macrophages as amastigotes. The percentage infection of macrophages as well as the number of parasites per infected macrophage were determined and are shown in Figure 4.20.

After 2 h no difference was seen in the average percentage infection between *L. donovani* WT and Δ*oas-tl* B. However, the number of Δ*oas-tl* B parasites per infected macrophage was significantly higher than WT ($p = 0.028$), with 2.48 ± 0.1 compared to 1.94 ± 0.1 parasites per macrophage respectively. This indicates that the parasites lacking OAS-TL are taken up by macrophages in higher numbers than WT. After the 12 h and 24 h time-points, no difference in either percentage infection or number of parasites per macrophage was observed between the two parasite lines. At 55 h post-infection, no difference was observed between the number of WT and Δ*oas-tl* B parasites per infected macrophage. However, there was a significant decrease in percentage infection of Δ*oas-tl* B parasites compared to WT ($p = 0.002$). *L. donovani* WT established an infection of 26 ± 1.3 % of macrophages compared to Δ*oas-tl* B parasites which infected 6 ± 1.2 % of macrophages.

These results suggest that parasites lacking OAS-TL are capable of being taken up by macrophages and surviving at a similar level to WT for a period of around 24 h post-infection, after which their numbers decrease rapidly. Since 24 h is the estimated time taken for *Leishmania* to transform into amastigotes, it is possible that *L. donovani* lacking OAS-TL cannot transform into amastigotes, and they are subsequently cleared by the host macrophages. Alternatively, if the parasites are capable of transformation into amastigotes, they may not be able to survive within the macrophage and proliferate as such.

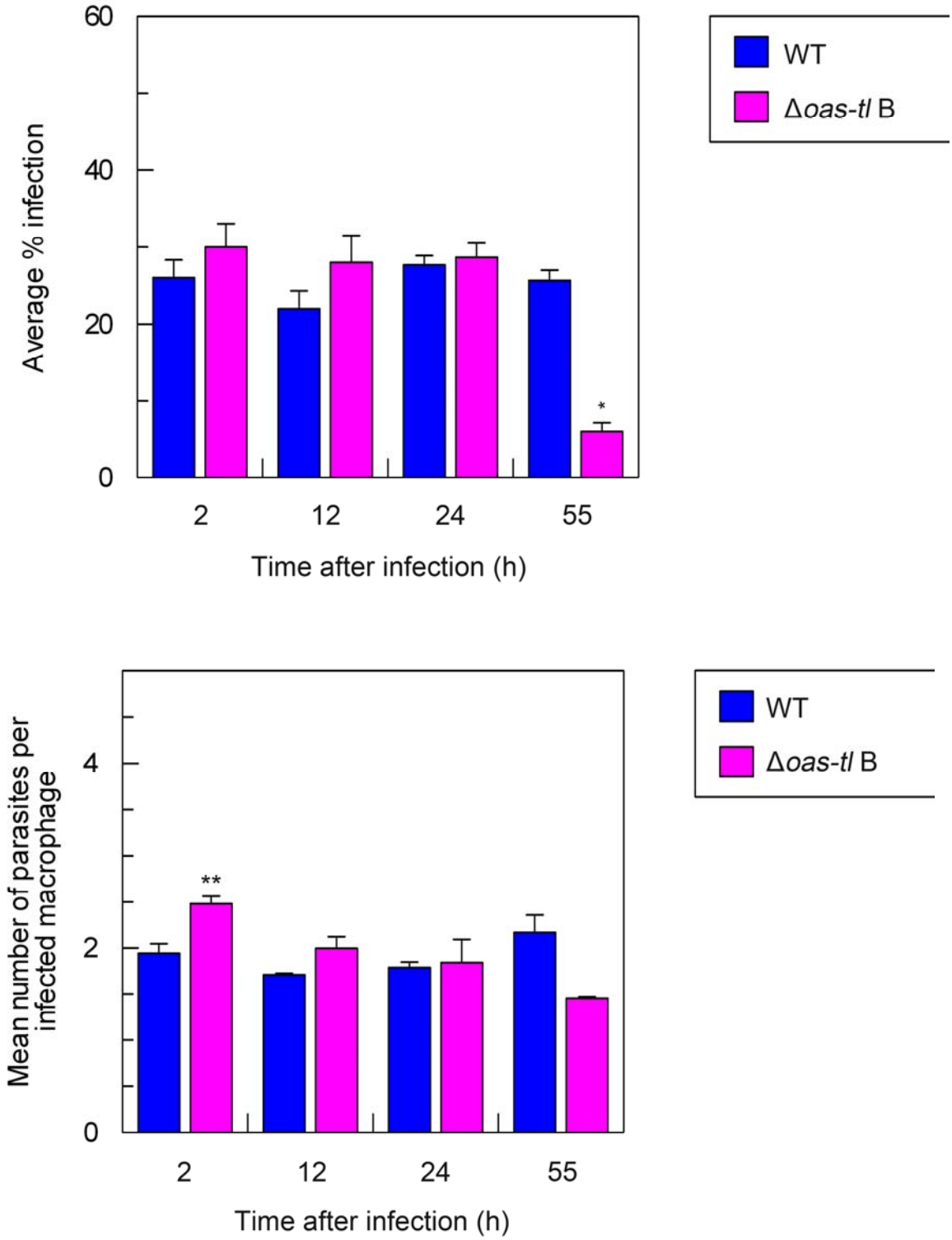

Figure 4.20 Infectivity of *L. donovani* WT and Δ*oas-tl* B promastigotes to macrophages at early time-points.
Stationary phase promastigotes were used to infect peritoneal macrophages at a ratio of 5:1, and slides were incubated for 2, 12, 24 and 55 h time-points. **A**: Percentage infection of *L. donovani* WT and Δ*oas-tl* B in macrophages after 2, 12, 24 and 55 h post-infection. Results show the mean ± S.E.M. of three replicates, and 100 macrophages were counted from each. **B**: Mean number of *L. donovani* WT and Δ*oas-tl* B parasites in infected macrophages after 2, 12, 24 and 55 h post-infection. Results show the mean ± S.E.M. of three replicates, and the number of parasites in 50 macrophages were counted from each. Values were statistically analysed by comparison to the WT value from the appropriate time-point. *, p = 0.002 and **, p = 0.028.

4.7.9 Effect of medium supplementation on *in vitro* infectivity to macrophages

The previous experiments showed that *L. donovani* Δ*oas-tl* A and B are not capable of surviving in macrophages in vitro for 6 days. Further investigation clarified that these parasites are taken up by macrophages and result in a similar percentage infection as WT after 2 h post-infection. The *OAS-TL* null mutants can survive for up to 24 hours post-infection at a similar percentage infection as WT, however after this time there is a significant decrease in percentage infection of these parasites compared to WT.

The *OAS-TL* null mutant parasites have been shown to be more susceptible to hydroperoxides that *L. donovani* WT. Since methionine is believed to be the limiting factor for the reverse transsulfuration pathway – the alternative cysteine biosynthesis pathway in *Leishmania* - it was hypothesised that by supplementing the medium with methionine, infection levels of *L. donovani* Δ*oas-tl* A and B may be restored to WT levels. In addition, glutathione was also used to supplement the medium, due to the ability of the parasite to break-down this low molecular weight thiol and use it as an alternative source of cysteine.

The effect of supplementing the medium on parasite development in macrophages was investigated at different timepoints. Macrophage infections were set up as described previously, and parasites were allowed to infect for 2 h before extracellular parasites were washed off. At all stages the medium used was either addition-free or contained the appropriate supplement (1 mM glutathione or 5 mM methionine). Slides of macrophage infections were fixed and stained after 2 h, 12 h, 24 h and 55 h.

After 2 h, the *OAS-TL* null mutant parasites appear to be taken up by macrophages at higher numbers than WT parasites, with percentage infections of 68 ± 3.6 % and 65.7 ± 0.3 % compared to the WT value of 40.3 ± 0.7 %, (Figure 4.21). The average percentage infection of Δ*oas-tl* A [OAS-TL] and Δ*oas-tl* B [OAS-TL], after 2 h post-infection, are 53.3 ± 2.3 % and 47.7 ± 1.2 % respectively, showing a partial recovery of the null mutants back to WT levels.

At this stage, no clear difference between the infection rates without additions to the medium, and those where the medium was supplemented with 1 mM glutathione or 5 mM methionine was seen. Despite the difference in average percentage infection between the knock-out lines and the WT at 2 h, at 12 h post-infection the difference no longer exists, indicating that a lower proportion of *OAS-TL* null mutant parasites are able to survive within host macrophages for 12 h than WT. 43.7 ± 2.0 % of macrophages were infected with *L. donovani* WT parasites after 12 h post-infection, which is not statistically different to the level of infection seen after 2 h for these parasites. No difference was observed between the average percentage infection of all of the parasite lines after 12 h. Furthermore, there is no significant difference in the infection rates of the experiments carried out using medium with either no addition, or supplemented with either 1 mM glutathione or 5 mM methionine.

After 24 h, the infection levels of the different parasite lines under different conditions show a change. The *OAS-TL* null mutant lines had infected almost half the number of macrophages than WT parasites. One of the re-expressing lines shows a percentage infection only very slightly higher than the knock-out lines, and the other, Δ*oas-tl* B [OAS-TL], is higher than all of the other lines. The addition of glutathione to the medium does not affect the average percentage of macrophages infection of all five lines. In the case of the methionine supplementation, WT parasites infected 51.7 ± 1.9 % of macrophages compared to Δ*oas-tl* A and Δ*oas-tl* B, which infected 32.3 ± 5.0 % and 37 ± 1 % respectively. The results suggest that there is no difference in percentage infection of the *OAS-TL* null mutant lines and the WT.

At 55 h post-infection, a clear difference between L. donovani WT and Δ*oas-tl* A and Δ*oas-tl* B had become apparent. WT parasites infected macrophages and survived for 55 h in over 52.3 ± 1.5 % of macrophages, compared to Δ*oas-tl* A and Δ*oas-tl* B which were almost completely cleared from all macrophages, with percentage infections of 0.7 ± 0.7 % and 1.0 ± 0 %. There was a partial recovery shown by the OAS-TL re-expressing lines, with infection rates of 18.3 ± 1.8 % and 19.3 ± 1.9 %.

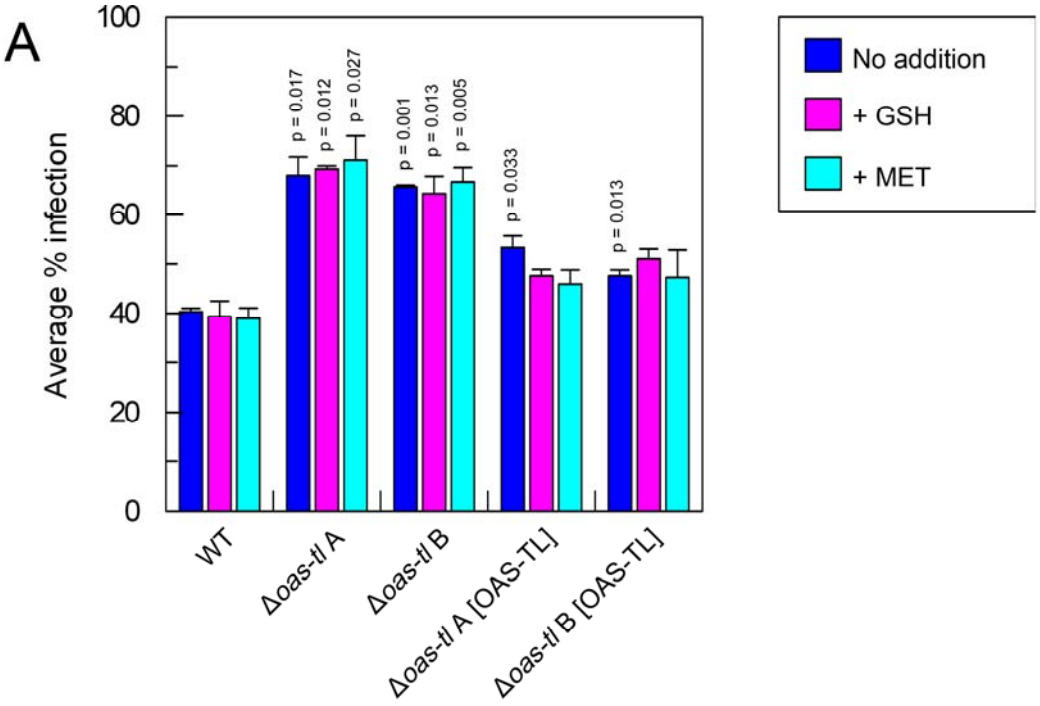
A
Average % infection
100
80
60
40
20
0
p = 0.017
p = 0.012
p = 0.027
p = 0.001
p = 0.013
p = 0.005
p = 0.033
p = 0.013
WT
Δoas-tl A
Δoas-tl B
Δoas-tl A [OAS-TL]
Δoas-tl B [OAS-TL]
No addition
+ GSH
+ MET

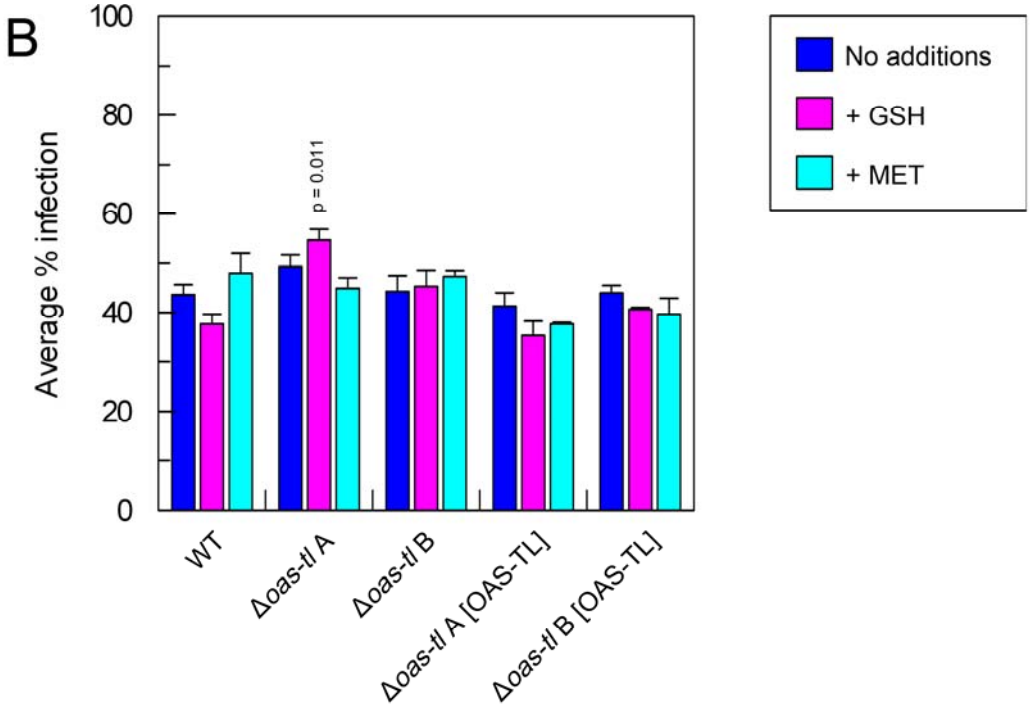
B
Average % infection
100
80
60
40
20
0
p = 0.011
WT
Δoas-tl A
Δoas-tl B
Δoas-tl A [OAS-TL]
Δoas-tl B [OAS-TL]
No additions
+ GSH
+ MET

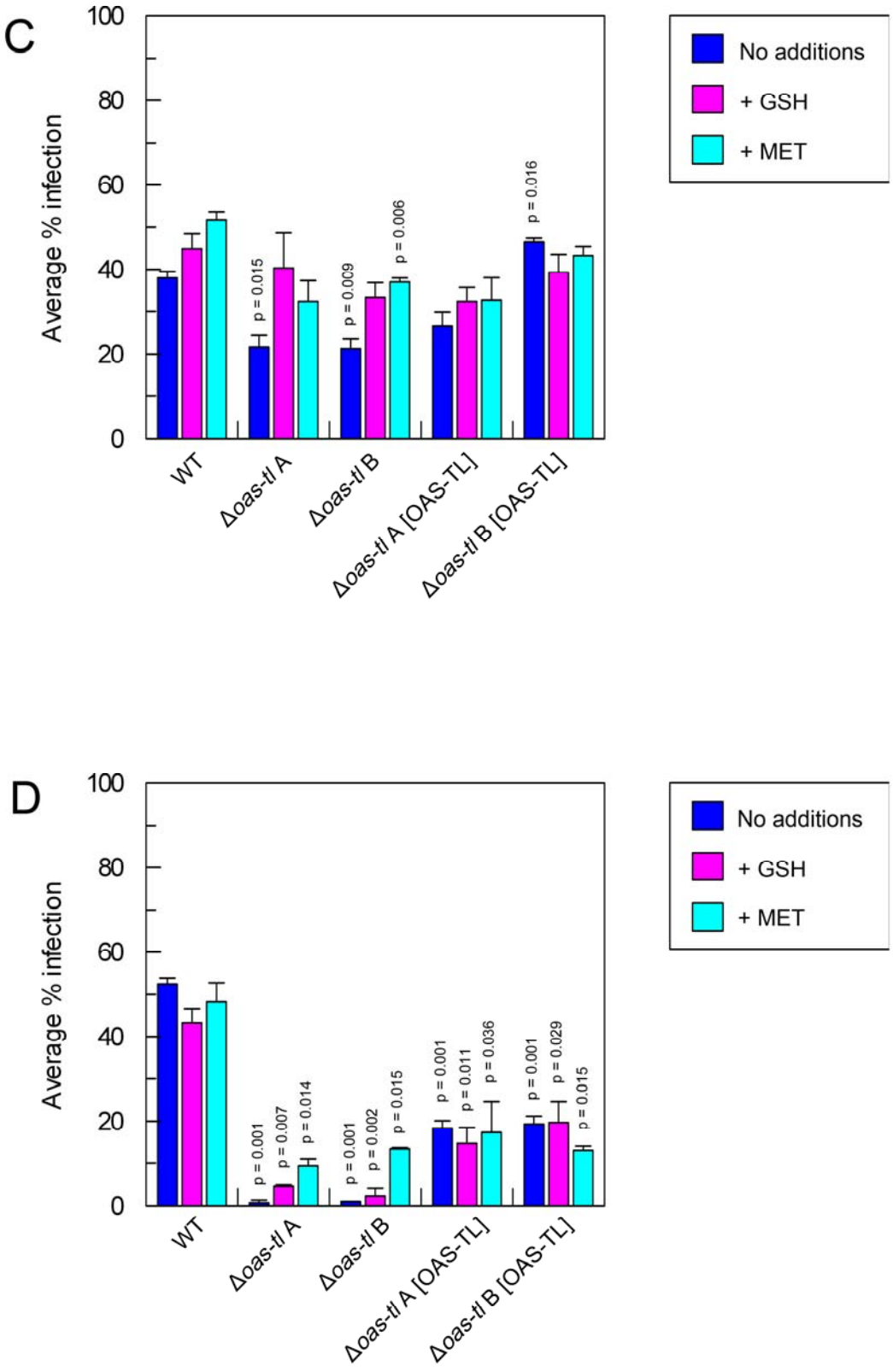

Figure 4.21 Effect of medium supplementation on the infectivity of *L. donovani* WT, Δ*oas-tl* A, Δ*oas-tl* B, Δ*oas-tl* A [OAS-TL] and Δ*oas-tl* B [OAS-TL] promastigotes to macrophages. Stationary phase promastigotes were used to infect peritoneal macrophages at a ratio of 5:1. The parasites and macrophages were incubated for 2 h before the parasites were washed off and replaced with fresh medium. Experiments were carried out with either no addition to the medium, or

supplemented with either 1 mM glutathione or 5 mM methionine, and were terminated after 2 h, 12 h, 24 h and 55 h. 1, WT; 2, Δ*oas-tl* A; 3, Δ*oas-tl* B; 4, Δ*oas-tl* A [OAS-TL]; 5, Δ*oas-tl* B [OAS-TL]. **A**: Percentage infection of *L. donovani* WT, Δ*oas-tl* A, Δ*oas-tl* B, Δ*oas-tl* A [OAS-TL] and Δ*oas-tl* B [OAS-TL] in macrophages after 2 h. **B**: Percentage infection of *L. donovani* WT, Δ*oas-tl* A, Δ*oas-tl* B, Δ*oas-tl* A [OAS-TL] and Δ*oas-tl* B [OAS-TL] in macrophages after 12 h. **C**: Percentage infection of *L. donovani* WT, Δ*oas-tl* A, Δ*oas-tl* B, Δ*oas-tl* A [OAS-TL] and Δ*oas-tl* B [OAS-TL] in macrophages after 24 h. **D**: Percentage infection of *L. donovani* WT, Δ*oas-tl* A, Δ*oas-tl* B, Δ*oas-tl* A [OAS-TL] and Δ*oas-tl* B [OAS-TL] in macrophages after 55 h. Results show the mean ± S.E.M. of three replicates, and 100 macrophages were counted. Values were statistically analysed by comparison to the WT value with the appropriate addition by unpaired t-test, and resulting p-values are given.

The addition of glutathione to the medium leads to a slight decrease in the average percentage infection of macrophages with WT parasites compared to when the medium was supplement-free, although this decrease was minimal. Δ*oas-tl* A and Δ*oas-tl* B show a slight increase in percentage infection when glutathione was added to the medium, with infections of 4.7 ± 0.3 % and 2.3 ± 1.9 % respectively. The re-expressing lines show the same partial recovery as those infections carried out under no medium supplementation. There is no significant difference between the infections of Δ*oas-tl* A [OAS-TL] and Δ*oas-tl* B [OAS-TL], carried out under the different medium supplementation conditions.

When methionine was added to the medium, Δ*oas-tl* A and Δ*oas-tl* B showed an increase in infection to 9.3 ± 1.7 % and 13.3 ± 0.3 %, compared to values close to 0 % when addition-free medium was used. Δ*oas-tl* A [OAS-TL] and Δ*oas-tl* B [OAS-TL] showed average percentage infections of 17.3 ± 7.4 % and 13 ± 1 % - marginally higher than the null mutant lines.

In addition to the average percentage infection, the mean number of parasites per infected macrophage was also determined and used as a measure of the infectivity, survival and proliferation of *L. donovani* WT, Δ*oas-tl* A, Δ*oas-tl* B, Δ*oas-tl* A [OAS-TL] and Δ*oas-tl* B [OAS-TL] in macrophages (Figure 4.22). At both 2 h and 12 h post-infection, the results show very little variation between the five parasite lines maintained in various media. After 24 h, the number of parasites per macrophage infected by the *OAS-TL* null mutants was similar to the WT and re-expressing lines.

At 55 h post-infection, a clear trend had emerged showing that with no addition to the medium 2.5 ± 0.3 WT parasites could be seen per infected macrophage on average, whereas no Δ*oas-tl* A and Δ*oas-tl* B parasites could be visualised in macrophages. The addition of both 1 mM glutathione and 5 mM methionine had a positive effect on the number of null mutant parasites per macrophage. Δ*oas-tl* A increased from 0 ± 0 parasites per infected macrophage to 1.7 ± 0.1 parasites per infected macrophage when supplemented with 1 mM glutathione and 1.8 ± 0.2 parasites per infected macrophage when supplemented with 5 mM methionine. Δ*oas-tl* B increased from 0 ± 0 parasites per infected macrophage to 2.0 ± 0.1 when supplemented with 1 mM glutathione and 2.1 ± 0.2 parasites per infected macrophage when supplemented with 5 mM methionine. Similar

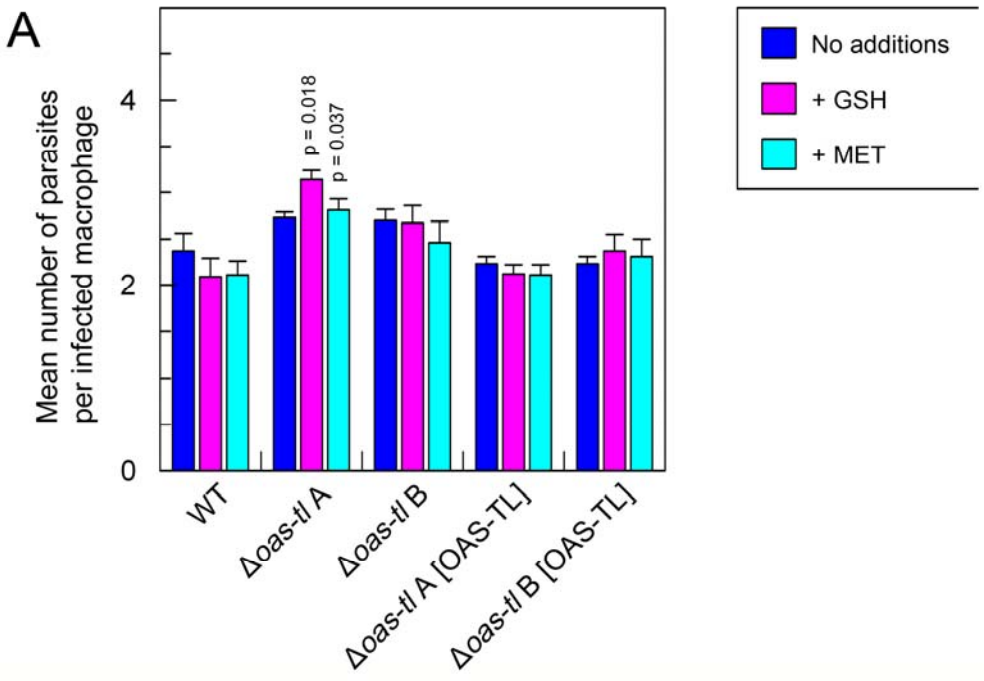
A
Mean number of parasites per infected macrophage
0
2
4
p = 0.018
p = 0.037
No additions
+ GSH
+ MET
WT
Δoas-tl A
Δoas-tl B
Δoas-tl A [OAS-TL]
Δoas-tl B [OAS-TL]

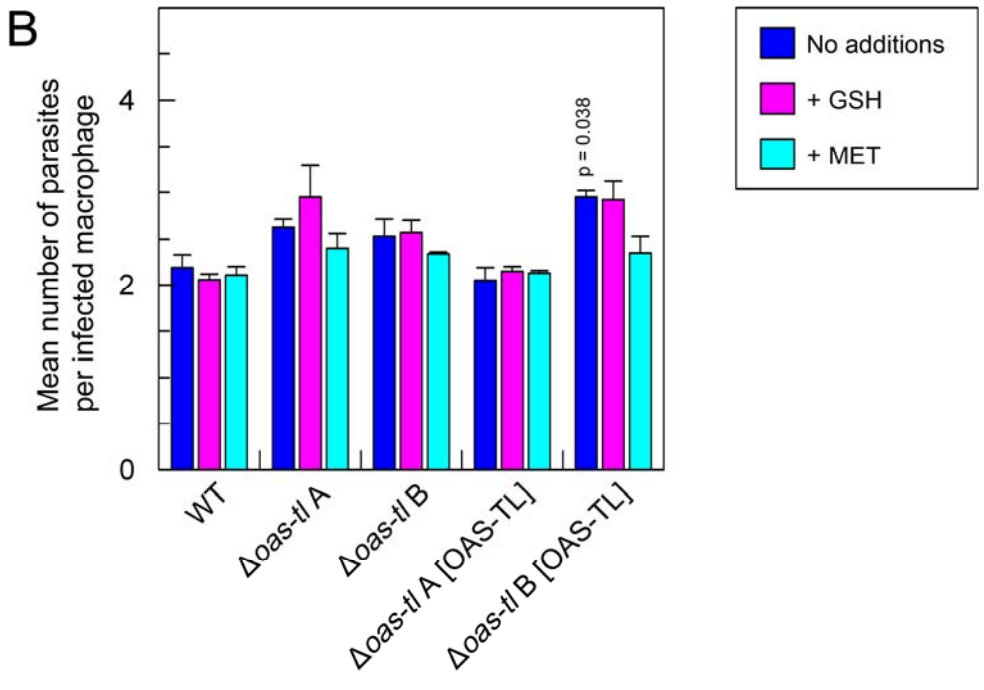
B
Mean number of parasites per infected macrophage
0
2
4
p = 0.038
No additions
+ GSH
+ MET
WT
Δoas-tl A
Δoas-tl B
Δoas-tl A [OAS-TL]
Δoas-tl B [OAS-TL]

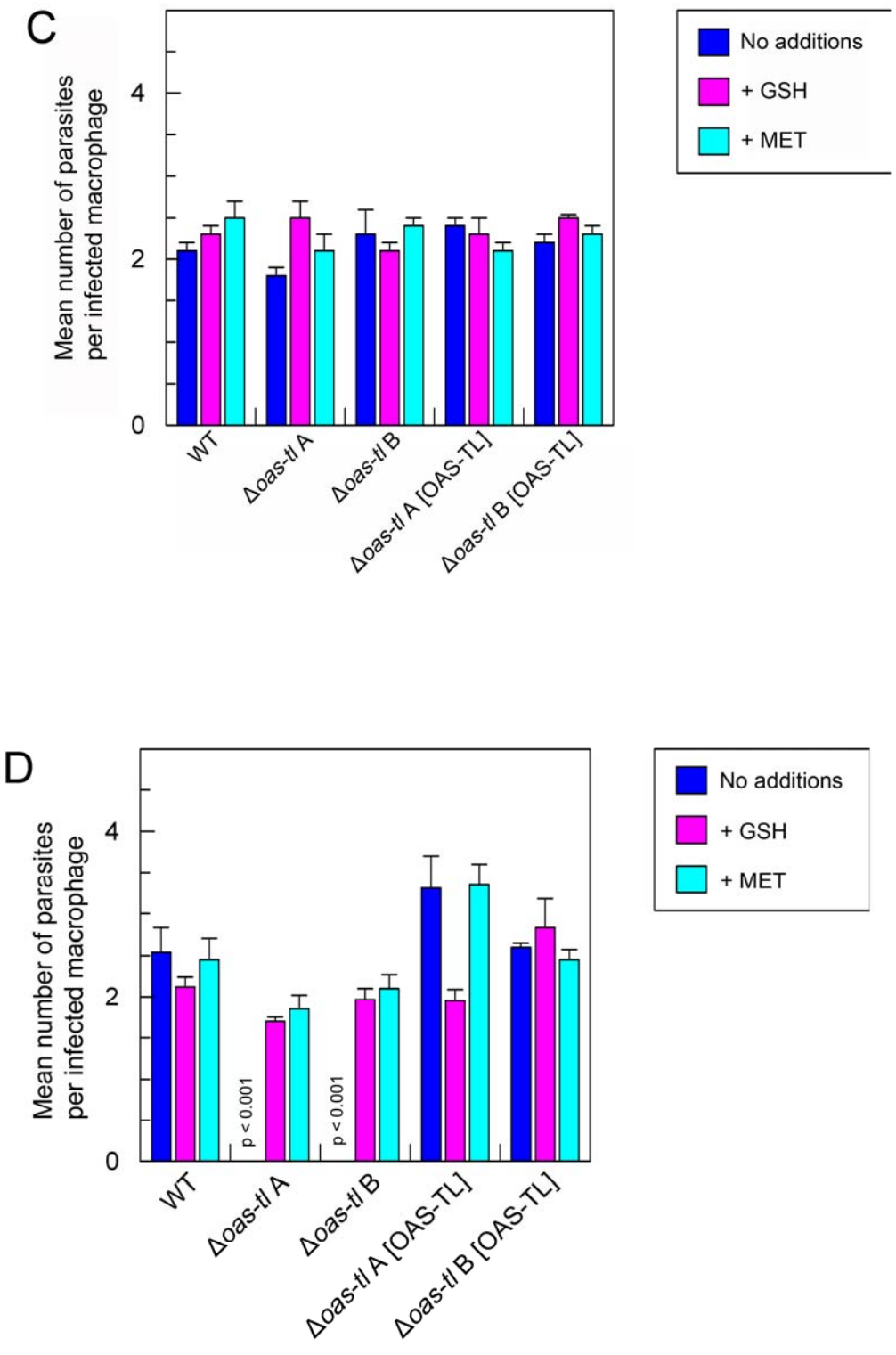

Figure 4.22 Effect of medium supplementation on the number of parasites per macrophage infected with *L. donovani* WT, Δ*oas-tl* A, Δ*oas-tl* B, Δ*oas-tl* A [OAS-TL] and Δ*oas-tl* B [OAS-TL] promastigotes.

Stationary phase promastigotes were used to infect peritoneal macrophages at a ratio of 5:1. The parasites and macrophages were incubated for 2 h before the parasites were washed off and replaced with fresh medium. Experiments were carried out with either no addition to the medium, or supplemented with either 1 mM glutathione or 5 mM methionine, and were terminated after 2 h, 12 h, 24 h and 55 h. 1, WT; 2, Δ*oas-tl* A; 3, Δ*oas-tl* B; 4, Δ*oas-tl* A [OAS-TL]; 5, Δ*oas-tl* B [OAS-TL]. **A**: Mean number of *L. donovani* WT, Δ*oas-tl* A, Δ*oas-tl* B, Δ*oas-tl* A [OAS-TL] and Δ*oas-tl* B [OAS-TL] parasites in infected macrophages after 2 h. **B**: Mean number of *L. donovani* WT, Δ*oas-tl* A, Δ*oas-tl*

B, Δ*oas-tl* A [OAS-TL] and Δ*oas-tl* B [OAS-TL] parasites in infected macrophages after 12 h. **C**: Mean number of *L. donovani* WT, Δ*oas-tl* A, Δ*oas-tl* B, Δ*oas-tl* A [OAS-TL] and Δ*oas-tl* B [OAS-TL] parasites in infected macrophages after 24 h. **D**: Mean number of *L. donovani* WT, Δ*oas-tl* A, Δ*oas-tl* B, Δ*oas-tl* A [OAS-TL] and Δ*oas-tl* B [OAS-TL] parasites in infected macrophages after 55 h. Results show the mean ± S.E.M. of three replicates and the number of parasites in 50 macrophages was counted from each. Values were statistically analysed by comparison to the WT with the appropriate addition by unpaired t-test, and resulting p-values are given.

numbers of re-expressing parasites were seen in macrophages as for WT parasites under all conditions.

The way the data has been presented in Figures 4.21 and 4.22 highlights any effect of the different supplementations made to the medium, and differences between the parasite lines. In order to clarify differences between the different parasite lines as the experiment progresses, the data was re-plotted to highlight this (Figure 4.23). When no supplement was added to the medium, the average percentage infection of WT parasites stays relatively constant from 2 h to 24 h, with a slight elevation after 55 h, suggesting that the parasite have started to proliferate. The null mutants, however, had a much higher percentage infection than the WT line after 2 h post-infection, indicating that these parasites are taken up by macrophages better than WT. The infection level of Δ*oas-tl* A and Δ*oas-tl* B progressively decreases at each time-point until at 55 h, the average percentage infections were 0.7 ± 0.7 % and 1 ± 0 % respectively. The largest decrease in percentage infection and number of parasites per infected macrophage was seen between 24 h and 55h, indicating that these parasites have difficulty either transforming into amastigotes or surviving as such. At 2 h, 12 h and 24 h post-infection, Δ*oas-tl* A [OAS-TL] and Δ*oas-tl* B [OAS-TL] show both percentage infections and number of parasites per macrophage similar to WT at each time-point. At 55 h, both re-expressing lines have an average percentage infection less than half that of WT, showing that the re-expression of OAS-TL results in the partial recovery of the null mutants. This partial recovery can be explained by the fact that Δ*oas-tl* A [OAS-TL] and Δ*oas-tl* B [OAS-TL] contain approximately half the amount of OAS-TL than *L. donovani* WT.

When glutathione was added to the medium, the same general trends as described above were seen in all parasite lines. However, the level of infection established by Δ*oas-tl* A and Δ*oas-tl* B does not drop as dramatically after 24 h and, by 55 h showed percentage infections of 4.7 ± 0.3 % and 2.3 ± 1.9 % respectively, compared to 0.7 ± 0.7 % and 1 ± 0 % when no addition was made to the medium. This shows that the addition of glutathione has a positive effect on the ability of the null mutant lines to survive within macrophages until 55 h post-infection.

When methionine was added to the medium, a similar pattern was seen. The percentage infection of the *OAS-TL* knock-out lines decreased as time progressed, as seen previously. However, after 55 h the level of infection was higher than when no addition was made to the medium and also when glutathione was added. 9.3 ± 1.7 % and 13.3 ± 0.3 % of macrophages remained infected my Δ*oas-tl* A and Δ*oas-tl* B respectively, compared to 0.7 ± 0.7 % and 1 ± 0 % when no addition was made to the medium.

The data corresponding to the number of parasites per macrophage were also re-plotted to clarify the pattern of infection over the four time-points investigated (Figure 4.24). With no additions to the medium, the WT has an approximately constant number of parasites per infected macrophage, across all the time-points investigated. At 2 h, 12 h and 24 h post-infection, all five of the parasite lines had roughly the same number of parasites per infected macrophage.

At 55 h, no Δ*oas-tl* A or Δ*oas-tl* B parasites could be seen in any visualised macrophages, while the OAS-TL re-expressing lines had a mean number of parasites per infected macrophage similar to the WT. Although the average percentage infection of the *OAS-TL* null mutants was greater than zero, the low nature of the infection meant that enough infected macrophages could not be found to calculate the mean number of parasites per macrophage. The fact that these parasites have difficulty surviving beyond 24 h in macrophages suggests that *OAS-TL* null mutants are unable to transform into amastigotes, or are unable to survive as amastigotes. When glutathione was used to supplement the medium, an increase in the number of null mutant parasites was seen per macrophage at this time-point. Interestingly, after 55 h post-infection, the mean number of null mutant parasites per infected macrophage was similar to the level seen in the WT and the Δ*oas-tl* A [OAS-TL], with Δ*oas-tl* B [OAS-TL] slightly higher. However, it was not possible to visually determine whether or not these parasites were in fact amastigotes. When the medium was supplemented with 5 mM methionine, no difference was seen in the number of parasites per infected macrophage between each of the five parasite lines at 2 h, 12 h and 24 h post-infection. Again, after 55 h, the mean number of *OAS-TL* knock-out parasites per infected macrophage is similar to the WT and Δ*oas-tl* B [OAS-TL], with Δ*oas-tl* A [OAS-TL] slightly higher. These data indicate that glutathione and methionine are able to partially overcome the detrimental effect of the lack of OAS-TL.

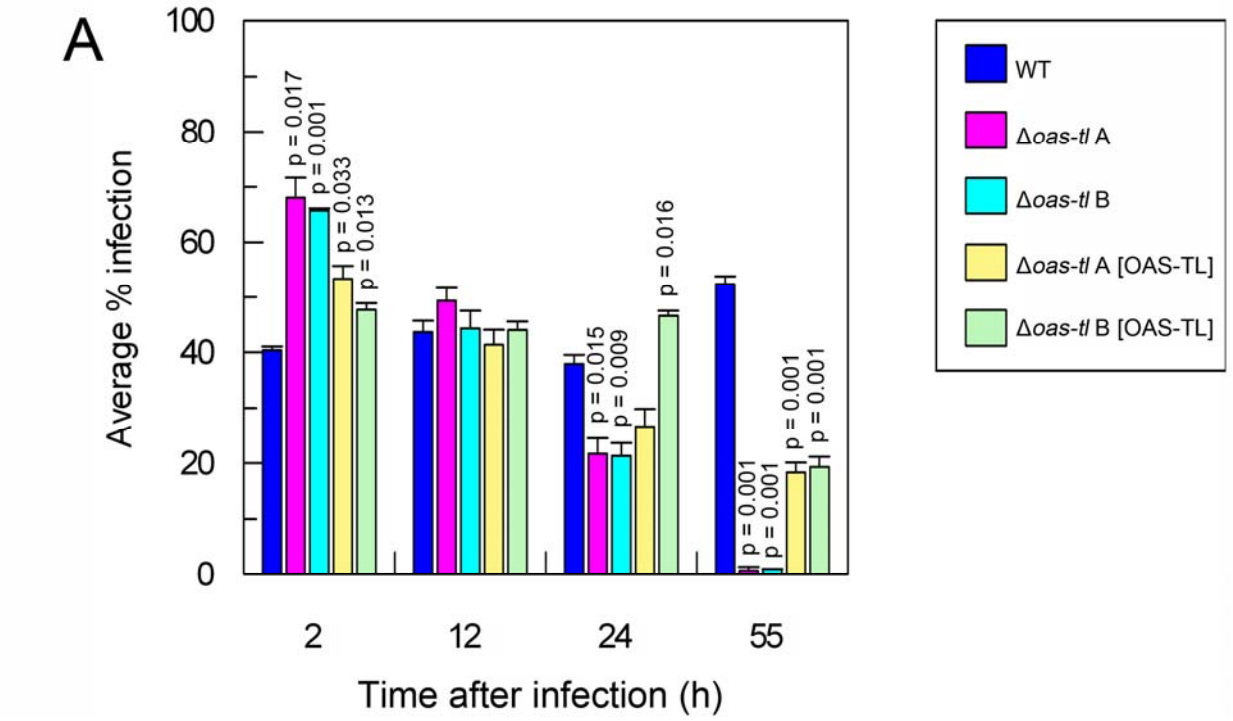
A
Average % infection
100
80
60
40
20
0
p = 0.017
p = 0.001
p = 0.033
p = 0.013
p = 0.015
p = 0.009
p = 0.016
p = 0.001
p = 0.001
p = 0.001
p = 0.001
2
12
24
55
Time after infection (h)
WT
Δoas-tl A
Δoas-tl B
Δoas-tl A [OAS-TL]
Δoas-tl B [OAS-TL]

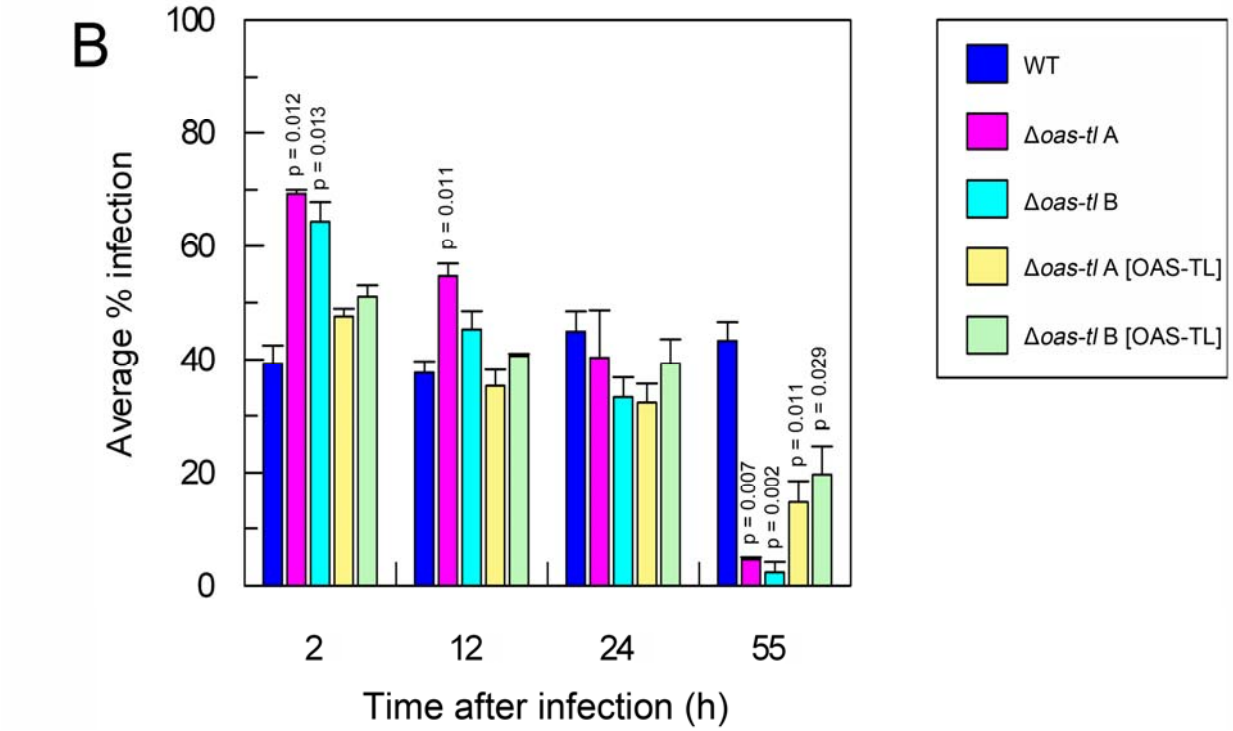
B
Average % infection
100
80
60
40
20
0
p = 0.012
p = 0.013
p = 0.011
p = 0.007
p = 0.002
p = 0.011
p = 0.029
2
12
24
55
Time after infection (h)
WT
Δoas-tl A
Δoas-tl B
Δoas-tl A [OAS-TL]
Δoas-tl B [OAS-TL]

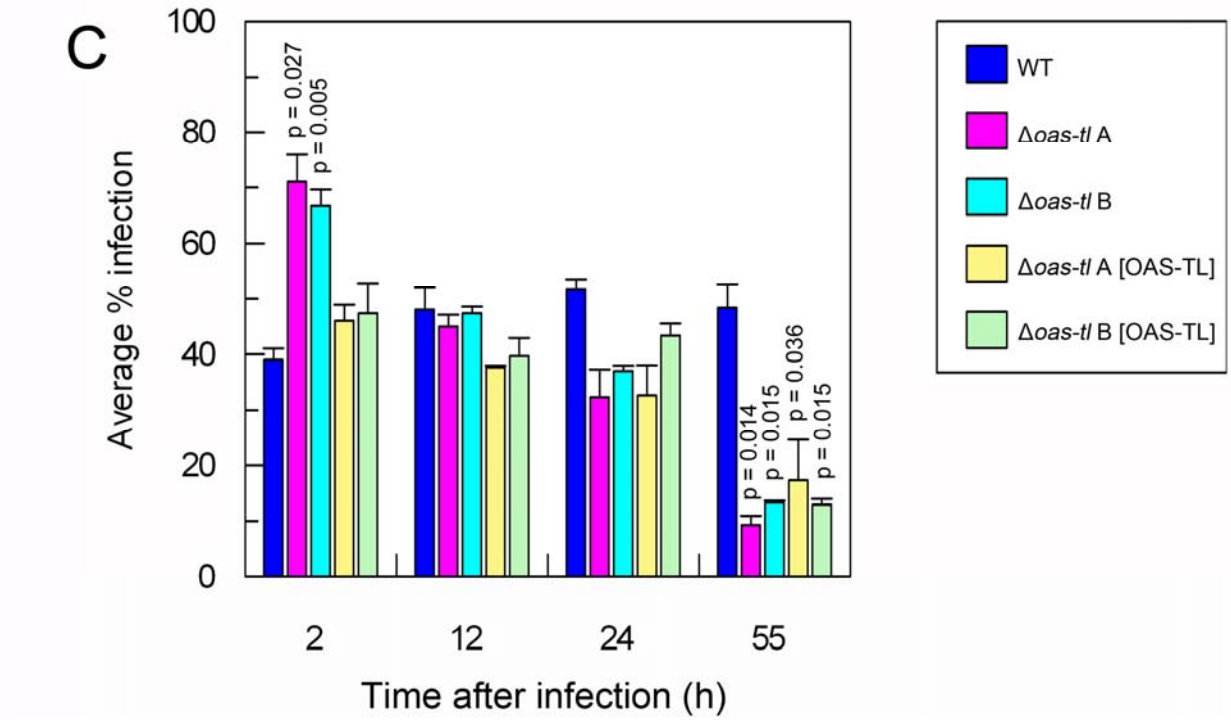

Figure 4.23 Infectivity of *L. donovani* WT, Δ*oas-tl* A, Δ*oas-tl* B, Δ*oas-tl* A [OAS-TL] and Δ*oas-tl* B [OAS-TL] promastigotes to macrophages, at various time-points.
Stationary phase promastigotes were used to infect peritoneal macrophages at a ratio of 5:1. The parasites and macrophages were incubated for 2 h before the parasites were washed off and replaced with fresh medium. Experiments were carried out with either no addition to the medium, or supplemented with either 1 mM glutathione or 5 mM methionine, and were terminated after 2 h, 12 h, 24 h and 55 h. 1, WT; 2, Δ*oas-tl* A; 3, Δ*oas-tl* B; 4, Δ*oas-tl* A [OAS-TL]; 5, Δ*oas-tl* B [OAS-TL]. **A**: Percentage infection of *L. donovani* WT, Δ*oas-tl* A, Δ*oas-tl* B, Δ*oas-tl* A [OAS-TL] and Δ*oas-tl* B [OAS-TL] in macrophages. **B**: Percentage infection of *L. donovani* WT, Δ*oas-tl* A, Δ*oas-tl* B, Δ*oas-tl* A [OAS-TL] and Δ*oas-tl* B [OAS-TL] in macrophages, when supplemented with 1 mM glutathione. **C**: Percentage infection of *L. donovani* WT, Δ*oas-tl* A, Δ*oas-tl* B, Δ*oas-tl* A [OAS-TL] and Δ*oas-tl* B [OAS-TL] in macrophages, when supplemented with 5 mM methionine. Results show the mean ± S.E. of three experiments, and 100 macrophages were counted from each. Values were statistically analysed by comparison to the WT value from the same time-point by unpaired t-test, and resulting p-values are given.

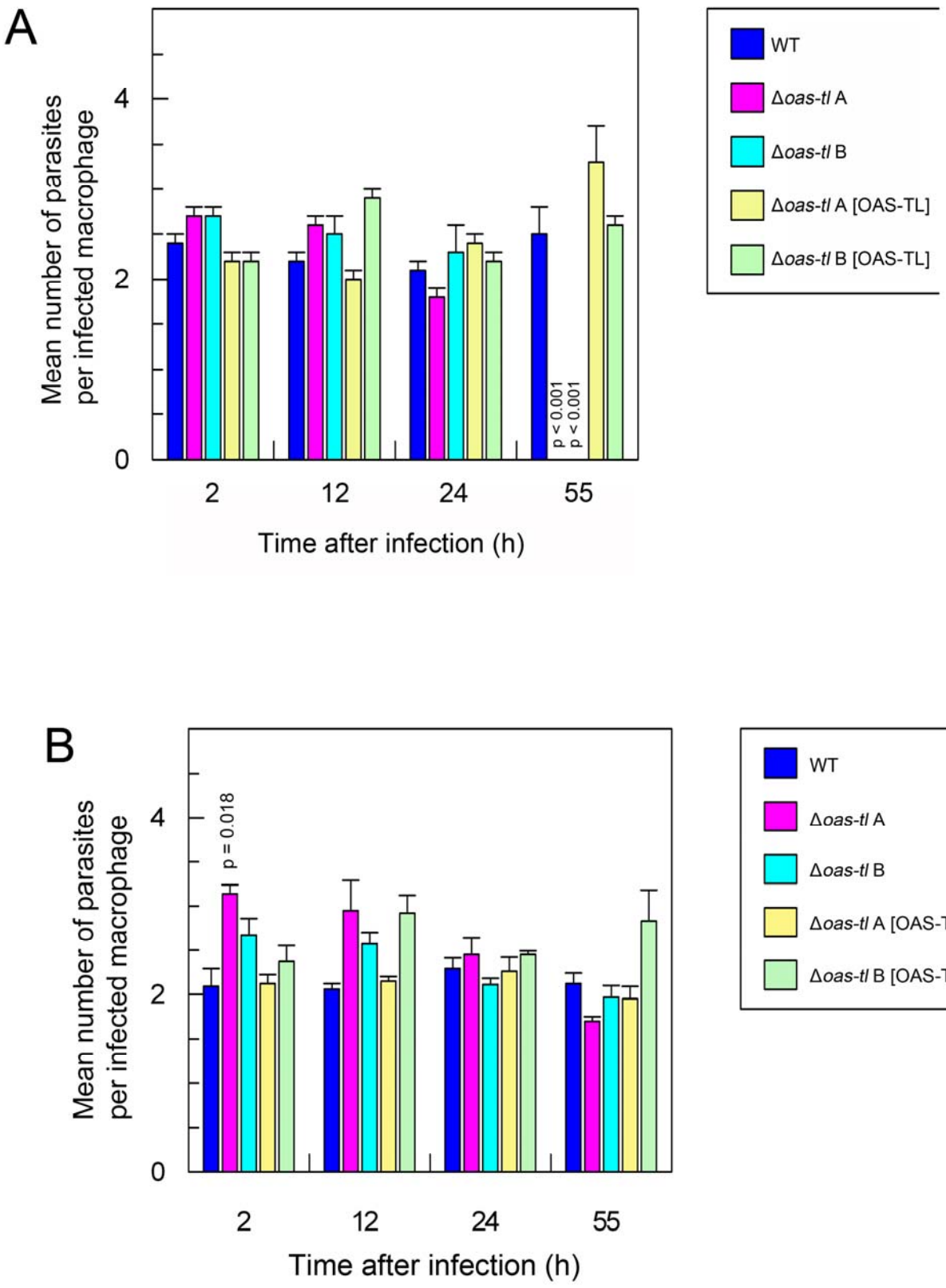
A
Mean number of parasites per infected macrophage
0
2
4
2
12
24
55
Time after infection (h)
p < 0.001
p < 0.001
WT
Δoas-tl A
Δoas-tl B
Δoas-tl A [OAS-TL]
Δoas-tl B [OAS-TL]
B
Mean number of parasites per infected macrophage
0
2
4
2
12
24
55
Time after infection (h)
p = 0.018
WT
Δoas-tl A
Δoas-tl B
Δoas-tl A [OAS-TL]
Δoas-tl B [OAS-TL]

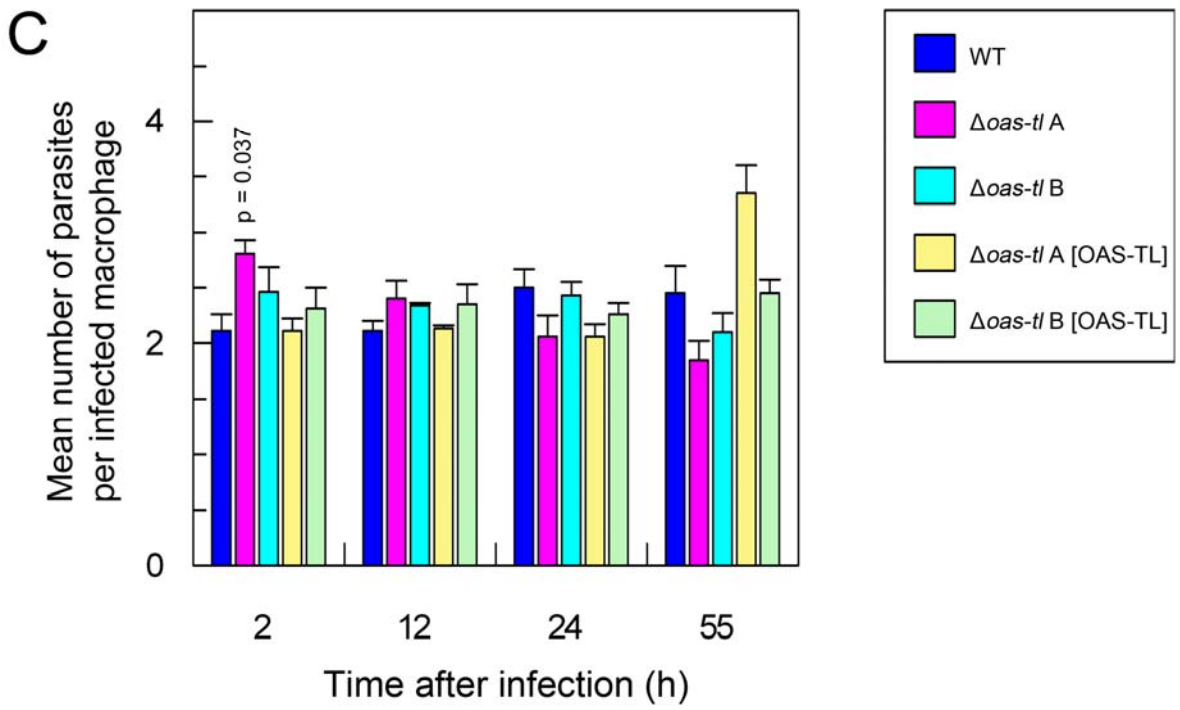

Figure 4.24 Mean number of parasites per macrophage infected with *donovani* WT, Δ*oas-tl* A, Δ*oas-tl* B, Δ*oas-tl* A [OAS-TL] and Δ*oas-tl* B [OAS-TL] promastigotes, at various time-points.

Stationary phase promastigotes were used to infect peritoneal macrophages at a ratio of 5:1. The parasites and macrophages were incubated for 2 h before the parasites were washed off and replaced with fresh medium. Experiments were carried out with either no addition to the medium, or supplemented with either 1 mM glutathione or 5 mM methionine, and were terminated after 2 h, 12 h, 24 h and 55 h. 1, WT; 2, Δ*oas-tl* A; 3, Δ*oas-tl* B; 4, Δ*oas-tl* A [OAS-TL]; 5, Δ*oas-tl* B [OAS-TL]. **A**: Mean number of *L. donovani* WT, Δ*oas-tl* A, Δ*oas-tl* B, Δ*oas-tl* A [OAS-TL] and Δ*oas-tl* B [OAS-TL] parasites in infected macrophages. **B**: Mean number of *L. donovani* WT, Δ*oas-tl* A, Δ*oas-tl* B, Δ*oas-tl* A [OAS-TL] and Δ*oas-tl* B [OAS-TL] parasites in infected macrophages, with medium supplemented with 1 mM glutathione. **C**: Mean number of *L. donovani* WT, Δ*oas-tl* A, Δ*oas-tl* B, Δ*oas-tl* A [OAS-TL] and Δ*oas-tl* B [OAS-TL] parasites in infected macrophages, when supplemented with 5 mM methionine. Results show the mean ± S.E. of three experiments and the number of parasites in 50 macrophages was counted from each. Values were statistically analysed by comparison to the WT value for the same time-point by unpaired t-test, and resulting p-values are given.

4.8 Infectivity of popliteal lymph nodes *in vivo*

To confirm the previous findings that the *L. donovani OAS-TL* null mutant parasites were unable to survive in macrophages beyond approximately 24 h, the *in vivo* infectivity of the parasites was assessed, using the rapid passage *in vivo* method described in Section 2.3.2.7.

8 x 10^6 late stationary phase promastigotes of L. donovani WT, Δ*oas-tl* A and Δ*oas-tl* A [OAS-TL] were injected into the footpads of five BALB/c mice. Infectivity was assessed by the migration and survival of parasites in the popliteal lymph node. The popliteal lymph nodes of infected mice were carefully removed after 8 weeks and passed through a 70 µm cell strainer into a final volume of 6 ml of HOMEM with 20 % (v/v) HIFCS. Serial dilutions of these cell suspensions were made in 96-well tissue culture plates, incubated at 25 ºC and monitored for growth of parasites. The most dilute well containing parasites was assumed to contain just one parasite and based on this the total number of parasites per popliteal lymph node was calculated.

The numbers of parasites contained in each popliteal lymph node are given in Table 4.6. Four out of the five lymph nodes contained *L. donovani* WT parasites, suggesting that these parasites were taken up by macrophages at the site of infection and were subsequently transported to the popliteal lymph node where they survived for 8 weeks. No *L. donovani* Δ*oas-tl* A parasites grew from the cell suspensions made from the removed popliteal lymph nodes, suggesting that they were either unable to transform into amastigotes or had difficulty surviving as amastigotes. This supports the *in vitro* findings that the *OAS-TL* null mutants were able to infect to a similar level as WT for a period of around 24 h, after which the parasite numbers declined rapidly. Of the five lymph nodes removed corresponding to the infection with the re-expressing line, parasites only grew from one. This could be due to the incomplete re-expression of OAS-TL in these parasites as there may not be enough of the protein in the cell to overcome the detrimental effects shown by the gene deletion.

Parasite line	Popliteal lymph node	Number of parasites present in popliteal lymph node
L. donovani WT	1	1 008
	2	4 032
	3	64 512
	4	504
	5	0
L. donovani Δ*oas-tl* A	1	0
	2	0
	3	0
	4	0
	5	0
L. donovani Δ*oas-tl* A [OAS-TL]	1	0
	2	0
	3	0
	4	0
	5	252

Table 4.6 *In vivo* infectivity of *L. donovani* WT, Δ*oas-tl* A and Δ*oas-tl* A [OAS-TL].
8 x 10^6 late stationary phase promastigotes of each parasite line were injected into footpads of 5 BALB/c mice. Mice were culled after 8 weeks. The popliteal lymph nodes of infected mice were removed and passed through a 70 μm cell strainer. Serial dilutions of cell suspensions were made in 96-well tissue culture plates, incubated at 25 ºC and monitored for growth of parasites. The most dilute well containing parasites was assumed to contain one parasite and the total number of parasites per popliteal lymph node was determined.

This experiment was only carried out once, and will have to be repeated before clear conclusions can be drawn. The *in vivo* method used has never been used on the *L. donovani* line used in this study before and, given the low numbers of parasites recovered, requires further development. The length of time parasites were allowed to infect as well as the final volume of cell suspension will have to be optimised. In addition, the remainder of each cell suspension was discarded after the serial dilutions were set up. The low numbers of parasites that grew was unexpected and the remaining cell suspensions, even of the lines that appeared to show no growth, could have contained a small number of parasites.

4.9 Discussion

Cysteine is a vital amino acid required for numerous cellular processes and is particularly important as the active component of low molecular weight thiols such as glutathione (Snoke et al., 1953) and, in trypanosomatid parasites like *Leishmania*, trypanothione (Fairlamb et al., 1985). This sulfur-containing amino acid is essential for the biosynthesis of coenzyme A, lipoic acid and a variety of vitamins such as biotin, pantothenate and thiamine pyrophosphate, to name only a few (Kessler, 2006). Furthermore, cysteine is a key component of redox active sulfhydryl-group containing proteins as well as structural proteins. It is also crucial for the generation of [Fe-S] clusters and thus the biosynthesis of [Fe-S]-containing proteins (Howard et al., 1976). It can therefore be inferred that the amino acid plays a key role in a wide variety of biosynthetic processes, which are likely to be essential for the survival of the cell or organism.

In some organisms, cysteine can also be a source of methionine, although this is an essential amino acid for mammals. In mammals, cysteine can either be taken up from the environment or generated via the reverse trans-sulfuration pathway from methionine (Figure 1.8). Bacteria, plants, fungi and some protozoa have the ability to generate cysteine *de novo*, by utilisation of the sulfhydrylation pathway, via the action of serine acetyltransferase and O-acetylserine (thiol) lyase (OAS-TL) (Figure 1.8) (Foglino et al., 1995; Bogdanova et al., 1995; Morzycka & Paszewski, 1979; Walker & Barrett, 1997). Protozoan parasites of the genus *Leishmania* possess and utilise both the reverse trans-sulfuration and the sulfhydrylation biosynthesis pathways to generate cysteine (Williams et al.,

2009). This study analysed the role of cysteine biosynthesis in *Leishmania*, particularly focussing on the enzyme OAS-TL, using a reverse genetic approach.

In order to analyse the value of *OAS-TL* as a potential drug target, the effect of removing the gene was investigated, and two independent null mutant lines (Δ*oas-tl* A and Δ*oas-tl* B) were generated for *L. donovani*. Only a small growth defect was observed and it was found that promastigote cultures of *L. donovani* Δ*oas-tl* A and Δ*oas-tl* B did not reach the same density as WT promastigotes (Figure 4.8). Extra-chromasomal expression of OAS-TL resulted in the complementation of this growth phenotype (Figure 4.8).

Morphologically, promastigotes of the *OAS-TL* null mutants appeared grossly deformed when compared with *L. donovani* WT promastigotes, having significantly shorter flagella and body lengths. The control of body size and organelle size (such as the flagellum length) are essential pre-requisites for the integrity of an organism and are therefore tightly regulated by signalling cascades (Berleman & Bauer, 2005). Signalling cascades are activated by many stimuli, including oxidative stress (Kurata, 2000; Kanterewicz et al., 1998) and may therefore indirectly depend upon the availability of cysteine.

A number of factors are known to be involved in maintaining the structural integrity of *Leishmania*. Several MAP kinases have been found to be involved in flagellum length during the promastigote stage of *Leishmania* (Rotureau et al., 2009). In addition, ADP-ribosylation factor-like protein (*Ld*ARL-3A) was identified as an essential gene involved in flagellum biogenesis (Cuvillier et al., 2000). Similarly, it has been shown that TC10, a GTPase belonging to a family of proteins involved in the regulation of MAP kinase cascades, plays a role in the regulation of cellular signalling to the actin cytoskeleton and processes associated with cell growth (Murphy et al., 1999). Given that cysteine is such an abundant amino acid involved in a plethora of biological functions, it is likely that alterations in the amount of cysteine available may either directly or indirectly affect the regulation of these pathways, despite the fact that in trypanosomatids the regulation of these pathways is poorly understood.

In recent years it has become apparent that a number of these pathways are regulated by other signalling molecules such as sphingosine and sphingosine-1-

phosphate. Sphingosine-1-phosphate is involved in proliferation, differentiation and apoptosis (Ohanian & Ohanian, 2001). Genes and proteins involved in these processes have been studied extensively in yeast (Dickson, 2008). In mammalian cells it was shown that the activity of serine-palmitoyltransferase responds directly to changes in the levels of the two substrates serine and palmitoyl-CoA resulting in an adjustment of sphingosine biosynthesis in response to the substrate levels (Linn et al., 2001). Although it was recently shown that *Leishmania* are auxotrophic for sphingosine (Zhang et al., 2007) they also have the ability to generate sphingolipids *de novo*. The fact that serine is used for the biosynthesis of cysteine suggests that the loss of *OAS-TL* may result in changes in levels of intracellular serine and therefore may alter the activity of serine-palmitoyltransferase. This in turn would lead to changes in the sphingolipid levels in the parasites, which could affect membrane composition and signal transduction pathways.

In *Leishmania major*, promastigotes lacking serine palmitoyltransferase were found to have a growth defect, which was recovered by the addition of ethanolamine (Zhang et al., 2007). In addition, these promastigotes displayed a morphological defect when compared to WT promastigotes, with 36 % of log-phase cells and 86 % of stationary phase cells appearing 'rounder' (Zhang et al., 2007). Although the serine-palmitoyltransferase promastigotes were viable in log phase, they failed to differentiate into metacyclic promastigotes, ultimately compromising virulence (Zhang et al., 2007).

In yeast, sphingolipids have been implicated in interactions with signalling cascades involved in a wide range of physiological functions such as heat stress, regulation of nutrient permeases, cytoskeleton changes, control of cell size, cell cycle progression and RNA translation to name only a few (Mathias et al., 1998). Furthermore, there is evidence to support the fact that the inhibition of sphingolipid biosynthesis results in alterations in the flagellar membrane of *Leishmania*, including a partial loss of internal axoneme and a complete loss of paraflagellar rod structures (Tull et al., 2004).

The levels of intracellular cysteine, glutathione and trypanothione in *L. donovani* WT, Δ*oas-tl* A and Δ*oas-tl* B were determined by reversed phase HPLC. The level of cysteine detected in *L. donovani* promastigotes was much less than previously

reported (Ariyanayagam & Fairlamb, 1999), and the levels of glutathione and trypanothione were found to be higher and lower respectively (Mandal et al., 2007). There are several possibilities for this variation including the use of different growth medium and the stage of growth at which the parasites were harvested for derivatisation. Furthermore, the *L. donovani* strain used in this study was a field isolate which has never been subject to thiol analysis previously, and therefore could account for the differences observed. Surprisingly, the levels of intracellular cysteine, glutathione and trypanothione were unaffected by the deletion of both *OAS-TL* alleles in *L. donovani*. The results are in agreement with a previous study by Heeg et al., 2008, where all three of the *OAS-TL* genes of *Arabidospis thaliana* were deleted and did not lead to any significant changes in the levels of low molecular weight thiols as well as cysteine. However, a later study where only cytosolic *OAS-TL* was deleted resulted in a clear reduction of cysteine and glutathione levels by about 30 % (Lopez-Martin et al., 2008). Given the growth defect and morphological defects observed in the OAS-TL null mutants, the uniformity of the thiol levels between the parasite lines suggests that the intracellular levels of cysteine, glutathione and trypanothione are preferentially maintained at the expense of other functions of the amino acid.

Despite the fact that the levels of intracellular cysteine were no different to WT in the *OAS-TL* null mutants, the amounts of the amino acid were only detected in promastigotes in stationary phase. Therefore any deficiency at an earlier stage of growth would not have been detected. A number of pathways may be affected by the availablility of cysteine, including methionine, glycine, serine and threonine metabolism. The availability of methionine would fundamentally affect the concentration of important molecules such as *S*-adenosylmethionine, which is not only a major methyl-donor, but also is a substrate for polyamine biosynthesis and acts as a co-factor for radical SAM proteins (Loenen, 2006). Furthermore, the generation of coenzyme A, which is of vital importance to both cellular metabolism in general and the formation of various t-RNAs required for protein biosynthesis, is affected by the availability of cysteine (Chua et al., 1984).

Alternatively, the morphological defects observed in *L. donovani* promastigotes lacking OAS-TL, could be a result of the accumulation of metabolic

intermediates caused by the inhibition of *de novo* cysteine synthesis. These molecules include O-acetylserine, which is the reaction product of serine acetyltransferase, and the sulfide source that is utilised for *de novo* cysteine biosynthesis, although this has never been reported.

It is reasonable to suggest that the morphological changes that were observed in this study are not directly attributable to changes in cysteine levels, rather that they are downstream effects of metabolic changes arising from compensatory efforts or as the result of changes in the metabolic balances within the parasite as suggested above. This is supported by the fact that *L. donovani* parasites re-expressing OAS-TL extra-chromasomally in the null mutant lines only partially recover flagellum length, and do not recover body length, but morphological features of the body were restored (Figure 4.9). Since the amount of OAS-TL in these parasites was determined to be approximately half the amount of OAS-TL as *L. donovani* WT, it can be hypothesised that if WT amounts of OAS-TL could be expressed in the *OAS-TL* null mutants, the morphology of these parasites would be completely recovered.

L. donovani Δ*oas-tl* A and Δ*oas-tl* B were found to be more susceptible to the heavy metals copper sulphate, cadmium chloride and potassium arsenate as well as the hydroperoxides cumene hydroperoxide and tert-butyl hydroperoxide than *L. donovani* WT and Δ*oas-tl* A [OAS-TL] and Δ*oas-tl* B [OAS-TL] (Figures 4.13, 4.14, 4.15, 4.17 and 4.18, and Tables 4.4 and 4.5). A possible explanation of this is that OAS-TL is involved in the compensatory reactions that help to maintain the thiol levels of parasites under normal conditions. However, when the mutant parasites are exposed to additional stress, the cysteine synthesised through the reverse transsulfuration pathway is insufficient to maintain normal thiol levels. This suggestion is supported by the fact that the activity of OAS-TL in *Phragmites* and *Typha* plants increases when stressed with sodium chloride and cadmium (Fediuc et al., 2005), suggesting that higher tolerance shown by *L. donovani* WT, Δ*oas-tl* A [OAS-TL] and Δ*oas-tl* B [OAS-TL] to the metals may reflect an increase in cysteine biosynthesis. Over-expressing OAS-TL in Tobacco plants has been shown to increase resistance against cadmium, selenium and nickel (Kawashima et al., 2004). In addition, expression of *E. coli* OAS-TL resulted in an increased resistance against cadmium in *Arabidopsis* (Howarth et al., 2003); it is therefore

consistent that removal of the protein resulted in an increased susceptibility to heavy metal stress.

The *OAS-TL* null mutant parasites had a defect in their ability to survive in macrophages for 6 days. After six days in macrophages *in vitro*, no *OAS-TL* null mutant parasites were observed, compared to both the WT and re-expressing parasites. On further investigation, it was found that the *OAS-TL* null mutants are capable of being taken up by macrophages and can survive for approximately 24 h after which numbers rapidly decline. The fact that after 55 h in macrophages, very few parasites are present and after 6 days none had survived, suggests that OAS-TL is involved in cellular processes that are vital to the differentiation of *L. donovani* into amastigotes or the survival of amastigotes.

Unfortunately, it was not possible to test for the presence of metacyclic promastigotes in stationary phase cultures, because the marker routinely used to test for metcyclic *L. major* promastigotes, HaspB (Flinn et al., 1994) could not be used for *L. donovani*. The widely used method of agglutination of promastigotes by peanut agglutinin (Louassini et al., 1998), to allow the quantification of metacyclics, was also not possible in the parasite line used. It was therefore not possible to check whether or not these parasites have an impaired ability to transform to the infective form. In addition, the differentiation of *L. donovani* WT into axenic amastigotes was attempted using the method described by Doyle et al., 1991, but proved unsuccessful. It could therefore not be established whether the null mutant parasites were able to differentiate into amastigotes.

When 5 mM methionine and 1 mM glutathione were used as additions to the medium, a partial recovery was seen in the ability of the parasites to survive in macrophages for at least 55 h (Figures 4.23 and 4.24). It was hypothesised that glutathione could be used by the parasites as a source of cysteine, and therefore increased the amount of cysteine available in the parasite to be used in various cellular processes essential for the differentiation/survival of amastigotes. It is likely that the availability of methionine results in some biosynthesis of cysteine via the reverse trans-sulfuration pathway. Therefore supplementing the medium with methionine is likely to have driven the reverse trans-sulfuration pathway to synthesise more cysteine, and, again, increased the amount of cysteine available

to be used for the various cellular processes used in the differentiation/survival of amastigotes.

These findings were in agreement with the fact that no *OAS-TL* null mutant parasites grew from the five popliteal lymph nodes extracted 8 weeks after inoculation of the parasites into the footpad of mice (Table 4.6). Only one of the five lymph nodes yielded OAS-TL re-expressing parasites. This is much less than for the WT parasites, where parasites grew from four out of the five lymph nodes. This is probably explained by the fact that *L. donovani* Δ*oas-tl* A [OAS-TL] and Δ*oas-tl* B [OAS-TL] only express approximately half the amount of OAS-TL compared to WT. This protocol had never previously been used with this line of *L. donovani*, and required further development, but due to time constraints was not possible within the scope of this study.

4.9.1 Conclusions and future directions

It has been shown that *OAS-TL* is not an essential gene for *L. donovani* promastigote growth. However, when the gene was removed from *L. donovani* promastigotes the resulting parasites displayed both a growth defect and severe morphological changes. These include a shorter body length with the loss of the spindle-like shape, and a shorter flagellum which was not present at all in many cases.

Intracellular levels of cysteine, glutathione and trypanothione were not found to be different in the *OAS-TL* null mutant compared to WT promastigotes. Since the intracellular thiol levels of the *L. donovani* Δ*oas-tl* promastigotes were quantified in stationary phase, it would be interesting to analyse the intracellular thiol levels of parasites in mid-log phase also. The thiol profile of *L. donovani* changes throughout the 7 days in liquid culture (Figure 3.12), suggesting that the amounts of thiols required by promastigotes differs over 7 days in liquid culture. Therefore, there may be differences in amounts of cysteine, glutathione and trypanothione at an earlier stage of growth that have not been detected in this study. The inclusion of the reducing agent DTT in the sample preparation means that total amounts of thiols were quantified. Any difference in the ratio of oxidised to reduced thiols due to the gene deletion were therefore also not detected. The removal of DTT from the sample

preparation would allow the quantification of only the thiols reduced at the time of parasite harvest.

Promastigotes lacking OAS-TL were also found to be more sensitive to heavy metals and hydroperoxides than *L. donovani* WT promastigotes, indicating that the cysteine generated through the reverse transsulfuration pathway is insufficient to maintain normal thiol levels when the parasites are exposed to stress. This could be further investigated by analysis of the expression of OAS-TL in *L. donovani* WT promastigotes that have been exposed to stress, to establish whether or not the protein is up-regulated in response to stress. In addition, it would be interesting to use HPLC to quantify the thiol levels of *L. donovani OAS-TL* null mutants that have been exposed to stress, and compare these to *L. donovani* WT parasites.

L. donovani was used in this study because it is the most important disease-causing species of *Leishmania*. The strain used was a field isolate from Nepal where visceral leishmaniasis is endemic and drug resistance is becoming an increasing problem. The parasite line was less easy to study than some other species as there are fewer tools available for analysis. For example, the tools commonly used to assess the ability of other species of *Leishmania* to differentiate into metacyclic promastigotes cannot be used on *L. donovani*. The determination of metacyclic differentiation has been assessed by a reduced ability to bind peanut agglutinin (Sacks et al., 1987). However, this method was not successful for the *L. donovani* BPK 206 clone 10, despite the fact that this method has been used for *L. donovani* before (Howard et al., 1987). Successful analysis of metacyclic differentiation by lectin agglutination has been reported in other species of *Leishmania*, including *L. major*, (Sacks et al., 1987; da Silva & Sacks, 1987), *L. infantum* (Louassini et al., 1998) and *L. braziliensis* (Almeida et al., 1993). Therefore the study of one of these species may facilitate the provision of conclusive evidence as to whether *OAS-TL* null mutants are capable of differentiation into the infective form of the parasite. Other methods of determining the presence of metacyclic forms have been reported, including flow cytometry, which has been used for *L. major*, *L. donovani*, *L. amazonensis* and *L. braziliensis* (Saraiva et al., 2005). However, this method relies upon the typical morphology of metacyclic forms, with a short, narrow cell body and an

elongated flagellum. Given the abnormal morphology of the *L. donovani OAS-TL* null mutants, it is clear that this is not a suitable method of analysis.

Conducting further analyses of OAS-TL through reverse genetics carried out on a species such as *L. mexicana*, would facilitate the use of many more analytical tools. Although the attempts to generate and maintain *L. donovani* axenic amastigotes were unsuccessful, many successful attempts have been reported (Doyle et al., 1991; Gupta et al., 1996). As previously mentioned, the *L. donovani* field isolate used in this study has never been analysed in this way before and therefore similar studies using an *L. mexicana* laboratory strain may prove fruitful, as the generation of *L. mexicana* axenic amastigotes is well documented (Pan, 1984; Bates et al., 1992; Pral et al., 1993). The ability of *OAS-TL* null mutants to differentiate into amastigotes could be determined in this way. In addition, it is also easier to identify intracellular amastigotes visually, due to the large parasitophorous vacuoles observed with *L. mexicana* macrophage infections.

Although the *in vivo* infectivity of *L. donovani* Δ*oas-tl* parasites was found to be much lower than WT parasites, the fact that the method used has never been previously used for *L. donovani* and was only carried out once, was not optimal and would require extensive development. The use of *L. mexicana* would again be advantageous, as the cutaneous nature of the disease manifestation means that routinely used mouse footpad infections could be utilised as a measure of *in vivo* infectivity.

The exploitation of the metabolic pathways associated with the sulfur-containing amino acids has been suggested as a rational target for the development of chemotherapeutic or prophylactic therapies against parasitic protozoa, due to the diversity between the organisms and their mammalian hosts (Nozaki et al., 2005). OAS-TL has been suggested as a possible drug target in *Trichomonas vaginalis* (Westrop et al., 2006). In addition, the related protein, serine acetyl transferase, also involved in the *de novo* synthesis of cysteine, has also been identified as a potential drug target against *Entamoeba hystolytica* (Agarwal et al., 2008). Given the inability of *L. donovani OAS-TL* null mutant parasites to survive within macrophages, together with the absence of the protein in the

mammalian host make OAS-TL an exciting prospect for the development of novel chemotherapeutics against visceral leishmaniasis.

References

Aga, E., Katschinski, D.M., van Zandbergen, G., Laufs, H., Hansen, B., Müller, K., Solbach, W. & Laskay, T. (2002) Inhibition of the spontaneous apoptosis of neutrophil granulocytes by the intracellular parasite *Leishmania major*. *J Immunol.*, **169**, 898-905.

Agarwal, S.M., Jain, R., Bhattacharya, A. & Azam, A. (2008) Inhibitors of *Escherichia coli* serine acetyltransferase block proliferation of *Entamoeba histolytica* trophozoites. *Int J Parasitol.*, **38**, 137-141.

Agren, D., Schnell, R., Oehlmann, W., Singh, M. & Schneider, G. (2008) Cysteine synthase (CysM) of *Mycobacterium tuberculosis* is an O-phosphoserine sulfhydrylase. *J Biol Chem.*, **283**, 31567-31574.

Allaoui, A., Francois, C., Zemzoumi, K., Guilvard, E. & Ouaissi, A. (1999) Intracellular growth and metacyclogenesis defects in *Trypanosoma cruzi* carrying a targeted deletion of a Tc52 protein-encoding allele. *Mol Microbiol.*, **32**, 1273-1286.

Almeida, M.C., Cuba, C.A.C., de Sa, C.M., Pharoah, M.M., Howard, K.M. & Miles, M.A. (1993) Metacyclogenesis of *Leishmania (Viannia) braziliensis in vitro*: evidence that lentil lectin is a marker of complement resistance and enhanced infectivity. *Trans R Soc Trop Med Hyg.*, **87**, 325-329.

Arana, F.E., Pérez-Victoria, J.M., Repetto, Y., Morello, A., Castanys, S. & Gamarro, F. (1998)) Involvement of thiol metabolism in resistance to glucantime in *Leishmania tropica*. *Biochem Pharmacol.*, **56**, 1201-1208.

Ariyanayagam, M.R. & Fairlamb, A.H. (1999) *Entamoeba histolytica* lacks trypanothione metabolism. *Mol Biochem Parasitol.*, **103**, 61-69.

Ashutosh, Sundar, S. & Goyal, N. (2007) Molecular mechanisms of antimony resistance in *Leishmania*. *J Med Microbiol.*, **56**, 143-153.

Baiocco, P., Colotti, G., Franceschini, S. & Ilari, A. (2009) Molecular Basis of Antimony Treatment in Leishmaniasis (dagger). *J Med Chem*. [Epub ahead of print].

Bankov, I., Timanova, A. & Barrett, J. (1996) Methionine and cysteine metabolism in *Fasciola hepatica*. *Int J Parasitol.*, **26**, 1401-1404.

Basselin, M., Denise, H., Coombs, G.H. & Barrett, M.P. (2002) Resistance to pentamidine in *Leishmania mexicana* involves exclusion of the drug from the mitochondrion. *Antimicrob Agents Chemother.*, **46**, 3731-3738.

Bateman, A. (1997) The structure of a domain common to archaebacteria and the homocystinuria disease protein. *Trends Biochem Sci.*, **22**, 12-13.

Bates, P.A., Robertson, C.D., Tetley, L. & Coombs, G.H. (1992) Axenic cultivation and characterization of *Leishmania mexicana* amastigote-like forms. *Parasitology.*, **105**, 193-202.

Belinsky, M.G., Chen, Z.S., Shchavelevam I., Zeng, H. & Kruh, G.D. (2002) Characterization of the drug resistance and transport properties of multidrug resistance protein 6 (MRP6, ABCC6). *Cancer Res.*, **62**, 6172-6177.

Berleman, J.E. & Bauer, C.E. (2005) A *che*-like signal transduction cascade involved in controlling flagella biosynthesis in *Rhodospirillum centenum*. *Mol Microbiol.*, **55**, 1390-1402.

Berman, J.D., Edwards, N., King, M. & Grogl, M. (1989) Biochemistry of Pentostam resistant *Leishmania*. *Am J Trop Med Hyg.*, **40**, 159-164.

Besteiro, S., Williams, R.A., Coombs, G.H. & Mottram, J.C. (2007) Protein turnover and differentiation in *Leishmania*. *Int J Parasitol.*, **37**, 1063-1075.

Blaszczyk, A., Brodzik, R. & Sirko, A. (1999) Increased resistance to oxidative stress in transgenic tobacco plants overexpressing bacterial serine acetyltransferase. *Plant J.*, **20**, 237-243.

Bogdanova, N., Bork, C. & Hell, R. (1995) Cysteine biosynthesis in plants: isolation and functional identification of a cDNA encoding a serine acetyltransferase from *Arabidopsis thaliana*. *FEBS Lett.*, **358**, 43-47.

Brochu, C., Wang, J., Roy ,G., Messier, N., Wang, X.Y., Saravia, N.G. & Ouellette, M. (2003) Antimony uptake systems in the protozoan parasite *Leishmania* and accumulation differences in antimony-resistant parasites. *Antimicrob Agents Chemother.*, **47**, 3073-3079.

Brosnan, J.T. & Brosnan, M.E. (2006) The sulfur-containing amino acids: an overview. *J Nutr.*, **136**, 1636S-1640S.

Bruinenberg, P.G., du Roo, G. & Limsowtin, K.Y. (1996) Purification and characterization of cystathionine γ-lyase from *Lactococcus lactis* subsp. *cremoris* SK11: Possible role in flavor compound formation during cheese maturation. *Appl Environ Microbiol.*, **63**, 561-566.

Brzywczy, J. & Paszewski, A. (1993) Role of O-acetylhomoserine sulfhydrylase in sulfur amino acid synthesis in various yeasts. *Yeast*, **9**, 1335-1342.

Brzywczy, J., Sieńko, M., Kucharska, A. & Paszewski, A. (2002) Sulphur amino acid synthesis in *Schizosaccharomyces pombe* represents a specific variant of sulphur metabolism in fungi. *Yeast*, **19**, 29-35.

Burnell, J.N. & Whatley, F.R. (1977) Sulphur metabolism in *Paracoccus denitrificans*. Purification, properties and regulation of serine transacetylase, O-acetylserine sulphydrylase and beta-cystathionase. *Biochim Biophys Acta.*, **481**, 246-265.

Callahan, H.L., Portal, A.C., Devereaux, R. & Grogl, M. (1997) An axenic amastigote system for drug screening. *Antimicrob Agents Chemother.*, **41**, 818-822.

Castro, H., Sousa, C., Santos, M., Cordeiro-da-Silva, A., Flohé, L. & Tomás, A.M. (2002) Complementary antioxidant defense by cytoplasmic and mitochondrial peroxiredoxins in *Leishmania infantum*. *Free Radic Biol Med.*, **33**, 1552-1562.

Castro-Pinto, D.B., Genestra, M., Menezes, G.B., Waghabi, M., Gonçalves, A., De Nigris Del Cistia, C., Sant'Anna, C.M., Leon, L.L. & Mendonça-Lima, L. (2008) Cloning and expression of trypanothione reductase from a New World *Leishmania* species. *Arch Microbiol.*, **189**, 375-384.

Chao, D., Chen, Y.A., Liu, J.K. & Huang, T.C. (1990) Analyses of surface membrane carbohydrates in parasitic flagellates of the order kinetoplastida using lectins. *Proc Natl Sci Counc Repub China B.*, **14**, 54-58.

Chappuis, F., Sundar, S., Hailu, A., Ghalib, H., Rijal, S., Peeling, R.W., Alvar, J. & Boelaert, M. (2007) Visceral leishmaniasis: what are the needs for diagnosis, treatment and control? *Nat Rev Microbiol.*, **5**, 873-882.

Cherest, H., Thomas, D. & Surdin-Kerjan, Y. (1993) Cysteine biosynthesis in Saccharomyces cerevisiae occurs through the trans-sulfuration pathway which has been built up by enzyme recruitment. *J Bacteriol.*, **175**, 5366-5374.

Chua, B.H., Giger, K.E., Kleinhans, B.J., Robishaw, J.D. & Morgan, H.E. (1984) Differential effects of cysteine on protein and coenzyme A synthesis in rat heart. *Am J Physiol.*, **247**, C99-106.

Coelho, A.C., Beverley, S.M. & Cotrim, P.C. (2003) Functional genetic identification of *PRP1*, an ABC transporter superfamily member conferring pentamidine resistance in *Leishmania major*. *Mol Biochem Parasitol.*, **130**, 83-90.

Cook, P.F. & Wedding, R.T. (1976) A reaction mechanism from steady state kinetic studies for O-acetylserine sulfhydrylase from *Salmonella typhimurium* LT-2. *J Biol Chem.*, **251**, 2023-2029.

Coombs, G.H., Tetley, L., Moss, V.A. & Vickerman, K. (1986) Three dimensional structure of the *Leishmania* amastigote as revealed by computer-aided reconstruction from serial sections. *Parasitology*, **92**, 13-23.

Cruz, A.K., Titus, R. & Beverley, S.M. (1993) Plasticity in chromosome number and testing of essential genes in *Leishmania* by targeting. *Proc Natl Acad Sci U S A.*, **90**, 1599-1603.

Cuvillier, A., Redon, F., Antoine, J.C., Chardin, P., DeVos, T. & Merlin, G. (2000) LdARL-3A, a *Leishmania* promastigote-specific ADP-ribosylation factor-like protein, is essential for flagellum integrity. *J Cell Sci.*, **113**, 2065-2074.

da Silva, R. & Sacks, D.L. (1987) Metacyclogenesis is a major determinant of *Leishmania* promastigote virulence and attenuation. *Infect Immun.*, **55**, 2802-2806.

Das, M., Banjara, M., Chowdhury, R., Kumar, V., Rijal, S., Joshi, A., Akhter, S., Das, P. & Kroeger, A. (2008) Visceral leishmaniasis on the Indian sub-continent: a multi-centre study of the costs of three interventions for the control of the sandfly vector, *Phlebotomus argentipes*. *Ann Trop Med Parasitol.*, **102**, 729-741.

Davies, C.R., Kaye, P., Croft, S.L. & Sundar, S. (2003) Leishmaniasis: new approaches to disease control. *BMJ.*, **326**, 377-382.

Dawidowicz, K., Hernandez, A.G., Infante, R.B. & Convit, J. (1975) The surface membrane of *Leishmania*. I. The effects of lectins on different stages of *Leishmania braziliensis*. *J Parasitol.*, **61**, 950-953.

de Souza, W. (2002) Special organelles of some pathogenic protozoa. *Parasitol Res.*, **88**, 1013-1025.

Decuypere, S., Rijal, S., Yardley, V., De Doncker, S., Laurent, T., Khanal, B., Chappuis, F. & Dujardin, J.C. (2005) Gene expression analysis of the mechanism of natural Sb(V) resistance in *Leishmania donovani* isolates from Nepal. *Antimicrob Agents Chemother.*, **49**, 4616-4621.

Denton, H., McGregor, J.C. & Coombs, G.H. (2004) Reduction of anti-leishmanial pentavalent antimonial drugs by a parasite-specific thiol-dependent reductase, TDR1. *Biochem J.*, **381**, 405-412.

Dey, S., Papadopoulou, B., Haimeur, A., Roy, G., Grondin, K., Dou, D., Rosen, B.P. & Ouellette, M. (1994) High level arsenite resistance in *Leishmania tarentolae* is mediated by an active extrusion system. *Mol Biochem Parasitol.*, **67**, 49-57.

Desjeux, P. (1996) Leishmaniasis. Public health aspects and control. *Clin Dermatol.*, **14**, 417-423.

Desjeux, P. (2004) Leishmaniasis: current situation and new perspectives. *Comp Immunol Microbiol Infect Dis.*, **27**, 305-318.

Dickson, R.C. (2008) Thematic review series: sphingolipids. New insights into sphingolipid metabolism and function in budding yeast. *J Lipid Res.*, **49**, 909-921.

Dodge, M.A., Waller, R.F., Chow, L.M., Zaman, M.M., Cotton, L.M., McConville, M.J. & Wirth, D.F. (2004) Localization and activity of multidrug resistance protein 1 in the secretory pathway of *Leishmania* parasites. *Mol Microbiol.* **51**, 1563-1575.

Doyle, P.S., Engel, J.C., Pimenta, P.F., da Silva, P.P. & Dwyer, D.M. (1991) *Leishmania donovani*: long-term culture of axenic amastigotes at 37 degrees C. *Exp Parasitol.*, **73**, 326-334.

Droux, M., Ruffet, M.L., Douce, R. & Job, D. (1998) Interactions between serine acetyltransferase and O-acetylserine (thiol) lyase in higher plants--structural and kinetic properties of the free and bound enzymes. *Eur J Biochem.*, **255**, 235-45.

Dwyer, D.M. (1974) Lectin binding saccharides on a parasitic protozoan. *Science*, **184**, 471-473.

El Fadili, K., Messier, N., Leprohon, P., Roy, G., Guimond, C., Trudel, N., Saravia, N.G., Papadopoulou, B., Légaré, D. & Ouellette, M. (2005) Role of the ABC transporter MRPA (PGPA) in antimony resistance in *Leishmania infantum* axenic and intracellular amastigotes. *Antimicrob Agents Chemother.*, **49**, 1988-1993.

Ephros, M., Bitnun, A., Shaked, P., Waldman, E. & Zilberstein, D. (1999) Stage-specific activity of pentavalent antimony against *Leishmania donovani* axenic amastigotes. *Antimicrob Agents Chemother.*, **43**, 278-282.

Fairlamb, A.H., Blackburn, P., Ulrich, P., Chait, B.T. & Cerami, A. (1985) Trypanothione: a novel bis(glutathionyl)spermidine cofactor for glutathione reductase in trypanosomatids. *Science*, **227**, 1485-1487.

Fediuc, E., Lips, S.H. & Erdei, L. (2005) O-acetylserine (thiol) lyase activity in *Phragmites* and *Typha* plants under cadmium and NaCl stress conditions and the involvement of ABA in the stress response. *J Plant Physiol.*, **162**, 865-872.

Feldman-Salit, A., Wirtz, M., Hell, R. & Wade, R.C. (2009) A mechanistic model of the cysteine synthase complex. *J Mol Biol.*, **386**, 37-59.

Fernandez-Gomez, R., Esteban, S., Gomez-Corvera, R., Zoulika, K. & Ouaissi, A. (1998) *Trypanosoma cruzi*: Tc52 released protein-induced increased expression of nitric oxide synthase and nitric oxide production by macrophages. *J Immunol.*, **160**, 3471-3479.

Ferreira, C. dos S., Martins, P.S., Demicheli, C., Brochu, C., Ouellette, M. & Frézard, F. (2003) Thiol-induced reduction of antimony(V) into antimony(III): a comparative study with trypanothione, cysteinyl-glycine, cysteine and glutathione. *Biometals*, **16**, 441-446.

Flinn, H.M., Rangarajan, D. & Smith, D.F. (1994) Expression of a hydrophilic surface protein in infective stages of *Leishmania major*. *Mol Biochem Parasitol.*, **65**, 259-270.

Foglino, M., Borne, F., Bally, M., Ball, G. & Patte, J.C. (1995) A direct sulfhydrylation pathway is used for methionine biosynthesis in *Pseudomonas aeruginosa*. *Microbiology*, **141**, 431-439.

Garzon, E., Borges, M.C., Cordeiro-da-Silva, A., Nacife, V., Meirelles, M.N., Guilvard, E., Bosseno, M.F., Guevara, A.G., Breniere, S.F. & Ouaissi, A. (2003)

Trypanosoma cruzi carrying a targeted deletion of a Tc52 protein-encoding allele elicits attenuated Chagas' disease in mice. *Immunol Let.*, **89**, 67-80.

Ghedin, E., Debrabant, A., Engel, J.C. & Dwyer, D.M. (2001) Secretory and endocytic pathways converge in a dynamic endosomal system in a primitive protozoan. *Traffic.*, **2**, 175-188.

Gilbert, H.F. (1990) Molecular and cellular aspects of thiol-disulfide exchange. *Adv Enzymol Relat Areas Mol Biol.*, **63**, 69-172.

Goldberg, B., Rattendi, D., Lloyd, D., Yarlett, N. & Bacchi, C.J. (2000) Kinetics of methionine transport and metabolism by Trypanosoma brucei brucei and Trypanosoma brucei rhodesiense. *Arch Biochem Biophys.*, **377**, 49-57.

Goodall, G. (2001) Studies on sulfur amino acid metabolising enzymes of *Trichomonas vaginalis*. Ref Type: Thesis/Dissertation.

Gossage, S.M., Rogers, M.E. & Bates, P.A. (2003) Two separate growth phases during the development of *Leishmania* in sand flies: implications for understanding the life cycle. *Int J Parasitol.*, **33**, 1027-1034.

Gourbal, B., Sonuc, N., Bhattacharjee, H., Legare, D., Sundar, S., Ouellette, M., Rosen, B.P. & Mukhopadhyay, R. (2004) Drug uptake and modulation of drug resistance in *Leishmania* by an aquaglyceroporin. *J Biol Chem.*, **279**, 31010-31017.

Griffith, O.W. (1987) Mammalian sulfur amino acid metabolism: an overview. *Methods Enzymol.*, **143**, 366-376.

Gull, K. (1999) The cytoskeleton of trypanosomatid parasites. *Annu Rev Microbiol.*, **53**, 629-655.

Gupta, N., Goyal, N., Kumar, R., Agrawal, A.K., Seth, P.K. & Rastogi, A.K. (1996) Membrane characterization of amastigote-like forms of *Leishmania donovani*. *Trop Med Int Health.*, **1**, 495-502.

Gupta, N., Goyal, N. & Rastogi, A.K. (2001) *In vitro* cultivation and characterization of axenic amastigotes of *Leishmania*. *Trends Parasitol.*, **17**, 150-153.

Haas, F.H., Heeg, C., Queiroz, R., Bauer, A., Wirtz, M. & Hell, R. (2008) Mitochondrial serine acetyltransferase functions as a pacemaker of cysteine synthesis in plant cells. *Plant Physiol.*, **148**, 1055-1067.

Haimeur, A., Guimond, C., Pilote, S., Mukhopadhyay, R., Rosen, B.P., Poulin, R. & Ouellette, M. (1999) Elevated levels of polyamines and trypanothione resulting from overexpression of the ornithine decarboxylase gene in arsenite-resistant *Leishmania*. *Mol Microbiol.*, **34,** 726-735.

Hamilton, C.J., Saravanamuthu, A., Eggleston, I.M. & Fairlamb, A.H. (2003) Ellman's-reagent-mediated regeneration of trypanothione *in situ*: substrate-economical microplate and time-dependent inhibition assays for trypanothione reductase. *Biochem J.*, **369**, 529-537.

Hanada, K., Hara, T. & Nishijima, M. (2000) D-Serine inhibits serine palmitoyltransferase, the enzyme catalyzing the initial step of sphingolipid biosynthesis. *FEBS Lett.*, **474**, 63-65.

Hansen, B.D., Webster, H.K., Hendricks, L.D. & Pappas, M.G. (1984) *Leishmania mexicana*: purine metabolism in promastigotes, axenic amastigotes, and amastigotes derived from Vero cells. *Exp Parasitol.*, **58**, 101-109.

Harms, K., von Ballmoos, P., Brunold, C., Höfgen, R. & Hesse, H. (2000) Expression of a bacterial serine acetyltransferase in transgenic potato plants leads to increased levels of cysteine and glutathione. *Plant J.*, **22**, 335-343.

Heeg, C., Kruse, C., Jost, R., Gutensohn, M., Ruppert, T., Wirtz, M. & Hell, R. (2008) Analysis of the Arabidopsis O-acetylserine(thiol)lyase gene family demonstrates compartment-specific differences in the regulation of cysteine synthesis. *Plant Cell.*, **20**, 168-185.

Hiraishi, H., Miyake, T. & Ono, B. (2008) Transcriptional regulation of *Saccharomyces cerevisiae CYS3* encoding cystathionine γ-lyase. *Curr Genet.*, **53**, 225-234.

Hirase, K. & Molin, W.T. (2001) Effect of inhibitors of pyridoxal-5'-phosphate-dependent enzymes on cysteine synthase in *Echinochloa crus-galli* L. *Pestic Biochem Physiol.*, **70**, 180-188.

Hojjati, M.R., Li, Z. & Jiang, X.C. (2005) Serine palmitoyl-CoA transferase (SPT) deficiency and sphingolipid levels in mice. *Biochim Biophys Acta.*, **1737**, 44-51.

Howard, J.B., Lorsbach, T., Que, L. (1976) Iron-sulfur clusters and cysteine distribution in a ferredoxin from *Azotobacter vinelandii*. *Biochem Biophys Res Commun.*, **70**, 582-588.

Howard, M.K., Sayers, G. & Miles, M.A. (1987) *Leishmania donovani* metacyclic promastigotes: transformation in vitro, lectin agglutination, complement resistance, and infectivity. *Exp Parasitol.*, **64**, 147-156.

Howarth, J.R., Roberts, M.A. & Wray, J.L. (1997) Cysteine biosynthesis in higher plants: a new member of the *Arabidopsis thaliana* serine acetyltransferase small gene-family obtained by functional complementation of an *Escherichia coli* cysteine auxotroph. *Biochim Biophys Acta.*, **1350**, 123-127.

Howarth, J.R., Dominques-Solis, J.R., Gutierrez-Alcala, G., Wray, J.L., Romero, L.C. & Gotor, C. (2003) The serine acetyltransferase gene family in *Arabidopsis thaliana* and the regulation of its expression by cadmium. *Plant Mol Biol.*, **51**, 589-598.

Hulanicka, M.D., Kredich, N.M. & Treiman, D.M. (1974) The structural gene for O-acetylserine sulfhydrylase A in *Salmonella typhimurium*. Identity with the trzA locus. *J Biol Chem.*, **249**, 867-872.

Hussain, S., Ali, V., Jeelani, G. & Nozaki, T. (2009) Isoform-dependent feedback regulation of serine O-acetyltransferase isoenzymes involved in L-cysteine biosynthesis of *Entamoeba histolytica. Mol Biochem Parasitol.*, **163**, 39-47.

Jha, T.K., Olliaro, P., Thakur, C.P.N., Kanyok, T.P., Singhania, B.L., Singh, N.K.P., Akhoury, S. & Jha, S. (1998) Randomised controlled trial of aminosidine (paromomycin) *v* sodium stibogluconate for treating visceral leishmaniasis in North Bihar, India. *BMJ.*, **316**, 1200-1205.

Jhee, K.H., McPhie, P. & Miles, E.W. (2000) Yeast cystathionine beta-synthase is a pyridoxal phosphate enzyme but, unlike the human enzyme, is not a heme protein. *J Biol Chem.*, **275**, 11541-11544.

Jhingran, A., Chawia, B., Saxena, S., Barrett, M.P. & Madhubaia, R. (2009) Paromomycin: uptake and resistance in *Leishmania donovani*. *Mol Biochem Parasitol.*, **164**, 111-117.

Johnson, C.M., Roderick, S.L. & Cook, P.F. (2005) The serine acetyltransferase reaction: acetyl transfer from an acylpantothenyl donor to an alcohol. *Arch Biochem Biophys.*, **433**, 85-95.

Joshi, P.B., Sacks, D.L., Modi, G. & McMaster, W.R. (1998) Targeted gene deletion of *Leishmania major* genes encoding developmental stage-specific leishmanolysin (GP63). *Mol Microbiol.*, **27**, 519-530.

Jost, R., Altschmied, L., Bloem, E., Bogs, J., Gershenzon, J., Hähnel, U., Hänsch, R., Hartmann, T., Kopriva, S., Kruse, C., Mendel, R.R., Papenbrock, J., Reichelt, M., Rennenberg, H., Schnug, E., Schmidt, A., Textor, S., Tokuhisa, J., Wachter, A., Wirtz, M., Rausch, T. & Hell, R. (2005) Expression profiling of metabolic genes in response to methyl jasmonate reveals regulation of genes of primary and secondary sulfur-related pathways in *Arabidopsis thaliana*. *Photosynth Res.*, **86**, 491-508.

Kanzaki, H., Nagasawa, T. & Yamada, H. (1987) Insight into the active site of Streptomyces cystathionine γ-lyase based on the results of studies on its substrate specificity. *Biochim Biophys Acta.*, **913**, 45-50.

Kamhawi, S. (2006) Phlebotomine sand flies and *Leishmania* parasites: friends or foes? *Trends Parasitol.*, **22**, 439-445.

Kandpal, M., Tekwani, B.L., Chauhan, P.M. & Bhaduri, A.P. (1996) Correlation between inhibition of growth and arginine transport of *Leishmania donovani* promastigotes in vitro by diamidines. *Life Sci.*, **59**, PL75-80.

Kanterewicz, B.I., Knapp, L.T. & Klann, E. (1998) Stimulation of p42 and p44 mitogen-activated protein kinases by reactive oxygen species and nitric oxide in hippocampus. *J Neurochem.*, **70**, 1009-1016.

Kawashima, C.G., Noji, M., Nakamura, M., Ogra, Y., Suzuki, K.T. & Saito, K. (2004) Heavy metal tolerance of transgenic tobacco plants over-expressing cysteine synthase. *Biotechnol Lett.*, **26**, 153-157.

Kawashima, C.G., Berkowitz, O., Hell, R., Noji, M. & Saito, K. (2005) Characterization and expression analysis of a serine acetyltransferase gene family involved in a key step of the sulfur assimilation pathway in *Arabidopsis*. *Plant Physiol.*, **137**, 220-230.

Kery, V., Bukovska, G. & Kraus, J.P. (1994) Transsulfuration depends on heme in addition to pyridoxal 5'-phosphate. Cystathionine beta-synthase is a heme protein. *J Biol Chem.*, **269**, 25283-25288.

Kessler, D. (2006) Enzymatic activation of sulfur for incorporation into biomolecules in prokaryotes. *FEMS Microbiol Rev.*, **30**, 825-840.

Killick-Kendrick, R., Molyneux, D.H. & Ashford, R.W. (1974a) *Leishmania* in phlebotomid sandflies. I. Modifications of the flagellum associated with attachment to the mid-gut and oesophageal valve of the sandlfy. *Proc R Soc Lond B Biol Sci.*, **187**, 409-419.

Killick-kendrick, R., Molyneux, D.H. & Ashford, R.W. (1974b) Ultrastructural observations on the attachment of *Leishmania* in the sandfly. *Trans R Soc Trop Med Hyg.*, **68**, 269.

Kredich, N.M. & Tomkins, G.M. (1966) The enzymic synthesis of L-cysteine in *Escherichia coli* and *Salmonella typhimurium*. *J Biol Chem.*, **241**, 4955-4965.

Kredich, N.M., Becker, M.A. & Tomkins, G.M. (1969) Purification and characterization of cysteine synthetase, a bifunctional protein complex, from *Salmonella typhimurium*. *J Biol Chem.*, **244**, 2428-2439.

Kredich, N.M. (1971) Regulation of L-cysteine biosynthesis in *Salmonella typhimurium*. I. Effects of growth of varying sulfur sources and O-acetyl-L-serine on gene expression. *J Biol Chem.*, **246**, 3474-3484.

Kredich, N.M., Hulanicka, M.D. & Hallquist, S.G. (1979) Synthesis of L-cysteine in *Salmonella typhimurium*. *Ciba Found Symp.*, **72**, 87-99.

Kurata, S. (2000) Selective activation of p38 MAPK cascade and mitotic arrest caused by low level oxidative stress. *J Biol Chem.*, **275**, 23413-13416.

Kuske, C.R., Hill, K.K., Guzman, E. & Jackson, P.J. (1996) Subcellular Location of O-Acetylserine Sulfhydrylase Isoenzymes in Cell Cultures and Plant Tissues of *Datura innoxia* Mill. *Plant Physiol.*, **112**, 659-667.

Lainson, R., Ready, P.D. & Shaw, J.J. (1979) *Leishmania* in phlebotomid sandflies. VII. On the taxonomic status of *Leishmania peruviana*, causative agent of Peruvian 'uta', as indicated by its development in the sandfly, *Lutzomyia longipalpis*. *Proc R Soc Lond B Biol Sci.*, **206**, 307-318.

Lainson, R., Ryan, L. & Shaw, J.J. (1987) Infective stages of *Leishmania* in the sanfly vector and some observations on the mechanism of transmission. *Mem Inst Oswaldo Cruz.*, **82**, 421-424.

Landfear, S.M. & Ignatushchenko, M. (2001) The flagellum and flagellar pocket of trypanosomatids. *Mol Biochem Parasitol.*, **115**, 1-17.

Laskay, T., van Zandbergen, G. & Solbach, W. (2003) Neutrophil granulocytes – Trojan horses for *Leishmania major* and other intracellular microbes? *Trends Microbiol.*, **11**, 210-214.

Lee, H.S. & Hwang, B.J. (2003) Methionine biosynthesis and its regulation in *Corynebacterium glutamicum*: parallel pathways of transsulfuration and direct sulfhydrylation. *Appl Microbiol Biotechnol.*, **62**, 459-467.

Légaré, D., Papadopoulou, B., Roy, G., Mukhopadhyay, R., Haimeur, A., Dey, S., Grondin, K., Brochu, C., Rosen, B.P. & Ouellette, M. (1997) Efflux systems and increased trypanothione levels in arsenite-resistant *Leishmania*. *Exp Parasitol.*, **87**, 275-282.

Légaré, D., Richard, D., Mukhopadhyay, R., Stierhof, Y.D., Rosen, B.P., Haimeur, A., Papadopoulou, B. & Ouellette, M. (2001) The Leishmania ATP-binding cassette protein PGPA is an intracellular metal-thiol transporter ATPase. *J Biol Chem.*, **276**, 26301-26307.

Leprohon, P., Légaré, D., Raymond, F., Madore, E., Hardiman, G., Corbeil, J. & Ouellette, M. (2009) Gene expression modulation is associated with gene amplification, supernumerary chromosomes and chromosome loss in antimony-resistant *Leishmania infantum*. *Nucleic Acids Res.*, **37**, 1387-1399.

Linn, S.C., Kim, H.S., Keane, E.M., Andras, L.M., Wang, E. & Merrill, A.H. Jr. (2001) Regulation of *de novo* sphingolipid biosynthesis and the toxic consequences of its disruption. *Biochem Soc Trans.*, **29**, 831-835.

Lira, R., Sundar, S., Makharia, A., Kenney, R., Gam, A., Saraiva, E. & Sacks, D. (1999) Evidence that the high incidence of treatment failures in Indian kala-azar is due to the emergence of antimony-resistant strains of *Leishmania donovani*. *J Infect Dis.*, **180**, 564-567.

Liszewska, F., Lewandowska, M., Płochocka, D. & Sirko, A. (2007) Mutational analysis of O-acetylserine (thiol) lyase conducted in yeast two-hybrid system. *Biochim Biophys Acta.*, **1774**, 450-455.

Liu, B., Liu, Y., Motyka, S.A., Agbo, E.E. & Englund, P.T. (2005) Fellowship of the rings: the replication of kinetoplast DNA. *Trends Parasitol.*, **21**, 363-369.

Lo, R., Turner, M.S., Barry, D.G., Sreekumar, R., Walsh, T.P. & Giffard, P.M. (2009) Cystathionine γ-lyase is a component of cysteine-mediated oxidative defense in *Lactobacillus reuteri* BR11. *J Bacteriol.*, **191**, 1827-1837.

Loenen, W.A. (2006) S-adenosylmethionine: jack of all trades and master of everything? *Biochem Soc Trans.*, **34,** 330-333.

López-Martín, M.C., Becana, M., Romero, L.C. & Gotor, C. (2008) Knocking out cytosolic cysteine synthesis compromises the antioxidant capacity of the cytosol to maintain discrete concentrations of hydrogen peroxide in *Arabidopsis. Plant Physiol.*, **147**, 562-572.

Louassini, M., Adroher, F.J., Foulquié, M.R. & Benítez, R. (1998) Investigations on the in vitro metacyclogenesis of a visceral and a cutaneous human strain of *Leishmania infantum*. *Acta Trop.*, **70**, 355-368.

Lunn, J.E., Droux, M., Martin, J. & Douce, R. (1990) Localization of ATP Sulfurylase and O-Acetylserine(thiol)lyase in Spinach Leaves. *Plant Physiol.*, **94**, 1345-1352.

Maclean, K.N., Janosík, M., Oliveriusová, J., Kery, V. & Kraus, J.P. (2000) Transsulfuration in *Saccharomyces cerevisiae* is not dependent on heme: purification and characterization of recombinant yeast cystathionine beta-synthase. *J Inorg Biochem.*, **81**, 161-171.

Mandal, G., Wyllie, S., Singh, N., Sundar, S., Fairlamb, A.H. & Chatterjee, M. (2007) Increased levels of thiols protect antimony unresponsive *Leishmania donovani* field isolates against reactive oxygen species generated by trivalent antimony. *Parasitology*, **134**, 1679-1687.

Marquis, N., Gourbal, B., Rosen, B.P., Mukhopadhyay, R. & Ouellette, M. (2005) Modulation in aquaglyceroporin AQP1 gene transcript levels in drug-resistant *Leishmania*. *Mol Microbiol.*, **57**, 1690-1699.

Marzluf, G.A. (1997) Molecular genetics of sulfur assimilation in filamentous fungi and yeast. *Annu Rev Microbiol.*, **51**, 73-96.

Mathias, S., Peña, L.A. & Kolesnick, R.N. (1998) Signal transduction of stress via ceramide. *Biochem J.*, **335**, 465-480.

Mbongo, N., Loiseau, P.M., Billion, M.A. & Robert-Gero, M. (1998) Mechanism of amphotericin B resistance in *Leishmania donovani* promastigotes. *Antimicrob Agents Chemother.*, **42**, 352-357.

McConville, M.J., Mullin, K.A., Ilgoutz, S.C. & Teasdale, R.D. (2002) Secretory pathway of trypanosomatid parasites. *Microbiol Mol Biol Rev.*, **66**, 122-154.

Medina-Acosta, E. & Cross, G.A. (1993) Rapid isolation of DNA from trypanosomatid protozoa using a simple 'mini-prep' procedure. *Mol Biochem Parasitol.*, **59**, 327-329.

Mehta, A. & Shaha, C. (2004) Apoptotic death in *Leishmania donovani* promastigotes in response to respiratory chain inhibition: complex II inhibition results in increased pentamidine cytotoxicity. *J Biol Chem.*, **279**, 11798-11813.

Mengeling, B.J., Beverley, S.M. & Turco, S.J. (1997) Designing glycoconjugate biosynthesis for an insidious intent: phosphoglycan assembly in *Leishmania* parasites. *Glycobiology*, **7**, 873-880.

Meyerhoff, A. (1999) U.S. Food and Drug Administration approval of AmBisome (liposomal amphotericin B) for treatment of visceral leishmaniasis. *Clin Infect Dis.*, **28**, 42-48.

Michels, P.A., Bringaud, F., Herman, M. & Hannaert, V. (2006) Metabolic functions of glycosomes in trypanosomatids. *Biochim Biophys Acta.*, **1763**, 1463-1477.

Mino, K., Yamanoue, T., Sakiyama, T., Eisaki, N., Matsuyama, A. & Nakanishi, K. (1999) Purification and characterization of serine acetyltransferase from *Escherichia coli* partially truncated at the C-terminal region. *Biosci Biotechnol Biochem.*, **63**, 168-179.

Mino, K. & Ishikawa, K. (2003) A novel O-phospho-L-serine sulfhydrylation reaction catalyzed by O-acetylserine sulfhydrylase from *Aeropyrum pernix* K1. *FEBS Lett.*, **551**, 133-138.

Miranda, K., Benchimol, M., Docampo, R. & de Souza, W. (2000) The fine structure of acidocalcisomes in *Trypanosoma cruzi*. *Parasitol Res.*, **86**, 373-384.

Mishra, J., Saxena, A. & Singh, S. (2007) Chemotherapy of leishmaniasis: past, present and future. *Curr Med Chem.*, **14**, 1153-1169.

Mishra, B.B., Kale, R.R., Singh, R.K. & Tiwari, V.K. (2009) Alkaloids: Future prospective to combat leishmaniasis. *Fitoterapia*, **80**, 81-90.

Mittal, M.K., Misra, S., Owais, M. & Goyal, N. (2005) Expression, purification, and characterization of *Leishmania donovani* trypanothione reductase in *Escherichia coli*. *Protein Expr Purif.*, **40**, 279-286.

Morzycka, E. & Paszewski, A. (1979) Two pathways of cysteine biosynthesis in *Saccharomycopsis lipolytica*. *FEBS Lett.*, **101**, 97-100.

Moutiez, M., Aumercier, M., Schöneck, R., Meziane-Cherif, D., Lucas, V., Aumercier, P., Ouaissi, A., Sergheraert, C. & Tartar, A. (1995) Purification and characterization of a trypanothione-glutathione thioltransferase from *Trypanosoma cruzi*. *Biochem J.*, **310**, 433-437.

Moutiez, M., Quemeneur, E., Sergheraert, C., Lucas, V., Tartar, A. & Davioud-Charvet, E. (1997) Glutathione-dependent activities of *Trypanosoma cruzi* p52 makes it a new member of the thiol:disulphide oxidoreductase family. *Biochem J.*, **322**, 43-48.

Mottram, J.C. & Coombs, G.H. (1985) *Leishmania mexicana*: enzyme activities of amastigotes and promastigotes and their inhibition by antimonials and arsenicals. *Exp Parasitol.*, **59**, 151-160.

Mukhopadhyay, R., Dey, S., Xu, N., Gage, D., Lightbody, J., Ouellette, M. & Rosen, B.P. (1996) Trypanothione overproduction and resistance to antimonials and arsenicals in *Leishmania*. *Proc Natl Acad Sci U S A.*, **93**, 10383-10387.

Mukhopadhyay, R. & Rosen, B.P. (2002) Arsenate reductases in prokaryotes and eukaryotes. *Environ Health Perspect.*, **110**, 745-748.

Müller, K., van Zandbergen, G., Hansen, B., Laufs, H., Jahnke, N., Solbach, W. & Laskay, T. (2001) Chemokines, natural killer cells and granulocytes in the early course of *Leishmania major* infection in mice. *Med Microbiol Immunol.*, **190**, 73-76.

Mullin, K.A., Foth, B.J., Ilgoutz, S.C., Callaghan, J.M., Zawadzki, J.L., McFadden, G.I. & McConville, M.J. (2001) Regulated degradation of an endoplasmic reticulum membrane protein in a tubular lysosome in *Leishmania mexicana*. *Mol Biol Cell.*, **12**, 2364-2377.

Murphy, G.A., Solski, P.A., Jillian, S.A., Pérez de la Ossa, P., D'Eustachio, P., Der, C.J. & Rush, M.G. (1999) Cellular functions of TC10, a Rho family GTPase: regulation of morphology, signal transduction and cell growth. *Oncogene*, **18**, 3831-3845.

Nagasawa, T., Kanzaki, H. & Yamada, H. (1984) Cystathionine γ-lyase of *Streptomyces phaeochromogenes*. *J Biol Chem*, **259**, 10393-10403.

Nakamori, S., Kobayashi, S.I., Kobayashi, C. & Takagi, H. (1998) Overproduction of L-cysteine and L-cystine by *Escherichia coli* strains with a genetically altered serine acetyltransferase. *Appl Environ Microbiol.*, **64**, 1607-1611.

Nakamura, T., Kon, Y., Iwahashi, H. & Eguchi, Y. (1983) Evidence that thiosulfate assimilation by *Salmonella typhimurium* is catalyzed by cysteine synthase B. *J Bacteriol.*, **156**, 656-662.

Nakamura, T., Iwahashi, H. & Eguchi, Y. (1984) Enzymatic proof for the identity of the *S*-sulfocysteine synthase and cysteine synthase B of *Salmonella typhimurium*. *J Bacteriol.*, **158**, 1122-1127.

Nakamura, M., Kuramata, M., Kasugai, I., Abe, M. & Youssefian, S. (2009) Increased thiol biosynthesis of transgenic poplar expressing a wheat O-acetylserine(thiol) lyase enhances resistance to hydrogen sulfide and sulfur dioxide toxicity. *Plant Cell Rep.*, **28**, 313-323.

Noji, M., Inoue, K., Kimura, N., Gouda, A. & Saito, K. (1998) Isoform-dependent differences in feedback regulation and subcellular localization of serine acetyltransferase involved in cysteine biosynthesis from *Arabidopsis thaliana*. *J Biol Chem.*, **273**, 32739-32745.

Notredame, C., Higgins, D.G. & Heringa, J. (2000) T-Coffee: A novel method for fast and accurate multiple sequence alignment. *J Mol Biol.*, **302**, 205-217.

Nozaki, T., Arase, T., Shigeta, Y., Asai, T., Leustek, T. & Takeuchi, T. (1998) Cloning and bacterial expression of adenosine-5'-triphosphate sulfurylase from the enteric protozoan parasite *Entamoeba hystolytica*. *Biochim Biophys Acta*, **1429**, 284-291.

Nozaki, T., Shigeta, Y., Saito-Nakano, Y., Imada, M. & Kruger, W.D. (2001) Characterization of transsulfuration and cysteine biosynthetic pathways0 in the protozoan hemoflagellate, *Trypanosoma cruzi*. Isolation and molecular characterization of cystathionine beta-synthase and serine acetyltransferase from *Trypanosoma*. *J Biol Chem.*, **276**, 6516-6523.

Nozaki, T., Ali, V. & Tokoro, M. (2005) Sulfur-containing amino acid metabolism in parasitic protozoa. *Adv Parasitol.*, **60**, 1-99.

Ohanian, J. & Ohanian, V. (2001) Sphingolipids in mammalian cell signalling. *Cell Mol Life Sci.*, **58**, 2053-2068.

Olliaro, P., Lazdins, J. & Guhl, F. (2002) Developments in the treatment of leishmaniasis and trypanosomiasis. *Expert Opin Emerg Drugs.*, **7**, 61-67.

Olsen, L.R., Huang, B., Vetting, M.W. & Roderick, S.L. (2004) Structure of serine acetyltransferase in complexes with CoA and its cysteine feedback inhibitor. *Biochemistry*, **43**, 6013-6019.

Opperdoes, F.R. (1987) Compartmentation of carbohydrate metabolism in trypanosomes. *Annu Rev Microbiol.*, **41**, 127-151.

Ouaissi, M.A., Dubremetz, J.F., Schöneck, R., Fernandez-Gomez, R., Gomez-Corvera, R., Billaut-Mulot, O., Taibi, A., Loyens, M., Tartar, A., Sergheraert, C. & Kusnierz, J.P. (1995) *Trypanosoma cruzi*: A 52 kDa protein sharing sequence homology with glutathione S-transferase is localized in parasite organelles morphologically resembling reservosomes. *Exp Parasitol.*, **81**, 453-461.

Ouellette, M., Drummelsmith, J. & Papadopoulou, B. (2004) Leishmaniasis: drugs in the clinic, resistance and new developments. *Drug Resist Updat.*, **7**, 257-266.

Ovádi J. (1991) Physiological significance of metabolic channelling. *J Theor Biol.*, **152**, 1-22.

Paget, M.S.B. & Buttner, M.J. (2003) Thiol-based regulatory switches. *Annu Rev Genet.*, **37**, 91-121.

Palumbo, E. (2008) Oral miltefosine treatment in children with visceral leishmaniasis: a brief review. *Braz J Infect Dis.*, **12**, 2-4.

Pan, A.A. (1984) *Leishmania mexicana*: serial cultivation of intracellular stages in a cell-free medium. *Exp Parasitol.*, **58**, 72-80.

Papadopoulos, A.I., Walker, J. & Barrett, J. (1996) A novel cystathionine beta-synthase from *Panagrellus redivivus* (Nematoda). *Int J Biochem Cell Biol.*, **28**, 543-549.

Parker, G., Walshaw, D., O'Rourke, K., Broad, S., Tingey, A., Poole, P.S. & Robson, R.L. (2001) Evidence for redundancy in cysteine biosynthesis in *Rhizobium leguminosarum* RL3841: analysis of a cysE gene encoding serine acetyltransferase. *Microbiology*, **147**, 2553-2560.

Parsons, M., Furuya, T., Pal, S. & Kessler, P. (2001) Biogenesis and function of peroxisomes and glycosomes. *Mol Biochem Parasitol.*, **115**, 19-28.

Parsons, M. (2004) Glycosomes: parasites and the divergence of peroxisomal purpose. *Mol Microbiol.*, **53**, 717-724.

Paszewski, A. & Grabski, J. (1974) Regulation of S-amino acids biosynthesis in *Aspergillus nidulans*. Role of cysteine and-or homocysteine as regulatory effectors. *Mol Gen Genet.*, **132**, 307-320.

Paszewski, A., Prazmo, W., Nadolska, J. & Regulski, M. (1984) Mutations affecting the sulphur assimilation pathway in *Aspergillus nidulans*: their effect on sulphur amino acid metabolism. *J Gen Microbiol.*, **130**, 1113-1121.

Pérez-Victoria, J.M., Parodi-Talice, A., Torres, C., Gamarro, F. & Castanys, S. (2001) ABC transporters in the protozoan parasite *Leishmania*. *Int Microbiol.*, **4**, 159-166.

Piotrowska, M. & Paszewski, A. (1990) A yeast with unusual sulphur amino acid metabolism. *J Gen Microbiol.*, **136**, 2283-2286.

Piotrowska, M. (1993) *Candida valida*--a yeast lacking the reverse transsulphuration pathway. *Acta Microbiol Pol.*, **42**, 35-39.

Poirot, O., O'Toole, E. & Notredame, C. (2003) Tcoffee@igs: A web server for computing, evaluating and combining multiple sequence alignments. *Nucleic Acids Res.*, **31**, 3503-3506.

Pral, E.M., Bijovsky, A.T., Balanco, J.M. & Alfieri, S.C. (1993) *Leishmania mexicana*: proteinase activities and megasomes in axenically cultivated amastigote-like forms. *Exp Parasitol.*, **77**, 62-73.

Puentes, S.M., Da Silva, R.P., Sacks, D.L., Hammer, C.H. & Joiner, K.A. (1990) Serum resistance of metacyclic stage *Leishmania major* promastigotes is due to release of C5b-9. *J Immunol.*, **145**, 4311-4316.

Pye, V.E., Tingey, A.P., Robson, R.L. & Moody, P.C. (2004) The structure and mechanism of serine acetyltransferase from *Escherichia coli*. *J Biol Chem.*, **279**, 40729-40736.

Rabeh, W.M. & Cook, P.F. (2004) Structure and mechanism of O-acetylserine sulfhydrylase. *J Biol Chem.*, **279**, 26803-26806.

Reguera, R., Balaña Fouce, R., Cubria, J.C., Alvarez Bujidos, M.L. & Ordoñez, D. (1994) Putrescine uptake inhibition by aromatic diamidines in *Leishmania infantum* promastigotes. *Biochem Pharmacol.*, **47**, 1859-1866.

Rijal, S., Yardley, V., Chappuis, F., Decuypere, S., Khanal, B., Singh, R., Boelaert, M., De Doncker, S., Croft, S. & Dujardin, J.C. (2007) Antimonial treatment of visceral leishmaniasis: are current *in vitro* susceptibility assays adequate for prognosis of *in vivo* therapy outcome? *Microbes Infect.*, **9**, 529-535.

Roberts, C.W., McLeod, R., Rice, D.W., Ginger, M., Chance, M.L. & Goad, L.J. (2003) Fatty acid and sterol metabolism: potential antimicrobial targets in *apicomplexan* and *trypanosomatid* parasitic protozoa. *Mol Biochem Parasitol.*, **126**, 129-142.

Roberts, W.L., Berman, J.D. & Rainey, P.M. (1995) *In vitro* antileishmanial properties of tri- and pentavalent antimonial preparations. *Antimicrob Agents Chemother.*, **39**, 1234-1239.

Robinson, K.A. & Beverley, S.M. (2003) Improvements in transfection efficiency and tests of RNA interference (RNAi) approaches in the protozoan parasite *Leishmania*. *Mol Biochem Parasitol.*, **128**, 217-228.

Rogers, M.E., Chance, M.L. & Bates, P.A. (2002) The role of promastigote secretory gel in the origin and transmission of the infective stage of *Leishmania mexicana* by the sandfly *Lutzomyia longipalpis*. *Parasitology*, **124**, 495-507.

Rogers, M.E., Ilg, T., Nikolaev, A.V., Ferguson, M.A. & Bates, P.A. (2004) Transmission of cutaneous leishmaniasis by sand flies is enhanced by regurgitation of fPPG. *Nature*, **430**, 463-467.

Rolland, N., Droux, M. & Douce, R. (1992) Subcellular Distribution of O-Acetylserine(thiol)lyase in Cauliflower (*Brassica oleracea L.*) Inflorescence. *Plant Physiol.*, **98**, 927-935.

Romão, P.R., Tovar, J., Fonseca, S.G., Moraes, R.H., Cruz, A.K., Hothersall, J.S., Noronha-Dutra, A.A., Ferreira, S.H. & Cunha, F.Q. (2006) Glutathione and the redox control system trypanothione/trypanothione reductase are involved in the protection of *Leishmania spp*. against nitrosothiol-induced cytotoxicity. *Braz J Med Biol Res.*, **39**, 355-363.

Roper, M.D. & Kraus, J.P. (1992) Rat cystathionine beta-synthase: expression of four alternatively spliced isoforms in transfected cultured cells. *Arch Biochem Biophys.*, **298**, 514-521.

Rosado, J.O., Salvador, M. & Bonatto, D. (2007) Importance of the trans-sulfuration pathway in cancer prevention and promotion. *Mol Cell Biochem.*, **301**, 1-12.

Rotureau, B., Morales, M.A., Bastin, P. & Späth, GF. (2009) The flagellum-MAP kinase connection in Trypanosomatids: a key sensory role in parasite signaling and development? *Cell Microbiol*. [Epub ahead of print].

Ruffet, M.L., Droux, M. & Douce, R. (1994) Purification and kinetic properties of serine acetyltransferase free of O-acetylserine (thiol) lyase from spinach chloroplasts. *Plant Physiol.*, **104**, 597-604.

Saar, Y., Ransford, A., Waldman, E., Mazareb, S., Amin-Spector, S., Plumblee, J., Turco, S.J. & Zilberstein, D. (1998) Characterization of developmentally-regulated activities in axenic amastigotes of *Leishmania donovani*. *Mol Biochem Parasitol.*, **95**, 9-20.

Sacks, D.L. & da Silva, R.P. (1987) The generation of infective stage *Leishmania major* promastigotes is associated with the cell-surface expression and release of a developmentally regulated glycolipid. *J Immunol.*, **139**, 3099-3106.

Sacks, D.L., Modi, G., Rowton, E., Späth, G., Epstein, L., Turco, S.J. & Beverley, S.M. (2000) The role of phosphoglycans in *Leishmania*-sand-fly interactions. *Proc Natl Acad Sci U S A.*, **97**, 406-411.

Sacks, D.L. (2001) *Leishmania*-sand-fly interactions controlling species-specific vector competence. *Cell Microbiol.*, **3**, 189-196.

Saito, K., Kurosawa, M., Tatsuguchi, K., Takagi, Y. & Murakoshi, I. (1994) Modulation of cysteine biosynthesis in chloroplasts of transgenic tobacco overexpressing cysteine synthase [O-acetylserine(thiol)-lyase]. *Plant Physiol.*, **106**, 887-895.

Saito, K., Yokoyama, H., Noji, M. & Murakoshi, I. (1995) Molecular cloning and characterization of a plant serine acetyltransferase playing a regulatory role in cysteine biosynthesis from watermelon. *J Biol Chem.*, **270**, 16321-16326.

Sands, M., Kron, M.A. & Brown, R.B. (1985) Pentamidine: a review. *Rv Infect Dis.*, **7**, 625-634.

Saraiva, E.M., Pinto-da-Silva, L.H., Wanderley, J.L., Bonomo, A.C., Barcinski, M.A. & Moreira, M.E. (2005) Flow cytometric assessment of *Leishmania spp* metacyclic differentiation: validation by morphological features and specific markers. *Exp Parasitol.*, **110**, 39-47.

Schnell, R., Oehlmann, W., Singh, M. & Schneider, G. (2007) Structural insights into catalysis and inhibition of O-acetylserine sulfhydrylase from *Mycobacterium tuberculosis*. *J Biol Chem.*, **282**, 23473-23481.

Schöneck, R., Plumas-Marty, B., Taibi, A., Billaut-Mulot, O., Loyens, M., Gras-Masse, H., Capron, A. & Ouaissi, A. (1994) *Trypanosoma cruzi* cDNA encodes a tandemly repeated domain structure characteristic of small stress proteins and glutathione S-transferases. *Biol Cell.*, **80**, 1-10.

Sereno, D., Cavaleyra, M., Zemzoumi, K., Maquaire, S., Ouaissi, A. & Lemesre, J.L. (1998) Axenically grown amastigotes of *Leishmania infantum* used as an in vitro model to investigate the pentavalent antimony mode of action. *Antimicrob Agents Chemother.*, **42**, 3097-3102.

Shaked-Mishan, P., Ulrich, N., Ephros, M. & Zilberstein, D. (2001) Novel Intracellular SbV reducing activity correlates with antimony susceptibility in *Leishmania donovani*. *J Biol Chem.*, **276**, 3971-3976.

Silvestre, R., Santarém, N., Cunha, J., Cardoso, L., Nieto, J., Carrillo, E., Moreno, J. & Cordeiro-da-Silva, A. (2008) Serological evaluation of experimentally infected dogs by LicTXNPx-ELISA and amastigote-flow cytometry. *Vet Parasitol.*, **158**, 23-30.

Simpson, L. & Kretzer, F. (1997) The mitochondrion in dividing *Leishmania tarentolae* cells is symmetric and circular and becomes a single asymmetric tubule in non-dividing cells due to division of the kinetoplast portion. *Mol Biochem Parasitol.*, **87**, 71-78.

Smacchi, E. & Gobbetti, M. (1998) Purification and characterization of cystathionine gamma-lyase from *Lactobacillus fermentum* DT41. *FEMS Microbiol Lett.*, **166**, 197-202.

Smith, D.A. (1971) S-amino acid metabolism and its regulation in *Escherichia coli* and *Salmonella typhimurium*. *Adv Genet.*, **16**, 141-165.

Snoke, J.E., Yanari, S. & Bloch, K. (1953) Synthesis of glutathione from gamma-glutamylcysteine. *J Biol Chem.*, **201**, 573-586.

Spies, H.S. & Steenkamp, D.J. (1994) Thiols of intracellular pathogens. Identification of ovothiol A in *Leishmania donovani* and structural analysis of a novel thiol from *Mycobacterium bovis*. *Eur J Biochem.*, **224**, 203-213.

Soares, M.J. & De Souza, W. (1988) Cytoplasmic organelles of trypanosomatids: a cytochemical and stereological study. *J Submicrosc Cytol Pathol.*, **20**, 349-361.

Srere, P.A. (1987) Complexes of sequential metabolic enzymes. *Annu Rev Biochem.*, **56**, 89-124.

Styblo, M., Del Razo, L.M., Vega, L., Germolec, D.R., LeCluyse, E.L., Hamilton, G.A., Reed, W., Wang, C., Cullen, W.R. & Thomas, D.J. (2000) Comparative

toxicity of trivalent and pentavalent inorganic and methylated arsenicals in rat and human cells. *Arch Toxicol.*, **74**, 289-299.

Sudhandiran, G. & Shaha, C. (2003) Antimonial-induced increase in intracellular Ca2+ through non-selective cation channels in the host and the parasite is responsible for apoptosis of intracellular *Leishmania donovani* amastigotes. *J Biol Chem.*, **278**, 25120-25132.

Sundar, S. (2001) Treatment of visceral leishmaniasis. *Med Microbiol Immunol.*, **190**, 89-92.

Sundar, S., Jha, T.K., Thakur, C.P., Sinha, P.K. & Bhattacharya, S.K. (2007) Injectable Paromomycin for visceral leishmaniasis in India. *N Engl J Med.*, **356**, 2571-2581.

Taoka, S., Ohja, S., Shan, X., Kruger, W.D. & Banerjee, R. (1998) Evidence for heme-mediated redox regulation of human cystathionine beta-synthase activity. *J Biol Chem.*, **273**, 25179-25184.

Taoka, S., West, M. & Banerjee, R. (1999a) Characterization of the heme and pyridoxal phosphate cofactors of human cystathionine beta-synthase reveals nonequivalent active sites. *Biochemistry*, **38**, 2738-2744.

Taoka, S., West, M. & Banerjee, R. (1999b) Characterization of the heme and pyridoxal phosphate cofactors of human cystathionine beta-synthase reveals nonequivalent active sites. *Biochemistry*, **38**, 7406.

Thakur, C.P., Singh, R.K., Hassan, S.M., Kumar, R., Narain, S. & Kumar, A. (1999) Amphotericin B deoxycholate treatment of visceral leishmaniasis with newer modes of administration and precautions: a study of 938 cases. *Trans R Soc Trop Med Hyg.*, **93**, 319-323.

Tull, D., Vince, J.E., Callaghan, J.M., Naderer, T., Spurck, T., McFadden, G.I., Currie, G., Ferguson, K., Bacic, A. & McConville, M.J. (2004) SMP-1, a member of a new family of small myristoylated proteins in kinetoplastid parasites, is

targeted to the flagellum membrane in *Leishmania*. *Mol Biol Cell.*, **15**, 4775-4786.

Wada, M. & Takagi, H. (2006) Metabolic pathways and biotechnological production of L-cysteine. *Appl Microbiol Biotechnol.*, **73**, 48-54.

Walker, J. & Barrett, J. (1997) Parasite sulphur amino acid metabolism. *Int J Parasitol.*, **27**, 883-897.

Waller, R.F. & McConville, M.J. (2002) Developmental changes in lysosome morphology and function *Leishmania* parasites. *Int J Parasitol.*, **32**, 1435-1445.

Westrop, G.D., Goodall, G., Mottram, J.C. & Coombs, G.H. (2006) Cysteine biosynthesis in *Trichomonas vaginalis* involves cysteine synthase utilizing O-phosphoserine. *J Biol Chem.*, **281**, 25062-25075.

Williams, R.A., Westrop, G.D. & Coombs, G.H. (2009) Two pathways for cysteine biosynthesis in *Leishmania major*. *Biochem J.*, Mar 18 [Epub ahead of print].

Winkel, B.S. (2004) Metabolic channeling in plants. *Annu Rev Plant Biol.*, **55**, 85-107.

Wirtz, M. & Droux, M. (2005) Synthesis of the sulfur amino acids: cysteine and methionine. *Photosynth Res.*, **86**, 345-362.

Wirtz, M. & Hell, R. (2006) Functional analysis of the cysteine synthase protein complex from plants: structural, biochemical and regulatory properties. *J Plant Physiol.*, **163**, 273-286.

Wirtz, M. & Hell, R. (2007) Dominant-negative modification reveals the regulatory function of the multimeric cysteine synthase protein complex in transgenic Tobacco. *Plant Cell.*, **19**, 625-639.

Woehl, E.U., Tai, C.H., Dunn, M.F. & Cook, P.F. (1996) Formation of the alpha-aminoacrylate immediate limits the overall reaction catalyzed by O-acetylserine sulfhydrylase. *Biochemistry*, **35**, 4776-4783.

Wyllie, S., Cunningham, M.L. & Fairlamb, A.H. (2004) Dual action of antimonial drugs on thiol redox metabolism in the human pathogen *Leishmania donovani*. *J Biol Chem.*, **279**, 39925-39932.

Yarlett, N. & Bacchi, C.J. (1988) Effect of DL-α-difluoromethylornithine on methionine cycle intermediates in *Trypanosoma brucei brucei*. *Mol Biochem Parasitol.*, **27**, 1-10.

Zhang, K., Pompey, J.M., Hsu, F.F., Key, P., Bandhuvula, P., Saba, J.D., Turk, J. & Beverley, S.M. (2007) Redirection of sphingolipid metabolism toward *de novo* synthesis of ethanolamine in *Leishmania*. *EMBO J.*, **26**, 1094-1104.

Zhao, F.J., McGrath, S.R. & Hawkesford, M.J. (2000) Sulphur nutrition and the sulphur cycle. *Institute of Arable Crops Research Report*, 36-39.

Zheng, Z., Butler, K.D., Tweten, R.K. & Mensa-Wilmot, K. (2004) Endosomes, glycosomes and GPI catabolism in *Leishmania major*. *J Biol Chem.*, **279**, 42106-42113.

Zhou, Y., Messier, N., Ouellette, M., Rosen, B.P. & Mukhopadhyay, R. (2004) *Leishmania major* LmACR2 is a pentavalent antimony reductase that confers sensitivity to the drug pentostam. *J Biol Chem.*, **279**, 37445-37451.

Zhou, Y., Bhattacharjee, H. & Mukhopadhyay, R. (2006) Bifunctional role of the leishmanial antimonate reductase LmACR2 as a protein tyrosine phosphatase. *Mol Biochem Parasitol.*, **148**, 161-168.

Zhu, W., Lin, A. & Banerjee, R. (2008) Kinetic properties of polymorphic variants and pathogenic mutants in human cystathionine gamma-lyase. *Biochemistry.*, **47**, 6226-6232.